

Changes in Concentration of Tetraoxane Produced During the Solution Polymerization of Trioxane Catalyzed by $\text{BF}_3 \cdot \text{O}(\text{C}_2\text{H}_5)_2$

T. MIKI, T. HIGASHIMURA, and S. OKAMURA,
Department of Polymer Chemistry, Kyoto University, Kyoto, Japan

Synopsis

The behavior of tetraoxane produced during the polymerization of trioxane was investigated kinetically. In the polymerization of trioxane, a short induction period for the formation of methanol-insoluble polymer was observed and during the induction period a certain amount of tetraoxane, depending on the polymerization conditions, was produced. This amount was independent of the initial concentration of catalyst but increased with an increase in the polymerization temperature and in the initial concentration of trioxane. So this amount was found to be determined by the equilibrium between the formation and consumption of tetraoxane. On the other hand, in the early stage of polymerization of trioxane, the formation of an appreciable amount of soluble polymer was estimated. Consequently the formation of tetraoxane was explained in terms of the "back-biting" reaction of the soluble growing chain with depolymerization.

INTRODUCTION

It has been found that in the solution polymerization of trioxane catalyzed by boron trifluoride etherate, tetraoxane is produced independently of the kind of a solvent. The formation mechanism of tetraoxane was discussed and a "back-biting" reaction of the growing chain end with depolymerization was proposed.¹ However, it has not been made clear why tetraoxane can exist in the polymerizing system of trioxane in spite of the fact that the cationic homopolymerizability is larger than that of trioxane. To answer this question the kinetic behavior of tetraoxane produced during the trioxane polymerization was investigated.

Tetraoxane was formed immediately on the addition of catalyst, and the methanol-insoluble polymer was formed in an appreciable reaction time. The addition of tetraoxane shortened the induction period for the formation of methanol-insoluble polymer. Thus, the tetraoxane formation plays an important role in the induction period for the formation of methanol-insoluble polymer.

EXPERIMENTAL

The polymerization procedures and the methods of purification of trioxane, solvent, and boron trifluoride etherate [$\text{BF}_3 \cdot \text{O}(\text{C}_2\text{H}_5)_2$] were the

same as described in the previous paper.² The yield of methanol-insoluble polymer was determined by a gravimetric method. The concentrations of trioxane and tetraoxane in the reaction system were determined by gas chromatography according to the internal standard method, as described in the previous papers.^{1,3} The concentration of water in the reaction system was measured by the Karl-Fischer method.

RESULTS

In the homopolymerization of trioxane, a polymer (polyoxymethylene) and tetraoxane are produced.¹ Accordingly, the relation between the polymer and tetraoxane yields under various conditions was determined in the polymerization of trioxane in ethylene dichloride with $\text{BF}_3 \cdot \text{O}(\text{C}_2\text{H}_5)_2$ as a catalyst at 30°C . except for one case.

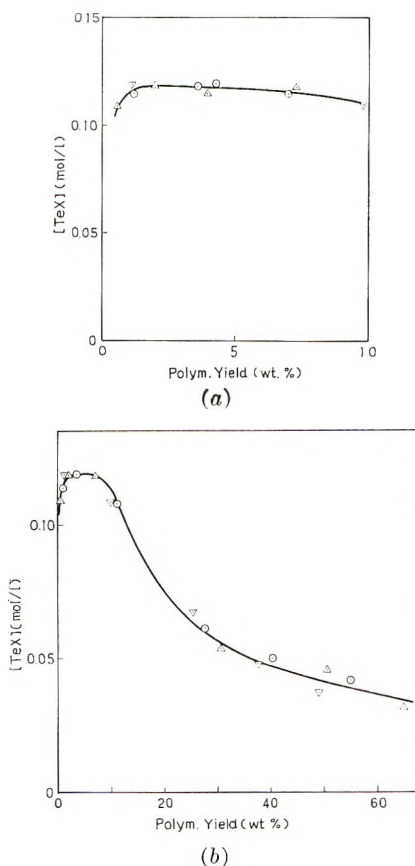


Fig. 1. Effect of initial catalyst concentration on the amount of tetraoxane produced in the polymerization of trioxane catalyzed by $\text{BF}_3 \cdot \text{O}(\text{C}_2\text{H}_5)_2$ in ethylene dichloride at 30°C . (a) at low conversion and (b) at high conversion: (Δ) $[\text{BF}_3 \cdot \text{O}(\text{C}_2\text{H}_5)_2]_0 = 20$ mmole/l.; (\circ) $[\text{BF}_3 \cdot \text{O}(\text{C}_2\text{H}_5)_2]_0 = 10$ mmole/l.; (∇) $[\text{BF}_3 \cdot \text{O}(\text{C}_2\text{H}_5)_2]_0 = 5$ mmole/l.; $[\text{ToX}]_0 = 3.17$ mole/l.; $[\text{H}_2\text{O}]_0 = 1.6$ mmole/l.

Effect of Catalyst Concentration and of Polymerization Temperature

The effect of the catalyst concentration on the amount of tetraoxane produced during the trioxane polymerization was investigated. Figures 1a and 1b show the results in the early stages and at long polymerization time, respectively. Figure 2 shows the time versus polymer yield curves in the early stage of polymerization; a induction period for polymer formation is evident. As is clear from Figure 1a, a certain amount of tetraoxane was produced in the very early stage of polymerization or during the induction period; this amount was independent of the initial concentration of catalyst. This suggests that the splitting of tetraoxane from the growing

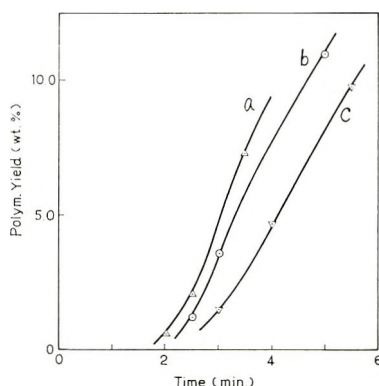


Fig. 2. Effect of initial catalyst concentration on the rate of formation of methanol-insoluble polymer in the polymerization of trioxane catalyzed by $\text{BF}_3 \cdot \text{O}(\text{C}_2\text{H}_5)_2$ in ethylene dichloride at 30°C .: (a) $[\text{BF}_3 \cdot \text{O}(\text{C}_2\text{H}_5)_2]_0 = 20$ mmole/l.; (b) $[\text{BF}_3 \cdot \text{O}(\text{C}_2\text{H}_5)_2]_0 = 10$ mmole/l.; (c) $[\text{BF}_3 \cdot \text{O}(\text{C}_2\text{H}_5)_2]_0 = 5$ mmole/l. $[\text{ToX}]_0 = 3.17$ mole/l.; $[\text{H}_2\text{O}]_0 = 1.6$ mmole/l.

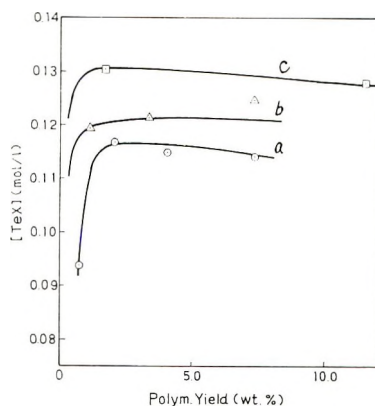


Fig. 3. Effect of polymerization temperature on the amount of tetraoxane produced in the polymerization of trioxane catalyzed by $\text{BF}_3 \cdot \text{O}(\text{C}_2\text{H}_5)_2$ in ethylene dichloride: (a) 30°C .; (b) 40°C .; (c) 50°C . $[\text{ToX}]_0 = 3.17$ mole/l.; $[\text{BF}_3 \cdot \text{O}(\text{C}_2\text{H}_5)_2]_0 = 20$ mmole/l.

chain does not depend on the initial catalyst concentration. Of course, the rate of formation of tetraoxane increased with increasing initial concentration of catalyst. However, as is seen in Figure 1*b*, the amount of tetraoxane in the reaction system decreased as the polymerization proceeded.

The effect of polymerization temperature on the amount of tetraoxane produced in the trioxane polymerization is shown in Figure 3. The amount of tetraoxane produced increased with increasing polymerization temperature.

Effect of Initial Concentration of Trioxane

The effect of initial trioxane concentration on the amount of tetraoxane produced in the trioxane polymerization was studied and was found to be very complicated. Figure 4 shows the change in the concentration of tetraoxane produced at various trioxane concentrations, and Figure 5 shows the relationship between polymer yield and tetraoxane produced at high initial concentrations of trioxane (more than 1.11 mole/l.). Figures 6–8 show the time–polymer yield and time–tetraoxane yield relationships at low initial concentrations of trioxane (less than 1.67 mole/l.). Figure 9 shows the relationship between the initial trioxane concentration and the maximum concentration of tetraoxane produced. As is seen in Figure 8, only a trace of methanol-insoluble polymer was obtained at a reaction time of 160 min. when the initial concentration of trioxane was 0.55 mole/l. At an initial trioxane concentration smaller than 0.55 mole/l., no methanol-insoluble polymer was obtained during the reaction time investigated in this paper, only tetraoxane being produced. As is also clear from Figure 6, the tetraoxane produced in the early stage was not consumed and remained in a certain concentration at an initial trioxane concentration lower than 1.11 mole/l. On the other hand, with an initial trioxane concentration

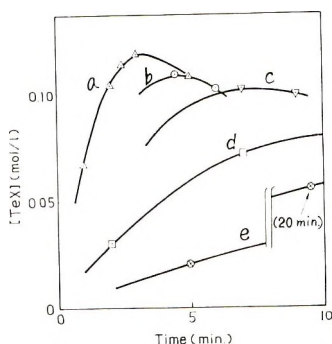


Fig. 4. Effect of the initial trioxane concentration on the rate of formation of tetraoxane in the polymerization of trioxane catalyzed by $\text{BF}_3 \cdot \text{O}(\text{C}_2\text{H}_5)_2$ in ethylene dichloride at 30°C . (at high concentrations of trioxane): (a) $[\text{ToX}]_0 = 3.17$ mole/l.; (b) 2.67 mole/l.; (c) 2.21 mole/l.; (d) 1.67 mole/l.; (e) 1.11 mole/l. $[\text{BF}_3 \cdot \text{O}(\text{C}_2\text{H}_5)_2]_0 = 10$ mmole/l.; $[\text{H}_2\text{O}]_0 = 1.6\text{--}2.5$ mmole/l.

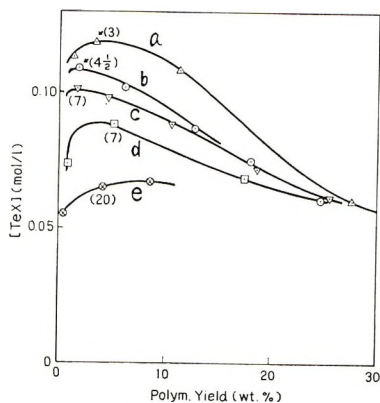


Fig. 5. Effect of the initial trioxane concentration on the amount of tetraoxane produced in the polymerization of trioxane catalyzed by $\text{BF}_3 \cdot \text{O}(\text{C}_2\text{H}_5)_2$ in ethylene dichloride at 30°C .: (a) $[\text{ToX}]_0 = 3.17$ mole/l.; (b) $[\text{ToX}]_0 = 2.67$ mole/l.; (c) $[\text{ToX}]_0 = 2.21$ mole/l.; (d) $[\text{ToX}]_0 = 1.67$ mole/l.; (e) $[\text{ToX}]_0 = 1.11$ mole/l. $[\text{BF}_3 \cdot \text{O}(\text{C}_2\text{H}_5)_2]_0 = 10$ mmole/l.; $[\text{H}_2\text{O}]_0 = 1.6$ – 2.5 mmole/l. The number in parentheses denotes the reaction time (min.).

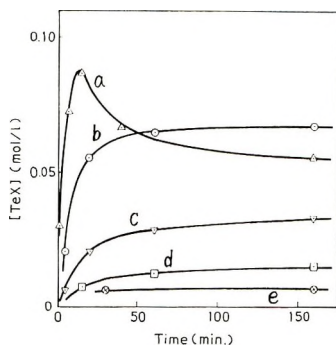


Fig. 6. Effect of the initial trioxane concentration on the rate of formation of tetraoxane in the polymerization of trioxane catalyzed by $\text{BF}_3 \cdot \text{O}(\text{C}_2\text{H}_5)_2$ in ethylene dichloride at 30°C . (at low concentrations of trioxane): (a) $[\text{ToX}]_0 = 1.67$ mole/l.; (b) $[\text{ToX}]_0 = 1.11$ mole/l.; (c) $[\text{ToX}]_0 = 0.55$ mole/l.; (d) $[\text{ToX}]_0 = 0.278$ mole/l.; (e) $[\text{ToX}]_0 = 0.167$ mole/l. $[\text{BF}_3 \cdot \text{O}(\text{C}_2\text{H}_5)_2]_0 = 10$ mmole/l.; $[\text{H}_2\text{O}]_0 = 1.1$ – 2.5 mmole/l.

higher than 1.67 mole/l., tetraoxane was consumed as the polymerization proceeds. The rate of formation of tetraoxane increased with increasing initial concentration of trioxane, as is seen in Figures 4 and 6. The maximum amount of tetraoxane produced in the early stage of polymerization also increased with increasing initial trioxane concentration, as is seen in Figure 9.

The amount of each component detected in the reaction system at a given time is shown in Figure 7, for a reaction in which an appreciable amount of methanol-insoluble polymer was produced and in Figure 8 for a reaction in which very little methanol-insoluble polymer was produced. The total amounts of trioxane, tetraoxane, and methanol-insoluble polymer

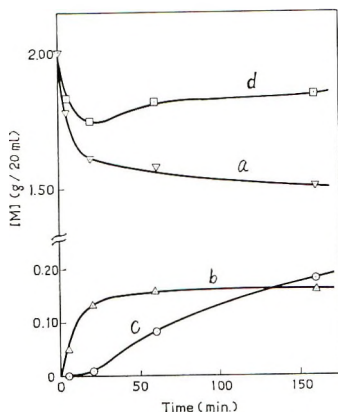


Fig. 7. Change in the concentration (in grams/20 ml.) of each component with the reaction time in the polymerization of trioxane catalyzed by $\text{BF}_3 \cdot \text{O}(\text{C}_2\text{H}_5)_2$ in ethylene dichloride at 30°C .: (a) consumption of trioxane; (b) formation of tetraoxane; (c) formation of methanol-insoluble polymer; (d) $a + b + c$. $[\text{ToX}]_0 = 1.11$ mole/l.; $[\text{H}_2\text{O}]_0 = 2.5$ mmole/l.; $[\text{BF}_3 \cdot \text{O}(\text{C}_2\text{H}_5)_2]_0 = 10$ mmole/l.

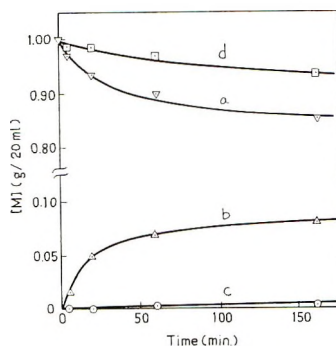


Fig. 8. Change in the concentration (in grams/20 ml.) of each component with reaction time in the polymerization of trioxane catalyzed by $\text{BF}_3 \cdot \text{O}(\text{C}_2\text{H}_5)_2$ in ethylene dichloride at 30°C .: (a) consumption of trioxane; (b) formation of tetraoxane; (c) formation of methanol-insoluble polymer; (d) $a + b + c$. $[\text{ToX}]_0 = 0.55$ mole/l.; $[\text{H}_2\text{O}]_0 = 1.7$ mmole/l.; $[\text{BF}_3 \cdot \text{O}(\text{C}_2\text{H}_5)_2]_0 = 10$ mmole/l.

did not coincide with the initial amount of trioxane charged, as reported previously.¹ It should be noticed that this difference increased with reaction time (Figs. 7 and 8) and then decreased again as soon as the methanol-insoluble polymer began to form, as is seen in Figure 7.

Effect of Water Concentration

The effect of water concentration on the amount of tetraoxane produced during the trioxane polymerization is shown in Figure 10. The induction period for the polymer formation increased with an increase in the initial water concentration, as has been reported.² The maximum amount of tetraoxane produced is almost independent of the initial water concentra-

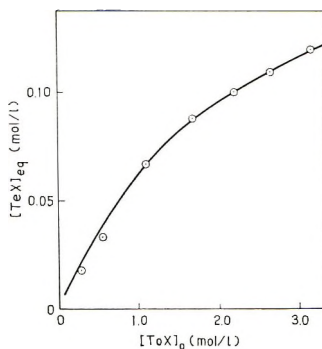


Fig. 9. Dependence of the equilibrium concentration of tetraoxane on the initial trioxane concentration in the polymerization of trioxane catalyzed by $\text{BF}_3 \cdot \text{O}(\text{C}_2\text{H}_5)_2$ in ethylene dichloride at 30°C . $[\text{BF}_3 \cdot \text{O}(\text{C}_2\text{H}_5)_2]_0 = 10$ mmole/l.; $[\text{H}_2\text{O}]_0 = 1.1$ – 2.5 mmole/l.

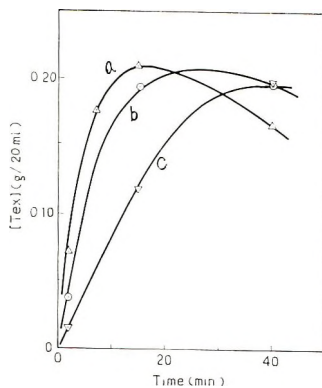


Fig. 10. Effect of the addition of water on the amount of tetraoxane produced in the polymerization of trioxane catalyzed by $\text{BF}_3 \cdot \text{O}(\text{C}_2\text{H}_5)_2$ in ethylene dichloride at 30°C .: (a) $[\text{H}_2\text{O}] = 1.8$ mmole/l.; (b) $[\text{H}_2\text{O}] = 4.0$ mmole/l.; (c) $[\text{H}_2\text{O}] = 7.0$ mmole/l. $[\text{ToX}]_0 = 1.67$ mole/l.; $[\text{BF}_3 \cdot \text{O}(\text{C}_2\text{H}_5)_2]_0 = 10$ mmole/l.

tion, while the rate of formation of tetraoxane decreased with increasing the initial water concentration. However, tetraoxane was formed without any induction period, in spite of the addition of water.

Effect of Tetraoxane Addition

The effect of addition of tetraoxane to the trioxane polymerization system was investigated. Figure 11 shows the time–polymer yield curves and Figure 12 shows the change in the tetraoxane concentration with reaction time. The induction period for polymer formation decreased with increasing initial concentration of tetraoxane added. As is clear from Figure 12, the concentration of tetraoxane was constricted to a certain value in the early stage of polymerization. The value is equal to the value shown in Figure 1a. This suggests the existence of an equilibrium between the formation and the consumption of tetraoxane.

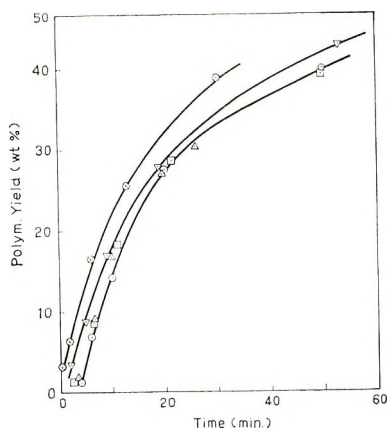


Fig. 11. Effect of the addition of tetraoxane on the formation of the methanol-insoluble polymer in the polymerization of trioxane catalyzed by $\text{BF}_3 \cdot \text{O}(\text{C}_2\text{H}_5)_2$ in ethylene dichloride at 30°C .: (O) no TeX added; (Δ) $[\text{TeX}] = 0.038$ mole/l.; (\square) $[\text{TeX}] = 0.076$ mole/l.; (∇) $[\text{TeX}] = 0.168$ mole/l.; (\otimes) $[\text{TeX}] = 0.305$ mole/l. $[\text{ToX}]_0 = 3.15$ mole/l.; $[\text{H}_2\text{O}]_0 = 4.6\text{--}5.4$ mmole/l.; $[\text{BF}_3 \cdot \text{O}(\text{C}_2\text{H}_5)_2]_0 = 10$ mmole/l.

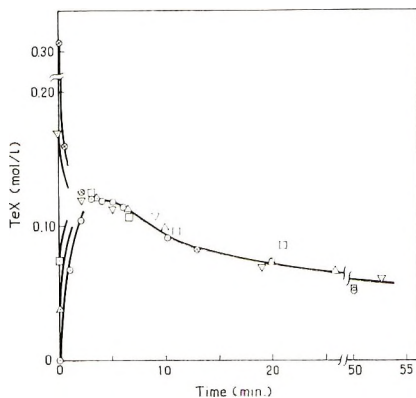


Fig. 12. Change in the tetraoxane concentration in the copolymerization of trioxane with tetraoxane catalyzed by $\text{BF}_3 \cdot \text{O}(\text{C}_2\text{H}_5)_2$ in ethylene dichloride at 30°C .: (O) no TeX added; (Δ) $[\text{TeX}] = 0.038$ mole/l.; (\square) $[\text{TeX}] = 0.076$ mole/l.; (∇) $[\text{TeX}] = 0.168$ mole/l.; (\otimes) $[\text{TeX}] = 0.305$ mole/l. $[\text{ToX}]_0 = 3.15$ mole/l.; $[\text{H}_2\text{O}]_0 = 4.6\text{--}5.4$ mmole/l.; $[\text{BF}_3 \cdot \text{O}(\text{C}_2\text{H}_5)_2]_0 = 10$ mmole/l.

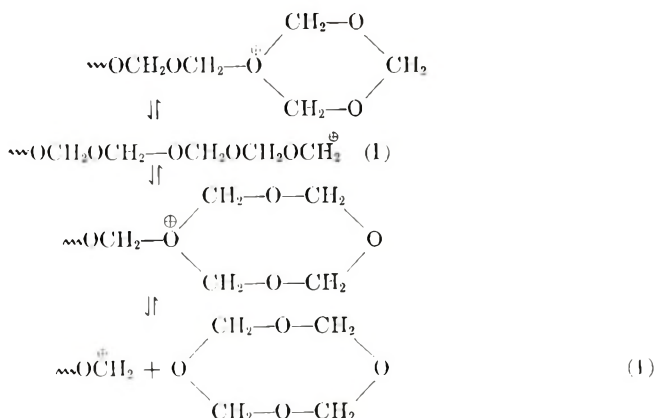
DISCUSSION

The behavior of tetraoxane produced during the polymerization of trioxane is very important to a study of the kinetics.¹ In the homopolymerization of trioxane, the amount of tetraoxane produced increased with the reaction time, reached the maximum value when the methanol-insoluble polymer began to form, and then decreased. From this it was concluded that tetraoxane is formed by a "back-biting" reaction in which an end of the soluble, low molecular weight, growing chain attacks its own chain, effecting polymerization until an equilibrium concentration of tetraoxane

is established in the early stage of polymerization and that the formation of tetraoxane by depolymerization is suppressed due to the heterogeneity of the reaction system as the reaction proceeds.

It should be noted that tetraoxane was formed before any methanol-insoluble polymer was obtained. The induction period for the polymer formation is one of the characteristics of the trioxane polymerization. Kern et al.⁴ explained the induction period in terms of the splitting of formaldehyde from the growing chain end and concluded that monomeric formaldehyde must be present in an equilibrium concentration before the polymerization of trioxane can take place. We have reported in detail the change in the formaldehyde concentration during the polymerization of trioxane.⁵ The amount of formaldehyde detected in the trioxane-BF₃·O-(C₂H₅)₂ polymerizing system increased even after the formation of a large amount of methanol-insoluble polymer (about 15 wt.-%). The addition of a small amount of formaldehyde did not cause disappearance of the induction period for the trioxane polymerization. However, as is seen in Figure 11, the addition of small amount of tetraoxane into the trioxane polymerization system shortened the induction period. Therefore, it was concluded that tetraoxane formation plays an important role in the induction period for the polymer formation in the trioxane polymerization.

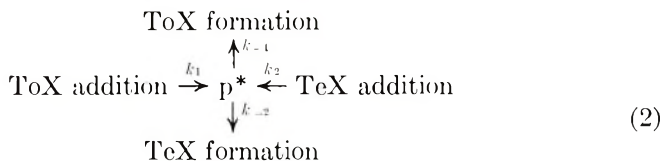
In the previous paper,¹ it was suggested that tetraoxane is formed not by an interaction of trioxane with formaldehyde liberated in the reaction system, but by a back-biting reaction of the growing chain end (I) with depolymerization, as is shown in eqs. (1).



On the other hand, tetraoxane has a larger cationic homopolymerizability than trioxane.¹ Thus, tetraoxane formed during the polymerization of trioxane takes part in the reaction of polyoxymethylene formation, and the tetraoxane formed should be consumed as the amount of tetraoxane formed increases. Finally, the rate of formation of tetraoxane becomes equal to the rate of consumption of tetraoxane, and thus the equilibrium between the formation and consumption of tetraoxane is established, as is shown

in Figures 7 and 12. From this moment the amount of methanol-insoluble polymer increases markedly. This equilibrium concentration of tetraoxane depends on the reaction conditions. It increases with an increase in the polymerization temperature (Fig. 3) and in the initial concentration of trioxane (Fig. 9). It is, however, independent of the initial concentration of catalyst (Fig. 1a).

Let p^* be the active center including both oxonium and carbonium ions. Then the behavior of p^* during the polymerization is limited to one of the probable four directions, as is shown in eqs. (2) where the reaction of p^* with impurities such as water is excluded, and where



ToX denotes trioxane, TeX denotes tetraoxane, and k_i are the rate constants. The rate of formation of tetraoxane is expressed as eq. (3).

$$d[\text{TeX}]/dt = k_{-2}[p^*] \quad (3)$$

The amount of tetraoxane produced is very small in comparison with that of trioxane charged (at $[\text{ToX}]_0 = 3.17$ mole/l., $[\text{TeX}]_{\text{produced}} < 0.12$ mole/l.). So the interaction of tetraoxane with p^* takes place with difficulty in the presence of trioxane in comparison with the case in the absence of trioxane, because trioxane itself also reacts with p^* . This retarding effect of tetraoxane must be taken into account in the reaction rate between p^* and tetraoxane during the polymerization of trioxane and may be stronger at the higher concentrations of trioxane. Then the consumption rate of tetraoxane can be expressed by eq. (4):

$$-d[\text{TeX}]/dt = (k_2/f)[p^*][\text{TeX}] \quad (4)$$

where f is a retarding factor depending on the concentration of trioxane. When the equilibrium between the formation and consumption of tetraoxane is established, eq. (5) is obtained from eqs. (3) and (4):

$$\begin{aligned}
 k_{-2}[p^*] &= (k_2/f)[p^*][\text{TeX}]_{\text{eq}} \\
 [\text{TeX}]_{\text{eq}} &= (k_{-2}/k_2)f
 \end{aligned}
 \quad (5)$$

If it is assumed that f is approximately proportional to a square root of trioxane concentration, eq. (5) can explain sufficiently the experimental relation between $[\text{TeX}]_{\text{eq}}$ and the trioxane concentration, as is shown in Figure 9. Equation (5) also shows that $[\text{TeX}]_{\text{eq}}$ is independent of the catalyst concentration. The increase in the equilibrium concentration of tetraoxane with increasing the polymerization temperature may be explained by the increase in k_{-2}/k_2 value. The phenomenon that the addition of water does not affect the maximum amount of tetraoxane formed and decreases the rate of formation of tetraoxane, may be explained in terms of the

decrease in the concentration of active centers due to the interaction with water.

As has been reported,¹ in the early stage of polymerization the amount of trioxane consumed did not coincide with the total amounts of tetraoxane and precipitant-insoluble polymer obtained. This fact was also observed in Figures 7 and 8. Low molecular weight cyclic compounds other than tetraoxane could not be detected by gas chromatography. These results suggest that an appreciable amount of soluble low molecular weight polymer is formed in the early stage of polymerization.

Other evidence for the formation of soluble low molecular weight polymer was noted. As has been reported,⁵ the concentration of formaldehyde in the reaction system was determined by the sodium sulfite method. The polymerization was stopped by adding a certain amount of aqueous sodium sulfite solution and the titration of NaOH liberated by reaction of CH_2O with Na_2SO_3 was carried out. In this procedure, the amount of NaOH liberated increased with the time between the polymerization to the beginning of the titration of NaOH. This is caused by the decomposition of soluble low molecular weight polyoxymethylene in the presence of alkali or acid.⁸ The existence of this soluble low molecular weight polymer was also suggested by Leese and Baumber.⁶ We shall hereafter term this soluble low molecular weight polymer the active prepolymer if it is growing and the dead prepolymer if it is dead.

We conclude that the active prepolymer plays an important role in the formation of tetraoxane by the back-biting reaction. The high molecular weight polyoxymethylene is insoluble in inert organic solvents such as benzene and ethylene dichloride. The molecular weight of methanol-insoluble polymer increases with the reaction time.⁷ As the active prepolymers grow, they can not exist in the soluble state and are precipitated from the solution, forming a polymer crystal. The propagation reaction still proceeds on the crystal surface, as pointed out by Leese and Baumber.⁶ Thus after the reaction system becomes heterogeneous, the polymerization proceeds both in the solution state homogeneously and on the crystal surface. When the propagation reaction proceeds on the crystal surface, the movement of the growing chain end may be limited due to its low flexibility. Consequently the back-biting reaction occurs with difficulty and the splitting of tetraoxane may be suppressed. On the other hand, the concentration of active prepolymer decreases after the methanol-insoluble polymer begins to form, as is shown in Figure 7. From these considerations, the decrease in the amount of tetraoxane formed in the early stage of polymerization after a given reaction time can be explained. As the amount of the crystal increases and the concentration of the soluble growing chain decreases with the reaction time, the rate of consumption of tetraoxane exceeds the rate of formation of tetraoxane; then the excess of tetraoxane is consumed till the rate of consumption of tetraoxane becomes equal to the rate of formation of tetraoxane. Thus tetraoxane is consumed to maintain the equilibrium.

References

1. T. Miki, T. Higashimura, and S. Okamura, *J. Polymer Sci. A-1*, **5**, 95 (1967).
2. T. Higashimura, T. Miki, and S. Okamura, *Bull. Chem. Soc. Japan*, **38**, 2067 (1965).
3. T. Higashimura, A. Tanaka, T. Miki, and S. Takamura, *J. Polymer Sci. A-1*, **5**, 1927 (1967).
4. W. Kern and V. Jaacks, *J. Polymer Sci.*, **48**, 399 (1960).
5. T. Miki, T. Higashimura, and S. Okamura, *Bull. Chem. Soc. Japan*, **39**, 36 (1966).
6. L. Leese and M. W. Baumber, *Polymer*, **6**, 269 (1965).
7. T. Higashimura, T. Miki, and S. Okamura, *Bull. Chem. Soc. Japan*, **39**, 25 (1966).
8. J. Löbering, *Ber.*, **69**, 1884 (1936).

Résumé

Le comportement du tétraoxane, produit en cours de polymérisation du trioxane, a été étudié cinétiquement. Dans la polymérisation du trioxane, la courte période d'induction pour la formation d'un polymère insoluble dans le méthanol a été observée et au cours de cette période d'induction une certaine quantité de tétraoxane, suivant les conditions de polymérisation, est produite. Cette quantité était indépendante de la concentration initiale en catalyseur, mais croissait avec une augmentation de la température de polymérisation et en concentration initiale de trioxane. Ainsi, cette quantité résultait d'un équilibre entre la formation et la consommation du tétraoxane. Par ailleurs, au cours des premières étapes de la polymérisation du trioxane, la formation d'une quantité appréciable de polymère soluble a été constatée. Conséquemment, la formation de tétraoxane était expliquée sur la base d'une réaction en retour des chaînes en croissance solubles saved dépolymérisation.

Zusammenfassung

Das Verhalten des während der Polymerisation von Trioxan gebildeten Tetroxans wurde kinetisch untersucht. Bei der Polymerisation von Trioxan wurde für die Bildung von methanolunlöslichem Polymeren eine kurze Induktionsperiode beobachtet, während der, je nach den Reaktionsbedingungen, eine gewisse Menge Tetroxan gebildet wurde. Diese Menge war von der Anfangskonzentration an Katalysator unabhängig, nahm jedoch bei Erhöhung der Polymerisationstemperatur und der Anfangskonzentration an Trioxan zu. Diesen Ergebnissen zufolge ist diese Menge durch das Gleichgewicht zwischen der Bildung und dem Verbrauch von Tetroxan bestimmt. Andererseits wurde die Bildung einer nennenswerten Menge eines "löslichen" Polymeren im Frühstadium der Trioxanpolymerisation festgestellt. Demzufolge wurde die Bildung von Tetroxan in Form einer "Rückbeiss"-Reaktion der wachsenden "löslichen" Kette unter Depolymerisation erklärt.

Received May 23, 1967

Prod. No. 120A

Effect of Solvent on the Amount of Tetraoxane Produced in the Solution Polymerization of Trioxane Catalyzed by $\text{BF}_3 \cdot \text{O}(\text{C}_2\text{H}_5)_2$

T. MIKI, T. HIGASHIMURA, and S. OKAMURA,

Department of Polymer Chemistry, Kyoto University, Kyoto, Japan

Synopsis

The amounts of tetraoxane produced in the polymerization of trioxane catalyzed by $\text{BF}_3 \cdot \text{O}(\text{C}_2\text{H}_5)_2$ were measured in various solvents. The maximum amount of tetraoxane produced depends on the nature of solvent used. This amount was independent of the initial concentration of the catalyst in ethylene dichloride and in nitrobenzene. On the other hand, in benzene, the amount of tetraoxane produced decreased slightly with increasing initial catalyst concentration. This result was explained by the reaction of tetraoxane produced with the residual catalyst as well as with the active center. The maximum amount of tetraoxane produced decreased, other conditions being similar, in the order, nitrobenzene > ethylene dichloride > benzene solvent. This order may be explained in terms of a longer lifetime of the active center in the more polar solvent, leading to the formation of tetraoxane.

INTRODUCTION

In the preceding paper,¹ it was found that a certain amount of tetraoxane is produced in the polymerization of trioxane in ethylene dichloride before the formation of methanol-insoluble polymer. The amount of tetraoxane is determined by an equilibrium between the formation and consumption of tetraoxane during the trioxane polymerization and increases with increasing polymerization temperature and initial trioxane concentration, but is independent of the initial catalyst concentration. Also, the addition of tetraoxane to the polymerization system of trioxane shortens the induction period for the methanol-insoluble polymer formation.

In this paper, the amounts of tetraoxane produced in the trioxane polymerizations with a less polar solvent, (benzene) and a more polar solvent (nitrobenzene) than ethylene dichloride, are measured and compared with the results obtained in ethylene dichloride.¹

The maximum amount of tetraoxane produced in the solution polymerization of trioxane catalyzed by $\text{BF}_3 \cdot \text{O}(\text{C}_2\text{H}_5)_2$ depends on a solvent used. This result may be explained in terms of the lifetime of the active center leading to the formation of tetraoxane.

The experimental procedures were the same as described in the preceding paper.¹

RESULTS AND DISCUSSION

The amount of tetraoxane produced in the polymerization of trioxane was measured in various solvents with $\text{BF}_3 \cdot \text{O}(\text{C}_2\text{H}_5)_2$ as a catalyst at 30°C . except in a particular case.

Effect of Catalyst Concentration

The effect of the initial catalyst concentration $[\text{C}]_0$ on the amount of tetraoxane (TeX) produced in the polymerization of trioxane (ToX) in benzene and in nitrobenzene are shown in Figures 1 and 2, respectively.

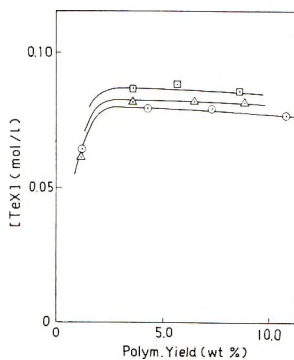


Fig. 1. Effect of the initial catalyst concentration $[\text{C}]_0$ on the amount of tetraoxane produced in the polymerization of trioxane catalyzed by $\text{BF}_3 \cdot \text{O}(\text{C}_2\text{H}_5)_2$ in benzene at 30°C .: (O) $[\text{C}]_0 = 20$ mmole/l.; (Δ) $[\text{C}]_0 = 10$ mmole/l.; (\square) 5 mmole/l. $[\text{ToX}]_0 = 3.27$ mole/l.; $[\text{H}_2\text{O}]_0 = 1.9$ mmole/l.

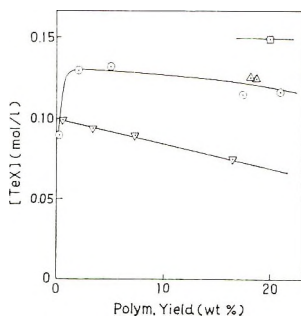


Fig. 2. Effect of the initial catalyst and trioxane concentrations and of the polymerization temperature on the amount of tetraoxane produced in the polymerization of trioxane catalyzed by $\text{BF}_3 \cdot \text{O}(\text{C}_2\text{H}_5)_2$ in nitrobenzene at $[\text{H}_2\text{O}]_0 = \text{ca. } 2$ mmole/l.: (\square) $[\text{ToX}]_0 = 3.17$ mole/l., $[\text{C}]_0 = 1.0$ mmole/l., 50°C .; (O) $[\text{ToX}]_0 = 3.17$ mole/l.; $[\text{C}]_0 = 1.0$ mmole/l., 30°C .; (Δ) $[\text{ToX}]_0 = 3.17$ mole/l., $[\text{C}]_0 = 10$ mmole/l., 30°C .; (∇) $[\text{ToX}]_0 = 1.08$ mole/l., $[\text{C}]_0 = 10$ mmole/l., 30°C .

The amount of tetraoxane produced seems to be independent of the initial catalyst concentration in nitrobenzene, as is the case with ethylene dichloride as solvent.¹ However, the amount of tetraoxane produced in

benzene depends on the initial concentration of catalyst and decreases slightly with increasing initial catalyst concentration.

The latter fact may be explained in terms of the reaction of tetraoxane with residual catalyst. The equilibrium concentration of tetraoxane in the trioxane polymerization is established when the rate of formation of tetraoxane becomes equal to the rate of consumption of tetraoxane. The formation of tetraoxane is due to the back-biting reaction of the active center, p^* , with depolymerization; the formation rate is expressed as eq. (1):

$$d[\text{TeX}]/dt = k_{-p}[p^*] \quad (1)$$

where k_{-p} is the rate constant of formation of tetraoxane by depolymerization. As for the consumption of tetraoxane, the reaction of tetraoxane with residual catalyst must not be neglected as well as the reaction of tetraoxane with active centers, because the reactivity of tetraoxane with p^* is not so large in benzene as in ethylene dichloride or nitrobenzene. Then the consumption rate of tetraoxane in benzene is expressed as eq. (2),

$$-d[\text{TeX}]/dt = (k_p/f)[p^*][\text{TeX}] + (k_i/f)[C][\text{TeX}] \quad (2)$$

where k_p is the rate constant of the reaction between p^* and tetraoxane, k_i is the rate constant of the reaction between the catalyst and tetraoxane, and f is the retarding factor depending on the trioxane concentration.¹ When the equilibrium is established, eq. (3) is obtained by setting eq. (1) equal to eq. (2).

$$\begin{aligned} k_{-p}[p^*] &= \{ (k_p/f)[p^*] + (k_i/f)[C] \} [\text{TeX}]_{\text{eq}} \\ [\text{TeX}]_{\text{eq}} &= f \{ k_{-p} / (k_p + k_i[C]/[p^*]) \} \end{aligned} \quad (3)$$

In the polymerization of trioxane catalyzed by $\text{BF}_3 \cdot \text{O}(\text{C}_2\text{H}_5)_2$ in benzene, the rate of formation of the methanol-insoluble polymer is increased by the addition of a small amount of water, and it was concluded that the polymerization of trioxane catalyzed by $\text{BF}_3 \cdot \text{O}(\text{C}_2\text{H}_5)_2$ in benzene does not occur in the absence of water.² Consequently the concentration of active centers $[p^*]$ is not proportional to the initial concentration of $\text{BF}_3 \cdot \text{O}(\text{C}_2\text{H}_5)_2$ at a fixed concentration of water. So the value of $[C]/[p^*]$ on establishment of equilibrium increases with increasing initial catalyst concentration at a fixed concentration of water. Thus $[\text{TeX}]_{\text{eq}}$ decreases with an increase in the initial concentration of catalyst, as is shown in Figure 1.

Effect of Polymerization Temperature

The effect of the polymerization temperature on the amount of tetraoxane was investigated. Figures 2 and 3 show the results in nitrobenzene and in benzene, respectively. In nitrobenzene the maximum amount of tetraoxane produced was larger at a higher polymerization temperature. In benzene the amount of tetraoxane produced also increased with increas-

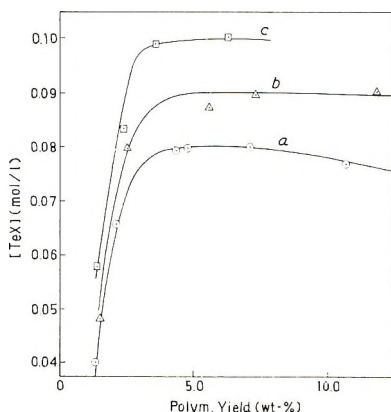


Fig. 3. Effect of the polymerization temperature on the amount of tetraoxane produced in the polymerization of trioxane catalyzed by $\text{BF}_3 \cdot \text{O}(\text{C}_2\text{H}_5)_2$ in benzene: (a) 30°C .; (b) 40°C .; (c) 50°C . $[\text{ToX}]_0 = 3.11$ mole/l.; $[\text{H}_2\text{O}]_0 = 1.3$ mmole/l.; $[\text{C}]_0 = 20$ mmole/l.

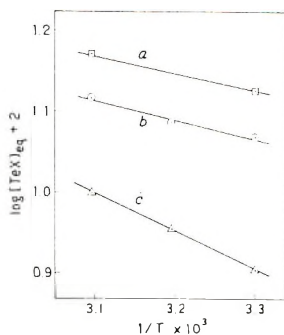


Fig. 4. Temperature coefficients of the equilibrium concentrations of tetraoxane during the polymerization of trioxane catalyzed by $\text{BF}_3 \cdot \text{O}(\text{C}_2\text{H}_5)_2$ in various solvents: (a) nitrobenzene, $[\text{C}]_0 = 1.0$ mmole/l.; (b) ethylene dichloride, $[\text{C}]_0 = 10$ mmole/l.; (c) benzene, $[\text{C}]_0 = 10$ mmole/l., $[\text{ToX}]_0 = 3.2$ mole/l.

ing polymerization temperature. Figure 4 shows the temperature coefficient of $[\text{TeX}]_{\text{eq}}$ in various solvents. As is clear from Figure 4, the value of the slope decreases in the order, benzene $>$ ethylene dichloride \approx nitrobenzene.

The equilibrium concentration of tetraoxane in the trioxane polymerization is expressed by eq. (3). In nitrobenzene and ethylene dichloride, the second term $[\text{C}]/[\text{p}^*]$, of the denominator of the right side in eq. (3) should be constant, because the equilibrium concentration of tetraoxane is independent of the catalyst concentration. This fact agrees with the result that $\text{BF}_3 \cdot \text{O}(\text{C}_2\text{H}_5)_2$ can initiate the polymerization of trioxane without water in a polar solvent.² Therefore, $[\text{TeX}]_{\text{eq}}$ depends primarily on the value of k_{-p}/k_p . Then $\log [\text{TeX}]_{\text{eq}}$ is approximately proportional to $1/T$ with $-(E_{-p} - E_p)/R$ as a proportionality constant. From the experimen-

tal results, it is concluded that the difference in activation energy between the depolymerization and polymerization with respect to tetraoxane during the trioxane polymerization, ($E_{-p} - E_p$), is similar in ethylene dichloride and nitrobenzene solvents. On the other hand, the larger temperature coefficient in benzene can be explained in terms of an additional decrease in $[C]/[p^*]$ with an increase in the polymerization temperature, because $[p^*]$ increases and then $[C]$ decreases with increasing polymerization temperature at a fixed initial concentration of catalyst ($[C]_0 = [C] + [p^*]$).

Effect of Trioxane Concentration

The effect of the initial trioxane concentration on the amount of tetraoxane produced in the trioxane polymerization was investigated. The result in nitrobenzene is shown in Figure 2. Figure 5 shows the equilibrium concentration of tetraoxane during the trioxane polymerization at various

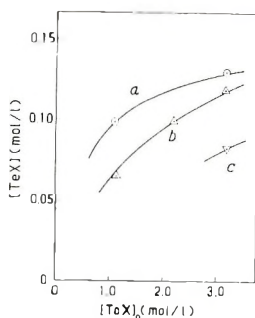
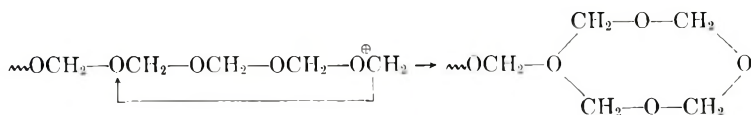


Fig. 5. Dependence of the equilibrium concentration of tetraoxane on the initial trioxane concentration in the polymerization of trioxane catalyzed by $\text{BF}_3 \cdot \text{O}(\text{C}_2\text{H}_5)_2$ in various solvents at 30°C .: (a) nitrobenzene; (b) ethylene dichloride; (c) benzene. $[C]_0 = 10$ mmole/l.

initial trioxane concentrations in various solvents. Clearly from Figure 5, the equilibrium concentration of tetraoxane at a fixed initial concentration of trioxane decreases in the order, nitrobenzene $>$ ethylene dichloride $>$ benzene. This order may be due to a higher value of k_{-p}/k_p and/or by a higher value of f in eq. (3) in the polar solvent. The higher value of k_{-p}/k_p in the polar solvent can be explained in terms of stabilization of the active center with solvent. The active center leading to the formation of the tetraoxane oxonium ion by the back-biting is a carbonium ion,³ as is shown in eq. (4).



The carbonium active center may be stabilized more strongly with the more polar solvent and the lifetime of the active center may be prolonged. The

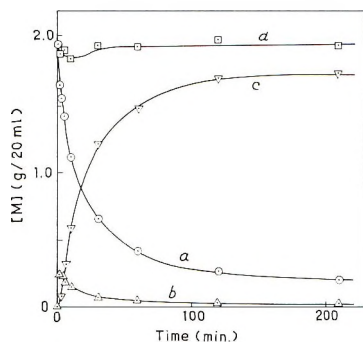


Fig. 6. Change in the concentration (in grams/20 ml.) of each component with the reaction time in the polymerization of trioxane catalyzed by $\text{BF}_3 \cdot \text{O}(\text{C}_2\text{H}_5)_2$ in nitrobenzene at 30°C .: (a) consumption of trioxane; (b) formation of tetraoxane; (c) formation of methanol-insoluble polymer; (d) $a + b + c$. $[\text{ToX}]_0 = 1.08$ mole/l.; $[\text{H}_2\text{O}]_0 = 1.7$ mmole/l.; $[\text{C}]_0 = 10$ mmole/l.

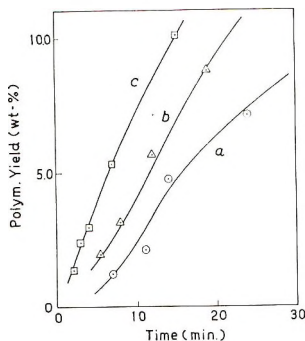


Fig. 7. Effect of the addition of tetraoxane on the formation of the methanol-insoluble polymer in the polymerization of trioxane catalyzed by $\text{BF}_3 \cdot \text{O}(\text{C}_2\text{H}_5)_2$ in benzene at 30°C .: (a) no TeX added; (b) $[\text{TeX}] = 0.095$ mole/l.; (c) $[\text{TeX}] = 0.188$ mole/l. $[\text{ToX}]_0 = 3.17$ mole/l.; $[\text{H}_2\text{O}]_0 = 1.3$ mmole/l.; $[\text{C}]_0 = 20$ mmole/l.

formation of tetraoxane by back-biting thus occurs with ease in the more polar solvent. The effects of the f factor is not clear at present.

Figure 6 shows the result of the trioxane polymerization in nitrobenzene at initial trioxane and catalyst concentrations of 1.11 mole/l. and 10 mmole/l., respectively, at 30°C . In the trioxane polymerization in ethylene dichloride under similar conditions, as shown in Figure 7 of the preceding paper,¹ tetraoxane produced in the early stage remained, and the induction period for the methanol-insoluble polymer was rather large (about 20 min.). However, in the trioxane polymerization in nitrobenzene, a certain amount of tetraoxane was produced instantly and tetraoxane immediately began to be consumed. An induction period for formation of the methanol-insoluble polymer was not observed. This fact supports strongly the conclusion drawn in the preceding paper¹ that the induction period for the methanol-insoluble polymer formation is related to the forma-

tion of tetraoxane and that the disappearance of tetraoxane observed in the later stages is caused by the formation of the polymer crystals on whose surface the polymerization proceeds, suppressing the back-biting reaction.

As is seen also in Figure 6, the material balance is incomplete in the early stage; this suggests the formation of the methanol-soluble polymer. The material balance is, however, completed in the later stage of polymerization (after 30 min.), and then the amount of tetraoxane is very small. This fact gives strong support to the conclusion drawn that the "soluble" growing chain grows to form the polymer crystal, that the formation of tetraoxane is due mainly to the back-biting of the "soluble" growing chain, and that the growing chain on the crystal surface has very little ability to participate in the back-biting reaction.

Effect of Addition of Tetraoxane

In the polymerization of trioxane in nitrobenzene, tetraoxane was produced immediately and no induction period for the methanol-insoluble polymer formation was observed if the water concentration in the reaction system was small, while addition of water brought about an appearance of the induction period.² In the polymerization of trioxane in ethylene dichloride a short induction period was observed under the conditions used, and during this period a certain amount of tetraoxane was produced. The addition of tetraoxane to the trioxane-(CH₂Cl)₂ polymerization system caused shortening of the induction period for formation of the methanol-insoluble polymer.¹

The effect of the addition of tetraoxane on the induction period for the methanol-insoluble polymer formation was investigated also in the trioxane polymerization in benzene. Figure 7 shows time versus yield of methanol-insoluble polymer and Figure 8 shows the change in the concen-

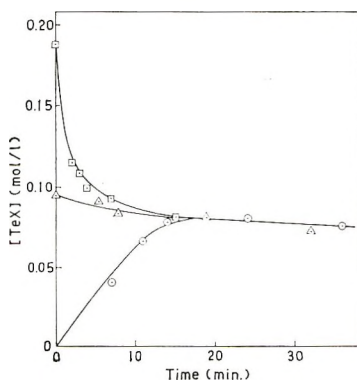


Fig. 8. Change in the tetraoxane concentration in the copolymerization of trioxane with tetraoxane catalyzed by $\text{BF}_3 \cdot \text{O}(\text{C}_2\text{H}_5)_2$ in benzene at 30°C .: (a) no TeX added; (b) $[\text{TeX}] = 0.095$ mole/l.; (c) $[\text{TeX}] = 0.188$ mole/l. $[\text{ToX}]_0 = 3.17$ mole/l.; $[\text{H}_2\text{O}]_0 = 1.3$ mmole/l.; $[\text{C}]_0 = 20$ mmole/l.

tration of tetraoxane with reaction time. It is evident from Figure 7 that the induction period was shortened on addition of tetraoxane. This may be due to the suppression by added tetraoxane of the formation of tetraoxane by depolymerization from the active center. On the other hand, the concentrations of tetraoxane in the various reaction systems were limited to a certain value, as observed with ethylene dichloride.¹

It is concluded that the kinetic behavior of tetraoxane produced in the polymerization of trioxane differs widely, depending on the nature of the solvent used.

References

1. T. Miki, T. Higashimura, and S. Okamura, *J. Polymer Sci. A-1*, **5**, 2977 (1967).
2. T. Higashimura, T. Miki, and S. Okamura, *Bull. Chem. Soc. Japan*, **38**, 2067 (1965).
3. T. Miki, T. Higashimura, and S. Okamura, *J. Polymer Sci. A-1*, **5**, 95 (1967).

Résumé

Les quantités de tétraoxane produit en cours de polymérisation du trioxane catalysée par $\text{BF}_3 \cdot \text{O}(\text{C}_2\text{H}_5)_2$ ont été mesurées dans différents solvants. La quantité maximum de tétraoxane produit dépend de la nature du solvant utilisé. Cette quantité est indépendante de la concentration initiale en catalyseur dans le dichloroéthylène et dans le nitrobenzène. Par ailleurs, dans le benzène la quantité de tétraoxane produit décroît faiblement avec une augmentation de concentration initiale en catalyseur. Ce résultat est expliqué par la réaction de tétraoxane produit avec le catalyseur résiduel aussi bien qu'avec le centre actif. La quantité maximum de tétraoxane produit décroissait dans des conditions semblables dans l'ordre nitrobenzène > dichlorure d'éthylène > benzène. Cet ordre peut être expliqué sur la base d'une durée de vie plus longue du centre actif amenant à la formation de tétraoxane dans les solvants les plus polaires.

Zusammenfassung

Die Tetroxanmengen, die bei der durch $\text{BF}_3 \cdot \text{O}(\text{C}_2\text{H}_5)_2$ katalysierten Trioxanpolymerisation gebildet werden, wurden in verschiedenen Lösungsmitteln bestimmt. Die maximal gebildete Tetroxanmenge hängt von der Natur des verwendeten Lösungsmittels ab. Diese Menge war in Äthylendichlorid und in Nitrobenzol von der Anfangskonzentration an Katalysator unabhängig. Andererseits nahm die Menge an gebildetem Tetroxan in Benzol geringfügig bei Erhöhung der Anfangskonzentration des Katalysators ab. Dieses Ergebnis wurde durch die Reaktion des gebildeten Tetroxans mit dem restlichen Katalysator sowie mit aktiven Zentren erklärt. Die maximal gebildete Menge an Tetroxan nahm unter sonst ähnlichen Bedingungen in der Reihenfolge der Lösungsmittel Nitrobenzol > Äthylendichlorid > Benzol ab. Diese Reihenfolge lässt sich vermittels einer längeren Lebensdauer der zur Bildung von Tetroxan führenden aktiven Zentren in stärker polaren Lösungsmitteln erklären.

Received May 23, 1967

Prod. No. 121A

Polymerization of Tetraoxane at Low Concentration Catalyzed by $\text{BF}_3 \cdot \text{O}(\text{C}_2\text{H}_5)_2$

T. MIKI, T. HIGASHIMURA, and S. OKAMURA,
Department of Polymer Chemistry, Kyoto University, Kyoto, Japan

Synopsis

In the solution polymerization of tetraoxane catalyzed by $\text{BF}_3 \cdot \text{O}(\text{C}_2\text{H}_5)_2$, trioxane and methanol-insoluble polymer were produced. However, the amounts of these products depend on the nature of solvent used. A critical concentration of tetraoxane is observed for the formation of methanol-insoluble polymer; at less than this critical concentration of tetraoxane no methanol-insoluble polymer is obtained, but trioxane is preferentially produced. This critical concentration of tetraoxane is higher in a more polar solvent, so the amount of methanol-insoluble polymer produced decreases and the amount of trioxane produced increases with increasing the polarity of solvent used. These results may be explained in terms of a stabilization of the active center leading to formation of trioxane by a solvation with solvent.

INTRODUCTION

The formation of tetraoxane during the polymerization of trioxane and the larger cationic reactivity of tetraoxane than trioxane have been already observed.¹ The kinetic behavior of tetraoxane produced during the polymerization of trioxane has also been investigated.^{2,3} In this paper, the polymerization of tetraoxane was carried out in various solvents to get more precise information on the kinetic behavior of tetraoxane produced during the trioxane polymerization.

In the polymerization of tetraoxane, trioxane and methanol-insoluble polymer were produced, but these amounts depended strongly on the initial concentration of tetraoxane and on the nature of solvent used. A critical concentration of tetraoxane was observed under which trioxane was produced exclusively, no methanol-insoluble polymer being found. This critical concentration of tetraoxane was higher in a more polar solvent, so the amount of methanol-insoluble polymer produced decreased with increasing the polarity of solvent used, at low initial tetraoxane concentration.

The procedures of polymerization were the same as described in the previous papers.^{2,3}

RESULTS

The polymerization of tetraoxane (TeX) was carried out at various initial concentrations of tetraoxane and in various solvents with $\text{BF}_3 \cdot \text{O}$ -

$(C_2H_5)_2$ as a catalyst at $30^\circ C$. The initial catalyst concentration was 10 mmole/l. in all cases.

Polymerization of Tetraoxane in Nitrobenzene

The results of the polymerization of tetraoxane at various initial concentrations of tetraoxane are shown in Figures 1-3. As is seen in Figures 1-3, tetraoxane was immediately consumed and trioxane was formed.

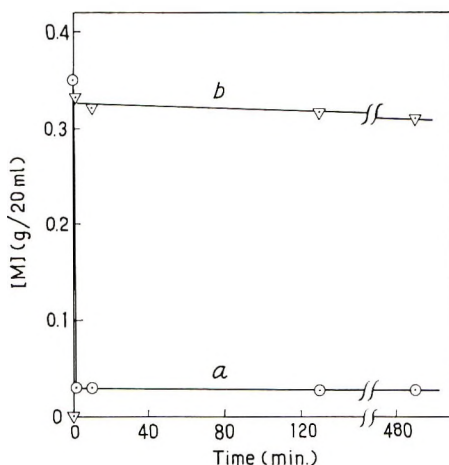


Fig. 1. Change in the concentration (in grams/20 ml.) of each component with reaction time in the polymerization of tetraoxane catalyzed by $BF_3 \cdot O(C_2H_5)_2$ in nitrobenzene at $30^\circ C$.: (a) consumption of tetraoxane; (b) formation of trioxane. $[TeX]_0 = 0.146$ mole/l.; $[BF_3 \cdot O(C_2H_5)_2]_0 = 10$ mmole/l.

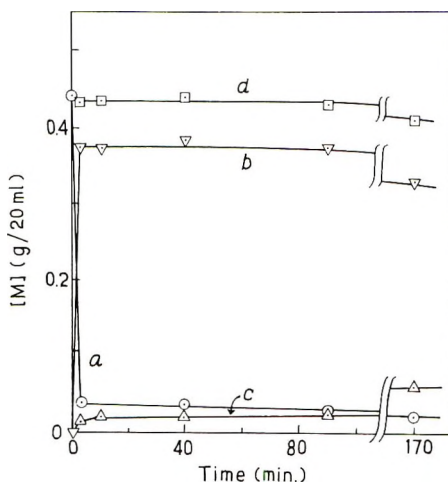


Fig. 2. Change in the concentration (in grams/20 ml.) of each component with reaction time in the polymerization of tetraoxane catalyzed by $BF_3 \cdot O(C_2H_5)_2$ in nitrobenzene at $30^\circ C$.: (a) consumption of tetraoxane; (b) formation of trioxane; (c) formation of methanol-insoluble polymer; (d) $a + b + c$. $[TeX]_0 = 0.183$ mole/l.; $[BF_3 \cdot O(C_2H_5)_2]_0 = 10$ mmole/l.

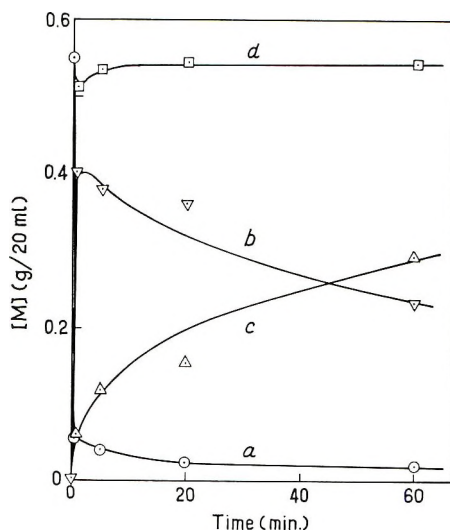


Fig. 3. Change in the concentration (in grams/20 ml.) of each component with reaction time in the polymerization of tetraoxane catalyzed by $\text{BF}_3 \cdot \text{O}(\text{C}_2\text{H}_5)_2$ in nitrobenzene at 30°C .: (a), (b), (c), (d) as in Fig. 2. $[\text{TeX}]_0 = 0.230$ mole/l.; $[\text{BF}_3 \cdot \text{O}(\text{C}_2\text{H}_5)_2]_0 = 10$ mmole/l.

At an initial tetraoxane concentration of 0.146 mole/l., no methanol-insoluble polymer was obtained during the time investigated, as is shown in Figure 1. At an initial tetraoxane concentration of 0.230 mole/l., an appreciable amount of methanol-insoluble polymer was obtained. In this case, however, trioxane (ToX) produced was gradually consumed as the amount of methanol-insoluble polymer increased, as is shown in Figure 3. At an initial tetraoxane concentration of 0.183 mole/l., the amount of the methanol-insoluble polymer produced was small, and the trioxane produced was slowly consumed, as is shown in Figure 2.

Polymerization of Tetraoxane in Ethylene Dichloride

The results of the polymerization of tetraoxane at various initial concentrations of tetraoxane are shown in Figures 4–6. At an initial tetraoxane concentration of 0.100 mole/l., no methanol-insoluble polymer was obtained (Fig. 4). At an initial tetraoxane concentration of 0.146 mole/l., an appreciable amount of the methanol-insoluble polymer was obtained (Fig. 6). However, it is evident that trioxane was formed in large quantities (in comparison with methanol-insoluble polymer).

Polymerization of Tetraoxane in Benzene

The results of the polymerization of tetraoxane at various initial concentrations of tetraoxane are shown in Figures 7–9. Trioxane was formed in all cases. Methanol-insoluble polymer was, however, obtained at initial tetraoxane concentrations of 0.146 and 0.065 mole/l. and was not obtained at 0.038 and 0.025 mole/l.

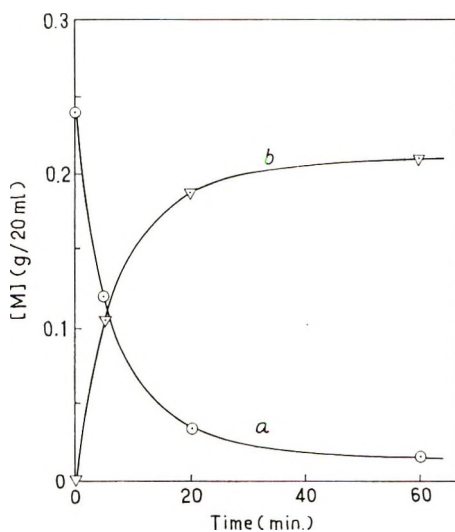


Fig. 4. Change in the concentration (in grams/20 ml.) of each component with reaction time in the polymerization of tetraoxane catalyzed by $\text{BF}_3 \cdot \text{O}(\text{C}_2\text{H}_5)_2$ in ethylene dichloride at 30°C .: (a), (b) as in Fig. 1. $[\text{TeX}]_0 = 0.100$ mole/l.; $[\text{BF}_3 \cdot \text{O}(\text{C}_2\text{H}_5)_2]_0 = 10$ mmole/l.

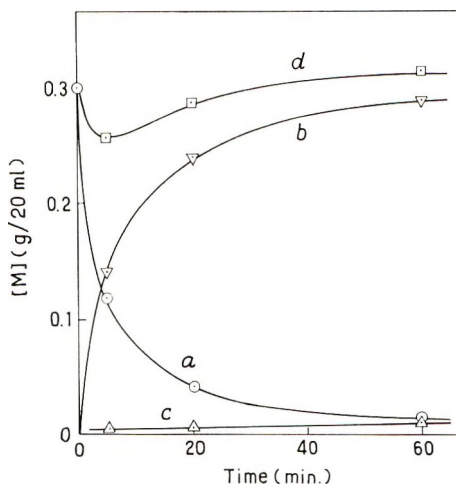


Fig. 5. Change in the concentration (in grams/20 ml.) of each component with reaction time in the polymerization of tetraoxane catalyzed by $\text{BF}_3 \cdot \text{O}(\text{C}_2\text{H}_5)_2$ in ethylene dichloride at 30°C .: (a), (b), (c), (d) as in Fig. 2. $[\text{TeX}]_0 = 0.125$ mole/l.; $[\text{BF}_3 \cdot \text{O}(\text{C}_2\text{H}_5)_2]_0 = 10$ mmole/l.

Effect of the Addition of Trioxane

The effect of the addition of trioxane (ToX) on the polymerization of tetraoxane in ethylene dichloride is shown in Figures 10 and 11. As is seen in Figure 10, tetraoxane was consumed and the amount of trioxane increased with the reaction time; no methanol-insoluble polymer was ob-

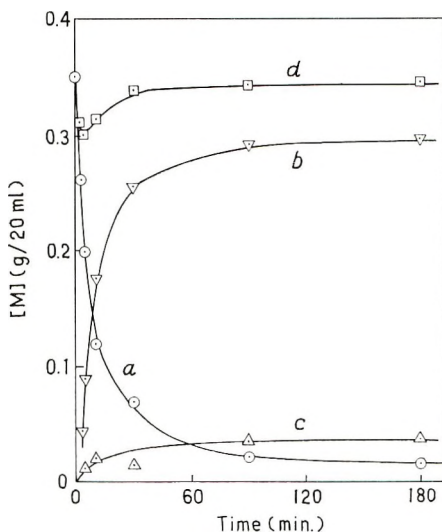


Fig. 6. Change in the concentration (in grams/20 ml.) of each component with reaction time in the polymerization of tetraoxane catalyzed by $\text{BF}_3 \cdot \text{O}(\text{C}_2\text{H}_5)_2$ in ethylene dichloride at 30°C .: (a), (b), (c), (d) as in Fig. 2. $[\text{TeX}]_0 = 0.146$ mole/l.; $[\text{BF}_3 \cdot \text{O}(\text{C}_2\text{H}_5)_2]_0 = 10$ mmole/l.

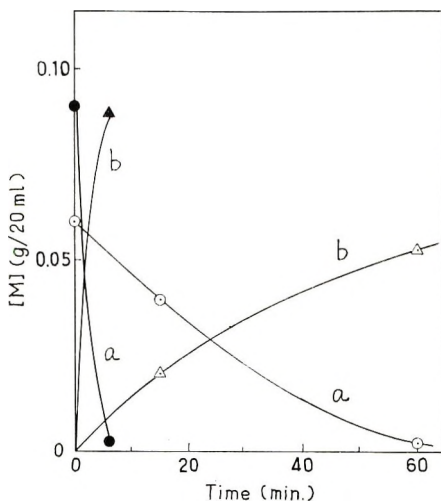


Fig. 7. Change in the concentration (in grams/20 ml.) of each component with reaction time in the polymerization of tetraoxane catalyzed by $\text{BF}_3 \cdot \text{O}(\text{C}_2\text{H}_5)_2$ in benzene at 30°C . with (●) $[\text{TeX}]_0 = 0.038$ mole/l. and (○) $[\text{TeX}]_0 = 0.025$ mole/l.: (a), (b) as in Fig. 1. $[\text{BF}_3 \cdot \text{O}(\text{C}_2\text{H}_5)_2]_0 = 10$ mmole/l.

tained during the reaction time investigated. In this case, however, both the rate of consumption of tetraoxane and the rate of formation of trioxane were smaller than the corresponding rates in the polymerization of tetraoxane without the addition of trioxane, as is seen in comparing Figure 10 with Figure 4. On the other hand, when the concentration of trioxane

added was large, methanol-insoluble polymer was obtained, and the amount of trioxane increased to a maximum and then decreased with the reaction time, as is shown in Figure 11.

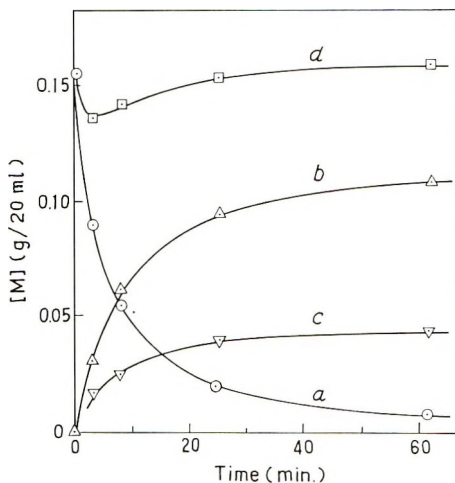


Fig. 8. Change in the concentration (in grams/20 ml.) of each component with reaction time in the polymerization of tetraoxane catalyzed by $\text{BF}_3 \cdot \text{O}(\text{C}_2\text{H}_5)_2$ in benzene at 30°C .: (a), (b), (c), (d) as in Fig. 2. $[\text{TeX}]_0 = 0.065$ mole/l.; $[\text{BF}_3 \cdot \text{O}(\text{C}_2\text{H}_5)_2]_0 = 10$ mmole/l.

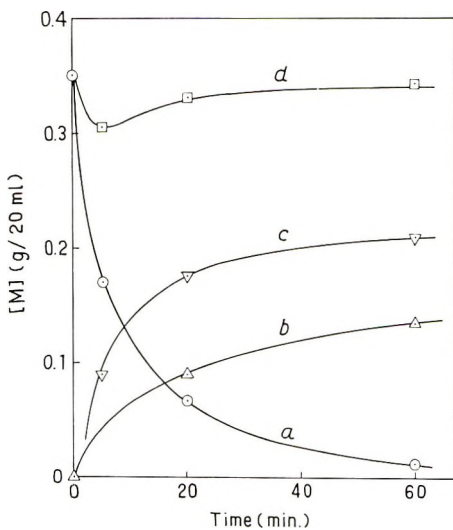


Fig. 9. Change in the concentration (in grams/20 ml.) of each component with reaction time in the polymerization of tetraoxane catalyzed by $\text{BF}_3 \cdot \text{O}(\text{C}_2\text{H}_5)_2$ in benzene at 30°C .: (a), (b), (c), (d) as in Fig. 2. $[\text{TeX}]_0 = 0.146$ mole/l.; $[\text{BF}_3 \cdot \text{O}(\text{C}_2\text{H}_5)_2]_0 = 10$ mmole/l.

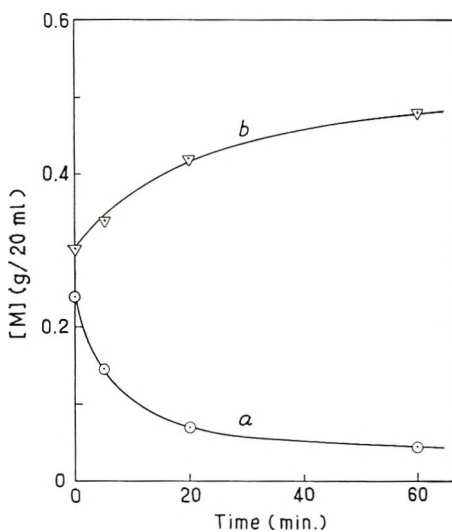


Fig. 10. Change in the concentration (in grams/20 ml.) of each component with reaction time in the polymerization of tetraoxane and trioxane catalyzed by $\text{BF}_3 \cdot \text{O}(\text{C}_2\text{H}_5)_2$ in ethylene dichloride at 30°C .: (a) concentration of tetraoxane; (b) concentration of trioxane. $[\text{TeX}]_0 = 0.100$ mole/l.; $[\text{ToX}] = 0.167$ mole/l.; $[\text{BF}_3 \cdot \text{O}(\text{C}_2\text{H}_5)_2]_0 = 10$ mmole/l.

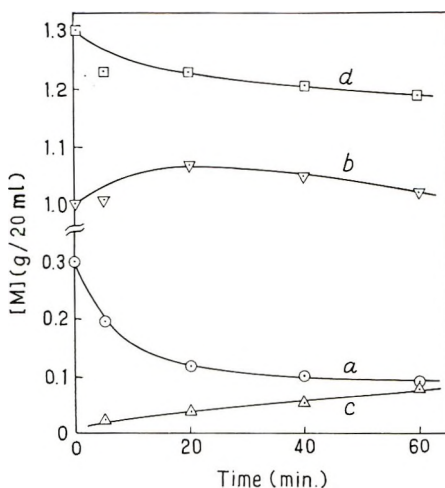


Fig. 11. Change in the concentration (in grams/20 ml.) of each component with reaction time in the polymerization of tetraoxane and trioxane catalyzed by $\text{BF}_3 \cdot \text{O}(\text{C}_2\text{H}_5)_2$ in ethylene dichloride at 30°C .: (a), (b), (c), (d) as in Fig. 2. $[\text{TeX}]_0 = 0.125$ mole/l., $[\text{ToX}]_0 = 0.555$ mole/l.; $[\text{BF}_3 \cdot \text{O}(\text{C}_2\text{H}_5)_2]_0 = 10$ mmole/l.

DISCUSSION

The formation of methanol-insoluble polymer and trioxane was observed in the homopolymerization of tetraoxane catalyzed by $\text{BF}_3 \cdot \text{O}(\text{C}_2\text{H}_5)_2$ in ethylene dichloride,¹ but the amounts of methanol-insoluble polymer and

TABLE I
 Conversions of Tetraoxane (TeX) to Methanol-Insoluble Polymer (P)
 and to Trioxane (ToX) in the Polymerization of Tetraoxane in Various Solvents^a

[TeX] ₀ , mole/l.	Nitrobenzene		Ethylene dichloride		Benzene	
	Conversion to P, wt.-%	Conversion to ToX, wt.-%	Conversion to P, wt.-%	Conversion to ToX, wt.-%	Conversion to P, wt.-%	Conversion to ToX, wt.-%
0.230	52.7	41.8	—	—	—	—
0.183	5.7	85.3	—	—	—	—
0.146	0	91.5	8.6	80.0	60.0	38.6
0.125	—	—	3.3	96.5	—	—
0.100	—	—	0	87.5	48.2 ^b	43.7 ^b
0.065	—	—	—	—	27.7	71.0
0.038	—	—	—	—	0	98.0

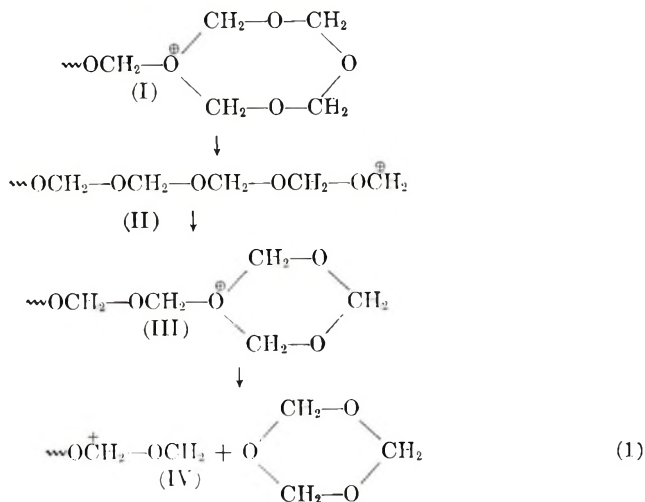
^a Reaction time, 60 min.; [BF₃·O(C₂H₅)₂]₀ = 10 mmole/l.; 30°C.

^b [TeX]₀ = 0.112 mole/l.

trioxane produced in the homopolymerization of tetraoxane were found to depend markedly on the initial tetraoxane concentration and on the nature of solvent used. In Table I, the conversions of tetraoxane to methanol-insoluble polymer and to trioxane at various initial tetraoxane concentrations are summarized in various solvents at a reaction time of 60 min. It is obvious from Table I that a "critical" concentration of tetraoxane for the formation of methanol-insoluble polymer exists and that this critical concentration of tetraoxane is higher in a more polar solvent, as is denoted by the horizontal staggered line in Table I. At an initial tetraoxane concentration lower than the critical concentration, methanol-insoluble polymer was not obtained, but trioxane was produced. This fact shows that tetraoxane reacts with catalyst even when the methanol-insoluble polymer is not obtained.

Because of a higher "critical" concentration of tetraoxane for the formation of methanol-insoluble polymer in a more polar solvent, the amount of methanol-insoluble polymer produced in the polymerization of tetraoxane decreased with increasing polarity of solvent used within the initial tetraoxane concentration investigated in this paper. However, the initial rate of formation of trioxane was larger in a more polar solvent. These results can be explained in terms of the lifetime of the growing chain end leading to the formation of trioxane.

The smaller rate of formation of methanol-insoluble polymer in a more polar solvent has been also observed in the homopolymerization of trioxane at a rather low concentration of trioxane, catalyzed by $\text{BF}_3 \cdot \text{O}(\text{C}_2\text{H}_5)_2$;⁴ an attempt was made to explain this phenomenon in terms of the selective solvation of the growing chain end with solvent rather than with trioxane. On the other hand, the formation of trioxane produced in the polymerization of tetraoxane may be explained in terms of the back-biting reaction of growing chain end (II) with depolymerization,¹ as is shown in eqs. (1) where the counterion was omitted for convenience.



According to eqs. (1), a chain end (II) is necessarily formed for the production of trioxane through the formation of the chain end (III), even though the chain end (II) may be partly consumed for the propagation by attack of tetraoxane. The chain end (II) may be formed with ease in a more polar solvent because it is stabilized by solvation with the solvent. Therefore, in a more polar solvent, the formation of trioxane occurs with ease and the formation of methanol-insoluble polymer is retarded.

The relation between the formation of methanol-insoluble polymer and of trioxane in the polymerization of tetraoxane at tetraoxane concentrations higher than the critical concentration for formation of the methanol-insoluble polymer should be noticed. No induction period for the formations of both methanol-insoluble polymer and trioxane was observed. Moreover, trioxane continued to form even after the formation of methanol-insoluble polymer in ethylene dichloride and benzene, as is seen in Figures 6 and 9. In nitrobenzene this phenomenon was not clearly observed because of the rapid disappearance of tetraoxane. The phenomenon in the tetraoxane polymerization in ethylene dichloride and benzene is different from the relation between the formation of tetraoxane and of methanol-insoluble polymer in the polymerization of trioxane. In the latter case, a short induction period was observed, and the amount of tetraoxane produced did not increase after the formation of methanol-insoluble polymer.^{2,3} The continued formation of trioxane after the formation of methanol-insoluble polymer in the tetraoxane polymerization may be due to the low reactivity of the trioxane with the active center, so that the trioxane may be consumed with difficulty.

The effect of the low reactivity of trioxane was also observed. Even when an amount of trioxane larger than that amount of trioxane produced in the homopolymerization of tetraoxane was added to the polymerization of tetraoxane, the amount of trioxane increased, although the initial rate of formation of trioxane was suppressed in comparison with the initial rate of formation of trioxane without added trioxane at a fixed concentration of tetraoxane, as is seen in Figures 10 and 4 and in Figures 11 and 5. Moreover, the initial rate of formation of trioxane was smaller in the larger concentration of trioxane added. Therefore, trioxane added serves as a suppressor for the formation of trioxane during the polymerization of tetraoxane. According to eqs. (1), the formation of trioxane through the third may be suppressed by the existence of trioxane, because trioxane can react with chain end IV to form chain end III. However, because of the low reactivity of trioxane, a large amount of trioxane is necessary to suppress entirely the formation of trioxane by depolymerization from the growing chain.

The kinetic behavior of tetraoxane in cationic polymerization is very interesting. The effect of the polymerization temperature should be necessarily investigated to obtain more precise knowledge of the tetraoxane polymerization. This will be the subject of a future paper.

The authors thank Dr. Y. Miyake in the Research Laboratory of the Tôyô Kô-atsu Co. Ltd. for the generous gift of tetraoxane.

References

1. T. Miki, T. Higashimura, and S. Okamura, *J. Polymer Sci. A-1*, **5**, 95 (1967).
2. T. Miki, T. Higashimura, and S. Okamura, *J. Polymer Sci. A-1*, **5**, 2977 (1967).
3. T. Miki, T. Higashimura, and S. Okamura, *J. Polymer Sci. A-1*, **5**, 2989 (1967).
4. T. Miki, T. Higashimura, and S. Okamura, *Bull. Chem. Soc. Japan*, **39**, 41 (1966).

Résumé

Dans la polymérisation en solution du tétraoxane catalysé par $\text{BF}_3 \cdot \text{O}(\text{C}_2\text{H}_5)_2$, du trioxane et un polymère insoluble dans le méthanol ont été formés. Toutefois, les quantités de ce produit dépendent de la nature du solvant utilisé. On observe une concentration critique de tétraoxane pour la formation du polymère insoluble dans la éthanol; en-dessous de cette concentration critique en tétraoxane, il n'y a pas de formation de polymère insoluble dans le méthanol, mais du tétraoxane est préférentiellement obtenu. Cette concentration critique en tétraoxane, est plus élevée dans un solvant plus polaire, de sorte que la quantité de polymère insoluble dans le méthanol produite décroît et la, quantité de trioxane produit s'accroît avec une augmentation de la polarité du solvant utilisé. Ces résultats peuvent être expliqués sur la base d'une stabilisation des centres actifs amenant à la formation de trioxane par solvatation avec un solvant.

Zusammenfassung

Bei der durch $\text{BF}_3 \cdot \text{O}(\text{C}_2\text{H}_5)_2$ katalysierten Lösungspolymerisation von Tetroxan wurden Trioxan und methanolunlösliches Polymeres gebildet. Die Mengen dieser Produkte hängen jedoch von der Natur des verwendeten Lösungsmittels ab. Für die Bildung von methanolunlöslichem Polymeren wurde eine "kritische" Tetroxankonzentration beobachtet: Unter dieser kritischen Konzentration an Tetroxan tritt kein methanolunlösliches Polymeres auf, sondern es bildet sich bevorzugt Trioxan. Diese kritische Konzentration ist in einem stärker polaren Lösungsmittel höher; daher nimmt die Menge des gebildeten methanolunlöslichen Polymeren mit steigender Polarität des Lösungsmittels ab und die Menge des gebildeten Trioxans zu. Diese Ergebnisse lassen sich in Form einer Stabilisierung des zur Bildung von Trioxan führenden aktiven Zentrums durch Solvatisierung mit dem Lösungsmittel erklären.

Received May 23, 1967
Prod. No. 122A

Di-isotacticity of Poly(methyl Propenyl Ether) and Double-Bond Opening of Methyl Propenyl Ether in Cationic Polymerization

Y. OHSUMI, T. HIGASHIMURA, and S. OKAMURA,
Department of Polymer Chemistry, Kyoto University,
Kyoto, Japan, and R. CHUJO and T. KURODA,
Katata Research Institute, Toyobo Co., Ltd., Katata, Shiga, Japan

Synopsis

The di-isotacticity of poly(methylpropenyl ether) obtained by the cationic polymerization has been studied by NMR spectra. The NMR spectra of β -methyl protons of the polymer are decoupled from the β -methine proton spectra to determine the di-isotactic fraction in a polymer. The signals of β -methyl protons at 8.78 and 8.89 τ are estimated as spectra based on *threo*- and *erythro*-di-isotactic diads, respectively. With $\text{BF}_3 \cdot \text{O}(\text{C}_2\text{H}_5)_2$ as a catalyst, the *trans* monomer yields a crystalline polymer and its structure is *threo*-di-isotactic. Otherwise, *cis* monomer produces an amorphous polymer, and it is a mixture of *threo*- and *erythro*-di-isotactic structure. From these results, it is concluded that the double bond in *trans* monomer is opened exclusively in the *cis* type, and in *cis* monomer *cis*- and *trans*-openings take place at almost the same rate.

INTRODUCTION

It is very important to know the type of double bond opening for the investigation of the propagation reaction in the ionic polymerization of vinyl monomers. Natta et al. have concluded from the di-isotactic structure of a polymer, as observed by x-ray diffraction, that the double bond of monomers opens in a definite type (*cis*) in the cationic polymerization of *trans*-propenyl ethers¹ and *trans*- and *cis*- β -chlorovinyl butyl ether.² However, by x-ray examination, it is impossible to determine quantitatively the steric structure of a polymer and to discuss the type of the opening of a monomer double bond if an amorphous polymer is produced. Thus, in the cationic polymerization, there are no reports dealing with the quantitative treatment of this problem.

On the other hand, in anionic polymerization, the opening of the double bond in the polymerization of α,β -*d*₂-acrylate has been studied by NMR spectra.^{3,4} It has been found that the type of the opening of the double bond is affected by polymerization conditions, e.g., the kind of catalyst, and that the changes in the opening are complicated.

In order to determine quantitatively the type of double-bond opening involved in the cationic polymerization of propenyl ether and to elucidate

the effects of catalyst variation and geometric isomerism of the monomer, the polymerization of methyl propenyl ether was investigated. In this paper is presented the effect of various polymerization conditions on the di-isotacticity of poly(methyl propenyl ether) as determined by NMR measurements.

The double-bond opening by homogeneous catalysts was found for the *trans* monomer to be exclusively of the *cis* type, whereas both *cis*- and *trans*-type opening occurred with the *cis* monomer.

EXPERIMENTAL

Materials

Methyl propenyl ether was synthesized by splitting off of alcohol from dimethyl acetal, the same procedure as that used for preparation of butyl propenyl ether.⁵ The crude product was purified by shaking with dilute sodium hydroxide solution. After drying with calcium chloride, methyl propenyl ether was fractionated by distillation on a column of 45 plates with a reflux ratio of 60:1. The *cis* and *trans* isomers could not be completely separated by the distillation because the boiling points of both isomers are very similar.

Therefore, two kinds of monomer mixtures having different mole ratios of *cis* and *trans* isomers were used, that is, *cis/trans* ratios of 1/9 and 4/1. The *cis* and *trans* contents of the methyl propenyl ether were determined by gas chromatography on a 3-m. dinonyl phthalate column at 40°C., H₂ flow rate of 50 ml./min.

Toluene was washed successively with concentrated sulfuric acid, water, dilute sodium hydroxide solution, and water, and was then dried over calcium chloride and distilled over sodium.

BF₃·O(C₂H₅)₂ and Al(C₂H₅)Cl₂ were distilled before use.

Procedures

Monomer and solvent were introduced into a 100 ml. flask sealed with a rubber cap at a fixed temperature. Catalyst was introduced through the rubber cap with a syringe. After a specified time, polymerization was stopped by addition of methanol and the polymer precipitated from the reaction mixture was washed with methanol and dried *in vacuo* at 40°C.

The NMR spectra of the poly(methyl propenyl ether) were measured in *o*-dichlorobenzene solution (10%, w/v) in a sealed tube at 160°C. with a Varian HR-60 instrument. The spin decoupling was performed by the side-bond method with a phase-sensitive detector operating at 2 kc./sec.

The intrinsic viscosity $[\eta]$ (in deciliters per gram) were measured in benzene at 30°C.

RESULTS AND DISCUSSION

Figure 1 shows the NMR spectra of polymers obtained with $\text{BF}_3 \cdot \text{O}(\text{C}_2\text{H}_5)_2$ at -78°C . The spectrum of β -methyl protons of polymer obtained from a monomer mixture having a high *trans* content (*cis/trans* = 1/9) is clearly different from that of polymer produced from monomer with a high *cis* content (*cis/trans* 4/1); the spectra of the methoxyl protons are also slightly different.

The spectrum of β -methyl protons is changed by the content of geometric isomers in the monomer mixture and the polymerization temperature. Therefore, it is expected that the spectral difference of β -methyl protons is due to the difference in the steric structure of the β -carbon with respect to the adjacent α -carbons, i.e., the di-isotactic structure of the polymer.

To study quantitatively the di-isotactic fractions of a polymer, the NMR spectra of β -methyl protons were decoupled from the β -methine proton. As shown in Figure 2, the spectra of β -methyl protons consist of two signals at 8.78 and 8.89 τ in all polymers. The intensity of 8.78 τ is much stronger than that of 8.89 τ in the polymers obtained from *trans*-rich monomer mixtures. On the other hand, the intensities of the two signals

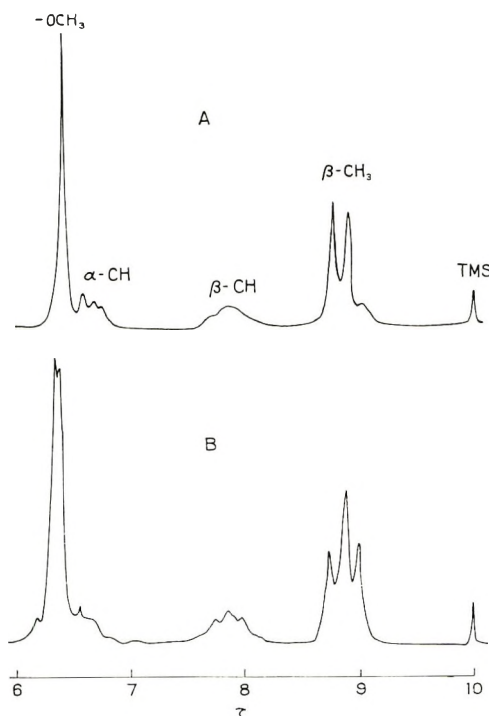


Fig. 1. NMR spectra of poly(methyl propenyl ethers) obtained by $\text{BF}_3 \cdot \text{O}(\text{C}_2\text{H}_5)_2$ in toluene at -78°C .: (A) *cis/trans* ratio in monomer mixture = 1/9; (B) *cis/trans* ratio in monomer mixture = 4/1; $[\text{M}]_0 = 10$ vol.-%, $[\text{C}] = 3$ mmole/l.

are almost the same in polymers obtained from *cis*-rich monomer mixtures. Also, it is found that with decreasing polymerization temperature the intensity of 8.78 τ increases in the predominantly *trans*-rich polymers and decreases in the *cis*-rich polymers.

An assignment of the two components of the proton resonance is not possible on the basis of spectral data alone. However, as shown in Table I, the spectrum of polymer obtained by $\text{BF}_3 \cdot \text{O}(\text{C}_2\text{H}_5)_2$ is substantially the same as that obtained by $\text{Al}(\text{C}_2\text{H}_5)_2\text{Cl}$. Natta et al. have shown that *trans*-alkenyl ethers produce *threo*-di-isotactic polymers with aluminum alkyl chloride¹ and that poly(β -chlorovinyl butyl ethers) obtained with

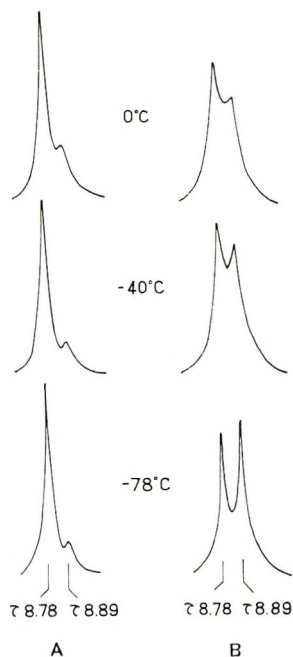


Fig. 2. NMR spectra of β -methyl protons decoupled from β -methine proton in poly(methyl propenyl ethers) obtained by $\text{BF}_3 \cdot \text{O}(\text{C}_2\text{H}_5)_2$ in toluene at various polymerization temperatures: (A) *cis/trans* ratio in monomer mixture = 1/9; (B) *cis/trans* ratio in monomer mixture = 4/1. $[\text{M}]_0 = 10$ vol.-%, $[\text{C}] = 3$ mmole/l.

this catalyst and with $\text{BF}_3 \cdot \text{O}(\text{C}_2\text{H}_5)_2$ are of the same structure.² Therefore, poly(*trans*-methyl propenyl ether) obtained by $\text{BF}_3 \cdot \text{O}(\text{C}_2\text{H}_5)_2$ at low temperature should have the *threo*-di-isotactic structure, and it seems reasonable to assign the signal at 8.78 τ to the *threo*-di-isotactic diad.

The intensity of the signal at 8.89 τ for the polymers obtained from *cis*-rich monomer mixture increases with decreasing polymerization temperature. As isotactic polymers are generally obtained at low temperature in the homogeneous cationic polymerization of vinyl ethers, the signal at 8.89 τ is also due to the isotactic structure. This signal

TABLE I
 Polymerization Conditions and Properties of Poly(methyl Propenyl Ether)*

Catalyst	<i>cis/trans</i> in monomer (mole ratio)	Polymerization		Con- version, %	[η], dl./g.	Melting point, °C.	Crystal- linity	<i>threo</i> -Di- isotactic fraction, %	<i>erythro</i> -Di- isotactic fraction, %
		Temp., °C.	Time, hr.						
BF ₃ ·OEt ₂	1:9	0	2	61	0.05	60	—	76.4	23.6
"	"	-40	"	55	0.10	150	Cryst.	82.6	17.4
"	"	-78	"	32	0.30	150	Cryst.	85.7	14.3
"	4:1	0	"	78	0.05	—	—	53.8	46.2
"	"	-40	"	68	0.09	40 ^b	Amorph.	51.9	48.0
"	"	-78	"	66	0.27	100 ^b	Amorph.	44.4	55.6
AlEtCl ₂	1:9	-78	20	82	0.19	140	Cryst.	84.5	15.5
"	4:1	-78	20	85	0.28	100 ^b	Amorph.	37.6	62.4

* Conditions: [M]₀ = 10 vol.-% [Cat] = 3 mmole/l., Solvent: toluene.

^b Softening point.

may be, therefore, assigned to another isotactic structure, i.e., the *erythro*-di-isotactic diad.

The di-syndiotactic fraction may exist in these polymers. The signal due to the di-syndiotactic diad can be expected to appear between the *threo*- and the *erythro*-di-isotactic signals. However, the signal corresponding to this diad is not found, as shown in Figure 2. It might be due to the existence of this small signal that the width of the signal for each sample is different.

The shape of the methoxyl protons signals also differs according to the polymerization conditions of the polymers, as shown in Figure 1. It is expected to be possible to analyze the configuration of poly(methyl propenyl ether) from the spectra of methoxyl protons as observed in poly(methyl vinyl ether).⁶ Although NMR spectra were measured in various solvents, e.g., benzene, chloroform tetrachloroethylene, and nitroethane, we could not find a suitable solvent which separated the signal sufficiently. Therefore, the analysis from the methoxyl proton was impossible in this study.

On the basis of the assignment of β -methyl protons, the content of the *threo*- and *erythro*-di-isotactic diads can be determined quantitatively. These results are shown in Table I together with the polymerization conditions and the properties of polymers.

The polymers obtained from *trans*-rich monomer mixtures in the presence of $\text{BF}_3 \cdot \text{O}(\text{C}_2\text{H}_5)_2$ are highly crystalline, and the fraction of the *threo*-di-isotactic diad is more than 80%. On the other hand, the polymers obtained from *cis*-rich monomer mixtures under the same condition are amorphous and are mixtures of the *threo*- and the *erythro*-di-isotactic structures.

In the cationic polymerization of alkenyl ethers, the *cis* isomer is generally more reactive than the *trans* isomer.⁵ Therefore, in the polymerization of a *cis-trans* mixture, the content of *cis* monomer in the polymer is higher than that in the monomer. The content of each monomer in a polymer can be determined experimentally from the content of the residual monomer in the polymerizing system.⁵

On the basis of these results dealing with polymer structure and monomer composition in the polymer, the type of double-bond opening can be quantitatively discussed. The probabilities of *trans* and *cis* openings in *cis* monomer are defined as a and $(1 - a)$, respectively, and those in *trans* monomer as b and $(1 - b)$, respectively. Then,

$$\begin{aligned} (d[\text{M}_c]/d[\text{M}])a + (d[\text{M}_t]/d[\text{M}])(1-b) &= (\textit{threo}\text{-di-isotactic fraction}) \\ &= 1 - (\textit{erythro}\text{-di-isotactic fraction}) \end{aligned}$$

where $d[\text{M}_c]$, $d[\text{M}_t]$ and $d[\text{M}]$ represent mole concentrations of *cis* isomer, *trans* isomer, and total monomer in a polymer obtained, respectively. If at a constant temperature the type of double-bond opening does not change with varying monomer composition and rotation of the newly

TABLE II
Fraction of Double Bond Opening at Various Polymerization Temperatures

Polymerization temperature, °C.	<i>cis</i> Isomer		<i>trans</i> Isomer	
	<i>cis</i> Opening, %	<i>trans</i> Opening, %	<i>cis</i> Opening, %	<i>trans</i> Opening, %
0	47	53	80	20
-40	50	50	89	11
-78	60	40	≈100	≈0

formed chain end does not occur, *a* and *b* can be calculated on the basis of the above results.

The fraction of *cis* and *trans* opening of the *cis* and *trans* monomer at various temperatures is summarized in Table II. In *trans* isomer, the monomer double bond is subject mainly to *cis*-type opening as reported by Natta et al.¹ On the other hand, in *cis* isomer, both types of the opening are observed. Even at -78°C ., the difference of both types of openings is small, and amorphous polymer is produced from *cis* isomer by a homogeneous catalyst. It is interesting that the type of opening of monomer is very different in the geometric isomers.

The determination of the type of double-bond opening is important for elucidation of the propagation mechanism in the cationic polymerization of vinyl monomers. The relationship between the type of double-bond opening and polymerization conditions will be described in detail in a subsequent paper.

References

1. G. Natta, *J. Polymer Sci.*, **48**, 219 (1960).
2. G. Natta, M. Peraldo, M. Farina, and G. Bressan, *Makromol. Chem.*, **55**, 139 (1962).
3. T. Yoshino and J. Komiyama, *J. Am. Chem. Soc.*, **86**, 4482 (1964); *ibid.*, **87**, 387 (1965); *ibid.*, **87**, 4404 (1965); *ibid.*, **88**, 176 (1966).
4. C. Schuerch, W. Fowells, A. Yamada, F. A. Bovey, F. P. Hood, and E. W. Anderson, *J. Am. Chem. Soc.*, **86**, 4481 (1964).
5. A. Mizote, S. Kusudo, T. Higashimura, and S. Okamura, *J. Polymer Sci. A-1*, **5**, 1727 (1967).
6. S. Brownstein and D. M. Wiles, *J. Polymer Sci. A*, **2**, 1901 (1964).

Résumé

La di-isotacticité de l'éther polyméthylpropénylique obtenu par polymérisation cationique a été étudiée par spectrométrie NMR. Les spectres NMR des protons β -méthyliques du polymère ont été découplés du proton β -méthinique de façon à connaître la quantité de fraction didactique au sein du polymère. Les signaux des protons β -méthyliques à τ 8.78 et 8.89 ont été admises comme correspondants aux diades *thréo*- et *érythro*-di-isotactiques respectivement. Utilisant $\text{BF}_3\text{O}(\text{C}_2\text{H}_5)_2$ comme catalyseur, le monomère *trans* produit un polymère cristallin et sa structure est *thréo*-di-isotactique. Par ailleurs le monomère *cis* produit un polymère amorphe et est un mélange de structure di-isotactique *thréo*- et *érythro*-. Au départ de ces résultats, on conclut que la double liaison d'un monomère *trans* est ouverte exclusivement en type-*cis* et que le

monomère *cis* est caractérisé par une ouverture *trans* et que les deux se passent à une vitesse sensiblement égale.

Zusammenfassung

Die Diisotaktizität von Polymethylpropenyläther, der durch kationische Polymerisation erhalten worden war, wurde an Hand der NMR-Spektren untersucht. Die NMR-Spektren der β -Methylprotonen werden vom β -Methinproton entkoppelt, um das Ausmass der diisotaktischen Fraktion im Polymeren festzustellen. Die Signale der β -Methylprotonen bei τ 8,78 und 8,89 wurden als die zu den *threo*- bzw. *erythro*-diisotaktischen Diaden gehörigen Spektren betrachtet. Bei Verwendung von $\text{BF}_3 \cdot \text{O}(\text{C}_2\text{H}_5)_2$ als Katalysator entsteht aus dem *trans*-Monomeren ein kristallines Polymeres mit *threo*-diisotaktischer Struktur. Andererseits liefert das *cis*-Monomere ein amorphes Polymeres, das eine Mischung von *threo*- und *erythro*-diisotaktischer Struktur darstellt. Aus diesen Ergebnissen wird geschlossen, dass sich die Doppelbindung im *trans*-Monomeren ausschliesslich nach dem *cis*-Typus öffnet, während im *cis*-Monomeren *cis*- und *trans*-Öffnung mit nahezu derselben Geschwindigkeit erfolgt.

Received March 29, 1967

Revised May 10, 1967

Prod. No. 5446A

Transition of Nylon 6 γ -Phase Crystals by Stretching in the Chain Direction

KEIZO MIYASAKA and KUNIO MAKISHIMA,
*Laboratory of Textile Chemistry, Tokyo Institute of Technology,
Ookayama, Meguro-ku, Tokyo, Japan*

Synopsis

A crystal transition was found in nylon 6 fibers from the γ -phase to α -phase on stretching in the chain direction. The γ -phase fiber prepared by iodine treatment was stretched under constant load and the crystal deformation was observed by an x-ray method. The critical stress for the transition was estimated as 4×10^3 kg./cm.² at room temperature. For this crystal transition the following conditions must be satisfied: (1) extension of the γ -phase chain to untwist the chain around the amide groups, (2) translational mobility of the chain to change the stacking in the crystallite. At the critical stress, the chain in the crystal is extended to nearly the same length as that of α -phase. The translational movement occurs under stress higher than about 3×10^3 kg./cm.², and the pseudohexagonal cell is deformed into a monoclinic form. However, the monoclinic crystallites present at a stress lower than the critical value estimated above are unstable and may be brought back to the original form by heat treatment at 100°C. No crystal transition occurs at low temperature.

INTRODUCTION

The structure and properties of nylon 6 γ -phase crystals have been studied by many authors, since Ueda et al.¹ and Turuta et al.² found that iodine treatment of the α -phase of nylon 6 is accompanied by a crystal transition to the γ -phase. However, no definite structure has so far been obtained. Arimoto³ proposed that hydrogen-bonded sheets are formed between parallel chains and that these sheets are stacked in such a way that the sense of the successive sheets is alternately up and down. In the structure proposed by Vogelsong,⁴ hydrogen-bonded sheets are not formed and, therefore, the sense of molecules is the same throughout the crystal. Recently Bradbury et al.⁵ suggested that the structure is of statistical nature, though hydrogen-bonded sheets are formed in the crystal.

The most characteristic feature of the γ -phase crystal is a shrinkage of about 3% in the chain repeat distance from that in the α -phase. The shortening of the chain length is attributed to the twisting of amide groups, which was first proposed by Kinoshita⁶ for another kind of nylon. The twisting of the chain is considered to be caused by the formation of stable hydrogen bonds between parallel chains. In this respect the authors quoted above agree with each other.

Sakurada et al.⁷ measured the stress-strain relations in the crystal in the chain direction and obtained a value of 2.1×10^5 kg./cm.² for the Young's modulus of the crystal. Miyasaka and Makishima⁸ measured the Poisson deformation of the crystal under tensile stress applied in the chain direction to find a crystal transition by stretching. The crystal transition on stretching is to be discussed in this report. The examination of the crystal transition may contribute something to knowledge of the structure and properties of the crystal.

EXPERIMENTAL

Sample Preparation

Nylon 6 multifilament yarns (ordinary and high tenacity) were treated with an aqueous iodine solution at 25°C. for 48 hr. The composition of

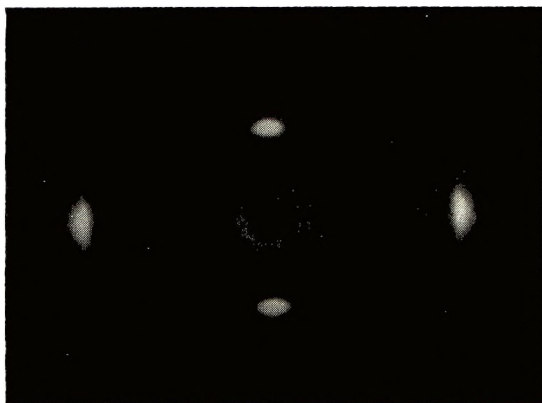


Fig. 1. X-ray diffraction photograph of γ -phase fiber of nylon 6. Fiber axis is vertical.

the treating solution was as follows: 39 g. I₂, 44 g. KI, and 300 cc. water for 4 g. fiber. These fibers were then deiodinized with Na₂S₂O₃ and washed with water. The length of the yarns was kept constant during

TABLE I
Density, Crystallite Orientation, and Long
Spacing of γ -Phase Yarns

Sample	Density at 25°C., g./cm. ³	Degree of crystallite orientation $\langle \sin^2 \varphi \rangle^a$	Long spacing, A.
Ordinary yarn	1.145	0.010	90
High-tenacity yarn	1.147	0.010	— ^b

^a Determined by x-ray method, where φ is the inclined angle of the chain axis to fiber axis.

^b Could not be determined from small-angle scattering.

the treatment. An x-ray diffraction photograph is shown in Figure 1, and some of the parameters defining the fine structure of the γ -phase yarn are given in Table I. As shown in Table I, the degree of crystallite orientation of these yarns is very high, and thus one can consider that the stress applied to the yarn is in the same direction as the chain axis of the crystallites. The lattice constants of the α - and γ -phase crystals are listed in Table II. As reported by Bradbury, the γ -phase crystal is rhombic, but the cell is approximately hexagonal at room temperature. Thus in this report, the pseudo-hexagonal cell is adopted for convenience.

TABLE II

	α -Phase (monoclinic) ^a	γ -Phase	
		Orthorhombic ^b	Pseudo-hexagonal ^c
a, A.	9.56	4.82	4.79
b, A.	17.24 (chain axis)	7.82	4.79
c, A.	8.01	16.70 (chain axis)	16.70 (chain axis)
β	67.5°		

^a Data of Holmes et al.⁹

^b Data of Bradbury et al.⁶

^c Data of Vogelsong.⁴

Procedure

Method of Measuring Crystal Deformation in the Chain Direction. A multifilament yarn with a cross-sectional area of about 2×10^{-3} cm.² was set on the x-ray goniometer attached by an apparatus devised for stretching a fiber by constant load.¹⁰ The yarn was so set as to keep the fiber axis at right angles to the goniometer axis and at the same time to keep an inclined angle, $90 - \theta$, with the incident x-ray beam. θ is the Bragg angle of the (00*l*) diffraction measured. The *c* axis is the chain axis in the hexagonal cell. A load was applied to the yarn through a pulley and the lattice spacing was measured by an x-ray GM counter. The spacing was also measured after removal of stress to obtain the irreversible strain. The x-ray measurements were made 10 min. after loading and after removal of stress. It was ascertained that most of the change in the spacing takes place in this time interval, though a small delayed recovery was observed beyond this interval. The load was increased stepwise. As a crystal transition occurred under high stress, measurement of the spacing became impossible in the high stress range. Ni-filtered CuK α was used in the Rigakudenki D-3F x-ray apparatus, using pin hole slits of 1.0 and 1.5 mm. diameter for the incident and scattering beams, respectively. The scanning speed of the counter was 0.5° (2*θ*)/min. and the chart speed was set at the rate of 40 mm./1.0° (2*θ*).

Observation of Crystal Deformation in the Direction Perpendicular to the Chain Axis. In this case the yarn was set coaxially to the goniometer

to be stretched vertically, and the x-ray measurements were made on the equator.¹¹ The x-ray procedure was the same as in the preceding section.

Atmospheric Conditions for Measurements. Experiments were made at 25°C. and 55–65% R.H. The water content of samples was about 3% under these conditions. For examination of the effect of water on the crystal deformation an experiment was performed in dry air, where samples absorbed about 0.5 wt.-% water. The results obtained in dry air, however, were not different from those obtained under the conditions shown above. It was very difficult to perform the x-ray measurements on a perfectly dry sample. This result may not always mean that water does not affect the crystal deformation. A small amount of water is expected to be absorbed within a crystallite, the defects of which may provide sites for water absorption. The small amount of water may affect the crystal deformation. In the examination of the effect of temperature on the crystal transition, samples were stretched in liquid nitrogen and a Dry Ice-methanol mixture.

Definition of Stress and Strain

A series model to connect the crystalline and amorphous regions is postulated for the fibers and, therefore, the stress applied to the fiber is assumed to be equal to that applied to crystalline region. This assumption is arbitrary. If a sample has very high crystallinity, as is the case with linear polyethylene, this assumption may be reasonable. In this case the crystallinity is not so high, and therefore a parallel connection between two regions should be considered as well as the series connection. Thus the real stress applied to crystallites must be higher than that estimated in this study, though the difference may not be large.

Two kinds of strain are defined, $e_1 = (d - d_0)/d_0$ and $e_0 = (d_0' - d_0)/d_0$, where d_0 , d , and d_0' are the spacing observed before stressing, under stress, and after removal of stress, respectively, and e_0 is irreversible strain.

RESULTS AND DISCUSSION

Stress-strain curves for γ -phase crystals of nylon 6 in the chain direction are shown in Figure 2. These were obtained on the (004) spacing. Strain increases linearly with stress except in the range of high stress. No difference in the stress-strain relation between the two kinds of sample can be observed in the lower range of stress. It should be noticed that the stress-strain relation does not follow the strict meaning in the high-stress range. As shown later, this stretching of the crystal is accompanied by a crystal transition. The (00 l) diffraction intensity is much weaker in the transformed crystal than that in the original γ -phase crystal. On the other hand, the crystal transition does not occur evenly throughout a sample. In the high-stress range, the (00 l) intensity observed comes mainly from γ -phase crystal which has not yet been transformed. Thus, in the high-stress range the results in Figure 2 no longer show the true stress-strain

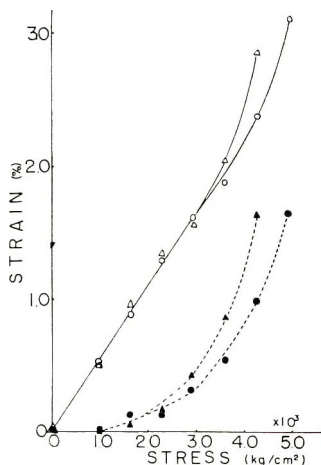


Fig. 2. Stress-strain curve of γ -phase crystallites of nylon 6 in the chain direction: (Δ) e_1 , ordinary yarn; (O) e_1 , high-tenacity yarn; (\blacktriangle) e_0 , ordinary yarn; (\bullet) e_0 , high-tenacity yarn.

relation; the true strain should be larger than that shown there. The deviation of the stress-strain relation from linearity in the high-stress range may be emphasized more than shown in Figure 2. Sakurada et al.⁷ have obtained a stress-strain curve on this crystal to determine Young's modulus. Their measurements were limited to the lower range of stress, and thus the deviation from linearity could not be observed.

The irreversible strain e_0 is also plotted against stress in Figure 2. The chain repeat distance increases irreversibly with stress, and the increase becomes appreciable at high stretching. It is interesting that the chain repeat distance extends gradually in the stressed samples, for a crystal should have a defined repeat distance. The force for stretching of a chain to unit strain is estimated as about 3×10^{-4} g. from the Young's modulus value of 1.8×10^5 kg./cm.² obtained in Figure 2. The force estimated is very small compared with that (44×10^{-4} g.) of polyethylene obtained by Sakurada.¹⁰ In addition to the high extensibility of the chain, this material has a strong cohesive force. Thus the chain may be affected easily by neighbors in recovery from tension. The gradual increase of the chain repeat distance observed in stressed crystallites may be related to these properties of this material and to the irregularity in the chain extension under stress. The broadening of the x-ray diffraction profile observed under stress suggests irregular deformation of chains within the crystallite.

Stress-strain curves of the yarns are shown in Figure 3. The stress-strain relation is markedly different for these two yarns in the high-stress range of stress. This suggests that the extension of crystallites is independent on the extension of yarns.

The stretching of the crystallites is accompanied by a marked decrease in the x-ray ($00l$) diffraction intensity. The change of the intensity obtained

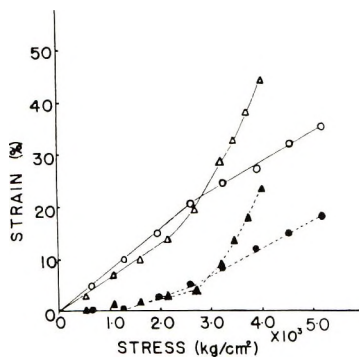


Fig. 3. Stress-strain curve of γ -phase fiber of nylon 6: (●) e_0 , high-tenacity yarn; (▲) e_0 , ordinary yarn; (○) e_1 , high-tenacity yarn; (Δ) e_1 , ordinary yarn.

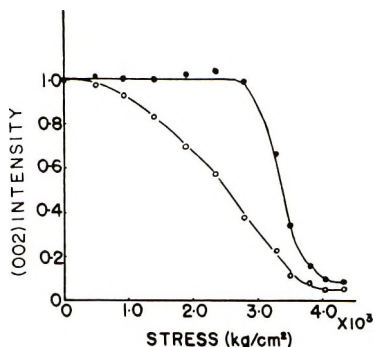


Fig. 4. Change in (002) diffraction intensity of γ -phase crystallites of nylon 6 on stretching in the chain direction: (●) after removal of stress; (○) under stress.

on the (002) diffraction is shown in Figure 4, where the intensity is normalized by that observed before stretching. The compensation for mass exposed to x-ray was made in the estimation of intensity. Similar results were obtained on the other (00 l) diffractions. The intensity decreases with stress reversibly up to about 3×10^3 kg./cm.² but irreversibly in high stretching. In this case also the intensity obtained in the high-stress range has no strict meaning for the same reasons as considered previously in the stress-strain relation.

As quoted above, the characteristic shrinkage of the chain in the γ -phase crystal is attributed to the twisting of the chain around amide groups. The chain has higher extensibility around the amide groups than in other parts, for the potential of the internal rotational angle is lower compared with these of bond length and bond angle. The extension of this part of the chain causes a change in the (00 l) diffraction intensity. However, the x-ray diffraction intensity on the meridian (chain direction) in nylon 6 crystal) is determined mainly by the chain stacking. The difference in (002) structure factor calculated on a chain is only about 10% between the extended (α) and twisted (γ) chains. In the γ -phase crystal the (002) structure factor is proportional approximately to that calculated for the chain. Thus if the crystal structure is not changed and the deformation

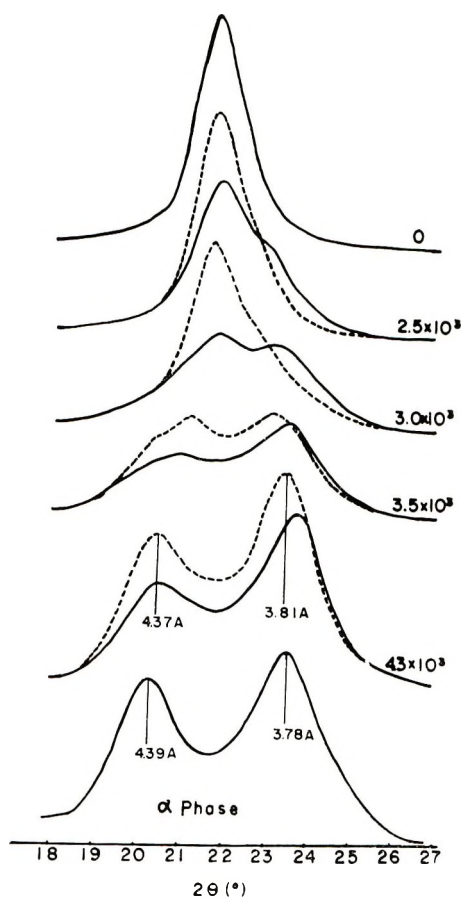


Fig. 5. Change of x-ray diffraction profile on the equator of γ -phase crystallites of nylon 6 on stretching in the chain direction: (—) under stress; (---) after removal of stress. Ordinary yarn: numbers on curves show the stress applied (in kilograms per square centimeter). The α -phase curve was obtained on the original fiber not treated by iodine.

caused by stretching is even, the decrease in (002) diffraction intensity is expected to be about 20% even when the crystal is fully extended. However, the change in the intensity shown in Figure 4 is much larger than that expected above and is irreversible at high stretching. This means there is an irreversible change in the chain stacking. At lower degrees of stretching, the intensity decreases markedly but recovers after removal of stress. In this case the irreversible change of the chain stacking can not be considered. It may be caused by an irregular deformation of chains within the crystallite, which causes a temporal change of chain stacking and decreases the diffraction intensity. The uneven deformation of the chain may be related to the defects in the crystallite and to the inhomogeneity of the crystallite surface perpendicular to chain axis. Tie molecules and the length of tie molecules and chain folding are the factors determining the state of the surface.

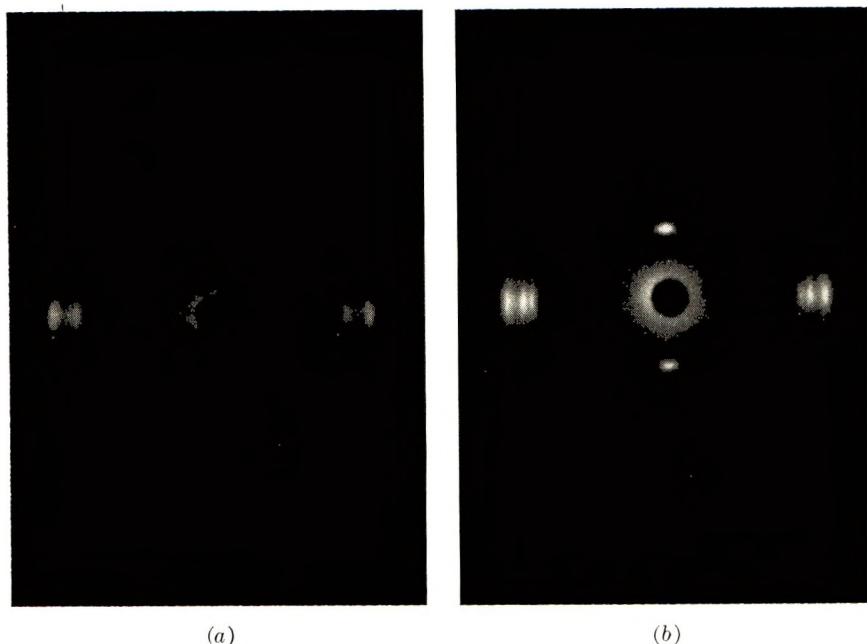


Fig. 6. X-ray diffraction photographs of γ -phase fiber of nylon 6 (ordinary yarn) stressed at 4.3×10^3 kg./cm.²: (a) before heat treatment, (b) after heat treatment.

The change of the x-ray diffraction profile on the equator on stretching is shown in Figure 5. One can observe a remarkable change of the profile. The (100) diffraction peak of the γ -phase crystal is extinguished by stretching and other two diffraction peaks appear on the equator. This change of profile is intimately related to the chain extension and especially to the change in the (002) diffraction intensity shown above. These diffraction peaks originated by stretching are similar to these of the (200) and (002) in the monoclinic α -phase crystal with respect to the spacing and intensity, where the b axis is in the chain direction. This change in the profile shows that the γ -phase pseudohexagonal cell is transformed into a monoclinic one.

For the purpose of examining the stability of the monoclinic crystal on stretching, the stressed samples were heat-treated at 100°C. for 1 min. in water, where the length was not kept constant. Figure 6 shows x-ray diffraction photographs obtained before and after the heat treatment for a sample stressed at 4.3×10^3 kg./cm.². A monoclinic pattern is observed on the equator before treating. On the other hand, two diffraction patterns from two crystal forms, hexagonal and monoclinic, are superimposed after the treatment. This means that some of the monoclinic crystallites formed as a result of stretching are unstable and brought back to the original form by the treatment. Others, however, are stable and remain in the monoclinic form after the treatment.

These monoclinic crystallites stable to the heat-treatment can be considered to be the α -phase crystal. When the heat treatment is applied to the sample stressed at 3.5×10^3 kg./cm.² (for which the equatorial scanning

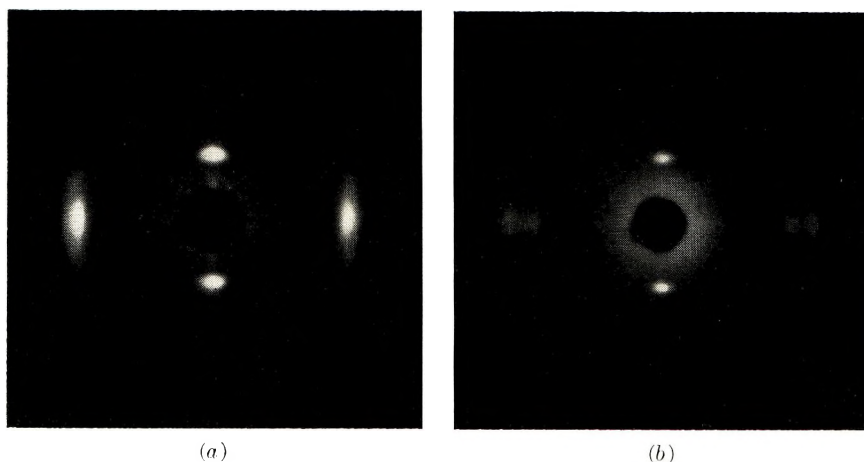


Fig. 7. X-ray diffraction photographs of γ -phase fibers of nylon 6 (high-tenacity yarn) stressed by 5.0×10^3 kg./cm.² at different temperatures: (a) in liquid nitrogen; (b) in Dry Ice-methanol mixture.

is shown in Fig. 5), the two diffraction peaks showing monoclinic form extinguish perfectly. The result and that shown above mean that the transition from hexagonal to monoclinic does not always involve a change of the crystal phase.

The chain repeat distance extends to nearly the same length as that in the α -phase under high stress as shown in Figure 2. The hydrogen bonds between parallel chains become unstable on extension. Thus the chains again form other stable bonds if they can find partners available among their neighbors. In this case the requirement for the new partner is that it can form stable hydrogen bonds with the chain considered in the extended conformation. This makes us conclude from Bunn's proposal that it is an antiparallel chain. The existence of an antiparallel chain in the unit cell was proposed by Arimoto³ and Bradbury⁴ and is also expected on the basis of the folding mechanism of polymer crystallization. When this formation of the bonds is performed, the γ -phase crystal is transformed into an α -phase crystal.

This discussion may be too much idealized, for the real structure of polymer crystal is more or less disordered, and, especially in this case, the chain deformation does not involve regular stretching. Roldan et al.¹² have defined an α -phase paracrystalline structure in this material and reported that the α -phase structure by Bunn is observed only in spherulites and that the paracrystalline structure prevails in oriented material. In this study a strict distinction between these two structures can not be discussed, and these structures are both noted as α -phase structures. In Roldan's structure, such a well defined hydrogen-bonded sheet is not formed as it is in Bunn's. It is natural, however, in Roldan's structure that hydrogen bonds formed between antiparallel chains prevail between parallel chains, and these are related to the chain repeat distance of the crystal. If this were not so, the chain repeat distance would have to be

shorter than that of the planar zigzag form. Thus, even when the paracrystalline structure is taken into consideration, the transition mechanism considered above may not need to be changed. The α -phase crystal obtained by stretching may be paracrystalline rather than conforming to Bunn's ideal structure.

It is concluded from the results obtained and the discussion that the γ -phase crystal is transformed into an α -phase crystal by stretching in the chain direction at room temperature. The crystal transition does not take place uniformly, and the transformed crystal is considered to be imperfect, containing many disordered regions. For the two kinds of samples the critical stress for the crystal transition is estimated from the stability of the crystal to the heat treatment as about 4×10^3 kg./cm.² This value of critical stress is supported by the stress-strain relation shown in Figure 2. Under this stress the chain extends to nearly the same length as that of the α -phase crystal with a planar zigzag conformation.

A monoclinic form can be observed on stretching at a stress lower than the critical stress. In these unstable monoclinic crystallites, the chain repeat distance is longer than that of the original γ -phase but most of the hydrogen bonds may remain in the γ -phase state. This unstable monoclinic crystallite is transformed to the α -phase by farther stretching.

For the crystal transition, the following conditions must be satisfied: (1) extension of chain to planar zigzag form, accompanied by untwisting around amide groups; (2) translational mobility of chain to change the stacking. Thus the crystal transition should be considered to be related to the mechanical relaxation phenomena of chains in a crystallite with respect to the following factors: stress, temperature, and time of stressing. The time effect is not appreciable at room temperature. Evidence for the temperature effect on the transition under constant stress and time is shown in Figure 7. These photographs were obtained on the samples stressed at 5.0×10^3 kg./cm.² for 150 min. in liquid nitrogen and a Dry Ice-methanol mixture. In the former no changes of the pattern can be observed (compare with Fig. 1), but a clear transition is observed in the latter. This result suggests the existence of a critical temperature between the liquid nitrogen and Dry Ice temperature. Nylon 6 has a mechanical dispersion at a temperature lower than about -100°C .¹³ which is identified as the local mode motion of amorphous chains and termed the γ dispersion. It is interesting that there seems to be a relation between the crystal transition and the γ dispersion observed in bulk nylon 6. Work concerning this temperature effect on the crystal transition is to be discussed in a subsequent paper from the view point of relaxation phenomena of nylon 6 chains in crystallites.

References

1. S. Ueda and T. Kimura, *Kobunshi Kagaku*, **15**, 243 (1958).
2. M. Turuta, H. Arimoto, and M. Ishibashi, *Kobunshi Kagaku*, **15**, 619 (1958).
3. H. Arimoto, *J. Polymer Sci. A*, **2**, 2283 (1964).
4. D. C. Vogelsong, *J. Polymer Sci. A*, **1**, 1055 (1963).

5. E. M. Bradbury, L. Brown, A. Elliot, and D. D. Parry, *Polymer*, **6**, 465 (1964).
6. Y. Kinoshita, *Makromol Chem.*, **33**, 1, 21 (1959).
7. I. Sakurada, T. Ito, and K. Nakamae, paper presented at 13th Annual Meeting, Society of Polymer Science Japan, June (1964).
8. K. Miyasaka and K. Makishima, *Kobunshi Kagaku*, **23**, 870 (1966).
9. D. R. Holmes, C. W. Bunn, and D. J. Smith, *J. Polymer Sci.*, **17**, 159 (1955).
10. I. Sakurada, K. Nukushina, and T. Ito, *J. Polymer Sci.*, **57**, 651 (1962).
11. K. Shirakashi, K. Ishikawa, and K. Miyasaka, paper presented at 13th Annual Meeting, Society of Polymer Science, Japan, June (1964).
12. L. G. Roldan and H. S. Kaufman, *J. Polymer Sci. B*, **1**, 603 (1963).
13. T. Kawaguchi, *J. Appl. Polymer Sci.*, **2**, 56 (1959).

Résumé

On a trouvé une transition cristalline du nylon-6 de la phase γ à la phase α par étirement dans le sens de la direction des chaînes. L'échantillon de phase γ a été préparé par traitement à l'iode de la fibre de phase α . L'échantillon de phase γ était étiré sous charge constante et la déformation des cristallites était mesuré par les méthodes aux rayons-X. La tension critique de transition était estimée à 4×10^3 Kg/cm². La distance périodique de la chaîne du cristal est étendue par l'étirement critique à la même longueur que la phase α du cristal alors que la chaîne a une configuration plane en zigzag. Sous cette tension, les liaisons hydrogènes de la phase γ entre les chaînes parallèles sont transformées en celles de la phase α formée en chaînes antiparallèles. Cette transitions du cristal montre l'existence de chaînes antiparallèles au voisinage d'une chaîne outre des chaînes parallèles avec lesquelles, elles forment des liaisons hydrogènes dans la phase cristalline α . La transition cristalline était également due à des formations inhomogènes des chaînes au sein des cristallites. La transition cristalline se rapport à des phénomènes de relaxation de chaînes au sein des cristallites. Ceci dépend de la température et de la durée d'étirement. La température critique pour la transition est liée à la dispersion gamma du nylon en bloc.

Zusammenfassung

Bei Ausübung einer Zugspannung in der Kettenrichtung erfolgt, wie gefunden wurde, eine Kristallumwandlung der Nylon 6- γ -Phase in die α -Phase. Die in der γ -Phase befindliche Probe wurde durch Behandlung einer Faser im α -Zustand mittels Jod hergestellt. Die γ -Phasen-Proben wurden unter konstanter Belastung verstreckt und die Deformation der Kristallite röntgenographisch gemessen. Die kritische Spannung für die Umwandlung wurde zu $4 \cdot 10^3$ kg/cm² bestimmt. Die Kettenidentitätsperiode wurde durch die kritische Spannung auf dieselbe Länge wie bei einem Kristall im α -Zustand vergrößert, wo die Ketten eine ebene Zickzack-Konfiguration besitzen. Unter dieser Spannung werden die γ -Phasen-Wasserstoffbindungen zwischen parallelen Ketten in solche umgewandelt, die sich in der α -Phase zwischen antiparallelen Ketten ausbilden. Diese Kristallumwandlung spricht für die Existenz antiparalleler Ketten in der Nachbarschaft einer Kette, zusätzlich zu den parallelen Ketten, zu denen sie im γ -Phasen-Kristall Wasserstoffbindungen ausbildet. Wegen der inhomogenen Deformation der Ketten innerhalb des Kristallits wird die Kristallumwandlung ungleichmässig ausgelöst. Die Kristallumwandlung steht mit den Relaxationsphänomenen der Ketten innerhalb des Kristallits in Beziehung. Demgemäss hängt sie von der Temperatur und der Beanspruchungsdauer ab. Die kritische Umwandlungstemperatur scheint mit der γ -Dispersion einer Nylon 6-Masse zusammenzuhängen.

Received December 21, 1966

Revised March 6, 1967

Prod. No. 5402A

Hydrodynamics of a Porous Sphere Molecule

TRUMAN SEELY, *The Institute of Paper Chemistry,
Appleton, Wisconsin 54911*

Synopsis

A mathematical model is proposed which treats a hypothetical polymer molecule as a porous sphere. Fluid flow within the sphere obeys Darcy's law while the creeping motion equations are used outside the sphere. Equations are derived relating the permeability and radius of the sphere to hydrodynamic properties of dilute solutions of the polymer. In checking against experimental data, it is found that the model, despite its simplicity, may be useful in explaining the hydrodynamic behavior of molecules which are highly branched or crosslinked.

Introduction

Viscosity and sedimentation data are often used to obtain information about the size and shape of polymer molecules in solution. Interpretation of the data is accomplished by recourse to an appropriate mathematical model of polymer hydrodynamics. There are several such models applicable in different situations.

Branched and crosslinked molecules present some difficulty in interpretation. Monomer unit positions relative to one another are not readily determined by the statistical methods used successfully on linear polymers. For this reason, hydrodynamic shielding effects cannot be correctly evaluated. A simple way around this problem will be suggested in the following paragraphs.

It will be noticed that the model used is similar to one suggested some time ago by Debye and Bucche,¹ whose starting equations are the same as Brinkman's.² There are, however, some differences which will be pointed out as they become important.

The following work was originally undertaken as a part of an investigation of the flow of wood fiber suspensions. The possible application to polymer hydrodynamics was not recognized until the intended task was nearly completed.

Theoretical

The following discussion is not a complete derivation. However, it should be sufficient to point out clearly the way in which a complete derivation may be constructed. Some attention will be given to the limitations of the model employed.

The model consists of a porous sphere of radius a in a viscous fluid. Darcy's law describes fluid motion inside the sphere, and the creeping motion equations are employed outside:

$$\nabla \cdot \mathbf{U}_* = 0 \quad r < a \quad (1)$$

$$\mathbf{U}_r = (K/\eta_0)\nabla P \quad (2)$$

$$\nabla \cdot \mathbf{U} = 0 \quad r > a \quad (3)$$

$$\eta_0 \nabla^2 \mathbf{U} = \nabla P \quad (4)$$

Equations (3) and (4) are quite common and need no explanation here. Equations (1) and (2) are less common and do require some explanation. The vector \mathbf{U}_* is the superficial velocity of the fluid in the porous medium. It is an average value of fluid velocity in an appropriately large region, the average being over the total volume rather than the fluid-occupied volume. Equation (1) is the equation of continuity, but is strictly valid only under steady flow conditions and when averaged over an appropriately large volume. The vector \mathbf{U}_r in eq. (2) refers to the superficial velocity of the fluid relative to the porous medium, while ∇P is the pressure gradient in the fluid. Equation (2) is the usual form of Darcy's law for a Newtonian fluid. The equation as written holds only for isotropic, homogeneous porous media. The porosity ϵ , and permeability coefficient K may not vary with position or direction.

The origin of Darcy's law is mainly empirical, or at best semiempirical. Recently, however, Whitaker³ was able to derive Darcy's law from the equations of motion under special conditions. His work clearly indicates that the equations are not readily generalized to materials which are not both isotropic and homogeneous.

For the time being, the situation will be limited to the case of the porous sphere being stationary and at the center of the reference coordinate system. Obviously, under these conditions $\mathbf{U}_r = \mathbf{U}_*$, and from eqs. (1)–(4) there is the important result:

$$\nabla^2 p = 0 \quad \text{all } r \quad (5)$$

Now fluid motion will be introduced. For reasons which will later be clear, the motion chosen will tend toward a hyperbolic velocity field far from the sphere. As additional boundary conditions, the pressure must be finite everywhere, while pressure and superficial velocity must be continuous across the sphere boundary. The last two conditions may be regarded as arbitrary, but are the most reasonable choices from a physical point of view.

Writing out the boundary conditions:

$$v_x \rightarrow \alpha x/2 \quad r \gg a \quad (6a)$$

$$v_y \rightarrow -\alpha y/2 \quad (6b)$$

$$v_z \rightarrow 0 \quad (6c)$$

$$\mathbf{U}_{*int} = \mathbf{U}_{ext} \quad \text{at } r = a \quad (7a)$$

$$p_{int} = p_{ext} \quad (7b)$$

The problem is not especially difficult to solve. Probably the easiest approach is the method of spherical harmonics, which is well described by Lamb.⁴ Briefly, this method depends upon the fact that the velocity of the fluid in creeping motion may be found by applying differential operators to a series of scalar harmonic functions. In problems of spherical symmetry, spherical harmonics are employed. From the boundary conditions, the user must select the spherical harmonics of the necessary orders and determine the coefficients which must be applied. Since the internal pressure is also a harmonic function, it is fairly easy to determine.

By using Lamb's notation, the external velocity field should be generated by the spherical harmonic functions:

$$\Phi_2 = \alpha(x^2 - y^2)/4 \quad (8a)$$

$$\Phi_{-3} = B_{-3}a^5(x^2 - y^2)/r^5 \quad (8b)$$

$$P_{-3} = A_{-3}\eta_0a^3(x^2 - y^2)/r^5 \quad (8c)$$

The internal pressure must match the external at the interface and remain finite at $r = 0$. Therefore, internally:

$$P_2 = (\eta_0A_2/a^2)(x^2 - y^2) \quad (9)$$

A clever mathematician could probably write down the coefficients by inspection. A less elegant but equally certain way to determine them is to proceed by successive approximations beginning with the solid sphere values as known from Einstein's work.⁵ The internal pressure is determined by requiring that it match the external pressure at $r = a$. The velocity condition is then not satisfied and the external field must be adjusted, etc. The results, valid for all K and a , are:

$$A_{-3} = A_2 = -5\alpha/2[1 + (10K/a^2)] \quad (10)$$

$$B_{-3} = -\alpha/4[1 + (10K/a^2)] \quad (11)$$

At this point, another harmonic function is introduced to the external field in accordance with Lamb's notation:

$$\chi_1 = -\alpha z/2 \quad (12)$$

The effect of this function is to give the external field an angular velocity:

$$\omega = -\alpha\mathbf{k}/2 \quad (13)$$

The boundary conditions may be matched by giving both the porous sphere and the fluid within it an identical angular velocity.

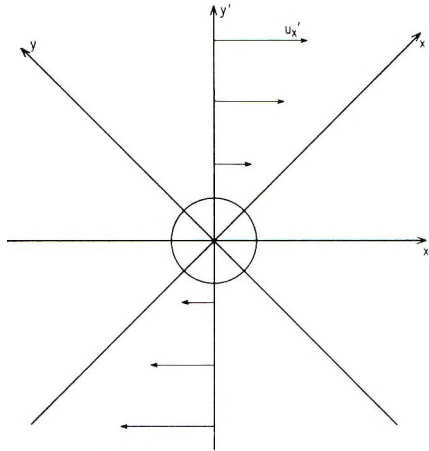


Fig. 1. Velocity field and coordinate systems.

The velocity field far from the sphere now tends to:

$$v_x = (\alpha/2)(x + y) \quad (14a)$$

$$v_y = (-\alpha/2)(x + y) \quad (14b)$$

$$v_z = 0 \quad (14c)$$

This field is immediately recognized as linear Couette flow in the x - y plane with the streamlines at a 45° angle to the x axis (see Fig. 1).

From this point it is easy to determine the viscosity of a dilute suspension of porous spheres by using the method described by Vand⁶ for solid spheres, or less rigorously one could employ the same shortcut Taylor⁷ used to compute the viscosity of a suspension of liquid spheres in a second liquid. By either method, the result obtained is:

$$\eta = \eta_0 \left\{ 1 + \frac{5}{2} \frac{\Phi}{[1 + (10K/a^2)]} \right\} \quad (15)$$

where Φ is the volume fraction of the suspension which is occupied by porous spheres, and must not be confused with the solid fraction.

The method outlined above may also be applied to a porous sphere settling in a viscous fluid of infinite extent. The most important result for the present discussion is the Stokes drag on such a sphere:

$$F_x = \frac{6\pi a \eta_0 v_x}{1 + (3K/2a^2)} \quad (16)$$

The radius of the sphere and the permeability coefficient enter fairly simply into both the viscosity and drag equations. The reader may wish to compare these expressions to the similar but more complex ones given by Debye.¹ Since the expressions are arrived at using different equations to describe the internal flow, Debye's $1/\sigma^2$ is not identical with K/a^2 . The

choice of Darcy's Law to describe internal flow is of course debatable. Brinkman² considers the equation he employs within a porous medium to be "a more or less arbitrary interpolation in the region where damping and viscous forces are of the same magnitude." As mentioned before, this equation is identical to Debye's. Using this sort of terminology, one could argue that the Darcy expression refers to a region where viscous damping is of a larger magnitude than any shear stress produced by variation in the superficial velocity.

Now it is necessary to describe the type of polymer molecule to which the model applies. This molecule must be nearly spherical at low but finite shear rate in the solvent employed. The permeability K must be constant throughout the sphere. This implies that when viewed on a sufficiently macroscopic scale, the internal structure of the molecule should be uniform. The requirement of uniformity eliminates the random coil and other configurations characteristic of linear polymers. It suggests instead a relatively rigid, branched, and/or crosslinked structure. For the model to be useful, permeability and porosity should not vary with molecular weight.

Given the molecule, determination of the relations between intrinsic viscosity, sedimentation constant, and molecular weight is straightforward.

Consider a solution of volume V containing n solute molecules which are uniform, porous spheres of radius a , permeability K , porosity ϵ , and solid density ρ_1 . Neglecting changes in solvent volume due to hydration, ρ_1 could be regarded as the reciprocal of the solute specific volume. The solid mass of a sphere is:

$$m = \rho_1 4/3 \pi a^3 (1 - \epsilon) \quad (17)$$

The total mass of solute molecules is

$$nm = \rho_1 \Phi (1 - \epsilon) V \quad (18)$$

Let c be the solute concentration in mass per unit volume, N be Avogadro's number, and M the molecular weight. Then:

$$\Phi = (cN/M)(4/3 \pi a^3) \quad (19)$$

From the definition of molecular weight:

$$M = \rho_1 (N 4 \pi a^3 / 3) (1 - \epsilon) \quad (20)$$

so:

$$\Phi = c / [(1 - \epsilon) \rho_1] \quad (21)$$

Now the viscosity of a dilute solution may be expressed as:

$$\eta = \eta_0 \left\{ 1 + \left[\frac{5c}{2(1 - \epsilon)\rho_1} \right] \left[\frac{1}{1 + (10K/a^2)} \right] \right\} \quad (22)$$

and for the intrinsic viscosity $[\eta]$ one has:

$$[\eta] = \frac{5}{2(1 - \epsilon)\rho_1} \left[\frac{1}{1 + (10K/a^2)} \right] \quad (23)$$

By use of eq. (20):

$$[\eta] = \frac{5/[2(1 - \epsilon)\rho_1]}{1 + 10K[4\pi N(1 - \epsilon)\rho_1/3M]^{2/3}} \quad (24)$$

$$[\eta] = A/(1 + BM^{-2/3}) \quad (25)$$

According to hypothesis, both A and B are independent of molecular weight. The limiting cases are:

$$BM^{-2/3} \gg 1 \Rightarrow [\eta]\alpha M^{2/3}$$

$$BM^{-2/3} \ll 1 \Rightarrow [\eta]\alpha M^0$$

For the sedimentation constant, by definition:

$$s = m(1 - \bar{V}_1\rho)/f \quad (26)$$

then:

$$s = [4\pi a^3(1 - \epsilon)/3f](\rho_1 - \rho) \quad (27)$$

And from eq. (16) the value of f is:

$$f = 6\pi\eta_0 a/[1 + (3K/2a^2)] \quad (28)$$

The sedimentation constant becomes:

$$s = (2/9\eta_0)(1 - \epsilon)(\rho_1 - \rho)[a^2 + (3K/2)] \quad (29)$$

A polydisperse sample may considerably complicate interpretation of the intrinsic viscosity-molecular weight relation. Suppose the species 1, 2, . . . n are present. Then the solution's viscosity is:

$$\eta = \eta_0 \left\{ 1 + \sum_{i=1}^n \frac{5c_i}{2\rho_1(1 - \epsilon)[1 + (10K/a_i^2)]} \right\} \quad (30)$$

where c_i is the concentration and a_i the radius of the i th species. If x_i is the mass fraction of the solute present as the i th species, the intrinsic viscosity may be expressed as:

$$[\eta] = \sum_{i=1}^n \frac{x_i A}{1 + BM_i^{-2/3}} = \frac{A}{1 + B\langle M \rangle_v^{-2/3}} \quad (31)$$

The viscosity-average molecular weight of the polydisperse sample is:

$$\langle M \rangle_v = \left[\frac{1}{B} \left(\sum_{i=1}^n \frac{x_i}{1 + BM_i^{-2/3}} \right)^{-1} - \frac{1}{B} \right]^{3/2} \quad (32)$$

To avoid such complications, samples should be as nearly monodisperse as possible. This is true even for well-behaved linear polymers, where the situation is somewhat simpler:

$$\langle M \rangle_v = \left[\sum_{i=1}^n x_i M_i^\alpha \right]^{1/\alpha}$$

When intrinsic viscosity data are available over a wide and appropriate range of molecular weights, values of A and B may be accurately determined. Given these and the density ρ_1 , from a separate determination one may find ϵ , K , and the hydrodynamic radius, a . Further interpretation of the permeability coefficient as an indicator of internal structure is possible and may prove useful on a comparative basis.

Comparison with Experimental Data

Several known polymeric materials have the branches and crosslinked structure necessary for the applicability of the proposed expressions. Among these are plant lignin, some natural hemicelluloses and several types of rubber. Vulcanized rubber and other macrogels represent extreme cases.

The sort of intrinsic viscosity behavior required is often encountered, but only a few specific examples will be discussed here.

The first example is the branched dextran studied experimentally by Senti et al.⁸ According to Oene and Cragg,⁹ even the highest molecular weight dextran studied by Senti et al. should yield viscosities essentially independent of shear rate. Therefore, significant deformation of the molecule due to shear is not likely to occur. The plot of intrinsic viscosity versus molecular weight is shown in Figure 2. The constants A and B in the theoretical equation have been adjusted to fit the data with the solid curve shown. The fit is very good over the entire range of the data. The values of A and B are:

$$A = 100 \text{ cm.}^3/\text{g.} \quad (33)$$

$$B = 5.6 \times 10^3 \quad (34)$$

which lead directly to the additional information:

$$K = 3.52 \times 10^{-13} \text{ cm.}^2 \quad (35)$$

$$a = 2.5 \times 10^{-8} M^{1/3} \text{ cm.} \quad (36)$$

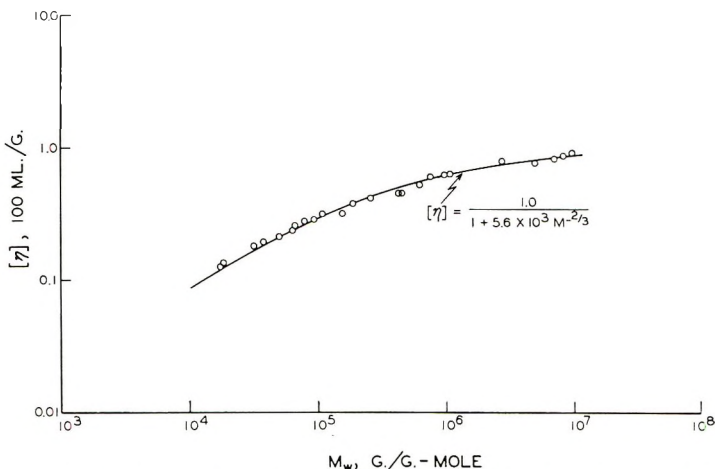


Fig. 2. Molecular weight $[\eta]$ for branched dextran (data from Senti et al.⁸).

Picking a reasonable value for ρ_1 of about 1.4 g./ml., the porosity becomes 0.982. Approximately 98% of the volume within the sphere is occupied by fluid. The value of the radius agrees pretty well with the root-mean-square radius obtained from light scattering as shown in Table I.

TABLE I
Comparison of Molecular Radii from Light Scattering and Intrinsic Viscosity for a Branched Dextran*

$M_w \times 10^{-3}$	M_w/M_n	Molecular radii, A.	
		From viscosity a	From light scattering $(\bar{R}^2)^{1/2}$
422	1.22	187	174
603	1.31	211	205
746	—	228	225
975	1.18	248	245
1040	—	254	258
2700	1.28	350	382

* Data of Senti et al.⁸

Chemical studies on the material⁸ indicate that it is an α -1,6 polymer of glucose. About 5% of the monomer units appear to be trifunctional with 1,3,6 linkages.

A similar dextran which apparently is more extensively branched has been investigated by Granath.¹⁰ The sample is designated A179 and exhibits lower intrinsic viscosity at a given molecular weight than does the first material.

Over the comparatively narrow range of molecular weights for which intrinsic viscosities are reported there is no reason to prefer the correlation

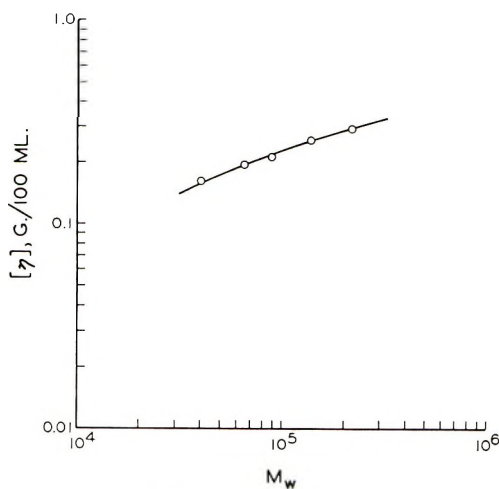


Fig. 3. \bar{M}_w vs. $[\eta]$ for dextran A-179.

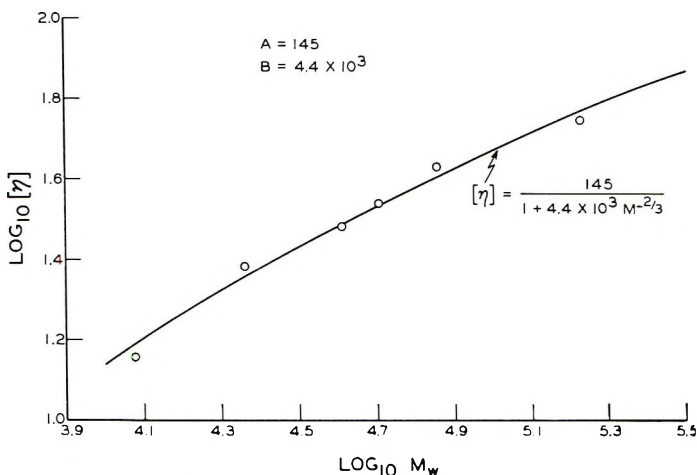


Fig. 4. $[\eta]$ vs. \overline{M}_w for spruce glucomannan (data from Linnell¹¹).

suggested in this paper over the standard form $[\eta] = KM^\alpha$. Nevertheless, the range is sufficient to determine approximate values of A and B assuming that the correlation is valid. Figure 3 shows Granath's experimental values and the correlation curve. The parameter values associated with this curve are

$$A = 50.8 \text{ cm.}^3/\text{g.} \quad (37)$$

$$B = 2.62 \times 10^3 \text{ cm.}^2 \quad (38)$$

The permeability constant and hydrodynamic radius are

$$K = 1.05 \times 10^{-13} \text{ cm.}^2 \quad (39)$$

$$a = 2.0 \times 10^{-8} M^{1/3} \quad (40)$$

This molecule is considerably more compact and less permeable than the previous example.

Linnell¹¹ has recently studied the triacetate derivative of a natural glucomannan occurring in black spruce and has found evidence of branching. Fractionation proved difficult, and the resulting distributions of molecular weight within fractions were rather broad. In spite of this difficulty, it appears that the behavior of this polymer is similar to those previously discussed (Fig. 4). In the present case, a fairly good fit of the data is obtained by taking:

$$A = 145 \text{ cm.}^3/\text{g.} \quad (41)$$

$$B = 4.4 \times 10^3 \quad (42)$$

which leads to the results:

$$(1 - \epsilon)\rho_1 = 1.72 \times 10^{-2} \text{ g./cm.}^3 \quad (43)$$

$$K = 3.58 \times 10^{-13} \text{ cm.}^2 \quad (44)$$

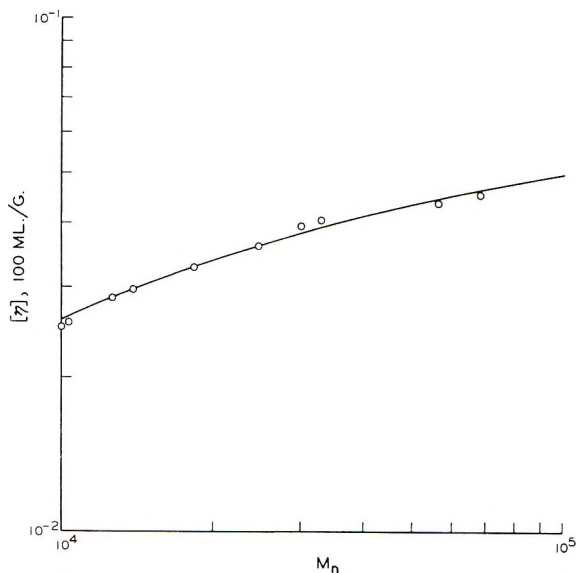


Fig. 5. Molecular weight vs. $[\eta]$ for a lignosulfonic acid (data from Tachi et al.¹²).

Linnell attributes branch points in his glucomannan to multifunctional lignin "monomers" which account for about 5% of the total number of units. The similarity of the porosities and permeabilities of the branched dextran and the glucomannan is therefore not surprising.

A contrasting example is the lignosulfonic acid studied by Tachi and co-workers.¹² This lignin derivative is the result of the action of sulfite cooking liquor on wood lignin in the sulfite pulping process. Its structure is not completely determined and is probably not regular. Each "monomer unit" may be at least trifunctional, and the material is a fairly strong acid. Intrinsic viscosities were determined on the sodium lignosulfonate in 0.5*M* NaCl.

One might suppose that the ionic environment and the expected high degree of crosslinking would lead to a very compact structure. The intrinsic viscosity-number-average molecular weight curve tends to bear out this idea. A portion of this curve is shown in Figure 5. On fitting the curve as before, values for *A* and *B* are obtained:

$$A = 6.8 \text{ cm.}^3/\text{g.} \quad (45)$$

$$B = 750 \quad (46)$$

and

$$(1 - \epsilon)\rho_1 = 0.368 \text{ g./cm.}^3 \quad (47)$$

$$K = 0.785 \times 10^{-14} \text{ cm.}^2 \quad (48)$$

$$a = 1.02 \times 10^{-8} M^{1/3} \text{ cm.} \quad (49)$$

Thus, the structure is much more compact and less permeable than in the previous cases.

Other branched polymers exhibit similar intrinsic viscosity behavior,^{13,14} but there is little to be gained by carrying out more sample calculations here.

Another interesting case is the molecule which is probably crosslinked but shows the limiting relation $[\eta] \propto M^{2/3}$. Molecules of this type include the natural rubber studied by Carter et al.¹⁵ and the Buna S synthetic rubber later investigated by the same authors.¹⁶ Of course, an exponent of 2/3 by no means demonstrates that the porous sphere model is applicable, as it may occur for linear polymers.

Permeability and Internal Structure

The permeability coefficient of a porous medium can often be related to the structure of the material. In fact, permeability measurements constitute an important part of the study of various media as dissimilar as oil-bearing rock¹⁷ and papermaking fibers.¹⁸ It is reasonable to suppose that some information about the internal structure of a porous sphere molecule could be extracted from its permeability constant by appropriate analysis.

Most estimates of the permeability coefficient in terms of particle size and porosity of the medium are designed for media with lower porosities than are encountered in porous molecules. This fact combines with the extremely small particle size to cast some doubt on the applicability of existing relations to the case of the porous sphere molecule.

Common estimates of K for a collection of spheres include the porosity and the radius of the spherical particles comprising the medium. For a "dense swarm" of spherical particles, Brinkman² suggests:

$$\lambda R = \{9 + 3[(8V/V_0) - 3]^{1/2}\} / [(4V/V_0) - 6] \quad (50)$$

where $\lambda = (\eta/K\eta')^{1/2} = (1/K)^{1/2}$ if $\eta = \eta'$. The quantities V and V_0 are the total volume and the particle-occupied volume, respectively, while R is the radius of an individual sphere. For packed beds of spheres having relatively low porosities ($\epsilon \leq 0.5$), an often used semiempirical relation is:¹⁹

$$K = D_p^2 \epsilon^3 / [150 (1 - \epsilon)^2] \quad (51)$$

In a molecule, the situation should be somewhat different from either a swarm or a packed bed of spheres. The usually nonspherical monomer units are arranged in chain segments which branch at certain units but are otherwise linear or partly coiled. Each unit in a segment is shielded in some directions by the units immediately attached to it and less well shielded in other directions by the surrounding segments. The monomer located at or near a branch point is probably better shielded than one located midway between two widely separated branch points.

Qualitatively, it appears that shielding by special configuration will lower the drag force on any one monomer unit leading to higher values of the permeability than would otherwise be supposed. An attempt to arrive at

the monomer radius by using eq. (50) or eq. (51) should yield a result that is somewhat large. Similarly, models which describe a regular array of spheres, as does Hasimoto's,²⁰ are not realistic for this case.

It would be nice to have a model for K which would yield information such as the average segment length, frequency of crosslinks, specific surface, and other information. Unfortunately, no such model is available at this time. It is likely that the best method of evaluating the significance of the permeability coefficient will vary from one type of molecule to another. The branched dextran and glucomannan previously referred to will be used again to demonstrate a method of attack.

The permeability coefficient may be related to an average "monomeric friction coefficient" which is simply the force exerted on a monomer unit divided by the approach velocity for that particle. Suppose that there are P monomer units in volume V' leading to permeability K . For high porosities, it is possible to approximate the approach velocity with the superficial velocity and:

$$K = V'_{\eta}/Pf \quad (52)$$

For Senti's dextran $f/\eta = 3.4 \times 10^{-8}$ cm., while for the glucomannan triacetate $f/\eta = 8.2 \times 10^{-8}$ cm. The larger value for the latter is explained by the less dense structure of the molecule and the larger size of the monomer unit. Both values are somewhat smaller than those obtained for the isolated monomers or low D.P. polymers, as should be the case.

Conclusion

Several theories and models exist which relate intrinsic viscosity to molecular weight and intramolecular structure of polymers. None may be regarded as absolute methods in the sense that the light-scattering and osmotic-pressure techniques are. The merits of the various concepts and models are determined solely by their usefulness.

The permeability coefficient has been highly useful in describing flow through porous media and in helping to define the physical characteristics of some of these media. It may prove equally useful on the molecular level. Further, the model proposed here appears to explain experimental observations in a consistent and simple manner over a large range of molecular weights. It is hoped that this model will prove useful in future studies of branched and crosslinked molecules.

During the course of the investigation described herein, the author was supported in part by a National Science Foundation Co-Op Graduate Fellowship, and in part by a scholarship from The Institute of Paper Chemistry where the author is currently a doctoral candidate.

The constant advice, criticism, and encouragement of Mr. Heribert Meyer is gratefully acknowledged.

References

1. P. Debye and A. Bueche, *J. Chem. Phys.*, **16**, 573 (1948).
2. H. Brinkman, *Appl. Sci. Res.*, **A1**, 27 (1947).
3. S. Whitaker, *Chem. Eng. Sci.*, **21**, 291 (1966).
4. H. Lamb, *Hydrodynamics*, Dover, New York, 6th Ed., 1945, Chap. XI.
5. A. Einstein, *Ann. Physik*, **19**, 289 (1906); *ibid.*, **34**, 591 (1911).
6. V. Vand, *J. Phys. Colloid Chem.*, **52**, 277 (1948).
7. G. Taylor, *Proc. Roy. Soc. (London)*, **A138**, 41 (1932).
8. F. Senti, N. Hellman, N. Ludwig, G. Babcock, R. Tobin, C. Glass, and B. Lambert, *J. Polymer Sci.*, **17**, 527 (1955).
9. H. van Oene and L. Cragg, *J. Polymer Sci.*, **57**, 175 (1962).
10. K. Granath, *J. Colloid Sci.*, **13**, 308 (1958).
11. W. Linnell, doctoral dissertation, The Institute of Paper Chemistry, Appleton, Wis., 1965.
12. I. Tachi, A. Nakai, S. Otuke, and Y. Kojima, *Kami-pa Gikyoshi*, **14**, 586 (1960).
13. C. Thurmond and B. Zimm, *J. Polymer Sci.*, **8**, 477 (1947).
14. L. Cragg and G. Ferm, *J. Polymer Sci.*, **10**, 185 (1953).
15. W. Carter, R. Scott, and M. Magat, *J. Am. Chem. Soc.*, **68**, 1480 (1946).
16. R. Scott, W. Carter, and M. Magat, *J. Am. Chem. Soc.*, **71**, 220 (1949).
17. A. Scheidegger, *The Physics of Flow through Porous Media*, University of Toronto Press, Toronto, Canada, 1960.
18. W. L. Ingmanson and B. D. Andrews, *Tappi*, **46**, 150 (1963).
19. R. Bird, W. Stewart, and E. Lightfoot, *Transport Phenomena*, Wiley, New York, 1960, Chap. 6.
20. H. Hasimoto, *J. Fluid Mech.*, **5**, 317 (1959).

Résumé

Un modèle mathématique est proposé dans lequel une molécule polymérique hypothétique est considérée comme une sphère poreuse. L'écoulement fluide à travers la sphère obéit à la loi de Darcy alors que l'équation du mouvement de fluage sont utilisées en dehors de la sphère. Des équations sont dérivées qui permettent de relier la perméabilité et le rayon de la sphère aux propriétés hydrodynamiques des solutions diluées du polymère. En confrontant ce modèle aux résultats expérimentaux, on trouve que le modèle malgré sa simplicité peut être utile pour expliquer le comportement hydrodynamique des molécules qui sont fortement branchées ou pontées.

Zusammenfassung

Ein mathematisches Modell wurde vorgeschlagen, das ein hypothetisches Polymermolekül als poröse Kugel behandelt. Der Fliessvorgang innerhalb der Kugel gehorcht dem Gesetz von Darcy, während ausserhalb der Kugel die Gleichungen für Kriechbewegung verwendet werden. Es werden Gleichungen abgeleitet, die die Permeabilität und den Kugelradius mit den hydrodynamischen Eigenschaften verdünnter Lösungen des Polymeren verknüpfen. Bei der Überprüfung mittels experimenteller Daten wurde gefunden, dass das Modell trotz seiner Einfachheit für die Erklärung des hydrodynamischen Verhaltens von stark verzweigten und vernetzten Molekülen von Nutzen sein kann.

Received January 27, 1967

Revised April 26, 1967

Prod. No. 5438A

Synthesis and Properties of Polyimidazopyrrolones*

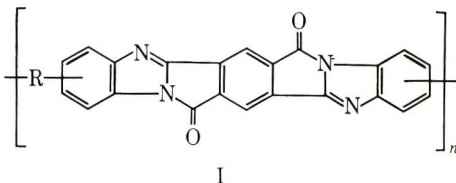
VERNON L. BELL and ROBERT A. JEWELL, *Langley Research Center, National Aeronautics and Space Administration, Langley Station, Hampton, Virginia 23365*

Synopsis

The preparation of polyimidazopyrrolones by three general synthetic methods has been presented. The effects of structure, conversion temperature, and conversion environment were determined. The polyimidazopyrrolones were shown to retain useful mechanical properties at elevated temperatures, after severe chemical treatment and after unusually high exposure to ionizing radiation. Thermogravimetric analysis of the polymers indicated the effect of structure on oxidative stability was relatively minor; furthermore, the relative stabilities of a series of eight polymers in air were not directly comparable to the order of stability in a vacuum environment.

INTRODUCTION

A number of aromatic-heterocyclic polymers with exceptional chemical and physical stability have been discovered during the past decade. More recent efforts have extended the aromatic-heterocyclic concept to a class of polymers derived from tetrafunctional acids and amines, thus leading to polymers with aromatic and heterocyclic rings fused into a polymeric structure which approaches a "ladder" or two-strand arrangement. These polymers (I), referred to as polyimidazopyrrolones,^{1,2} polybenzoylenebenzimidazoles,^{3,4} and polybenzimidazobenzophenanthrolines,⁵ not only have excellent resistance to thermal degradation but also withstand unusually high levels of ionizing radiation.^{1,2}



This combination of properties has generated considerable effort to study the polymers to determine their suitability for application as spacecraft materials. The research presented herein has extended our investigation of the polyimidazopyrrolones to encompass alternative methods of synthesis, variations in polymer structures, and the effects of conversion (curing)

* Paper presented in part at the 153rd National Meeting of the American Chemical Society, Miami Beach, Florida, April 9-14, 1967.

and environmental conditions on the useful properties of the polymers. Certain questions, such as which isomeric arrangements prevail in the polymer structures and the relative stabilities of such isomers, remain unanswered; nevertheless, the possible utility of this unusual polymer class has been expanded and the results are being used to advantage in the fabrication of the polymers.

RESULTS AND DISCUSSION

Monomer Synthesis

The two most frequently used aromatic dianhydrides in this study, pyromellitic dianhydride (PMDA) and 3,3',4,4'-benzophenone tetracarboxylic acid dianhydride (BTDA), were obtained from commercial sources and purified as previously described.² 3,3'-Diaminobenzidine was also obtained commercially and was recrystallized from water. 1,2,4,5-Tetraaminobenzene was purified as the tetrahydrochloride salt from hydrochloric acid.

Three other tetraamines used in this work 3,3',4,4'-tetraaminodiphenyl ether (TADPO), 3,3',4,4'-tetraaminodiphenylmethane (TADPM), and 3,3',4,4'-tetraaminobenzophenone (TABP), were synthesized by the general procedure described in the literature.⁶ This method involved acetylation and nitration of the corresponding 4,4'-diamino compounds, followed by deacetylation and catalytic reduction of the dinitro diamines to the tetraamines.

In our synthetic work, we found that catalytic reduction of the dinitro diamines with platinum oxide, specifically in ethyl acetate, led to better yields and products of higher purity than the usual tin or stannous chloride reductions which involved a difficult separation of the tetraamines from tin salts. The preferred method for preparation of 3,3',4,4'-tetraaminobenzophenone was to oxidize 4,4'-diacetamino-3,3'-dinitrodiphenylmethane to 4,4'-diacetamino-3,3'-dinitrobenzophenone with chromic acid in glacial acetic acid, followed by deacetylation and hydrogenation.

2,5-Dicarbomethoxyterephthaloyl chloride was prepared by dissolving pyromellitic dianhydride in refluxing methanol. The *para* isomer, which was isolated by recrystallization, was then reacted with thionyl chloride.

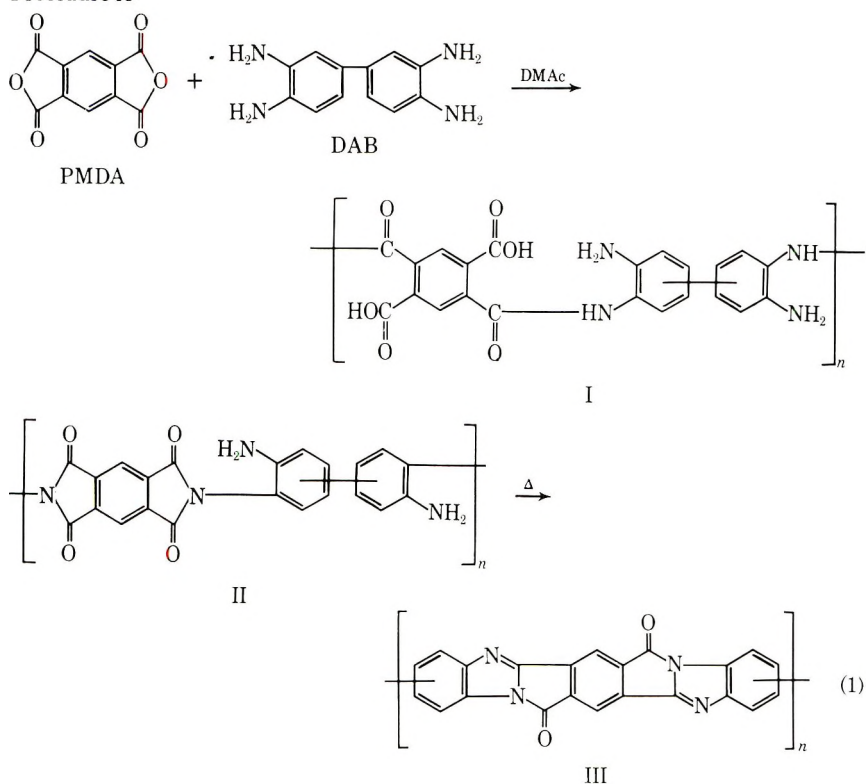
Polymerization

Three general methods of polymerization were used to prepare the polyimidazopyrrolones. Procedure A involved the addition of a solution of dianhydride to a solution of tetraamine, utilizing aprotic solvents of the amide type, e.g., *N,N*-dimethylformamide (DMF), *N,N*-dimethylacetamide (DMAc), *N*-methyl-2-pyrrolidinone (NMP), dimethyl sulfoxide (DMSO), and hexamethylphosphoramide (HMP). Procedure B was carried out by the reaction of dianhydride solution with a slurry of the tetrahydrochloride salt of the tetraamine, in the presence of an acid acceptor. Procedure C

also utilized the tetraamine tetrahydrochloride salt and 2,5-dicarboxymethoxyterephthaloyl chloride instead of pyromellitic dianhydride.

In each procedure the initial reaction of polymerization resulted in a soluble polyamide intermediate I, substituted with carboxylic acid (or ester) and amino groups. Thermal conversion of polymer I proceeded through an aminopolyimide structure II to the fused imidazopyrrolone ring structure III. The mechanism for the sequence was based primarily on model compounds^{3,4} and infrared spectroscopy.^{2,4} The reaction schemes for the three polymerization procedures are as given in eqs. (1)–(3) for the example of the pyromellitic dianhydride–diaminobenzidine polymer system.

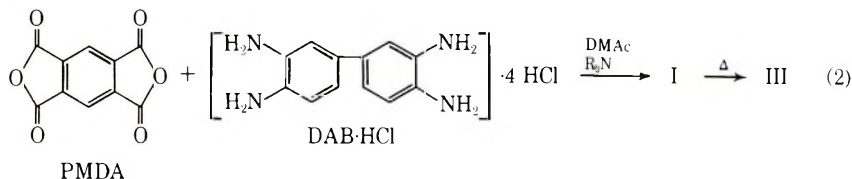
Procedure A:



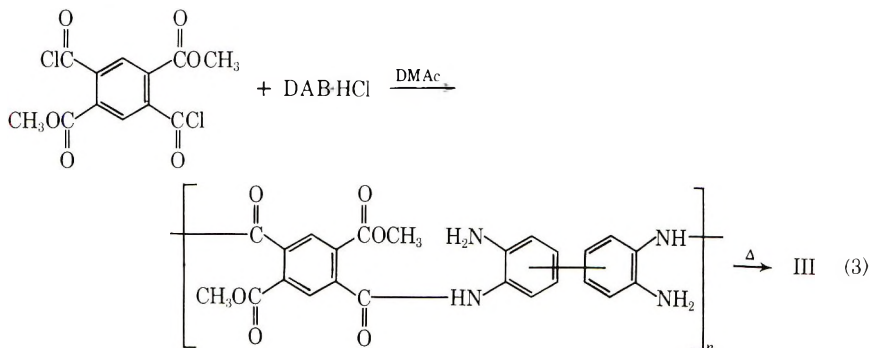
No attempt has been made to specify any definite isomer arrangements, which could not only be expected from random participation of the tetraamine in the polymerization, but could also result from *cis* and *trans* isomers about the basic dianhydride unit.

Procedure A. The major portion of this investigation utilized procedure A for polymer synthesis. Although this method was seemingly simple in operation, in actuality it required adherence to a rather rigid set of conditions to obtain high molecular weight polymer. One of the difficulties encountered resulted from the relatively poor solubility of pyromellitic

Procedure B:



Procedure C:

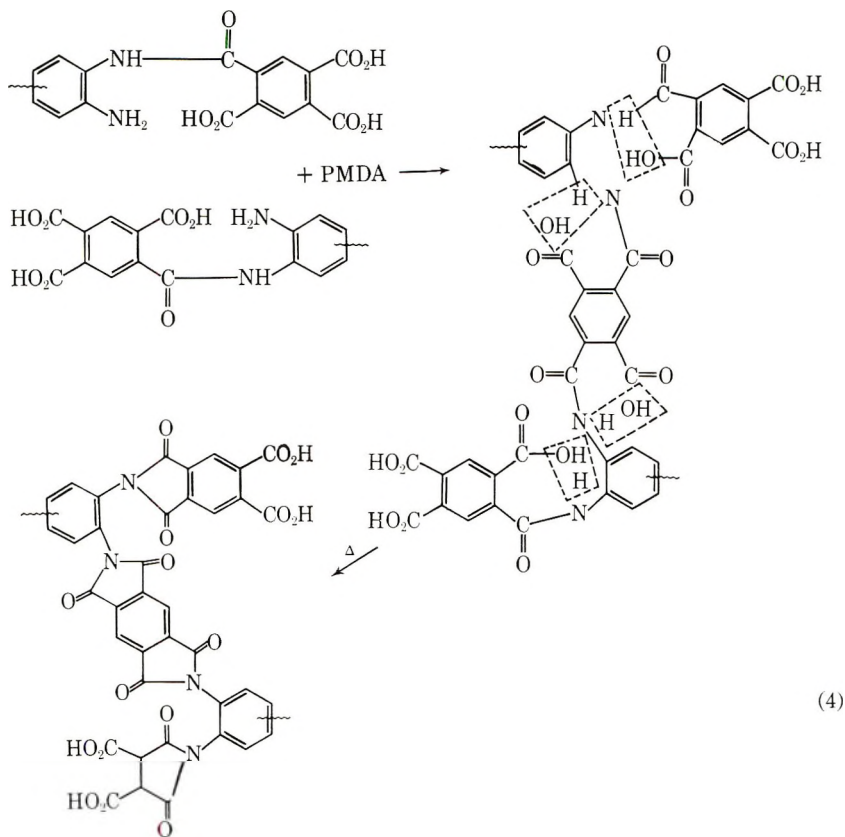


dianhydride in the amide solvents (<10%). Variations in the polymerization procedure which led to the presence of any solid PMDA in tetraamine solution inevitably led to gel formation. Examples were the addition of large portions of solid PMDA to tetraamine solution, and the addition of PMDA solution to cold tetraamine solution which resulted in precipitation of the anhydride before reaction could occur. Reversal of the order of addition, that is, addition of tetraamine solution to the anhydride solution, always led to massive gelation. These observations led to the conclusion that high concentrations of dianhydride at any time during the polymerization were to be avoided, thus making efficient stirring a necessity.

The polymerization was conveniently carried out in a Waring Blender and blanketed with nitrogen. The most rapid technique involved addition of 95% of the theoretical amount of dianhydride solution at one time to the rapidly stirred tetraamine solution. The anhydride ring-opening reaction was rapid, resulting in a rise in temperature to 35–50°C., depending on concentrations. Moderate cooling was occasionally used, but with caution, since excessively cooled surfaces which precipitated anhydride at the surfaces led to gel formation. No adverse effect due to the heat of reaction was observed, even when applied to gallon-size polymerizations. After the initial low molecular weight polymer solution was allowed to cool to near room temperature, the viscosity of the solution was increased by careful, dropwise addition of the remaining dianhydride solution. The viscosity was monitored either visually or with a Brookfield viscometer. The amount of dianhydride required to reach intrinsic viscosities ranging from about 0.5 to 1.5 dl./g., varied depending on the purities of the intermediates and solvents. The use of extremely pure starting materials required excesses of dianhydride as little as 1–2% beyond the

theoretical amount to reach the maximum solution viscosity attainable before gelation (at a 10% polymer solids concentration). On the other hand, the use of less rigorously purified intermediates required amounts of excess dianhydride of 5–10% to reach a comparable viscosity level. Nevertheless, such polymer solutions could be used to prepare solvent-cast films which had tensile properties and thermal stabilities indistinguishable from those obtained using high purity materials.

It was assumed that this ability to polymerize to high viscosity in spite of the presence of chain-terminating impurities was related to the presence of the free amino groups on the polyamide. Although impurities such as water would be expected to terminate a chain by hydrolysis of an anhydride group, an increase in molecular weight could still be achieved by the reaction of a molecule of excess dianhydride with free amino groups on two terminated chains. This mechanism would not only introduce an element of nonlinearity into the polymer structure, but would also create imide groups in the chain and crosslinks at the expense of imidazopyrrolone units. This mechanism is illustrated in eqs. (4) for the polymerization of PMDA and DAB.



An unusual feature of the polymerization was the observation that the intrinsic viscosities attainable from a practical standpoint appeared to reach a limit near 2.0 when polymer solutions were prepared with solids contents of 10%. Careful attempts to increase the viscosities to even higher levels always led to gelation. The cause of this was not definitely established; however, it was felt that at the initial stages the gelation was simply polymer insolubility, since dilution of the "pseudo-gel" restored it to a smooth solution.

Procedure B. This polymerization procedure, which employed the tetrahydrochloride salts of the tetraamines, was found to be useful for polymerization of the most readily oxidized free tetraamines. A notable example was 1,2,4,5-tetraaminobenzene. The experimental procedure was similar to procedure A except that sufficient tertiary amine was included to accept the hydrogen chloride which was generated upon reaction of the dianhydride with the tetraamine hydrochloride salt. While procedure A was an extremely rapid reaction, the use of the tetraamine hydrochlorides led to a much slower polymerization. Consequently, ample time was allowed for reaction to occur. The reaction time was of the order of 2-6 hr. for DMAc-soluble tetraamine tetrahydrochlorides, such as 3,3'-diaminobenzidine; with tetraaminobenzene tetrahydrochloride, which was insoluble in DMAc, dianhydride solutions had to be added dropwise over a 10-20 hr. time period.

Elemental analyses indicated hydrogen chloride was not retained in the thermally cured (300°C.) polymer; thus, it was probably lost via sublimation of the pyridine salt. Insofar as they were examined, the polymers prepared by this procedure appeared to be identical to those prepared from the free tetraamine, since the thermogravimetric analyses, infrared spectra,^{1,2} and tensile properties of films from both types of polymers were essentially identical.

Procedure C. A variation of the method described above was to use the symmetrical dimethyl ester diacid chloride of pyromellitic acid, rather than the dianhydride, for reaction with tetraamine hydrochloride salts. Amide-type solvents such as DMAc were used but, in contrast to procedure A, tetraamine tetrahydrochloride salts were employed inasmuch as reaction of the acid chloride with the free tetraamines led to a very rapid reaction which resulted in insoluble polymer. However, the use of tertiary amines as acid acceptors was not essential. Interesting, too, is the fact that addition of the stoichiometric amount of pyridine to a solution of tetraamine tetrahydrochloride in dimethylacetamide did not automatically produce the free base. Thus, it appears that the tertiary amine functioned primarily as a catalyst while the amide solvent employed functioned as the acid acceptor.

Polymer Properties

A summary of the polymers which were prepared in this investigation, together with the solution properties of the intermediate polyamide stage, is

TABLE I
Solution Properties of Polyimidazopyrrolones at Polyamide Stage

Polymer ^a	Method ^b	Solvent	Viscosity of polyamide ^c	Molecular weight M_n ^d
PMDA-DAB	A	DMF	0.99	—
PMDA-DAB	B	DMAc	0.47	—
PMDA-TADPO	A	DMAc	0.59	8,000
PMDA-TADPM	A	DMAc	0.74	—
PMDA-TABP	A	DMF	0.64	14,300
PMDA-TAB	C	DMAc	0.77	—
BTDA-DAB	A	DMF	1.45	—
BTDA-TADPO	A	DMAc	1.11	14,700
BTDA-TADPM	A	DMAc	0.72	—
BTDA-TABP	A	DMF	0.43	13,800

^a PMDA = pyromellitic dianhydride; BTDA = 3,3',4,4'-benzophenone tetracarboxylic dianhydride; DAB = 3,3'-diaminobenzidine; TADPO = 3,3',4,4'-tetraaminodiphenyl ether; TADPM = 3,3',4,4'-tetraaminodiphenylmethane; TABP = 3,3',4,4'-tetraaminobenzophenone; TAB = 1,2,4,5-tetraaminobenzene.

^b Procedure A, dianhydride + tetraamine; Procedure B, dianhydride + tetraamine tetrahydrochloride; Procedure C, diester diacyl chloride + tetraamine tetrahydrochloride.

^c Intrinsic viscosity in the specified solvent at 25°C.

^d Via membrane osmometry in the polymerization solvent at 37°C.

given in Table I. The viscosities cited should be considered typical rather than optimum, since some of the polymer combinations were prepared numerous times with variations in procedure (A, B, or C) and conditions, resulting in corresponding variation in solution properties.

Mechanical Properties of Films. Films were conveniently prepared by casting the intermediate polyamides onto glass plates, while regulating the

TABLE II
Typical Tensile Properties of Polyimidazopyrrolone Films^a

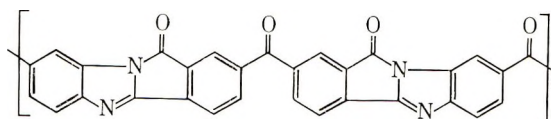
Polymer ^b	Tensile strength, psi	Elongation, %	Tangent modulus, psi	Color
PMDA-DAB	20,400	2.8	950,000	Deep red
PMDA-DAB ^c	13,600	2.0	810,000	Deep red
PMDA-TADPO	21,800	4.8	812,000	Red
PMDA-TADPM	13,900	3.9	534,000	Orange
PMDA-TABP	13,300	2.6	593,000	Yellow
BTDA-DAB	20,300	4.3	601,000	Red
BTDA-TADPO	18,900	3.8	627,000	Red-orange
BTDA-TADPM	9,700	1.9	599,000	Yellow
BTDA-TABP	12,000	3.1	498,000	Yellow

^a Films cast from amide solvents onto glass plates, dried, and cured in air at temperatures progressing to 300°C. Final film thicknesses ranged from 0.7 to 1.0 mils.

^b See Table I for explanation of abbreviations.

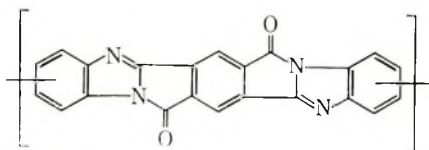
^c Polymer prepared from PMDA and tetrahydrochloride salt of DAB (procedure B).

thickness with doctor blades. The solvent was removed and the films were converted to the final imidazopyrrolone stage by heating in forced-draft air ovens at temperatures progressing up to 300–325°C. The tensile properties of some of the films are listed in Table II. The data are not necessarily the highest values obtained, but rather reflect general trends for the specific structural compositions. Although considerable variations in film quality were observed, the tensile strengths were excellent, while the elongations were consistently very low and the modulus values very high. The latter two features, as a measure of stiffness, were not unexpected for such rigid, ladderlike polymeric structures although it is believed that an indeterminate amount of crosslinking was present. Nevertheless, the film properties were for the most part reflective of the imidazopyrrolone units since the tangent modulus, a measure of chain stiffness and rigidity, decreased with anticipated increases in polymer chain flexibility. For example, films prepared from both the benzophenone dianhydride and tetraamine (BTDA-TABP) had tangent moduli of about 500,000 psi, reflecting the structure of only four fused rings separated by carbonyl groups:



BTDA-TABP

On the other hand, the PMDA-DAB system resulted in films with moduli of over 900,000 psi, thus reflecting the structure of seven fused rings separated by a single carbon-carbon bond:



The colors of the films also emphasized the conjugative effect of the fused ring structures, those prepared using PMDA being darker than those from the benzophenone anhydride. The extreme case was the deep black (suggestive of extensive ladder segments) films from the PMDA-tetraaminobenzene (TAB) polymer. No reliable mechanical property data were obtained for this polymer system due to film brittleness.

Most of the films were cured in a forced-draft air oven. As seen from the results of Table III, no significant differences (within experimental error) in film tensile properties were observed when conversions were made in air, nitrogen, and vacuum.

However, it was observed that the tensile properties of films were quite dependent upon the degree of conversion. As noted in Table IV, there

TABLE III
Effect of Heating Environment on Film Tensile Properties^a

Polymer	Heating atmosphere	Tensile strength, psi	Elongation, %	Modulus, psi
PMDA-DAB	Air	15,600	4.0	697,000
PMDA-DAB	Vacuum	15,800	3.8	681,000
PMDA-DAB	Nitrogen	14,100	2.1	860,000

^a Films were cured at 250°C. for 3 hr.

TABLE IV
Effect of Curing Temperature on Film Properties^a

Polymer	Curing temperature, °C. ^b	Strength, kpsi		Modulus, kpsi	Elongation, %
		Yield	Tensile		
BTDA-TADPO	150	11.1	16.3	509	5.4
BTDA-TADPO	225	13.1	17.1	545	4.1
BTDA-TADPO	300	14.7	18.9	627	3.8

^a All samples from single sheet of 1-mil film.

^b Curing time, 1 hr.

TABLE V
Effect of Temperature on Tensile Properties of PMDA-DAB Films^a

Testing temperature, °C.	Yield strength, psi	Tensile strength, psi	Elongation, %	Tangent modulus, psi
25	12,900	17,000	2.8	857,000
100	9,800	15,800	3.7	713,000
200	7,400	11,500	3.7	526,000

^a Films were prepared at 225°C. for 1 hr.

was a general increase in tensile strength and modulus and a decrease in the elongation as the conversion temperature was increased.

The retention of tensile properties of films at elevated temperatures was excellent as seen in Table V. PMDA-DAB films (0.6 mil) retained 70% of the room temperature tensile strength when tested at 200°C. in an air atmosphere. The retention of elongation as the temperature was increased from 100 to 200°C. might be attributed to an unknown amount of cross-linked structure.

Radiation Stability. An especially attractive characteristic of the polyimidazopyrrolones was their excellent resistance to ionizing radiation. Previous studies of these polymers noted virtually no adverse effect on tensile properties of PMDA-TADPO films in vacuum with 2 M.e.v. electron doses up to 10,000 Mrad, and PMDA-DAB films in air at up to 22,000 Mrad of 3 M.e.v. electrons.² These results have been extended to irradiation

TABLE VI
Effect of Radiation on PMDA-DAB Films^a

Dose, Mrad ^b	Yield strength, psi	Tensile strength, psi	Elongation, %	Tangent modulus, psi
0	13,300	16,700	3.2	811,000
1,100	14,200	20,900	4.5	883,000
5,500	14,400	20,900	3.9	889,000
11,000	14,600	19,100	3.1	891,000
21,000	15,600	22,200	3.3	988,000
58,300	12,500	15,300	2.7	826,000

^a Films converted at 300°C.; environment temperature during irradiation was approximately 250°C.

^b 3 M.e.v. electrons at a dose rate of 5500 Mrad/hr.

tion in air with 3 M.e.v. electrons at a dose rate of 5,500 Mrad/hr. and exposures ranging to 58,000 Mrad. The data in Table VI indicate that although some degradation may have begun after 21,000 Mrad, the tensile properties after the extreme exposure of 58,000 Mrad were still nearly equivalent to the initial values. Therefore, it could be expected that such material would remain functional if utilized in a high radiation environment.

Thermal Stability. The thermal stabilities of the polyimidazopyrrolones were measured in air and in vacuum using thermogravimetry (TGA). The TGA weight loss curves for the polymers when heated in air are shown in Figure 1. The samples used were 2.0-mg. portions of films (0.6–1.0 mil thick) which had been cured for 1 hr. at 300°C. Samples were pre-treated by aging for 30 min. at 100°C., after which they were heated at a rate of 5°C./min.

The shaded area within the bounds of the two curves contains the TGA curves for all eight polymer combinations based on PMDA and BTDA as the dianhydrides and DAB, TADPO, TADPM, and TABP as the tetraamines. It was concluded that the effect of structure on the thermal (or

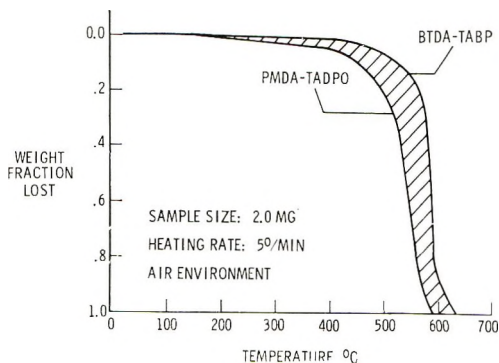


Fig. 1. TGA weight loss of polyimidazopyrrolones in air.

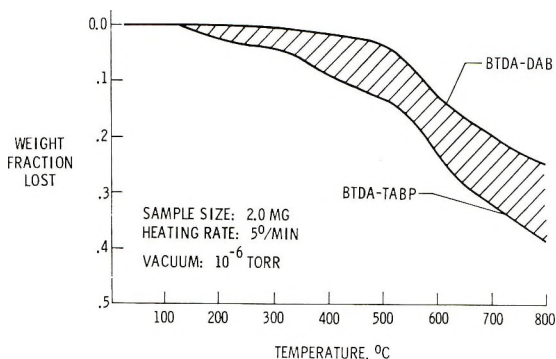


Fig. 2. TGA weight loss of polyimidazopyrrolones in vacuum.

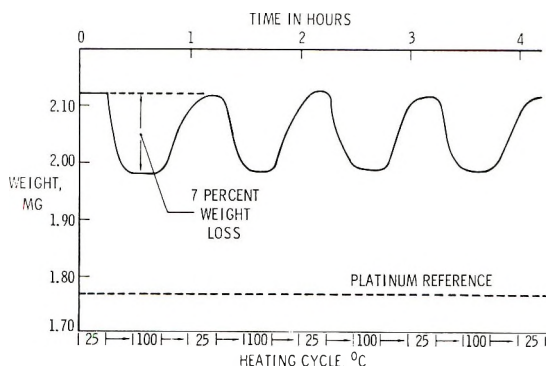


Fig. 3. Loss and regain of water by PMDA-DAB film.

oxidative) stability of the polymers in air was only moderate, since in the regions of maximum rate of weight loss, the difference between the most stable polymer (BTDA-TABP) and the least stable (PMDA-TADPO) was of the order of 40–50°C.

Figure 2 shows the weight loss behavior of the same eight polyimidazopyrrolones when they were heated in vacuum (10^{-6} torr). Once again, the TGA curves for all eight combinations have been encompassed within the bounds of the shaded area. However, the polymer which had displayed the lowest relative weight loss in air (BTDA-TABP) was observed to lose the most weight when heated in a high vacuum environment.

There were indications that the fully converted polyimidazopyrrolones readily formed a dihydrated structure. Figure 3 shows the weight loss as a 0.7-mil PMDA-DAB film, previously cured at 350°C. for 2 hr., was cycled in air through four stages: (a) heated from 25°C. to 100°C., (b) maintained at 100°C., (c) cooled from 100°C. to 25°C., and (d) maintained at 25°C. Each stage was 15 min. in duration. The figure indicates a ready gain of 7% upon cooling in the atmosphere and an equally facile loss of the same amount of water upon reheating to 100°C. The theoretical percentage of water for $\text{PMDA-DAB} \cdot 2\text{H}_2\text{O}$ is 9%. The formation of a weakly com-

TABLE VII
Effect of 2*N* NaOH and 96% H₂SO₄ Immersion
on Properties of PMDA-DAB Films^a

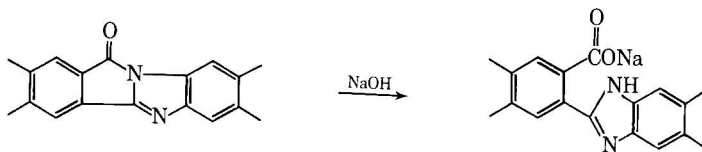
Exposure ^b	Tangent modulus, psi	Elongation, %	Tensile strength, psi
Untreated	612,000	5.5	22,300
2 <i>N</i> NaOH	393,000	7.5	12,800
96% H ₂ SO ₄	595,000	4.6	17,000

^a One-mil films, cured at 250°C. for 1 hr.; Instron measurements made with 1-in. gage length specimens.

^b Specimens immersed at room temperature for 1 hr., washed with water, and dried 1 hr. at room temperature.

plexed dihydrate was further substantiated by elemental analyses and vapor phase chromatography of trapped volatiles.

Chemical Stability. An unusual resistance to corrosive chemicals was found for the polyimidazopyrrolones. The 1-mil film retained its original shape and integrity after immersion for 2 days at room temperature in 2*N* sodium hydroxide solution, concentrated sulfuric acid, and yellow fuming nitric acid. Although it is most probable that this insolubility is related to the indeterminate amount of crosslinking, nevertheless this property could be invaluable for applications of the polymers. The retention of useful tensile properties of 1-mil PMDA-DAB films after 1 hr. immersion in 2*N* sodium hydroxide solution and concentrated sulfuric acid can be seen from the results in Table VII. After treatment, the films were washed in distilled water and dried at room temperature for 1 hr. While the sulfuric acid treatment appeared to show no evidence of severe degradation, the decrease in modulus and increase in elongation for the sodium hydroxide-treated samples indicated a significant effect on tensile properties. In addition, the deep red color of the untreated films changed to a light yellow-brown color. In contrast, films from a supposedly linear, uncrosslinked aromatic polyimide were completely dissolved by the identical caustic and acidic exposures. A possible explanation for the chemical reaction, though not investigated, might be hydrolysis of the imidazopyrrolone structure to a carboxylic-substituted polybenzimidazole structure.⁷



EXPERIMENTAL

Properties

Intrinsic Viscosity. Viscosity measurements were performed with Ubbelohde viscometers at 25°C. and the solvents in which the polymers

were prepared (DMAc and DMF). The intrinsic viscosity was measured by means of a four-point extrapolation to infinite dilution.

Molecular Weights (\bar{M}_n). Number-average molecular weights were measured in dimethylacetamide at 37°C. by using a Mechrolab 501A membrane dynamic osmometer.

Thermogravimetric Analysis (TGA). The thermal behaviors of the polyimidazopyrrolones were investigated by use of a null-balancing automatic recording electrobalance (Cahn RG Electrobalance) using films of 2.05 ± 0.03 mg. sample size. Vacuum measurements were made at a pressure of 10^{-6} torr maintained by a 250 l./sec. capacity ion pump.

Differential Thermal Analysis (DTA). These measurements were made with a Du Pont 900 differential thermal analyzer.

Radiation. Polymer films were irradiated in air and in evacuated (10^{-6} torr), sealed Pyrex tubes with 3×10^6 electron-volt (3 M.e.v.) electrons from a 3 M.e.v. Dynamitron.

Mechanical Properties. Mechanical properties were determined on an Instron tensile tester by using film strips 0.5 in. wide and having a gage length of 3.0 in. at a crosshead speed of 0.2 in./min.

Monomer Synthesis

Pyromellitic dianhydride and 3,3',4,4'-benzophenone tetracarboxylic acid dianhydride were obtained from commercial sources and purified by sublimation as reported earlier.² 3,3'-Diaminobenzidine and 1,2,4,5-tetraaminobenzene tetrahydrochloride were obtained from Burdick and Jackson Laboratories, Inc., Muskegon, Michigan, and were purified by reported methods.² Dimethylformamide was obtained from Burdick and Jackson Laboratories, Inc. and was used without additional purification.

3,3',4,4'-Tetraaminodiphenyl Ether (TADPO). This tetraamine was synthesized by a general procedure involving diacetylation and dinitration of *p,p'*-oxydianiline with 70% nitric acid in acetic anhydride at 10–15°C. in 65% yield, followed by deacetylation with Claisen's alkali⁸ to give an 81% yield of 4,4'-diamino-3,3'-dinitrodiphenyl ether. This compound could be reduced with tin and hydrochloric acid to the tetraamine, but the difficulty in completely removing tin salts from the free base made catalytic hydrogenation a preferred method. Catalytic hydrogenation was accomplished by reducing 72.5 g. (0.25 mole) of 4,4'-diamino-3,3'-dinitrodiphenyl ether in a stirred Parr reactor with the use of 1.25 liters of ethyl acetate and 4 g. of 5% platinum-on-carbon catalyst. A pressure of 50 psig and ambient temperature (up to 50°C.) was used. The insoluble gray crystals were recrystallized from water with charcoal treatment to give 35.7 g. (62%) of tan flakes of 3,3',4,4'-tetraaminodiphenyl ether, m.p. 151–152°C. (lit.⁶ m.p., 149.5–151°C.).

3,3',4,4'-Tetraaminodiphenylmethane (TADPM). The same procedure employed for preparation of TADPO was used successfully to prepare TADPM. Acetylation of 198 g. (1.0 mole) *p,p'*-methylenedianiline in refluxing 1:1 glacial acetic acid–acetic anhydride for 2 hr. gave 264 g. (95%)

of 4,4'-bismethylenediacetanilide, a yellow solid, m.p. 234–236°C. (lit.⁹ m.p. 237°C.). Nitration of 264 g. (0.95 mole) of the diacetylated compound was performed by dropwise addition of 240 ml. of 70% nitric acid to a stirred slurry of the compound in 2.1 liters of acetic anhydride, the temperature being maintained at 12–15°C. A yield of 215 g. (63%) of 4,4'-diacetamino-3,3'-dinitrodiphenylmethane was obtained as a yellow solid, m.p. 271–273°C., after recrystallization from dimethylacetamide.

ANAL. Calcd. for $C_{17}H_{16}N_4O_6$: C, 54.84%; H, 4.33%; N, 15.05%. Found: C, 54.94%; H, 4.36%; N, 14.58%.

Deacetylation of the above diacetaminodinitro compound was accomplished using Claisen's alkali, by adding 205 g. (0.55 mole) of the compound to a stirred solution of 315 ml. of alcoholic potassium methoxide. Stirring was continued for 15 min. while heating the thick mixture on a steam bath. Following the addition of 300 ml. of water, stirring and heating was continued for 15 min. The mixture was cooled in ice water, the dark brown solid was collected by filtration, and the product was washed repeatedly with water. Recrystallization of the 4,4'-diamino-3,3'-dinitrodiphenylmethane from *n*-propanol gave 151 g. (95%) of orange crystals, m.p. 234–236°C.

ANAL. Calcd. for $C_{13}H_{12}N_4O_4$: C, 54.16%; H, 4.20%; N, 19.44%. Found: C, 54.09%; H, 4.18%; N, 18.68%.

The corresponding tetraamine was obtained by catalytic hydrogenation of 50 g. (0.17 mole) of the above dinitro compound in a stirred Paar reactor by using 1000 ml. ethyl acetate and 2.0 g. of 5% platinum on carbon. Hydrogenation was carried out at 50 psig and ambient temperature (up to 55°C.). The insoluble product was recrystallized twice from water, with charcoal treatment, to give 20 g. (50%) of light tan crystals of 3,3',4,4'-tetraaminodiphenylmethane, m.p. 137.5–139°C. (lit.⁹ m.p., 137–138°C.).

ANAL. Calcd. for $C_{13}H_{16}N_4$: C, 68.39%; H, 7.06%; N, 24.54%. Found: C, 68.39%; H, 7.09%; N, 24.57%.

3,3',4,4'-Tetraaminobenzophenone (TABP). The preferred method for preparation of the tetraamine was by oxidation of 4,4'-diacetamino-3,3'-dinitrodiphenylmethane followed by deacetylation and hydrogenation.

The oxidation was performed by dissolving 105 g. (0.28 mole) of the diacetamino compound in 1700 ml. of refluxing glacial acetic acid. A total of 150 g. of chromium trioxide was added in small portions sufficient to control the oxidation. The solution was refluxed for 4 hr. after the addition was complete. The crude product was precipitated by dilution with 2 liters of water. The yellow solid was washed repeatedly with water, followed by a final wash with 1:1 ethanol-water. This solid was then hydrolyzed with Claisen's alkali, and the dinitrodiamine was sublimed at 280–300°C./0.5 mm. Hg to give 40 g. (47%) of 4,4'-diamino-3,3'-dinitrobenzophenone as yellow solid or red needles (depending on the crystalline modification), m.p. 293°C. (lit.¹⁰ m.p. 293.5°C.).

The dinitrodiamine (20 g., 0.066 mole) was reduced in a stirred Paar reactor at 50 psi and 55–60°C. with the use of 700 ml. of ethyl acetate as solvent and 3 g. of 5% platinum on carbon. The resulting mixture was cooled and the solid was recrystallized, first from water and then from pyridine-benzene to give 10.4 g. (65%) of 3,3',4,4'-tetraaminobenzophenone as yellow crystals, m.p. 217°C. (lit.¹⁰ m.p., 217°C.).

2,5-Dicarbomethoxyterephthaloyl Chloride. Sublimed pyromellitic dianhydride, 54.5 g. (0.25 mole), was added to 500 ml. of dry methanol and the mixture was refluxed until the anhydride had dissolved. The clear solution was concentrated to approximately 250 ml. and allowed to stand at room temperature for 24 hr. The solid which precipitated was collected by filtration. This crop of white solid was recrystallized twice from methanol. The resulting product, 2,5-dicarbomethoxyterephthalic acid, melted at 238°C.

A 25-g. portion (0.089 mole) of the diester diacid was added to 75 ml. of thionyl chloride and several drops of dimethylformamide were added. The mixture was refluxed for 4½ hr. after which time all of the diacid had dissolved. The excess thionyl chloride was removed by distillation under reduced pressure. The crystalline residue was then recrystallized twice from a benzene-heptane solution. The white crystals (21.8 g., 77%) melted at 136.5–138°C.

Anal. Calcd. for $C_{12}H_8O_6Cl_2$: C, 45.16%; H, 2.56%; Cl, 22.22%. Found: C, 46.14%; H, 2.76%; Cl, 21.28%.

Polymerization

Procedure A. A typical example of this method of polymerization is demonstrated by the reaction of pyromellitic dianhydride (PMDA) with 3,3'-diaminobenzidine (DAB).

A solution of 21.4 g. (0.10 mole) of DAB in 190 ml. of DMAc was prepared in a Waring Blendor, which was blanketed with nitrogen. A solution of 21.8 g. (0.10 mole) of PMDA in 195 ml. of DMAc was prepared and 190 ml. of this solution was added quickly to the rapidly stirred DAB solution. The resulting polymer solution was stirred slowly for 15–30 min., after which time it had cooled from 35–40°C. back to near room temperature. Then the remainder of the PMDA-DMAc solution was added in a dropwise manner. At this point (1:1 PMDA-DAB) the straw-yellow polymer solution was moderately viscous if very pure starting materials and solvents were used. The solution viscosity could be increased to a level which depended on the end use desired. This was accomplished by slow, dropwise addition from a solution of 1.09 g. (0.005 mole) of PMDA in 10 ml. of DMAc. The viscosity could be monitored by eye or by some more precise method, such as a Brookfield viscometer. The maximum viscosity which could be attained without attendant gelation resulted in polymer solution that "tailed" when dropped from a medicine dropper or pipet. However, extreme caution had to be exercised to prevent gelation due to the addition

of too great an excess of PMDA solution. At this stage, the intrinsic viscosity in DMAc at 25°C. ranged from 1.0 to 1.5 dl./g. The polymer solution was then centrifuged to remove heterogeneous matter and was either used for further study or stored under nitrogen at -20°C.

Solid polymer at this polyamide acid amine stage was obtained by precipitation with a nonsolvent such as acetone, ethanol, or benzene. After the powder was washed well with the nonsolvent, it was dried *in vacuo* at room temperature. If drying was complete, it was usually not possible to obtain complete redissolution in the amide-type solvents.

Procedure B for PMDA-DAB. The same polymer described in procedure A (PMDA-DAB) was prepared by using 3,3'-diaminobenzidine tetrahydrochloride (DAB·HCl).

A solution of 3.60 g. (0.01 mole) of DAB·HCl in 35 ml. of DMAc was prepared in a Waring Blendor jar, and the jar was blanketed with nitrogen. Pyridine (3.20 g., 0.041 mole) was added, after which approximately 90% of a solution of 2.18 g. (0.01 mole) of PMDA in 25 ml. DMAc was added at one time, with rapid stirring of the DAB·HCl-DMAc solution. The resulting solution was allowed to stir slowly for 2 hr., after which time the remainder of the PMDA solution was added dropwise. The resulting solution was allowed to stand overnight at room temperature. At this point (1:1 DAB·HCl-PMDA) the red-orange polymer solution was moderately viscous. A 4% excess of PMDA (0.09 g., 0.0004 mole) in 1 ml. of DMAc was added dropwise over a 4-hr. period. The intrinsic viscosity in DMAc at 25°C. was 0.47 dl./g. Films could be obtained by the usual solvent-casting techniques and cured by heating at temperatures progressing up to 300°C. Analysis of the polymer indicated no retention of hydrogen chloride in the polymer.

Procedure B for PMDA-TAB. Procedure B was used successfully to prepare the polyimidazopyrrolone from pyromellitic dianhydride and 1,2,4,5-tetraaminobenzene tetrahydrochloride (TAB·HCl).

A slurry of 5.45 g. (0.025 mole) of finely powdered TAB·HCl in 50 ml. of DMAc was prepared in a 250-ml. Erlenmeyer flask fitted with a serum bottle cap and a magnetic stirring bar. Before sealing the flask, nitrogen was passed into the slurry for 1-2 min. Then 7.9 g. (0.10 mole) of pyridine was added to the slurry via syringe through the serum bottle cap. Next a solution of 5.45 g. (0.025 mole) of PMDA in 50 ml. of DMAc was added via syringe in a slow, dropwise manner over about 10-20 hr., while the slurry was stirred magnetically.

Usually, when approximately 50-60% of the dianhydride solution had been added, a clear or slightly hazy solution resulted. If addition was too rapid, insoluble particles were formed. The complete addition of PMDA solution resulted in a light to moderately viscous polymer solution. The viscosity could be increased by the careful dropwise addition of 2-5% excesses of PMDA in DMAc. In this particular experiment, the addition of 0.16 g. (0.006 mole) of PMDA in 2 ml. DMAc resulted in PMDA-DAB polymer solution with an intrinsic viscosity of 0.45 dl./g. in DMAc at

25°C. Films could be prepared by casting the solution onto glass plates and drying the films in an air oven at 125°C. for 1 hr. and curing at 200°C./1 hr. The resulting black films were quite rigid and inflexible. Elemental analyses were inconclusive and indicative of incomplete cyclization to the polyimidazopyrrolone structure.

Procedure C for PMDA-DAB. A solution of 1.80 g. (0.005 mole) of 3,3'-diaminobenzidine tetrahydrochloride (DAB·HCl) in 10 ml. of DMAc was prepared in a 1-oz. serum bottle, equipped with a magnetic stirring bar and a serum bottle cap. A solution of 1.59 g. (0.005 mole) of 2,5-dicarbomethoxyterephthaloyl chloride in 12 ml. of DMAc was added to the stirred DAB·HCl solution via syringe. The light yellow solution increased markedly in viscosity to a clear, very thick solution over 2 hr. This polymer solution was cast onto a glass plate, and the solvent was removed by drying in an air oven at 125°C. for 1 hr. The resulting yellow film was then cured at 200°C for 1 hr. and 300°C. for 1 hr. The resultant deep red film was tough and stiff but flexible. The infrared spectrum was identical to that of the PMDA-DAB polymer prepared by procedures A and B.

Procedure C for PMDA-TAB. A solution of 1.55 g. (0.0049 mole) of 2,5-dicarbomethoxyterephthaloyl chloride in 15 ml. of DMAc was added dropwise over 3 hr. to a stirred slurry of 1.42 g. (0.0050 mole) of TAB·HCl in 10 ml. of DMAc in a sealed 1-oz. serum bottle. The resulting orange solution was very viscous ($[\eta] = 0.77$ dl./g. in DMAc at 25°C.). This polymer solution was cast onto a glass plate, and the resulting film was dried and cured in an air oven at 100°C. for 2 hr. and 300°C. for 1 hr. The infrared spectrum of the black, rigid film was essentially identical to that of the PMDA-TAB polymer film prepared by procedure B.

The authors express their appreciation to Mr. Howard L. Price for the mechanical property measurements, to Dr. George D. Sands for solution properties, and to Dr. Norman J. Johnston and Dr. George F. Pezdirtz for their helpful discussions of this work.

References

1. V. L. Bell and G. F. Pezdirtz, paper presented at 150th Meeting, American Chemical Society, Philadelphia, Pa., Sept. 14, 1965; *Polymer Preprints*, **6**, 747 (1965).
2. V. L. Bell and G. F. Pezdirtz, *J. Polymer Sci. B*, **3**, 977 (1965).
3. F. Dawans and C. S. Marvel, *J. Polymer Sci. A*, **3**, 3549 (1965).
4. J. G. Colson, R. H. Michel, and R. M. Paufler, *J. Polymer Sci. A-1*, **4**, 59 (1966).
5. R. L. Van Deusen, *J. Polymer Sci. B*, **4**, 211 (1966).
6. R. T. Foster and C. S. Marvel, *J. Polymer Sci. A*, **3**, 417 (1965).
7. J. Arient and J. Marham, *Collection Czechoslovak. Chem. Commun.*, **26**, 98 (1961).
8. P. F. Fanta and D. S. Tarbell, in *Organic Syntheses*, Coll. Vol. III, E. C. Horning, Ed., New York, 1955, p. 661.
9. J. Meyer and M. Rohmer, *Ber.*, **33**, 257 (1900).
10. P. J. Montague, *Ber.*, **48**, 1027 (1915).

Résumé

La préparation de polyimidazopyrrolones par trois méthodes synthétiques générales est présentée ici. Les effets de la structure, de la température de conversion et des conditions de conversion ont été déterminés. Les polyimidazopyrrolones conservent des

propriétés mécaniques utiles à des températures élevées après avoir subi des traitements chimiques sévères et une exposition anormalement élevée sur radiations ionisantes. L'analyse thermogravimétrique des polymères indique que l'effet de la structure sur la stabilité à l'oxydation est relativement faible; en outre, les stabilités relative d'une série de huit polymères dans l'air ne sont pas directement comparables à l'ordre des stabilités mesurées sous vide.

Zusammenfassung

Drei allgemeine synthetische Methoden zur Herstellung von Polyimidazopyrrolonen wurden dargelegt. Der Einfluss von Struktur, Umsetzungstemperatur und Umsetzungsmedium wurde bestimmt. Die Polyimidazopyrrolone behalten, wie gezeigt wurde, nach harter chemischer Behandlung und nach ungewöhnlich starker Bestrahlung mit ionisierenden Strahlen nützliche mechanische Eigenschaften bei höherer Temperatur bei. Die thermogravimetrische Analyse der Polymeren zeigte, dass der Einfluss der Struktur auf die Oxydationsstabilität relativ gering war. Darüber hinaus waren die relativen Stabilitäten einer Reihe von acht Polymeren in Luft nicht direkt mit der Reihenfolge ihrer Stabilität im Vakuum vergleichbar.

Received March 1, 1967

Revised May 1, 1967

Prod. No. 5439A

Kinetics of Bulk Polymerization of Trimeric Phosphonitrilic Chloride

J. R. MACCALLUM and A. WERNINCK, *Department of Chemistry, St. Salvator's College, St. Andrews, Scotland*

Synopsis

The kinetics of the pure bulk polymerization of trimeric phosphonitrilic chloride were investigated in the temperature range 240–255°C. The reaction was found to be second-order with an activation energy of 57 kcal./mole. Polymerization catalyzed by benzoic acid was first-order, and the reactivities of benzoic acid and sodium benzoate at 235°C. were found to be about similar. The volatile decomposition products for the benzoic acid reaction were identified. Mechanisms are postulated for the catalyzed and uncatalyzed reactions.

INTRODUCTION

The conversion of trimeric phosphonitrilic chloride (PNCl_2)₃ to high polymers which have potential use as thermostable materials has been extensively studied.^{1a} The kinetics of the polymerization reaction in bulk and in solution are complicated by the production of an increasing proportion of crosslinked gel. The separation of gel, soluble polymer, and unreacted trimer has led to difficulties in measuring the rate of reaction which has been reported as second-order without catalyst,² and both first-order^{3,4} and second-order⁵ with catalyst. Gimblett^{1a} has pointed out that the method of analysis employed by Patat and co-workers removes not only trimer but also soluble polymer which can amount to a significant proportion of the total polymer formed.

It has never been firmly established whether the reaction involves ionic or free-radical intermediates, and the role of catalysts such as benzoic acid is not clear. Gimblett^{1a} has suggested that polymerization takes place by an anionic mechanism, whereas Konecny et al.³ favor a cationic process.

In this investigation the kinetics of the bulk polymerization with and without catalyst are examined, and the volatile products of benzoic acid-catalyzed polymerization identified.

EXPERIMENTAL

Phosphonitrilic chloride trimer (Albright and Wilson Limited, Oldbury, Birmingham) was purified by sublimation and stored under vacuum till required, m.p. 112–113°C. Benzoic acid (Analar grade) was sublimed

before use, m.p. 120–121°C. Sodium benzoate was dried in a vacuum oven at 100°C. overnight before use.

About 1 g. of trimer and the required weight of catalyst, when one was used, were placed in a clean thick-walled tube (tube volume in milliliters to weight trimer in grams was kept constant at 2:1). The tube was then evacuated to a pressure of 10^{-4} mm. Hg and sealed. A series of trial experiments showed that variation of $\pm 20\%$ in the volume to weight of trimer ratio had no effect on the rate of the reaction.

The sealed tubes were immersed in a thermostatted oil bath (controlled to $\pm 1^\circ\text{C}$.), and removed at time intervals chosen to give moderate conversion. The capsule after cleaning and weighing was opened, and weighed again. There was usually a very small change in weight due to loss of volatile products such as hydrogen chloride. All the opened capsules for a single run were then placed in a vacuum oven which incorporated a water-cooled copper spiral. Unreacted trimer was sublimed out of the tubes by heating to 105°C. in a vacuum of 10^{-3} mm. Hg. Normally a period of at least 24 hr. was required before constant weight was attained, and for capsules containing higher proportions of polymer 48 hr. subliming was necessary to remove all the trimer.

For analysis of products by gas-liquid chromatography the contents of the capsule were washed into a 10 ml. beaker by adding a few milliliters of dried Analar benzene and analyzed immediately. Products were identified by comparing retention times on two different columns with authentic samples. The instrument used was a Griffin and George D.6 employing a gas density balance as detector.

RESULTS

Kinetics of Pure Bulk Polymerization

The most convenient temperature range for studying the pure bulk polymerization was found to be 240–255°C. In all runs times were so

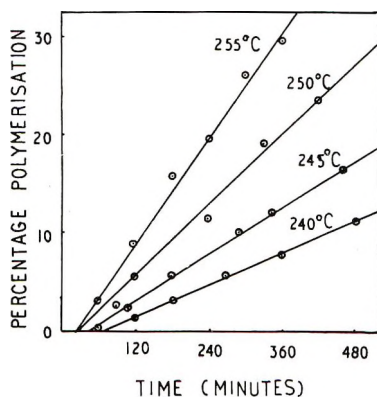


Fig. 1. Percentage polymerization vs. time for the uncatalyzed bulk reaction.

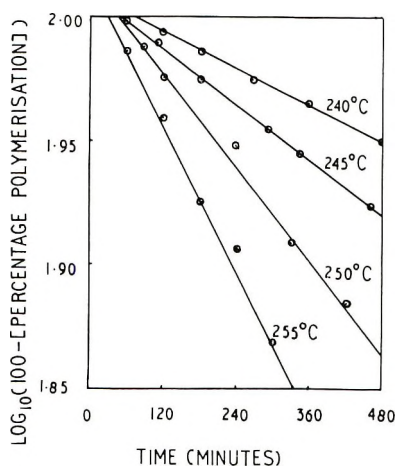


Fig. 2. Data for the uncatalyzed bulk polymerization plotted as a first-order reaction with respect to trimer.

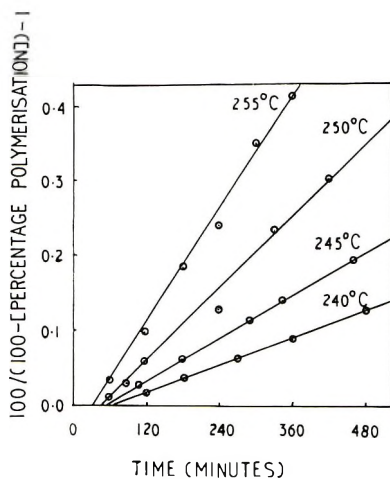


Fig. 3. Data for the uncatalyzed bulk polymerization plotted as a second-order reaction with respect to trimer.

chosen that the conversion to polymer did not exceed 30%. Figure 1 shows the extent of polymerization as a function of time, and in Figures 2 and 3 the appropriate plots for first- and second-order kinetics are depicted. The rather extraordinary fact emerges from these figures that within experimental error reasonably good straight lines can be drawn for zero-, first-, and second-order kinetics, although the origin is not a common point on any of the plots. In Figure 4 the activation energy is obtained for each set of rate constants, and the values obtained are shown. It is apparent from this figure that second-order kinetics would seem to be the most likely, a conclusion in agreement with the findings of Patat and

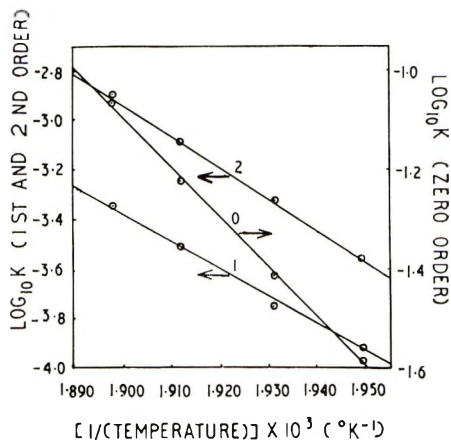


Fig. 4. Arrhenius plot for activation energies for the rate constants from the data shown in Figs. 1, 2, and 3. Zero-order, 47 ± 1.5 kcal./mole; first order, 50 ± 1.5 kcal./mole; second-order, 57 ± 1 kcal./mole.

Frombling² in spite of the differing methods of analysis. There is, however, a marked difference between the activation energy reported by these authors, 42 kcal./mole and that of the present work, 57 kcal./mole.

Kinetics of Catalyzed Bulk Polymerization

Gimblett⁴ has studied the bulk polymerization catalyzed by benzoic acid. He found first-order kinetics and an activation energy of 24.3 kcal./mole. An unusual feature of his results was the observation of the existence of an induction period the length of which varied with the tem-

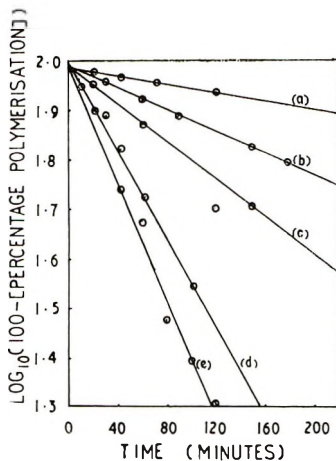


Fig. 5. Benzoic acid-catalyzed bulk polymerization plotted as a first-order reaction with respect to trimer at various concentrations of catalyst: (a) 10.1 mg./g. trimer; (b) 15.4 mg./g.; (c) 20.2 mg./g.; (d) 30.0 mg./g.; (e) 35.1 mg./g. $T = 252^\circ\text{C}$. Data are corrected for thermal polymerization.

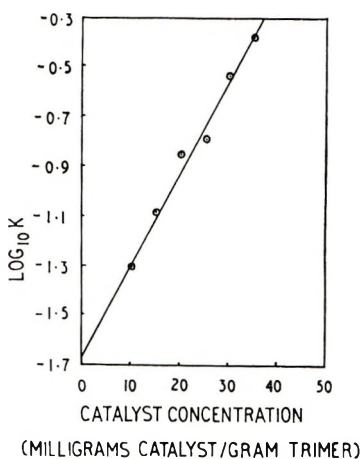


Fig. 6. Logarithm of the first-order rate constants for benzoic acid-catalyzed polymerization vs. the concentration of catalyst. The conversion to polymer is uncorrected for the purely thermal reaction.

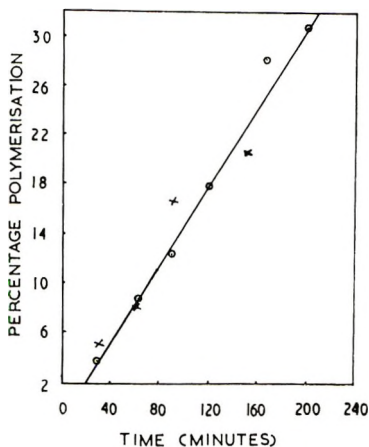


Fig. 7. Comparison of the conversion to polymer catalyzed by benzoic acid (1.4×10^{-4} mole/g. trimer) and sodium benzoate (1.4×10^{-4} mole/g. trimer): (○) benzoic acid; (×) sodium benzoate. $T = 235^\circ\text{C}$.

perature of polymerization up to 225°C . Most of Gimblett's data were collected between 25% and 60% polymerization. It seemed desirable to investigate the earlier part of the polymerization reaction by obtaining data for lower conversions. Figure 5 shows first-order plots for a series of runs at 252°C . with varying amounts of benzoic acid as catalyst. The data were found not to fit second-order kinetics. The percentage conversion to polymer was corrected for the purely thermal reaction using the results obtained for pure bulk polymerization.

A plot of the logarithm of the measured, uncorrected, rate constants against the catalyst concentration is illustrated in Figure 6. A linear re-

relationship exists similar to that already reported by Gimblett^{1a} for both bulk and solution polymerization. It is possible to calculate the rate constant for the pure thermal polymerization at 211°C. from Figure 4. The value obtained is an order of magnitude less than that calculated from Gimblett's data.

In order to throw some further light on catalytic activity a comparative study of the reactivities of benzoic acid and sodium benzoate was made at 235°C. The degree of dissociation of benzoic acid in molten phosphonitrilic trimer at elevated temperatures is a matter for speculation, but it is reasonable to assume that sodium benzoate is much more dissociated and such a study should give some indication of the role of the benzoate ion. Some data are represented in Figure 7 from which it can be concluded that the relative catalytic activity is about similar.

Volatile Products of Polymerization

The volatile products of benzoic acid-catalyzed polymerization were examined by using gas-liquid chromatography. The direct breakdown products of the benzoic acid were found to be benzoyl chloride and benzonitrile. Hydrogen chloride was also produced. No other volatile species was detected for low conversion polymerization. The ratio of C_6H_5CN to C_6H_5COCl increased as the reaction proceeded. It was not possible to measure the amounts quantitatively because of the very low concentrations. Nevertheless, it was estimated that practically all the benzoic acid had reacted very early in the reaction.

The fact that there is little difference in the catalytic activity of C_6H_5COOH and C_6H_5COONa would seem to suggest that the reactive species in the polymerization process is some subsidiary compound. This conclusion is further substantiated by the fact that at least in the case of benzoic acid very little of the original catalyst remains as such after a short period of heating.

Some experiments were carried out to investigate the effect of water on the polymerization reaction. Table I summarizes the results of these experiments. Detectable amounts of chlorine were found in the water-catalyzed reactions. In another run a trace of water vapor was added to a tube containing white soluble polymer obtained by extracting a trimer-free sample of uncatalyzed bulk polymer. The sealed tube was heated

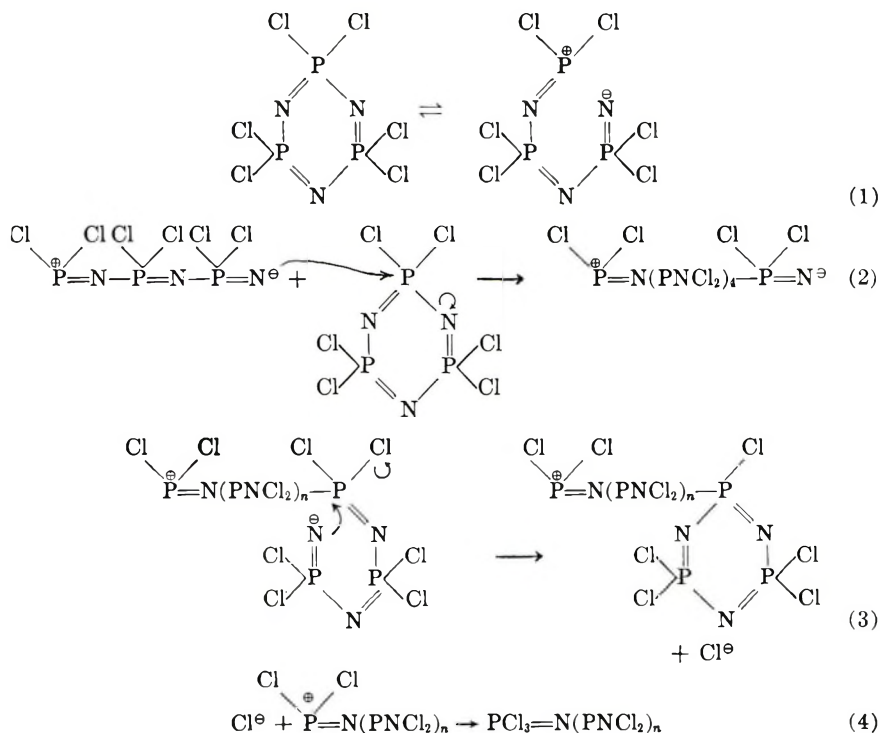
TABLE I
Samples Heated for 24 hr. at 236°C.

Sample	Water concn., %	Polymerization, %	Color of polymer	Chlorine detected
1	0	38	White	No
2	1×10^{-2}	38	Light brown	No
3	2×10^{-2}	62	Brown	Yes
4	3×10^{-2}	89	Black	Yes

overnight at 240°C., resulting in a black, almost totally insoluble, product. These experiments show conclusively that very small amounts of water can have a profound effect on both the rate and product of polymerization.

DISCUSSION

From the kinetic data shown it is possible to deduce that the bulk polymerization of phosphonitrilic chloride is first-order with catalyst, and second-order without. The evidence available from Allcock and Best's work⁶ involving conductivity and dielectric constant measurements almost certainly precludes the likelihood of a free-radical mechanism. This is in agreement with the observation that a large number of organic molecules which do not produce free radicals on heating to 300°C. catalyze the polymerization of phosphonitrilic chloride.⁷ The nature of the reactive species in the polymerization reaction is highly speculative. However, it is possible to suggest a mechanism for the uncatalyzed bulk reaction which is consistent with the kinetic data and also the known susceptibility of trimeric phosphonitrile chloride to nucleophilic attack.⁸ It is proposed that in the



molten bulk at the elevated temperatures of polymerization studies an equilibrium exists according to eq. (1). Step (2) is a nucleophilic attack on a cyclic trimeric molecule and is the propagation step of the polymeriza-

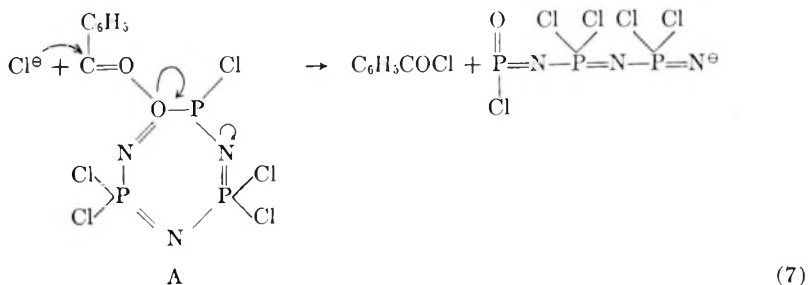
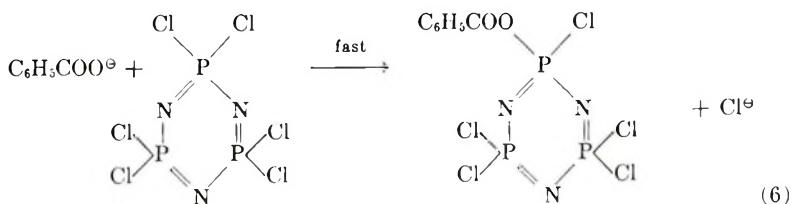
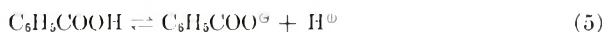
tion reaction. Step (3) is an intramolecular termination process, yielding linear, soluble macromolecules. Similar intermolecular reactions can occur equally well, giving rise to branched and finally crosslinked polymeric structures, in accord with the experimental observations. The final reaction, step (4), is the addition of Cl^- to the positively charged terminal phosphorus atom.

By the usual kinetic analysis the following second-order expression is obtained for the rate of polymerization;

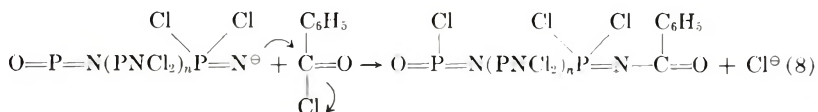
$$-d[\text{T}]/dt = d[\text{P}]/dt = (k_1 k_2 / k_3) [\text{T}]^2$$

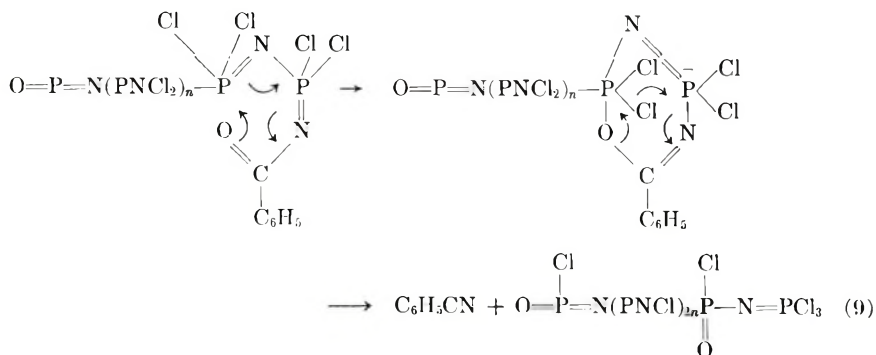
in which $[\text{T}]$ and $[\text{P}]$ represent the concentrations of trimer and polymer, respectively, and k_1 , k_2 , and k_3 are the rate constants for the initiation, propagation, and termination reactions, respectively.

The nature of the catalyzed polymerization is a much more complex problem. In line with the anionic nature of the noncatalyzed reaction the mechanism of eqs. (5)–(7) is tentatively suggested.



Propagation and inter- and intramolecular transfer are by the same steps as proposed above. In order to account for the observed production of $\text{C}_6\text{H}_5\text{CN}$ at the expense of $\text{C}_6\text{H}_5\text{COCl}$ the steps (8) and (9) are proposed.





On the assumption that step (7) is slow and rate-controlling in the initiation process then the following first-order expression can be deduced for the rate equation;

$$-d[\text{T}]/dt = d[\text{P}]/dt = k_7 k_2 / k_3 [\text{Cl}^-][\text{A}][\text{T}]$$

in which k_7 is the rate constant for the decomposition of $\text{C}_6\text{H}_5\text{COOP}(\text{Cl}) = \text{N}(\text{PNCl}_2)_2(\text{A})$. Termination by $\text{C}_6\text{H}_5\text{COCl}$ is considered to have negligible effect on the kinetics, and the term $[\text{Cl}^-][\text{A}]$ is assumed to be relatively constant.

Both the above mechanisms fit the requirements of the experimental results. It seems unlikely however that they should describe the reaction for high conversions to polymer when the presence of significant proportions of crosslinked molecules will drastically increase the viscosity and inevitably have a profound effect on the rate of reaction.

An interesting feature of the experimental results is the marked effect which very low concentrations of water have on both the rate of polymerization and the polymer itself. These results indicate that great experimental care must be exercised to eliminate water during kinetic investigations. This conclusion is particularly relevant to solution studies.

Great interest^{1b} has been shown in the possible existence of an equilibrium between trimer and polymer $n(\text{PNCl}_2)_3 \rightleftharpoons -(\text{PNCl}_2)_{3n}-$, and measured activation energies have been compared with a view to confirming that such a situation exists. It should be noted, however, that activation energies obtained experimentally are rarely those of simple one-step reactions, and before measured values can be applied to the above equilibrium the values for the constituent steps must be evaluated separately.

A. W. gratefully acknowledges the award of a Research Studentship by the Science Research Council.

References

1. F. G. R. Gimblett, *Inorganic Polymer Chemistry*, Butterworths, London, 1963, (a) Chap. 5; (b) Chap. 7.
2. F. Patat and K. Frombling, *Monatsh. Chem.*, **86**, 718 (1955).
3. J. O. Konecny, C. M. Douglas, and M. Y. Gray, *J. Polymer Sci.*, **42**, 383 (1960).
4. F. G. R. Gimblett, *Polymer*, **1**, 418 (1960).

5. F. Patat and F. Kollinsky, *Makromol. Chem.*, **6**, 292 (1951).
6. H. R. Allcock and R. J. Best, *Can. J. Chem.*, **42**, 447 (1964).
7. J. O. Konecny and C. M. Douglas, *J. Polymer Sci.*, **36**, 195 (1959).
8. N. L. Paddock, *Quart. Rev.*, **18**, 168 (1964).

Résumé

Les cinétiques de polymérisation en bloc du chlorure de phosphonitrile trimère ont été étudiées à une température de 240–255°C. La réaction est du second-ordre avec une énergie d'activation de 57 Kcal/mole. La polymérisation catalysée par l'acide benzoïque est du premier-ordre et les réactions de l'acide benzoïque et du benzoate de sodium à 235°C sont à peu près semblables. Les produits volatiles de décomposition de la réaction avec l'acide benzoïque ont été identifiés. Des mécanismes sont proposés pour interpréter les réactions catalysées et non-catalysées.

Zusammenfassung

Die Kinetik der reinen Bulkpolymerisation des trimeren Phosphornitrilchlorids wurde im Temperaturbereich von 240° bis 255°C untersucht. Die Reaktion verläuft, wie gefunden wurde, nach zweiter Ordnung mit einer Aktivierungsenergie von 57 Kcal/Mol. Die durch Benzoesäure katalysierte Polymerisation war erster Ordnung und die Reaktivitäten von Benzoesäure und Natriumbenzoat waren bei 235°C den Ergebnissen zufolge einander etwa gleich. Für die Benzoesäure-Reaktion wurden die flüchtigen Zersetzungsprodukte identifiziert. Für die katalysierte und unkatalysierte Reaktion werden Mechanismen postuliert.

Received April 18, 1967

Prod. No. 5440A

Viscosity of Polydimethylsiloxane Blends

TADAO KATAOKA and SHIGEYUKI UEDA,
Textile Research Institute of the Japanese Government,
Kanagawaku, Yokohama, Japan

Synopsis

Zero shear viscosities of two-component blends of polydimethylsiloxane with different molecular weights were measured over the whole range of composition. Results are analyzed on the basis of the conventional treatments for the viscosity of polymer blends and some comments are made on such treatments of data. After that, an empirical equation is derived:

$$\log \eta_{bl} = \frac{v_1(1-a)}{1-av_1} \log \eta_1 + \frac{v_2}{1-av_1} \log \eta_2$$

where η is the viscosity, v the volume fraction, subscripts 1, 2, and *bl* denote the lower and higher molecular weight component and the blend, respectively, and a is a constant independent of composition. The equation is not only applicable to all series of blends of polydimethylsiloxane but also to other polymers.

INTRODUCTION

Many investigators¹⁻¹¹ have reported on the viscous properties of blends composed of two polymeric components of different molecular weights.

The extensive studies of Flory¹ and Fox and co-workers²⁻⁶ are eminent in this field. They found that the viscosities of mixtures of sharp fractions of polymers are about equal to the viscosities of sharp fractions having molecular weights equal to the weight-average molecular weights of the mixtures, and suggest that the viscosity of a polydisperse polymer is an explicit function of its weight-average molecular weight. Busse and Longworth^{7,8} reported that the viscosities of polyethylene-wax mixtures are related to their viscosity-average molecular weights.

As for the viscosity-composition relationship, Ninomiya and co-workers⁹⁻¹¹ derived a blending law for homologous polymer mixtures and experienced some success in describing the viscoelastic properties of the mixtures in terms of the respective properties of the components.

In an earlier paper¹² we reported an investigation of the viscosity of polydimethylsiloxane-pentamer systems and discussed the effect of short-chain molecules on the viscosity. The treatment followed that of earlier work by Allen and Fox.⁵

This paper describes the viscosity of polydisperse polydimethylsiloxane polymers and two-component blends of these polymers of different molecular weights. The main objectives of this work were, first, to determine experimentally the viscosity–composition relationships for such systems and, secondly, to test the applicabilities of the theoretical and empirical relationships reported in the literatures^{4,7,8,11} to the results, we have derived a relatively simple empirical equation for the viscosity–composition relationship of homologous polymer blends with wide applicability.

EXPERIMENTAL

Materials used in this study are given in Table I. All are commercial products of Shin-etsu Chemical Industry Co., Ltd. Samples L and M are

TABLE I
Samples

Sample designation	$\bar{M}_v \times 10^{-4}$	$\bar{M}_n \times 10^{-4}$	$\bar{M}_w \times 10^{-4}$
A	0.29	0.19	0.29
C	1.03	0.58	1.12
E	3.34	1.80	3.60
G	8.05	4.40	8.80
I	14.0	7.60	15.2
K	20.6	11.2	22.4
L	41	0.45	44.6
M	45	0.38	49.0

hydroxy end-blocked polydimethylsiloxane and the others are trimethyl end-blocked polydimethylsiloxane. The content of the cyclic compound (octamethyl cyclic tetrasiloxane) was negligible for trimethyl end-blocked species and was several per cent for hydroxy end-blocked species. Since it was difficult to remove the cyclic material completely from large amounts of highly viscous samples L and M, we utilized these samples without further purification.

Viscosity-average molecular weights \bar{M}_v were calculated from the intrinsic viscosities of toluene solutions at 25°C. by using eq. (1)¹³ for sample A, and eq. (2)¹⁴ for the others.

$$[\eta] = 4.97 \times 10^{-4} M^{0.5} + 3.28 \times 10^{-6} M \quad (1)$$

$$[\eta] = 2.15 \times 10^{-4} M^{0.65} \quad (2)$$

Number-average molecular weights \bar{M}_n for samples A, C, L, and M were measured by using a Mechrolab vapor-pressure osmometer, Type 301. Because of the high content of low molecular weight cyclic compound ($M = 296$), samples L and M have \bar{M}_n of several thousand, while their \bar{M}_v are above 400,000. From the values of \bar{M}_n we estimated the cyclic compound content to be about 7 and 8% for samples L and M, respectively.

TABLE II
 Viscosities of Polydimethylsiloxane Blends

Blend	Weight fraction w_2	Viscosity, η , poises		
		Observed values	Calculated from	
			eq. (16)	eq. (12)
AL	0.000	2.7×10^{-1}		
	0.022	8.7×10^{-1}	6.6×10^{-1}	
	0.042	1.45	1.36	
	0.081	4.3	4.8	
	0.107	1.00×10^1	1.02×10^1	
	0.209	1.16×10^2	1.05×10^2	
	0.302	4.8×10^2	5.0×10^2	
	0.402	1.93×10^3	1.86×10^3	
	0.501	4.7×10^3	5.1×10^3	
	0.612	1.05×10^4	1.27×10^4	
	0.692	1.80×10^4	2.2×10^4	
	0.788	3.4×10^4	3.8×10^4	
	0.902	6.3×10^4	6.8×10^4	
	0.950	8.0×10^4	8.4×10^4	
1.000	1.02×10^5			
CL	0.000	2.5		
	0.021	4.4	4.8	
	0.048	8.5	8.3	
	0.080	1.73×10^1	2.3×10^1	
	0.127	5.5×10^1	6.6×10^1	
	0.199	2.4×10^2	2.4×10^2	
	0.301	1.05×10^3	1.02×10^3	
	0.401	3.0×10^3	3.0×10^3	
	0.504	7.2×10^3	7.5×10^3	
	0.598	1.30×10^4	1.48×10^4	
	0.694	2.3×10^4	2.7×10^4	
	0.801	4.4×10^4	4.1×10^4	
	0.897	6.4×10^4	6.9×10^4	
	0.947	8.7×10^4	8.4×10^4	
AK	0.081	2.1	1.84	
	0.136	5.1	5.3	
	0.241	2.5×10^1	2.8×10^1	
	0.324	8.4×10^1	8.2×10^1	
	0.381	1.55×10^2	1.53×10^2	
	0.466	3.5×10^2	3.5×10^2	
	0.599	1.00×10^3	9.8×10^2	
	0.730	2.4×10^3	2.2×10^3	
	0.875	4.6×10^3	5.1×10^3	
	0.953	7.3×10^3	6.7×10^3	
	1.000	8.2×10^3		

(continued)

The apparatus is not appropriate for \bar{M}_n larger than 10,000, and we were not able to determine \bar{M}_n for samples E, G, I, and K by the apparatus.

The molecular weight distribution of conventional polydimethylsiloxane is approximately the most probable one,¹⁵ if low molecular weight parts

TABLE II (continued)

Blend	Weight fraction w_2	Viscosity η , poises		
		Observed values	Calculated from	
			eq. (16)	eq. (12)
CK	0.071	8.8	8.5	
	0.141	2.1×10^1	2.3×10^1	
	0.234	6.5×10^1	7.2×10^1	
	0.309	1.40×10^2	1.54×10^2	
	0.421	4.1×10^2	3.5×10^2	
	0.513	7.4×10^2	7.8×10^2	
	0.622	1.50×10^3	1.54×10^3	
	0.746	2.8×10^3	2.9×10^3	
	0.881	5.2×10^3	5.3×10^3	
	0.928	6.2×10^3	6.3×10^3	
EM	0.000	2.5×10^1		
	0.011	3.2×10^1	3.1×10^1	4.5×10^1
	0.036	4.6×10^1	5.2×10^1	1.00×10^2
	0.075	1.00×10^2	1.07×10^2	2.1×10^2
	0.150	3.4×10^2	3.5×10^2	5.5×10^2
	0.289	2.0×10^3	1.94×10^3	1.85×10^3
	0.492	1.10×10^4	1.13×10^4	7.6×10^3
	0.678	2.85×10^4	3.2×10^4	2.3×10^4
	0.864	7.4×10^4	8.4×10^4	6.7×10^4
	0.964	1.05×10^5	1.18×10^5	1.15×10^5
GM	0.000	2.3×10^2		
	0.011	2.7×10^2	2.7×10^2	3.1×10^2
	0.020	2.9×10^2	3.0×10^2	3.9×10^2
	0.058	4.0×10^2	4.9×10^2	7.4×10^2
	0.084	6.3×10^2	6.7×10^2	1.02×10^3
	0.150	1.30×10^3	1.36×10^3	1.97×10^3
	0.308	5.4×10^3	5.4×10^3	5.7×10^3
	0.499	1.85×10^4	1.85×10^4	1.60×10^4
	0.761	6.0×10^4	6.2×10^4	5.2×10^4
	0.901	1.03×10^5	1.03×10^5	9.4×10^4
IM	0.946	1.15×10^5	1.18×10^5	1.13×10^5
	0.000	2.4×10^3		
	0.010	2.7×10^3	2.6×10^3	2.7×10^3
	0.022	3.0×10^3	2.8×10^3	3.0×10^3
	0.039	3.4×10^3	3.2×10^3	3.5×10^3
	0.071	3.9×10^3	3.9×10^3	4.4×10^3
	0.149	6.1×10^3	6.4×10^3	7.3×10^3
	0.251	1.12×10^4	1.13×10^4	1.25×10^4
	0.463	2.8×10^4	2.8×10^4	2.8×10^4
	0.711	6.4×10^4	6.6×10^4	6.2×10^4
0.905	1.13×10^5	1.12×10^5	1.08×10^5	
0.960	1.28×10^5	1.28×10^5	1.27×10^5	

(continued)

are removed from the materials as in the cases for trimethyl end-blocked species used in this work. When such a distribution is assumed and \bar{M}_v is calculated from eq. (2), the ratio \bar{M}_n/\bar{M}_v should be 0.544. The value of

TABLE II (continued)

Blend	Weight fraction w_2	Viscosity η , poises		
		Observed values	Calculated from	
			eq. (16)	eq. (12)
EK	0.090	5.4×10^1	5.7×10^1	7.2×10^1
	0.149	8.5×10^1	1.03×10^2	1.17×10^2
	0.277	2.4×10^2	2.5×10^2	2.7×10^2
	0.331	3.8×10^2	3.5×10^2	3.8×10^2
	0.452	7.3×10^2	7.3×10^2	7.2×10^2
	0.546	1.20×10^3	1.22×10^2	1.13×10^3
	0.632	1.85×10^3	1.86×10^3	1.69×10^3
	0.780	3.2×10^3	3.6×10^3	3.3×10^3
	0.914	6.0×10^3	6.1×10^3	5.8×10^3
	0.950	7.1×10^3	6.9×10^3	6.7×10^3
GK	0.080	3.4×10^2	3.5×10^2	3.8×10^2
	0.131	4.5×10^2	4.6×10^2	4.8×10^2
	0.230	7.3×10^2	7.3×10^2	7.5×10^2
	0.288	9.4×10^2	9.0×10^2	9.4×10^2
	0.417	1.50×10^3	1.53×10^3	1.49×10^3
	0.521	2.2×10^3	2.2×10^3	2.1×10^3
	0.650	3.5×10^3	3.3×10^3	3.1×10^3
	0.774	4.6×10^3	4.7×10^3	4.4×10^3
	0.848	5.7×10^3	5.7×10^3	5.5×10^3
	0.911	7.0×10^3	6.9×10^3	6.5×10^3
IK	0.081	2.8×10^3	2.8×10^3	2.8×10^3
	0.135	3.1×10^3	3.0×10^3	3.1×10^3
	0.234	3.6×10^3	3.5×10^3	3.6×10^3
	0.318	4.0×10^3	4.0×10^3	4.1×10^3
	0.403	4.3×10^3	4.4×10^3	4.6×10^3
	0.513	5.0×10^3	5.1×10^3	5.2×10^3
	0.581	5.5×10^3	5.5×10^3	5.9×10^3
	0.757	6.4×10^3	6.6×10^3	6.7×10^3
	0.867	7.1×10^3	7.3×10^3	7.3×10^3
	0.942	7.7×10^3	7.8×10^3	7.8×10^3

\bar{M}_n/\bar{M}_v for the sample C is 0.563, which is close to the value in the case of the most probable distribution. Thus, we assumed \bar{M}_n for samples E, G, I, and K to be $0.544\bar{M}_v$.

The weight-average molecular weight \bar{M}_w for sample A was assumed to be equal to its \bar{M}_v . Values of \bar{M}_w for the others were calculated from the relation $\bar{M}_w/\bar{M}_v = 1.088$ which can be derived from the assumption of the most probable distribution.

The critical molecular weight M_c for chain entanglements is about 27,000 for this polymer.¹² Samples A and C have lower molecular weights than M_c .

A typical series of blends denoted as AL was prepared by mixing relative amounts of the two components A and L. In Table II the various blends studied are listed. Note that the series AK, AL, CK, and CL have $M_1 < M_c$ and $M_2 > M_c$; the others have $M_1 > M_c$ and $M_2 > M_c$, where

suffixes 1 and 2 denote the lower and higher molecular weight components of the blend, respectively. All blends were prepared by weight. Volume fractions v_1 and v_2 were calculated from weight fractions w_1 and w_2 by assuming negligible volume change on mixing.

Viscosity measurements were made at 30°C. by using a cone-plate viscometer. In each case the zero shear viscosity η was obtained at a shear stress less than several hundred dynes/cm.².

RESULTS

Viscosity data are summarized in Table II along with calculated values described in the latter sections.

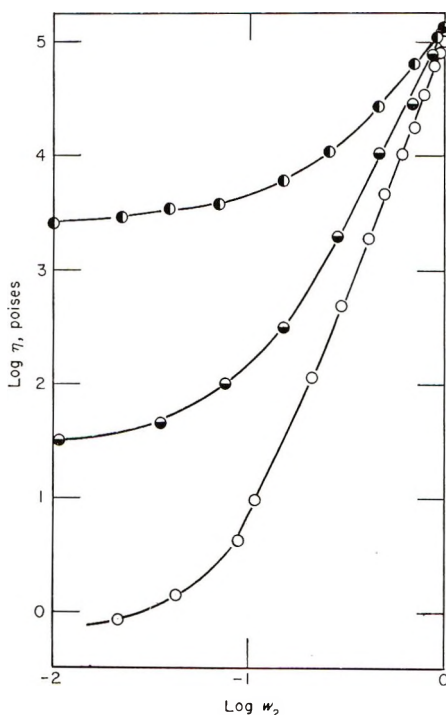


Fig. 1. Relations between $\log \eta$ and $\log w_2$ for various series: (O) AL; (●) EM; (◐) IM. Solid lines are smoothed curves for those plots.

Plots of $\log \eta$ versus $\log w_2$ for typical series are shown in Figure 1. The slope of the curve ($d \log \eta / d \log w_2$) increases with increasing w_2 and approaches a nearly constant value $(d \log \eta / d \log w_2)_{\text{limit}}$ at high w_2 in each case.

In Figure 2 values of $(d \log \eta / d \log w_2)_{\text{limit}}$ are plotted against M_1/M_2 , where molecular weights are viscosity-average values. For comparison, results for polymer-pentamer systems¹² are also shown. Plots in Figure 2 fall into two groups, depending on the molecular weight of component 1

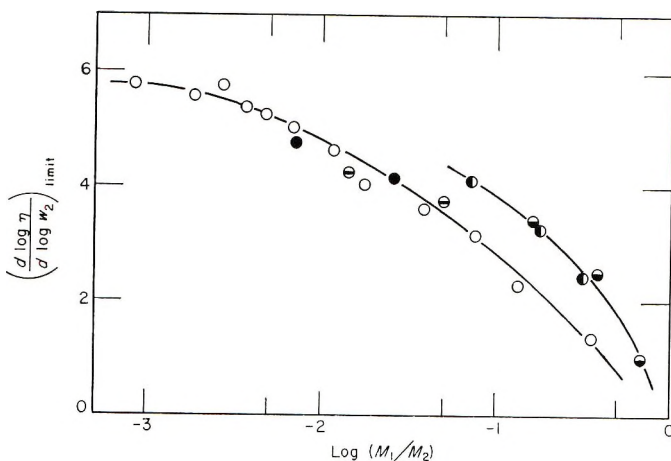


Fig. 2. Relations between the limiting slopes $(d \log \eta / d \log w_2)_{\text{limit}}$ and $\log (M_1/M_2)$ for various series: (●) AL and CL; (⊖) AK and CK; (◐) EM, GM, and IM; (◑) EK, GK, and IK; (○) polymer-pentamer.

relative to M_c . The value $(d \log \eta / d \log w_2)_{\text{limit}}$ increases with decreasing M_1/M_2 and tends towards about 5.7 at a very small value of M_1/M_2 in the case of $M_1 < M_c$, but it is not certain whether it tends towards the same value (5.7) in the case of $M_1 > M_c$.

DISCUSSION

Considerable controversy currently exists in regard to which average molecular weight should be employed to correlate the viscosity of polydisperse polymers. Fox and Flory,² from their work on sharp fractions of polymers, suggest that the viscosity is an explicit function of the weight-average molecular weight. Other workers^{4,16,17} have reported similar findings for polydisperse polymers. Busse and Longworth^{7,8} in their studies on polyethylene-wax systems suggest a good correlation between viscosity and viscosity-average molecular weight. Bueche¹⁸ theoretically predicts a dependence of viscosity on a molecular weight somewhere between the weight- and z -average value.

An investigation of the correlation of viscosity with viscosity-average (\bar{M}_v) and weight-average (\bar{M}_w) molecular weight was conducted. Since cases where $M_1 \ll M_c$ and $M_2 > M_c$ are of particular interest, data on the polymer-pentamer system¹² is also examined.

To correlate viscosity with \bar{M}_v , it is necessary to apply a chain-end effect correction^{4-6,19,20} to systems with $\bar{M}_n \ll M_c$. The need for this correction is evidenced by the lowering of T_g with decreasing chain length.

In an earlier publication,¹² we calculated the average frictional coefficient ζ per chain atom at constant \bar{M}_n for polydimethylsiloxane-pentamer systems on the basis of the treatment of Fox and Allen^{5,6} and obtained eq. (3) for $\bar{M}_n > 1000$.

$$\zeta = 7.4 \times 10^{-9} - 4.2 \times 10^{-6} / \bar{M}_n \quad (3)$$

By using eq. (3) we can correct the viscosity as follows;

$$\eta_{\text{corr}} = \eta(\zeta_{\infty}/\zeta) \quad (4)$$

where ζ_{∞} is the friction coefficient per chain atom for sufficiently high \bar{M}_n materials and is equal to 7.4×10^{-9} . This correction is required for blends of $\bar{M}_n < M_c$ and not for those of $\bar{M}_n > M_c$ since the latter systems have ζ practically equal to ζ_{∞} .

Figure 3 shows plots of $\log \eta_{\text{corr}}$ versus $\log \bar{M}_w$, where data of polymer-pentamer mixtures having $\bar{M}_n > 1000$ are also plotted. In the higher \bar{M}_w region a line of 3.5 slope is drawn. The value 3.5 is based on the experimental results on the original (nonblended) polymers and on the polymer-pentamer systems in our previous papers.^{12,21,22} As is shown in Figure 3, the data points fit the 3.5 slope line in the higher \bar{M}_w region.

In the region of molecular weights, $10,000 < \bar{M}_w < 50,000$, some scatter occurs. It is expected that the data for polymer-pentamer systems give a composite curve, since eq. (3) is derived from data on these systems.

Viscosity in the region of M_c is further complicated by the effects of chain entanglements in addition to the previously mentioned chain-end effect. The nature of entanglements and the manner in which their presence is manifested in the neighborhood of M_c is currently open to conjecture. Merker²³ has supported the view that entanglements become pro-

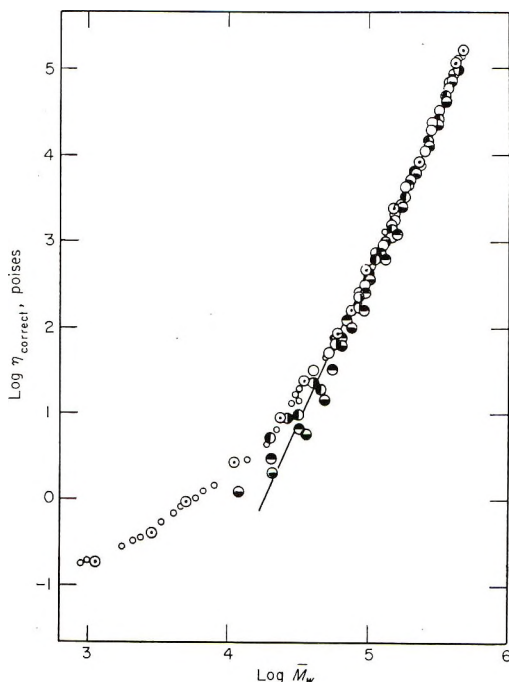


Fig. 3. Plots of $\log \eta_{\text{corr}}$ vs. $\log \bar{M}_w$; (○) original samples; (◐) series AL; (◑) series AK; (◒) series CL; (◓) series CK; (◔) series EM, GM, IM, EK, GK, and IK; (◕) polymer-pentamer.

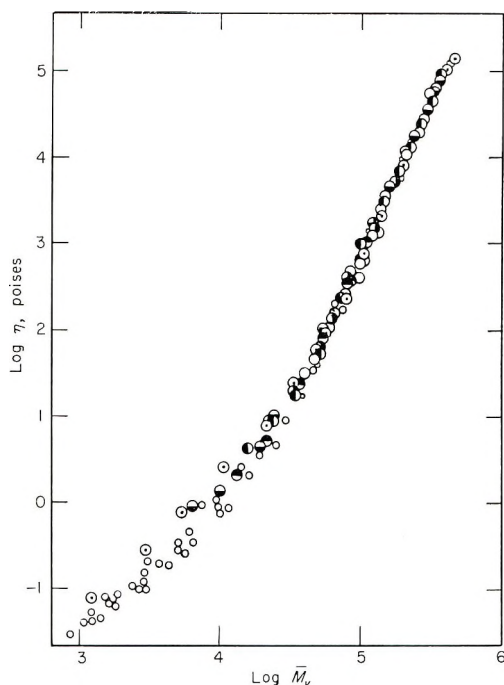


Fig. 4. Plots of $\log \eta$ vs. $\log \bar{M}_v$: (\odot) original samples; (\ominus) series AL; (\bullet) series AK; (\circ) series CL; (\bullet) series CK; (\circ) series EM, GM, IM, EK, GK, and IK; (\circ) polymer-pentamer.

gressively effective in the region of M_c . If the degree of interaction is not a function of \bar{M}_n alone, the value ζ of the same \bar{M}_n material might vary depending on the systems on which ζ is calculated. If so, relation (3) is valid only for polymer-pentamer systems, and more elaborate corrections may be required for systems other than those of polymer-pentamer.

Busse and Longworth^{7,8} made measurements on the viscosities of polyethylene-wax mixtures and found that the limiting slope of the plots of $\log \eta$ versus $\log w_2$ in the higher w_2 region is nearly equal to that of the plots of $\log \eta$ versus $\log \bar{M}_w$ in the higher \bar{M}_w region, that is, $(d \log \eta / d \log w_2)_{\text{limit}} = (d \log \eta / d \log \bar{M}_w)_{\text{limit}}$. Based on their findings, they suggest the dependence of the viscosity of a blend on its viscosity-average molecular weight \bar{M}_v . \bar{M}_v can be expressed in terms of the components of the blend by

$$\bar{M}_v = (w_1 M_1^\alpha + w_2 M_2^\alpha)^{1/\alpha} \quad (5)$$

where α is defined as

$$\alpha = 3.4 / (d \log \eta / d \log w_2)_{\text{limit}} \quad (6)$$

By using relations (5) and (6), \bar{M}_v was calculated for each composition of various series of blends. In Figure 4 the resulting plot of $\log \eta$ versus $\log \bar{M}_v$ is given. Data for polymer-pentamer systems are also plotted in

the figure. The superposition of data points seems to be somewhat better than that of Figure 3, particularly in the middle region of molecular weight.

The range of validity for relation (6) is somewhat in doubt, since in Figure 2 a considerable dependence of $(d \log \eta / d \log w_2)_{\text{limit}}$ on (M_1/M_2) is observed. Nevertheless, relation (6) may be accepted for systems of $M_1 \ll M_c$ and $M_2 > M_c$, because the value $(d \log \eta / d \log w_2)_{\text{limit}}$ for such systems is nearly the same as is shown in Figure 2. For polydimethylsiloxane-pentamer systems, the value $(d \log \eta / d \log w_2)_{\text{limit}}$ at the small value of M_1/M_2 is about 5.7, thus $\alpha = 3.4/5.7 = 0.6$. The value of 0.6 is in fair agreement with the exponent of \bar{M} in the relation of $[\eta]$ and \bar{M} [eq. (2)]. Therefore, the use of \bar{M}_v for correlation with viscosity may be accepted if it is restricted to systems with $M_1 \ll M_c$ and $M_2 > M_c$.

Test of Ninomiya's Equation

From the consideration of the viscoelastic properties of homologous polymer blends composed of two components with different molecular weights, Ninomiya and Ferry⁹⁻¹¹ have derived the following equation for viscosity of such systems:

$$\eta_{b1} = v_1 \lambda_1 \eta_1 + v_2 \lambda_2 \eta_2 \quad (7)$$

where λ_i is regarded as the ratio of the average frictional resistance encountered by a molecule of species i in the blend to the resistance it would encounter surrounded by other molecules of its own kind. The factor λ_i can be estimated from stress relaxation data.

From their data, Ninomiya and Ferry¹¹ define the two parameters

$$N_{21} \equiv \lambda_2 \eta_2 / \lambda_1 \eta_1 \quad (8)$$

and

$$D \equiv \lambda_1^{v_1} \lambda_2^{v_2} \quad (9)$$

In terms of these parameters, eq. (7) can be rewritten as

$$\eta_{b1} = D \eta_1^{v_1} \eta_2^{v_2} [1 + (N_{21} - 1)v_2] / N_{21}^{v_2} \quad (10)$$

If both components of the blend have molecular weights higher than M_c , the following relations are satisfied:¹¹

$$D = 1 \quad (11)$$

and

$$(\partial N_{21} / \partial v) = 0$$

Thus, eq. (10) reduces to

$$\eta_{b1} = \eta_1^{v_1} \eta_2^{v_2} [1 + (N_{21} - 1)v_2] / N_{21}^{v_2} \quad (12)$$

Thus, under the given conditions, eqs. (11) we can express the viscosity of a blend in terms of the components and their respective viscosities by means of the parameter N_{21} . Data for the series of blends EM, GM, IM, EK, GK, and IK give examples for testing eq. (12). Values of N_{21} were

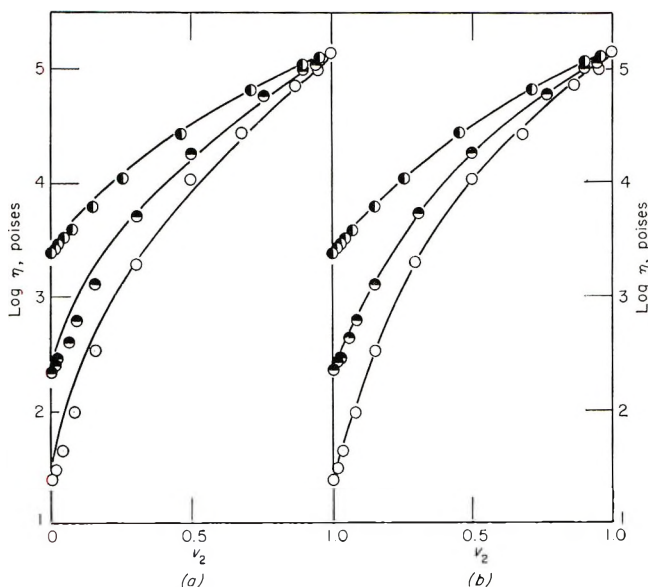


Fig. 5. Relations between $\log \eta$ and v_2 for various series: (O) EM; (◐) GM; (●) IM. Solid lines are those calculated (a) from eq. (12) and (b) from eq. (16).

estimated so as to give the best fit to the experimental data and are given in Table III. Viscosities calculated from eq. (12) are given in Table II. Figure 5a shows the relations between $\log \eta_{b1}$ and v_2 for typical series, where curves calculated from eq. (12) are shown by solid lines. Disagreements with data points are minor for systems of relatively small M_2/M_1 but become remarkable with increasing M_2/M_1 . There are definite tendencies that calculated values are too large in the region of low v_2 and too small in the region of higher v_2 . Similar discrepancies were shown in the original paper of Ninomiya and Ferry¹¹ (Fig. 4 in ref. 11).

TABLE III
Values of N_{21}

Blends	M_2/M_1	N_{21}
EK	6.17	14
GK	2.58	6
IK	1.47	3
EM	13.5	70
GM	5.59	30
IM	3.21	10

An Empirical Equation

The theoretical approach to obtain an expression for the viscosity-composition relationship of blended polymers encompassing a broad molecular weight range has several marked shortcomings. The possibility

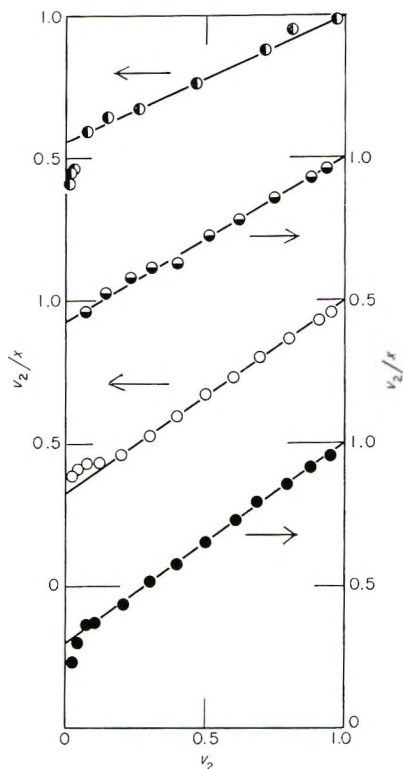


Fig. 6. Plots of v_2/x vs. v_2 for various series: (●) AL; (○) CL; (◐) CK; (◑) IM.

of arriving at an empirical relationship applicable to a variety of polymer systems was investigated.

We define a parameter x as

$$x \equiv (\log \eta_{bl} - \log \eta_1) / (\log \eta_2 - \log \eta_1) \quad (13)$$

Rewriting eq. (13), we have

$$\log \eta_{bl} = (1 - x) \log \eta_1 + x \log \eta_2 \quad (14)$$

Upon examination of our data, plots of v_2/x versus v_2 were observed to give a straight line (Fig. 6). We see from the equation for the curve

$$v_2/x = 1 - av_1 \quad (15)$$

that our parameter x is defined in terms of the volume fractions of the components and the parameter a , which is constant for a particular series of blends. Substituting eq. (15) into eq. (14), we obtain;

$$\log \eta_{bl} = [v_1(1 - a)/(1 - av_1)] \log \eta_1 + (v_2/1 - av_1) \log \eta_2 \quad (16)$$

or

$$\eta_{bl} = \eta_1^{v_1} \eta_2^{v_2} (\eta_2/\eta_1) \exp \{ av_1 v_2 / (1 - av_1) \} \quad (17)$$

TABLE IV
Values of a

Blend	a	
	Observed values	Calculated from eq. (18)
AK	0.62	0.62
CK	0.57	0.59
EK	0.41	0.52
GK	0.37	0.38
IK	0.32	0.20
AL	0.70	0.67
CL	0.67	0.66
EM	0.60	0.64
GM	0.54	0.57
IM	0.44	0.48
O _r A ^a	0.05	0.07
O _r A	0.11	0.17
O _r B	0.23	0.23
O _v C	0.30	0.30
O _r D	0.31	0.36
O _v E	0.44	0.42
O _r F	0.49	0.49
O _v G	0.55	0.52
O _r H	0.56	0.54
O _v I	0.59	0.57
O _r K	0.62	0.62
O _v M	0.70	0.69

^a The O_v series are mixtures of polymers and pentamer O_v(\bar{M}_n of O_v is 385).

Values of a are listed in Table IV, where values for polymer-pentamer systems and calculated values are also given. Viscosities calculated by eq. (16) are given in Table II. Typical results are shown in Figure 5b for the systems with $M_1 > M_c$ and $M_2 > M_c$ and in Figure 7 for the systems with $M_1 < M_c$ and $M_2 > M_c$.

Satisfactory agreement is observed except for the series O_vM with the major discrepancies occurring in the lower v_2 region. Consistently similar behavior was observed for other systems, with component 1 being pentamer. The maximum deviation in the lower v_2 region is a factor of about 3 for the series O_vM. The magnitude of this discrepancy is considerably lessened when we recall that the viscosity ratio of the two components is of the order 10⁷.

The values of a listed for systems in Table IV are those obtained from data in the higher v_2 region. From these values were obtained the relation:

$$a = 0.225[\log(M_2/385)][1 - (M_1/M_2)] \quad (18)$$

where molecular weights are viscosity-average values. Values calculated from eq. (18) are given in Table IV. While eq. (18) is not complete, as is

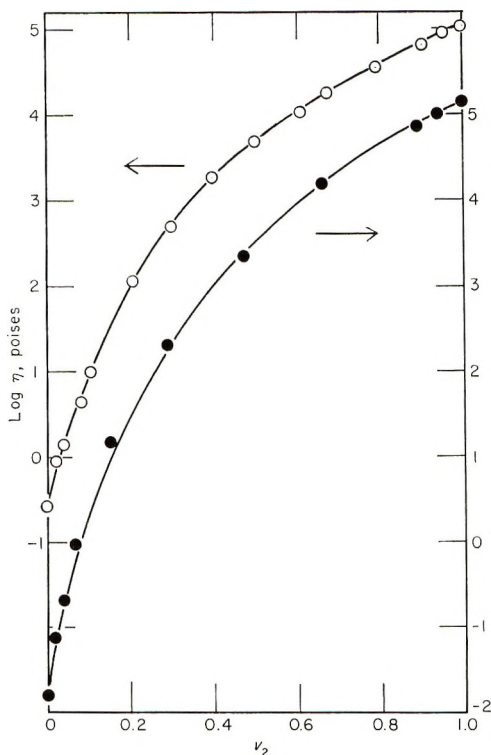


Fig. 7. Relations between $\log \eta$ and v_2 for various series: (O) AL; (●) O₂M. Solid lines are those calculated from eq. (16).

evident from the comparison of observed and calculated values of a , we can predict the viscosity at least for practical purposes of any blend of any two-component systems of polydimethylsiloxane.

Application of Equation (16) to Other Polymer Systems

Equation (16) was found to be applicable to blends of other polymer systems for which sufficient data were found in the literature.^{1,7,11,17,25-26} An exception to our finding was the result reported by Leaderman²⁴ for polyisobutylene blends.

Table V shows the systems tested and values of a . Typical results are given in Figures 8 and 9 and Table VI. Figure 8 shows plots of v_2/x versus v_2 for linear polyethylene-wax systems;⁷ straight-line relations as predicted by eq. (15) are practically satisfied. Figure 9 shows the relations between $\log \eta$ and v_2 for branched polyethylene-wax systems;⁷ calculated curves represent the data points fairly well over nine decades of viscosity. Table VI gives the comparison of observed and calculated viscosities for poly(decamethylene adipate) blends¹ and poly(decamethylene adipate)-diethyl succinate systems;¹ in the latter case diethyl succinate may be regarded as the lower member of the decamethylene adipate polymers;

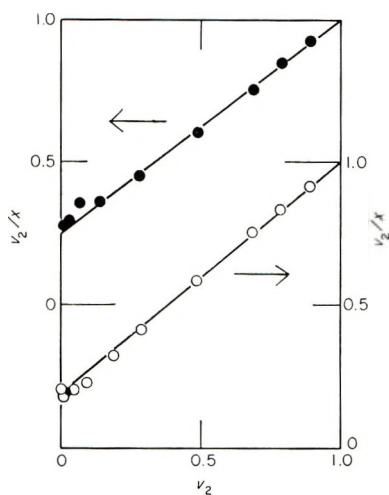


Fig. 8. Plots of v_2/x vs. v_2 : (○) linear PE ($\bar{M}_w = 1.75 \times 10^5$)-wax system; (●) linear PE ($\bar{M}_w = 7.3 \times 10^4$)-wax system.

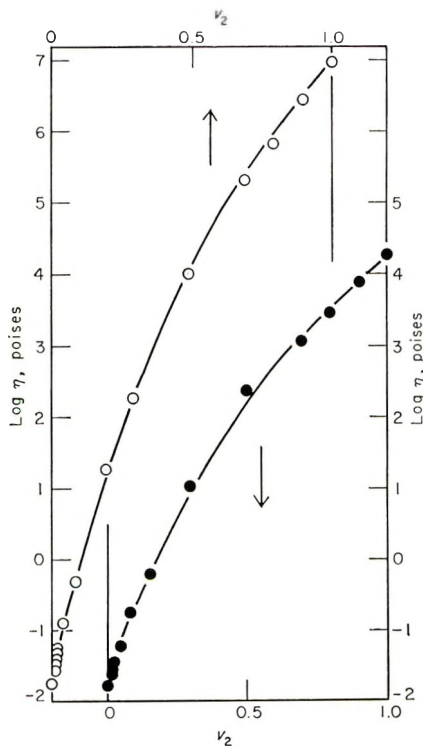


Fig. 9. Relations between $\log \eta$ and v_2 : (○) branched PE ($\bar{M}_w = 1.15 \times 10^6$)-wax system; (●) branched PE ($\bar{M}_w = 1.9 \times 10^5$)-wax system. Solid lines are those calculated from eq. (16).

TABLE V
Values of a for Some Homologous Polymer Blends

Polymer	Component 1 ^a	Component 2 ^a	Temp., °C.	a	Note ^b
Polyethylene ^c	Wax, $M = 435$	w, l, $\bar{M}_w = 1.75 \times 10^5$	150	0.81	s
"	"	w, l, $\bar{M}_w = 7.3 \times 10^4$	"	0.75	"
"	"	w, b, $\bar{M}_w = 1.15 \times 10^5$	"	0.52	"
"	"	w, b, $\bar{M}_w = 1.9 \times 10^5$	"	0.48	"
Polyethylene ^d	w, b, MI = 20	w, b, MI = 2.2	160	0.0	d
Polypropylene ^e	n-Heptane extract $\bar{M}_w = 2.7 \times 10^4$	w, $\bar{M}_w = 2.69 \times 10^5$	200	0.65	"
Polystyrene ^f	f, $\bar{M}_w = 1.1 \times 10^5$	f, $M_w = 6.9 \times 10^5$	135	0.54	t
Polystyrene ^g	f, $\bar{M}_w = 8.25 \times 10^4$	f, $M_w = 2.67 \times 10^5$	227	0.43	s
Poly(decamethylene adipate) ^h	Diethyl succinate MI = 174	f, $M = 1.6 \times 10^4$	79	0.50 ⁱ	"
"	$Z_w = 92.5$	$Z_w = 893$	109	0.40 ⁱ	"

^a Component 1: lower molecular weight component; component 2: higher molecular weight component; w: whole polymer; f: fraction; l: linear; b: branched; M : molecular weight, MI: melt index, Z : numbers of chain atoms.

^b s: steady shear viscosity, d: dynamic viscosity, t: tensile viscosity.

^c Data of Busse and Longworth.⁷

^d Data of Horio et al.²⁵

^e Data of Onogi et al.²⁶

^f Data of Ninomiya et al.¹¹

^g Data of Rudd.¹⁷

^h Data of Flory.¹

ⁱ The value of a was estimated from eq. (15) by using weight fractions.

TABLE VI
Viscosities of Poly(decamethylene Adipate) Blends and Poly(decamethylene Adipate)-Diethylsuccinate Systems^a
Poly(decamethylene adipate)-diethyl succinate systems

Weight fraction w_2^b	Viscosity η , poises		Weight fraction w_2^b	Viscosity η , poises	
	Observed value	Calculated from eq. (16)		Observed value	Calculated from eq. (16)
0.000	4.66×10^{-1}		0.000	9.6×10^{-3}	1.05×10^{-2}
0.163	1.75	1.72	0.00422	1.055×10^{-2}	1.17×10^{-2}
0.285	4.1	3.93	0.00928	1.195×10^{-2}	1.34×10^{-2}
0.504	1.35×10^1	1.43×10^1	0.01585	1.40×10^{-2}	1.62×10^{-2}
0.664	2.75×10^1	2.80×10^1	0.0249	1.72×10^{-2}	2.75×10^{-2}
0.818	5.3×10^1	5.17×10^1	0.0517	3.07×10^{-2}	6.80×10^{-2}
1.000	9.7×10^1		0.1007	7.33×10^{-2}	3.30×10^{-1}
			0.199	3.67×10^{-1}	1.34
			0.300	1.46	2.22
			0.341	2.28	1.20×10^1
			0.500	1.22×10^1	6.43×10^1
			0.700	6.10×10^1	1.69×10^2
			0.844	1.47×10^2	
			1.000	4.25×10^2	

^a Data of Flory.¹

^b Weight fractions were employed in eqs. (15) and (16).

it is seen that the calculated values are nearly the same as the observed values over the whole range of composition.

The magnitude of a depends on the molecular weights of both components of the blend and on the polymer structure. It is interesting to note that the values of a are much larger for linear polyethylene-wax systems than those for branched polyethylene-wax systems.

The applicability of eq. (16) for polydimethylsiloxane blends appears to be better for systems with $M_1 > M_c$ and $M_2 > M_c$ than for those with $M_1 < M_c$ and $M_2 > M_c$. However, in other systems these criteria appeared to play a much less serious role. The broad range of applicability of this empirical relationship is quite encouraging.

In formulating eq. (16) we employed the volume fractions as the unit of composition. The choice of the composition unit is somewhat arbitrary, but the use of the volume fraction may be preferable from the theoretical point of view, although the theoretical interpretation or physical significance of eq. (16) is not clear at the present time.

References

1. P. J. Flory, *J. Am. Chem. Soc.*, **62**, 1057 (1940); *J. Phys. Chem.*, **46**, 870 (1942).
2. T. G. Fox and P. J. Flory, *J. Am. Chem. Soc.*, **70**, 2384 (1948).
3. T. G. Fox and P. J. Flory, *J. Phys. Colloid Sci.*, **55**, 221 (1951).
4. T. G. Fox, S. Gratch, and S. Loshaek, in *Rheology*, F. Eirich, Ed., Vol. 1, Academic Press, New York, 1956, Chap. 12.
5. V. R. Allen and T. G. Fox, *J. Chem. Phys.*, **41**, 337 (1964).
6. T. G. Fox and V. R. Allen, *J. Chem. Phys.*, **41**, 344 (1964).
7. W. F. Busse and R. Longworth, *J. Polymer Sci.*, **58**, 49 (1962).
8. R. Longworth and W. F. Busse, *Trans. Soc. Rheol.*, **6**, 179 (1962).
9. K. Ninomiya, *J. Colloid Sci.*, **14**, 49 (1959).
10. K. Ninomiya, *J. Colloid Sci.*, **17**, 759 (1962).
11. K. Ninomiya and J. D. Ferry, *J. Colloid Sci.*, **18**, 421 (1963).
12. T. Kataoka and S. Ueda, *J. Polymer Sci.*, in press.
13. T. Sakai, private communication.
14. A. Kolorelov, K. A. Andrianov, L. S. Uchecheva, and T. E. Vuegenskaya, *Dokl. Akad. Nauk SSSR*, **89**, 65 (1959).
15. A. J. Barlow, G. Harrison, and J. Lamb, *Proc. Roy. Soc. (London)*, **A282**, 228 (1964).
16. L. H. Tung, *J. Polymer Sci.*, **46**, 409 (1960).
17. J. F. Rudd, *J. Polymer Sci.*, **44**, 459 (1960).
18. F. Bueche, *J. Polymer Sci.*, **43**, 527 (1960).
19. F. Bueche, C. J. Coven, and B. J. Kinzig, *J. Chem. Phys.*, **39**, 128 (1963).
20. F. Bueche, *J. Chem. Phys.*, **20**, 1959 (1952); *Physical Properties of Polymers*, Interscience, New York, 1962.
21. T. Kataoka and S. Ueda, *J. Polymer Sci. B*, **4**, 317 (1966).
22. T. Kataoka and S. Ueda, *Bull. Textile Res. Inst. Japan*, **79**, 7 (1966).
23. R. L. Merker, *J. Polymer Sci.*, **22**, 353 (1956).
24. H. Leaderman, R. G. Smith, and L. C. Williams, *J. Polymer Sci.*, **36**, 233 (1959).
25. M. Horio, T. Fujii, and S. Onogi, *J. Phys. Chem.*, **68**, 421 (1963).
26. S. Onogi, S. Ueki, and H. Kato, paper presented at 14th Rheology Symposium, Sendai, Japan, October 1965.

Résumé

Les viscosités à tension de cisaillement nulle de mélanges à deux composants de polydiméthylsiloxane de différents poids moléculaires ont été mesurées sur toute la gamme de compositions. Les résultats sont analysés sur la base du traitement conventionnel de la viscosité de mélanges polymériques et certains commentaires sont faits à ce sujet.

En outre, une équation empirique a été trouvée: $\log \eta_{bl} = \frac{v_1(1-a)}{1-av_1} \log \eta_1 + \frac{v_2}{1-av_1} \log \eta_2$, où η est la viscosité, v , la fraction de volume, et où les indices 1 et 2 et bl dénotent les composants de bas et haut poids moléculaires et le mélange, et a est une constante indépendante de la composition. L'équation ci-dessus n'est pas seulement applicable à toutes sortes de mélanges de polydiméthylsiloxane mais également à d'autres polymères.

Zusammenfassung

An Zweikomponentengemischen von Polydimethylsiloxanen verschiedenen Molekulargewichts wurden die Viskositäten für Scherspannung Null über den ganzen Zusammensetzungsbereich gemessen. Die Ergebnisse werden auf der Grundlage der für die Viskosität von Polymerlösungen üblichen Verfahren analysiert und einige Bemerkungen über diese Art der Datenbehandlung gemacht. Danach wird eine empirische Gleichung

abgeleitet: $\log \eta_{bl} = \frac{v_1(1-a)}{1-av_1} \log \eta_1 + \frac{v_2}{1-av_1} \log \eta_2$ wobei η die Viskosität, v der

Volumbruch ist und die Suffixe 1, 2 und bl die nieder- und die höhermolekulare Komponente bzw. die Mischung bezeichnen; a ist eine von der Zusammensetzung unabhängige Konstante. Die obige Gleichung ist nicht nur für alle Reihen von Polydimethylsiloxan-Mischungen, sondern auch für andere Polymere anwendbar.

Received November 30, 1966

Revised April 26, 1967

Prod. No. 5441A

Polymer Reactions. V. Kinetics of Autoxidation of Polypropylene

JAMES C. W. CHIEN and C. R. BOSS,
*Research Center, Hercules Incorporated,
Wilmington, Delaware 19899*

Synopsis

The rate constants for the autoxidation of polypropylene were determined by a combined ESR, volumetric, and chemical method. The values of k_i , k_p , and k_t at 110°C. are 3×10^{-4} sec.⁻¹, 1.9 l./mole-sec., and 3×10^6 l./mole-sec., respectively. The values of k_t and its activation energy are the same as those for the decomposition of polypropylene hydroperoxide, thus identifying the latter as the principal initiation process. The values of the temperature-independent k_t suggest that secondary peroxy radicals are the terminating species. The rate constants are compared with rate constant ratios for initiated autoxidations of squalane and other related systems.

INTRODUCTION

Most investigations of the autoxidation of polyolefins make use of oxygen absorption techniques alone to measure induction periods and the rates of oxidation. The results thus obtained can be expressed only as some combinations of rate constants.^{1,2} The use of initiator allowed Tobolsky et al.³ to determine accurate ratios of rate constants.

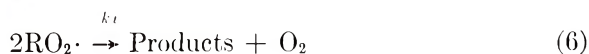
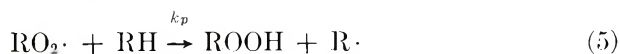
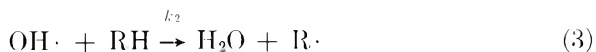
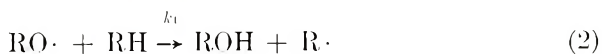
To define the kinetics of autoxidation requires at least three rate constants for the most simplified reaction sequence. That these rate constants are not readily determined is evident from the scarcity of results. Most of the values⁴ were obtained by the rotating-sector method. This method cannot be readily adapted to study solid polymer samples. On the other hand, electron spin resonance (ESR) appears to be ideal, although to the authors' knowledge, it has not been applied in this context.

This paper describes a method which enabled us to determine rate constants in the autoxidation of polypropylene. The results are compared with the rate constant ratios of oxidation of squalane and related systems.

KINETIC METHOD

The branched chain autoxidation of polyolefins is characterized by an induction period; during this time hydroperoxides are produced.⁵ The decomposition of these hydroperoxides is commonly assumed^{6,7} as the

process responsible for the ensuing faster oxidation. In a previous paper,⁸ each —OOH, upon decomposition, was observed to yield 1.8 radicals. The initiation reaction and the subsequent processes may be represented by the familiar sequence:



Under the chosen experimental conditions of 100- μ polymer particles and a pressure of oxygen of 1 atm., termination is predominantly by eq. (6).¹² In the region of constant autoxidation rate, steady-state assumptions for $\text{RO}\cdot$, $\text{OH}\cdot$, $\text{R}\cdot$, and ROOH give

$$k_i = (-d[\text{O}_2]/dt)_s/2[\text{ROOH}]_s \quad (7)$$

$$k_p = (-d[\text{O}_2]/dt)_s/2[\text{RO}_2\cdot]_s[\text{RH}] \quad (8)$$

$$k_t = (-d[\text{O}_2]/dt)_s/2[\text{RO}_2\cdot]_s^2 \quad (9)$$

and

$$(-d[\text{O}_2]/dt)_s = k_i[\text{ROOH}]_s + (k_p[\text{RH}]/k_t^{1/2})(k_i[\text{ROOH}]_s)^{1/2} \quad (10)$$

where the subscript *s* designates steady-state quantities.

To obtain the "step" rate constants, the rate of oxidation was measured continuously by a gas absorption apparatus connected to the ESR cell; the ESR output gave instantaneous $[\text{RO}_2\cdot]_s$. The sample was quenched afterwards for iodimetric determination of $[\text{ROOH}]_s$.

EXPERIMENTAL

Materials

Crystalline polypropylene from Hercules Incorporated was used in this work. Eastman white label squalane was purified by fractional distillation.

Kinetic Measurements

Most of the autoxidation experiments were carried out in conjunction with ESR measurements. In these experiments, the quartz ESR sample

tube (containing 0.08 g. of polymer and 0.2 g. of Linde 5A sieves) was connected via O-ring joints and 1 in. of Tygon tubing to a gas absorption apparatus. The flexible tubing allows rapid transfer of the sample tube from the resonant cavity into a quenching bath without opening the system to the atmosphere. The cell and the associated absorption apparatus were evacuated and flushed with oxygen. All experiments were carried out at one atmosphere of oxygen.

Monitoring of the ESR spectrometer began as soon as the desired temperature was attained in the resonant cavity. The oxygen uptake caused a pressure drop and imbalance between the two arms of a mercury pressure-sensing device. A rise in the mercury level of the arm containing two platinum-tipped tungsten electrodes closed the circuit which activated a motor to raise the mercury leveling bulb of a thermostatted gas buret to compensate for the pressure drop. The motor was also mechanically coupled to a potentiometer, the output of which was recorded by a 6-in. Leeds & Northrup Speedomax recorder. The system responds to the uptake of 0.01 ml. of oxygen.

After the steady-state condition had been attained, as indicated by constant rate of oxidation and ESR signal intensity, the sample tube was quickly transferred into a Dewar flask containing a mixture of Dry Ice and trichloroethylene. The total amount of oxygen absorbed was about 4 ml., which is equivalent to 50 ml. of oxygen per gram of polymer.

To assure that autoxidation was occurring at a normal rate, the rates of oxidation in the ESR tube and in the oven were compared. The cell was placed in a constant temperature oven and the rate of oxidation was measured. When the two rates agreed, the autoxidation in the ESR sample tube was said to be normal.

At 140°C., the rate of oxidation in the ESR cavity was considerably slower than that in the oven. Apparently, oxygen consumption was too fast to be accommodated by its diffusion through the 3-mm. i.d. sample tube. At this temperature, therefore, small pieces of Teflon (about 0.5 mm. in diameter) were mixed with the polypropylene flake to reduce the net oxygen consumption. Autoxidations under this condition have normal rates.

The effective length of the resonant cavity was 0.9 in.; the maximum temperature gradient between different portions of the cavity was about 2°C. The temperature of the cavity was maintained within $\pm 1^\circ\text{C}$.

The radical concentration was calculated from the first moment of its spectrum and that of standard α,α -diphenylpicrylhydrazyl solutions. A curve follower was used to take 75 or more data points from a spectrum and the first moment was calculated by a Bendix G15 computer. Baseline fluctuation was compensated by assuming a linear baseline between the first three and last three points of the spectrum.

The radical was found to be stable at -60°C . almost indefinitely. The sample could be warmed up and the spectrum taken again at room temperature without significant loss of intensity. The line shape, however, was different from that obtained at elevated temperatures.

The hydroperoxide in the sample was determined by iodimetry. The intrinsic viscosity was measured in 1% decalin solution at 135°C. The carbonyl contents were analyzed with a Beckmann IR-7 spectrophotometer in the 1600–1850 cm^{-1} region.⁹

RESULTS

Autoxidation Profile

Several preliminary experiments were carried out on the autoxidation of polypropylene both in the solid state and in solutions of trichlorobenzene. The results, illustrated in Figures 1 and 2, can be summarized as follows. During the induction period, the drop in intrinsic viscosity, the formation of hydroperoxide and carbonyl functionalities, and the consumption of

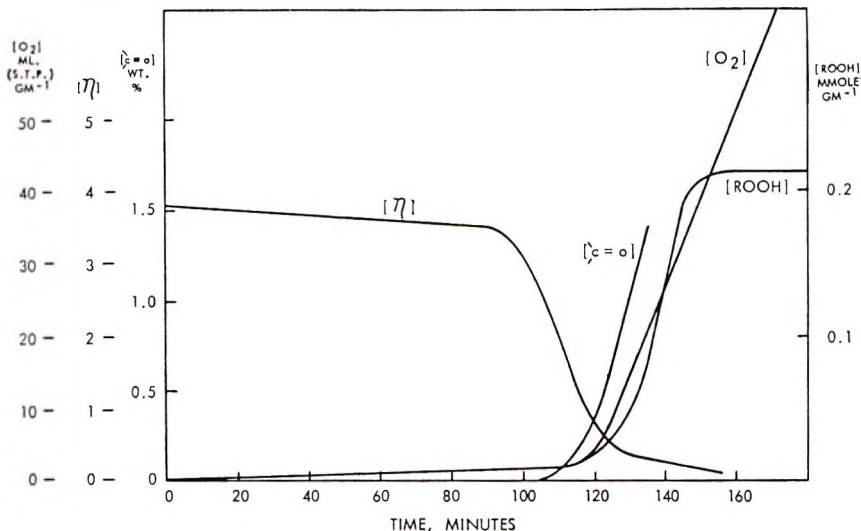


Fig. 1. Autoxidation of polypropylene flake at 140°C.

oxygen were minor. Significant changes were observed toward the end of the induction period. During steady-state oxidation, the rate of oxygen uptake and the hydroperoxide concentration remained approximately constant, whereas the intrinsic viscosity decreased and carbonyl concentration increases with time. From these results, the steady-state condition was chosen between 40 and 60 ml. of oxygen reacted per gram of polymer.

The amount of radicals present during the induction period was too low to be detected by ESR. All subsequent kinetic measurements were made during the steady-state period.

TABLE I
 Autooxidation of Polypropylene

Temp., °C.	$\left(\frac{-d[O_2]}{dt}\right)_s \times 10^4$, mole/l.-sec.	[ROOH] _s , mole/l.	[ROO·] _s × 10 ⁶ , mole/l.	$k_t \times 10^4$, sec. ⁻¹	k_p , l./mole-sec.	$k_t \times 10^{-6}$, l./mole-sec.
110	2.86	0.47	6.9	3.0	1.9	3.0
110	2.63	0.46	6.4	2.9	1.9	3.2
110	2.80	0.46	6.8	3.0	1.9	3.0
			Avg.	3.0 ± 0.1	1.9	3.1 ± 0.1
120	5.65	0.48	8.2	5.9	3.1	3.8
120	5.63	0.38	7.9	7.8	3.2	4.5
120	5.70	0.42	7.4	6.8	3.5	5.2
120	5.70	0.43	7.9	6.6	3.3	4.5
			Avg.	6.8 ± 0.8	3.3 ± 0.1	4.5 ± 0.6
130	10.1	0.26	9.4	19	4.9	5.8
130	10.3	0.32	11.0	16	4.3	4.3
130	8.8	0.28	10.3	16	3.8	4.1
130	8.8	0.30	10.1	15	4.0	4.0
			Avg.	16.5 ± 1.7	4.2 ± 0.5	4.5 ± 0.8
140	15.7	0.26	14.5	30	4.9	3.7
140	16.2	0.24	15.0	34	4.9	3.6
140	15.7	0.25	17.5	31	4.1	2.6
			Avg.	32 ± 2	4.6 ± 0.5	3.3 ± 0.6
ΔE , kcal./mole				25	9	~0

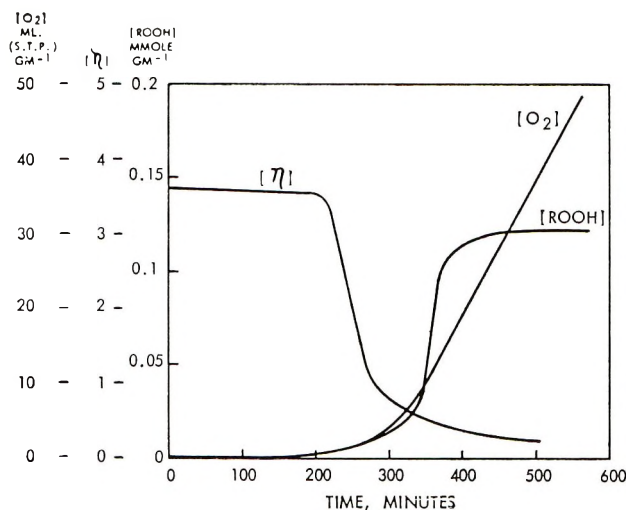


Fig. 2. Autoxidation of polypropylene in solution at 140°C. (50 g./l. in trichlorobenzene).

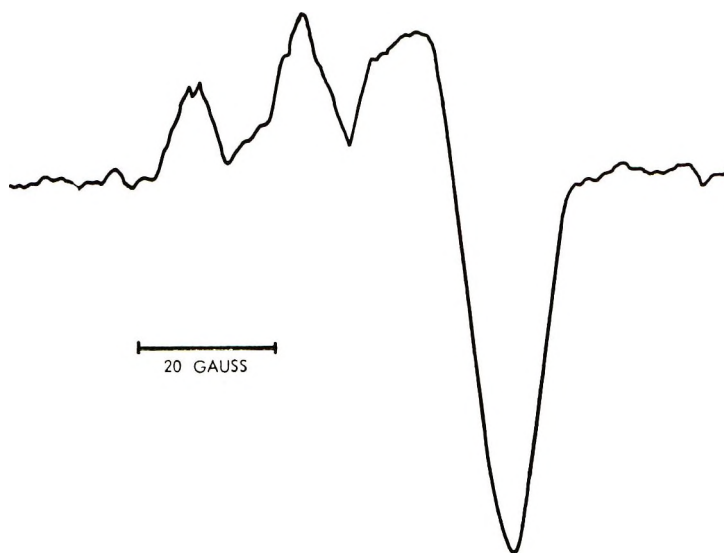


Fig. 3. ESR spectrum of polypropylene peroxy radical at 25°C.

Autoxidation of Polypropylene

Of the radical species postulated in reaction sequence (1)–(6), only $\text{ROO}\cdot$ is expected to be detected by ESR. Experimental confirmation of this expectation as well as description of variations of g anisotropy of peroxy radicals with temperature and phase changes are described in another paper.¹⁰ Typical spectra of polypropylene peroxy radicals are shown in Figures 3 and 4.

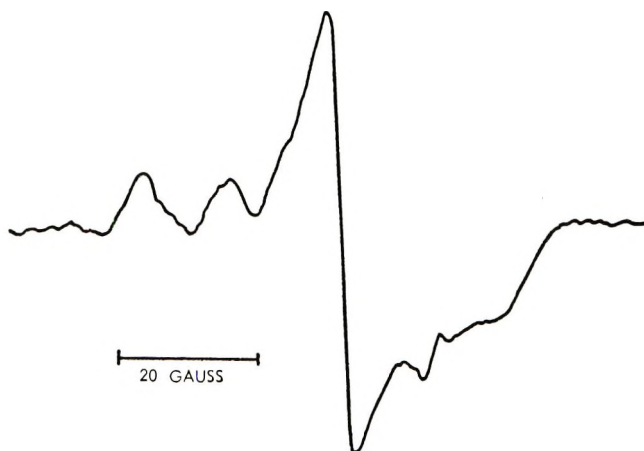


Fig. 4. ESR spectrum of polypropylene peroxy radical at 130°C.

The results of the experiments are presented in Table I. The rate constants were calculated from eqs. (7)–(9). The value of $[RH]$ was chosen with two simplifying assumptions; only tertiary hydrogen atoms were reacted,¹¹ and only the amorphous phase of the sample was oxidized.¹² Since the polypropylene used in this work was rated 50% crystalline by x-ray and by density measurements, $[RH]$ was taken to be 11 mole/l.

Table I also gives average values of rate constants, their standard deviations, and their energies of activation. Experiments at temperatures higher than 140°C. were found to be unfeasible: use of the Teflon dilution technique still did not allow the oxidation to proceed at the "normal" rate.

DISCUSSION

For a given set of reaction sequences containing m step rate constants, determinations of m observable quantities allow the calculation of a set of rate constants. These constants are self-consistent in the sense that if one of them is wrong, all others are proportionately off by factors which relate these constants in the rate expressions. To establish the validity of such a set of rate constants, one of them must be verified by an independent measurement.

Of the rate constants defined in the eqs. (1)–(6), only that of the initiation process can be separately determined. This process has been postulated as the decomposition of hydroperoxides. Therefore, the rate constant of decomposition of polypropylene hydroperoxide k_d obtained earlier³ may be identified with the rate constant of initiation k_i for autoxidation obtained here. The agreement between the two sets of results, shown in Figure 5, is quite remarkable. It lends support to our postulated mechanism and kinetics of autoxidation of polypropylene and indicates the correctness of the other rate constants k_p and k_t .

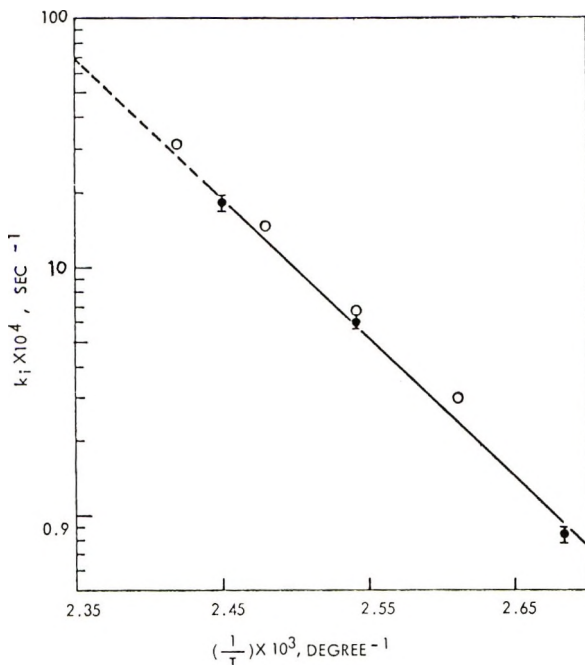


Fig. 5. Temperature dependence of (○) the rate constant of initiation for autoxidation of polypropylene and (●) the rate constant of decomposition of polypropylene hydroperoxide.⁸

The diffusional activation energy of polypropylene¹³ is 9.7 kcal./mole at temperatures below the melting point of the polymer. On the other hand, our values of k_t show no temperature dependence within experimental accuracy. This indicates that the termination reaction occurs either via an intramolecular process or between proximity sites on immediate neighboring polymer molecules. It could involve termination by very mobile, low molecular weight peroxy radicals. Our values of k_t are comparable to those found¹⁴ for other secondary peroxy radicals and are about two to three orders of magnitude faster than the k_t values for tertiary peroxy radicals. The most likely explanation is that intramolecular hydrogen abstraction during chain propagation also proceeds via seven-membered ring transition states.¹⁵ This type of abstraction produces secondary peroxy radicals which are capable of rapid terminations. An alternative explanation for the rapid termination observed is that direct cage combination reaction of tertiary peroxy radicals occurs; this, however, is contrary to the results of Traylor et al.¹⁶

The results reported here are comparable with those given by Tobolsky et al.³ At 110°C., their rate constant ratio for initiated oxidation of amorphous polypropylene is

$$(k_p/k_t^{1/2})e_i^{1/2}[\text{RH}] = 2.3 \times 10^9 \text{ ml.}^{1/2}/\text{molecule}^{1/2}\text{-sec.}^{1/2} \quad (11)$$

where e_i is the efficiency of initiator. For amorphous polypropylene $[\text{RH}] = 22 \text{ mole/l.}$, the ratio $k_p e_i^{1/2}/k_t^{1/2} = 4.2 \times 10^{-3} \text{ l.}^{1/2}/\text{mole}^{1/2}\text{-sec.}^{1/2}$.

Our value is $1.1 \times 10^{-3} \text{ l.}^{1/2}/\text{mole}^{1/2}\text{-sec.}^{1/2}$. The agreement should be considered as encouraging.

Tobolsky et al.³ found the ratio of $k_p e_t^{1/2} [\text{RH}]/k_t^{1/2}$ for ethylene-propylene copolymer to that for polypropylene to be 0.45 and concluded that intramolecular propagation down the polymer chain through a six-membered transition state is no more favored than interchain random propagation. The similarity of the two ratios can be readily accounted for if the kinetic chain length is short. With the known structure for polypropylene hydroperoxide,¹⁷ we believe that propagation via cyclic transition states is definitely favored over random reactions.

Table II compares the values of $k_p/k_t^{1/2}$ for polypropylene autoxidation and initiated autoxidation of squalane. The remarkable agreement indicates similar mechanisms for the two systems. The absence of phase and molecular weight dependences suggests that translational diffusion of the peroxy radicals in the propagation and termination steps are not involved in polypropylene autoxidation.

The picture for autoxidation of polypropylene evolved from this work is the following. There is slow oxidation during the induction period. Intramolecular hydrogen abstraction via the favored six-membered transition state results in the formation of neighboring hydroperoxides during this period.

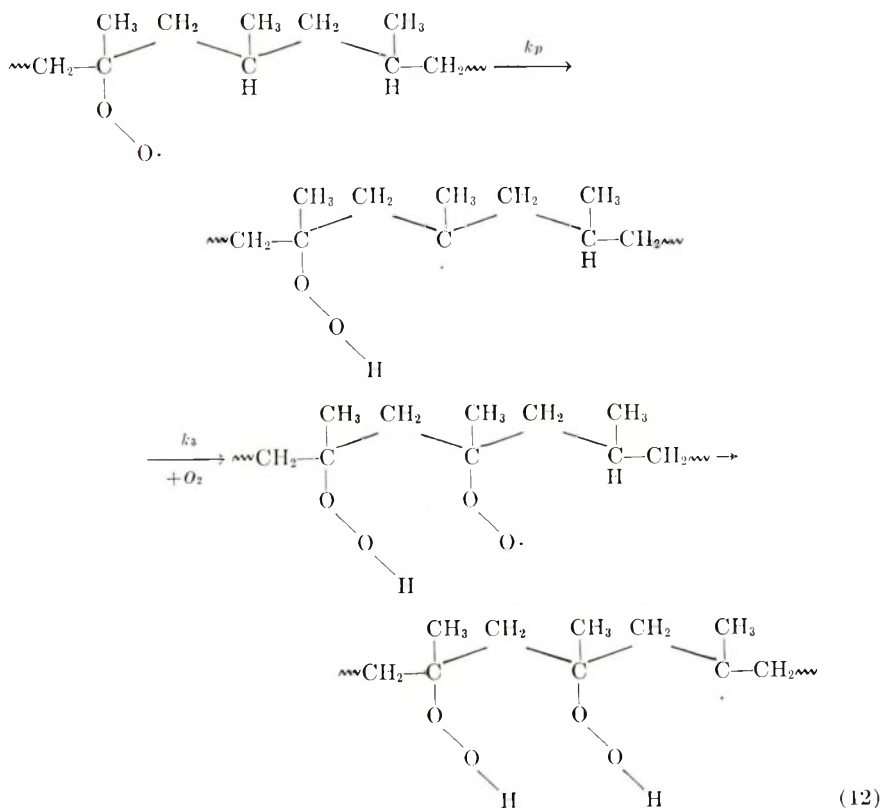


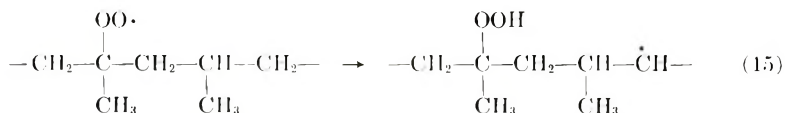
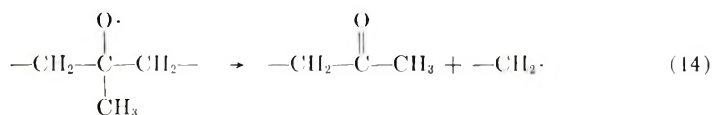
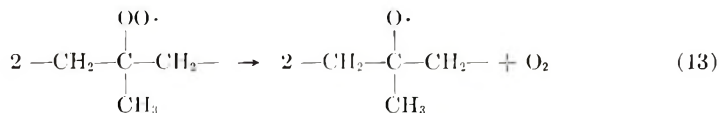
TABLE II
Rate Constants for Polypropylene and Squalane Autoxidation

Temp., °C.	$(k_p/k_t^{1/2}) \times 10^3, \text{l.}^{1/2}/\text{mole}^{1/2}\text{-sec.}^{-1/2}$	
	Polypropylene	Squalane
110	1.1	
115		1.2
120	1.6	
125		1.9
130	2.0	
140	2.5	2.8

By this process, the build-up rate of hydroperoxide is an exponential function.¹⁸

The hydroperoxides attached to the polymer chain decompose predominantly by a rapid intramolecular radical chain process. A steady state is achieved when the hydroperoxides decompose as fast as they are formed. This state is characterized by an approximately constant rate of oxidation.

Termination is primarily via the disproportionation of a primary or a secondary peroxy radical with another peroxy radical. The former could be formed by two types of reactions, the sequence of eqs. (13) and (14) or reaction (15).



In the autoxidation of polypropylene, some of the primary products^{19,20} are water, formaldehyde, acetaldehyde, acetic acid, acetone, and 2,5-hexanedione. It is possible to rationalize the formation of these products by the initiation, propagation, and termination mechanisms suggested here involving neighboring interactions in many of the processes.

References

1. N. T. Notley, *Trans. Faraday Soc.*, **58**, 1 (1962); *ibid.*, **60**, 1 (1964).
2. S. S. Stivola, L. Reich, and P. G. Kelleher, *Makromol. Chem.*, **59**, 28 (1963).
3. A. V. Tobolsky, P. M. Norling, N. H. Frick, and H. Yu, *J. Am. Chem. Soc.*, **86**, 3925 (1964).
4. C. Walling, *Free Radicals in Solution*, Wiley, New York, 1957, p. 503.

5. K. U. Ingold, *Chem. Rev.*, **61**, 563 (1961).
6. J. L. Bolland, *Quart. Rev.*, **3**, 1 (1949).
7. L. Bateman, *Quart. Rev.*, **8**, 147 (1954).
8. J. C. W. Chien and H. Jabloner, *J. Polymer Sci. A-1*, in press.
9. L. P. Luongo, *J. Polymer Sci.*, **42**, 139 (1960).
10. J. C. W. Chien and C. R. Boss, *J. Am. Chem. Soc.*, **89**, 571 (1967).
11. H. C. Beachell and D. L. Beck, *J. Polymer Sci. A*, **3**, 457 (1965).
12. F. H. Winslow and W. L. Hawkins, in *Crystalline Olefin Polymers*, R. A. V. Raff and K. W. Doak, Eds., Interscience, New York, 1965, pp. 838-840.
13. P. S. Francis, unpublished results.
14. J. A. Howard and K. U. Ingold, *Can. J. Chem.*, **44**, 1119 (1966).
15. F. F. Rust, *J. Am. Chem. Soc.*, **79**, 4000 (1957).
16. A. Factor, C. A. Russell, and T. G. Traylor, *J. Am. Chem. Soc.*, **87**, 3692 (1965).
17. J. C. W. Chien and H. Jabloner, *J. Polymer Sci. A-1*, in press.
18. A. V. Tobolsky, D. J. Metz, and R. B. Mesrobian, *J. Am. Chem. Soc.*, **72**, 1942 (1950).
19. E. M. Bevilacqua, E. S. English, and J. S. Gall, *J. Appl. Polymer Sci.*, **8**, 1969 (1964).
20. E. M. Bevilacqua and P. M. Norling, *Nature*, **147**, 289 (1965).

Résumé

Les constantes de vitesse d'autoxydation du polypropylène ont été déterminées en combinant l'E.S.R. et des méthodes volumétriques et chimiques. Les valeurs de k_i , k_p et k_t à 110°C sont de 3×10^{-6} /sec, 1,9 litres/mole-sec et 3×10^4 litres/mole-sec, respectivement. Les valeurs de k_i et de son énergie d'activation sont les mêmes que celles caractérisant la décomposition de l'hydroperoxyde de polypropylène, ce qui permet d'identifier le processus d'initiation principal. Les valeurs de k_i indépendantes de la température suggèrent que les radicaux peroxy secondaires sont les espèces terminantes. Les constantes de vitesse sont comparées aux rapports de constante de vitesse pour l'autoxydation initiée du squalène et d'autres systèmes voisins.

Zusammenfassung

Die Geschwindigkeitskonstanten für die Autoxydation von Polypropylen wurden durch eine kombinierte ESR, volumetrische und chemische Methode bestimmt. Die Werte von k_i , k_p und k_t betragen bei 110°C 3×10^{-6} /sec, 1,9 Liter/Mol-sec bzw. 3×10^4 Liter/Mol-sec. Die Werte von k_i und dessen Aktivierungsenergie gleichen denen für den Zerfall von Polypropylenhydroperoxyd; damit ist dieser als der wesentliche Startprozess identifiziert. Die temperaturunabhängigen Werte von k_i lassen vermuten, dass sekundäre Peroxyradikale die abbrechende Spezies darstellen. Die Geschwindigkeitskonstanten werden mit den Verhältnissen der Geschwindigkeitskonstanten bei der gestarteten Autoxydation von Squalan und anderen verwandten Systemen verglichen.

Received March 20, 1967

Revised May 1, 1967

Prod. No. 5444A

Hydrophobic Interaction in Poly(2-hydroxyethyl Methacrylate) Homogeneous Hydrogel

MIGUEL F. REFOJO,

*Departments of Cornea and Retina Research,
Institute of Biological and Medical Sciences,
Retina Foundation, Boston, Massachusetts 02114*

Synopsis

Homogeneous poly(2-hydroxyethyl methacrylate) (PHEMA) hydrogel exhibits a narrow range of swelling at equilibrium in water (% H₂O, 41.09 ± 0.15 standard error of the mean of 24 samples), regardless of the dilution of the monomer solution and relatively low level of crosslinking. It is postulated that PHEMA hydrogel has, in addition to its covalently linked network structure, a secondary structure stabilized by hydrophobic bonding. The addition of microsolute to the hydrogel seems to confirm this hypothesis. The hydrogel swells beyond its swelling equilibrium in water in presence of urea and its methyl derivatives. Swelling is also induced by organic solvents like alcohol and acetone, and by anions like iodide, acetate, trichloroacetate, and thiocyanate. Chlorides and sulfates produce a less swollen hydrogel than pure water, while bromides and cetylpyridinium chloride, in the concentrations tested, induce only a slight deswelling of the gel. When PHEMA gel prepared in organic solvent-water solutions is placed in water, the gel passes through an opaque state before becoming transparent again. This phenomenon is interpreted as being caused by the inability of water to solvate the hydrophilic ends of the unorganized polymer segments. Homogeneity returns to the gel after a rearrangement of the chains, directed by the interaction of the hydrophobic portions of the polymer segments, exposing to the solvent-water most of the hydrophilic sites in the network.

INTRODUCTION

Homogeneous poly(2-hydroxyethyl methacrylate) (PHEMA) hydrogel is of practical interest for the manufacture of soft contact lenses and for certain other medical uses.^{1,2} PHEMA gel may be prepared by polymerization of HEMA with a small amount of ethylene glycol dimethacrylate as a crosslinking agent in ethylene glycol-water solution or in any other good solvent medium for both monomer and polymer. Although linear PHEMA is insoluble in water, it is soluble in aqueous solutions of certain organic solvents. Homogeneous PHEMA hydrogel was found to exhibit³ a narrow range of swelling at equilibrium in water (% H₂O, 41.09 ± 0.15 standard error of the mean of 24 samples), regardless of the initial dilution of the monomer solution and relatively low level of crosslinking.³⁻⁵ The polymer obtained in bulk swells in water to about the same degree as the gel prepared in solution. Therefore, it appears that PHEMA hydrogel

may have, in addition to its covalently linked primary structure, a secondary structure stabilized by noncovalent forces. The forces stabilizing the secondary structure of PHEMA in water may be similar to some of the forces which contribute to stabilize the compact structure of globular proteins, the so-called hydrophobic interactions.⁶ If such is the case, the addition of agents that interfere with these forces should lead to changes in the structure of PHEMA hydrogel manifested by variations in its swelling equilibrium.

With hydrophobic interactions having already been found to contribute greatly to stabilization of the secondary structure of un-ionized poly-(methacrylic acid) (PMAA) in aqueous solutions^{7,8} and with the chemical similarity between un-ionized PMAA and PHEMA molecules, one may assume *a priori* that hydrophobic interactions between the methyl groups in the α position may also be the principal factors contributing to the stability of the secondary structure of PHEMA hydrogel. Hydrophobic interactions may induce PHEMA molecules to assume compact conformations, as far as the covalent crosslinks will allow, in the same way that they were found to induce this in un-ionized PMAA.^{7,8} In water, most of the hydrophobic portions of the chains tend to aggregate, avoiding contact with the solvent, while the water will hydrogen-bond the polar groups in the chains which accumulate preferentially on the periphery.

PHEMA hydrogel is a relatively strong and easy to handle material. The slight variations in the degree of equilibrium swelling of different PHEMA samples in pure water affords one an easy way to analyze the nature of these forces which bind the polymer chains together. The object of this investigation, then, was to determine the effect of the addition of electrolytes, urea and its derivatives, and water-soluble organic solvents on the hydration of PHEMA hydrogel, depending on the predominant mechanism by which these compounds may act toward the polymer-polymer (hydrophobic bonds), and polymer-water interactions.

From a practical point of view, the swelling behavior of PHEMA hydrogel in varied aqueous solutions is also interesting. Periodically, a hydrogel contact lens should be boiled in water or in saline solution for the purpose of cleaning and sterilization. The lens will then require some time to reach a different swelling equilibrium in the tear fluid. This change in swelling state, be it ever so slight, will affect the shape and indeed the optics of the lens. Also, certain aqueous solutions such as artificial tears⁹ and fluorescein solutions used by some contact lens wearers and fitters will more or less alter the shape of the lens as compared to its shape when kept or boiled in a saline solution or water.

When PHEMA hydrogel is used to make surgical implants, its swelling state before being implanted in the body may vary from that after implantation, when it has attained a different equilibrium swelling with the surrounding body fluids. The consequence of these facts must be considered. For example, it was found that PHEMA hydrogel swells in steer aqueous humor to about 68% water content at equilibrium, which means

a significant change in dimensions over the same material equilibrated in water or in physiological saline solution. The significance of this fact is that if a PHEMA implant is placed in the eye, in some way in contact with aqueous fluid, one should expect some changes in the swelling state of the implant, which implies changes in size and in its optical quality.

EXPERIMENTAL

The preparation of homogeneous HEMA hydrogel was described previously.^{3,4} A typical batch of PHEMA hydrogel was made from a mixture of 3 parts by volume of HEMA, containing 1.77% ethylene glycol dimethacrylate, 1.5 parts of ethylene glycol, 1.5 parts of water, and 0.1 part each of 6% ammonium persulfate and 12% sodium metabisulfite. The polymerization was carried out for 2 hr. at 60°C. After polymerization, the gel was allowed to equilibrate in distilled water. Slight variations in this procedure and in the constituents of the mixture produced hydrogels with small variations in water content at equilibrium swelling of no significance for the results of this work.

The effect of various solutes in aqueous solution on PHEMA structure was determined in the following manner. Two or more pieces of water-equilibrated gel (0.5–1.0 cc.) were allowed to remain at room temperature in approximately 50 cc. of each of the solutions tested. After 3 months, equilibrium swelling was assumed to have been reached. With a few of the samples, the state of equilibrium swelling was confirmed by repeated water determinations at 1-month intervals. In each case, the final water content was determined for two pieces of hydrogel. Good agreement was found in the degree of swelling of both pieces, each having the same history, the average of the two determinations being given. The water content was determined in the standard manner, by blotting the superficial aqueous solution and weighing the specimens both in their swollen state and after drying to constant weight.

All solutes used in the swelling experiments were of the purest grade available commercially, no further purification being done in any case.

RESULTS

Urea and Methylureas

The effect of urea and its derivatives on PHEMA swelling is given in Figures 1 and 2. Each of these compounds was found to induce a further swelling of PHEMA from its equilibrium swelling in water. Unsubstituted urea shows the highest swelling activity, demonstrating this property at very low concentrations. *N,N*-Dimethylurea, also a very powerful swelling agent for PHEMA although somewhat weaker than unsubstituted urea, is surprisingly enough stronger than the monomethylurea, possibly due to the presence of some urea impurities with the dimethyl derivative. Tetramethylurea exhibited the lowest swelling effect on PHEMA of the related compounds in the concentrations tested.

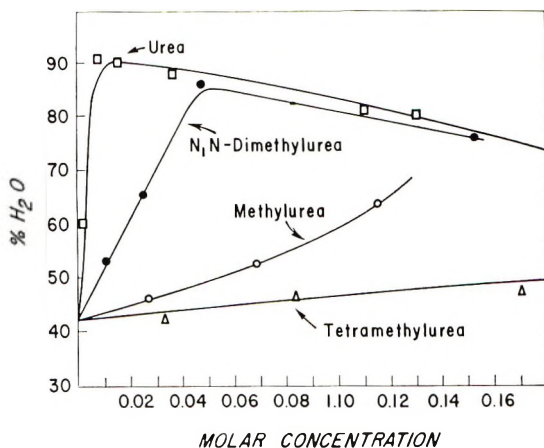


Fig. 1. Water content of PHEMA hydrogel in low concentrations of urea and methylureas.

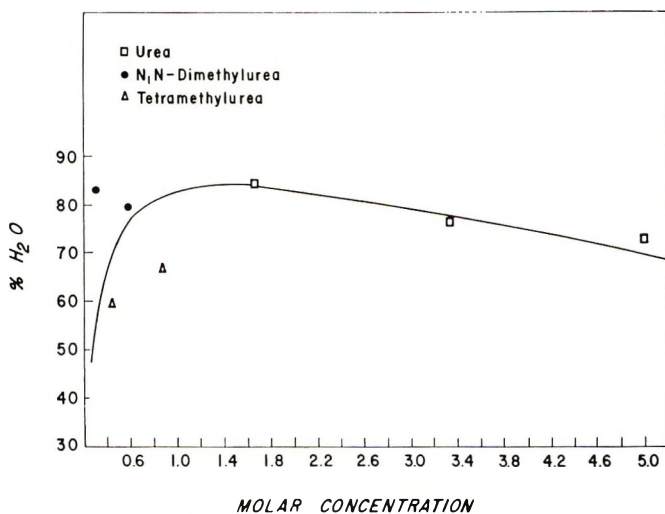


Fig. 2. Water content of PHEMA hydrogel in higher concentrations of urea and methylureas.

Acetone and Ethanol

The effects of acetone and ethanol, shown in Figure 3, demonstrate a strong swelling power on PHEMA as compared with pure water. The gel sample used in these swelling experiments was prepared from a monomer mixture containing an unusually high content of crosslinking diester, producing a tighter network and hence a lower initial water content for the gel equilibrated in water.

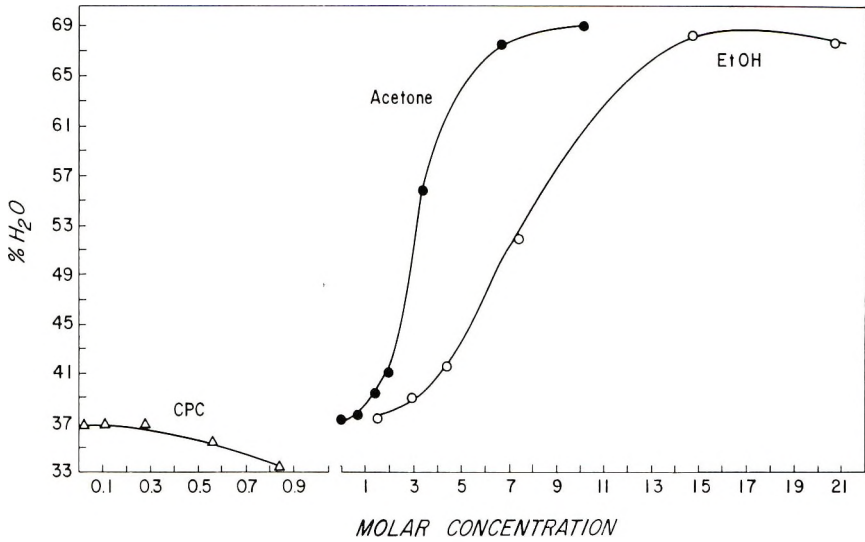


Fig. 3. Effect of acetone, ethanol, and cetylpyridinium chloride on water content of PHEMA hydrogel.

Cetylpyridinium Chloride

The same type of gel tested with acetone and ethanol was used in the experiments with cetylpyridinium chloride (CPC) solutions. The effect of this detergent, as shown in Figure 3, on the swelling of the hydrogel, is to induce a slight deswelling. Higher concentrations of CPC in water could

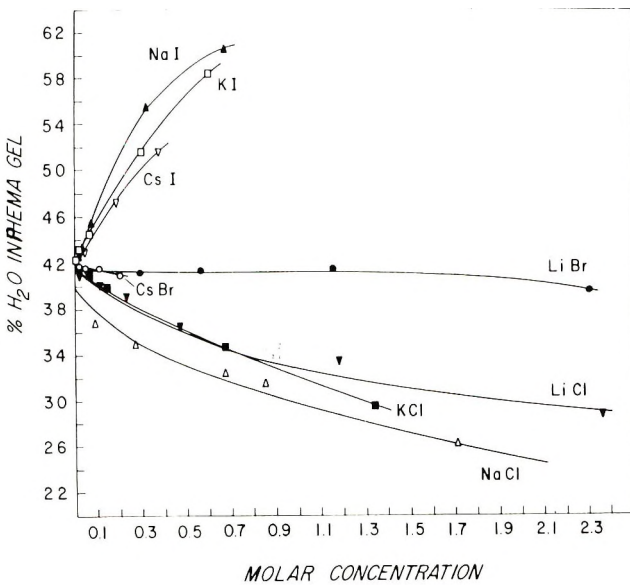


Fig. 4. Effect of alkali halides on the swelling of PHEMA hydrogel.

not be tested because of the limited solubility of this compound in water at room temperature. The two higher CPC concentrations used in these experiments crystallized repeatedly at room temperature, and were kept at 36°C. for the time allowed for the gel to equilibrate.

Alkali Halides

The effect of some alkali halides on the swelling state of PHEMA hydrogel is given in Figure 4. The chlorides have a marked salting out or deswelling effect on the PHEMA hydrogel, while bromides show a very slight, if any, deswelling in comparison with pure water. Iodides exhibit a marked swelling or salting-in effect on the hydrogel.

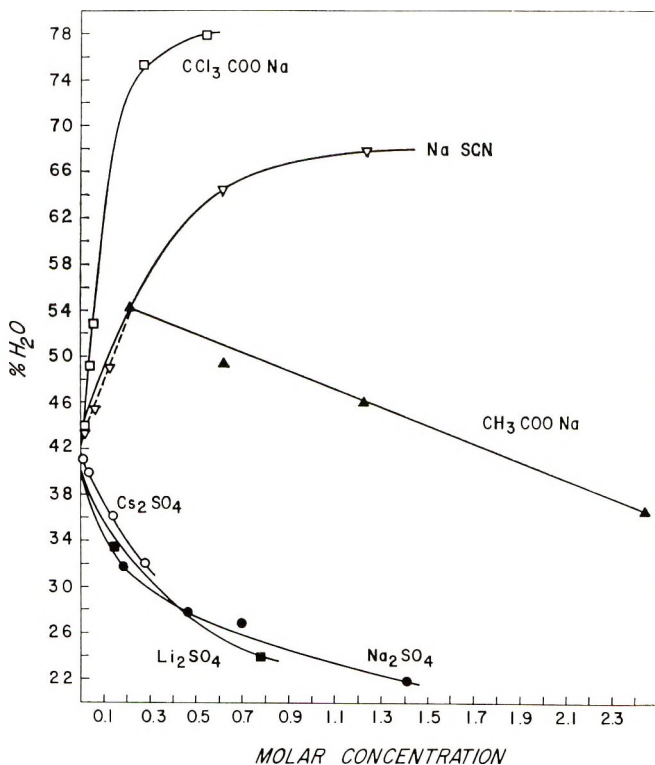


Fig. 5. Water content of PHEMA hydrogel in alkali sulfate solutions and in solutions of sodium acetate, sodium trichloroacetate, and sodium thiocyanate.

In spite of having left the iodide solutions in the dark during the time required for the PHEMA to equilibrate, some iodide ions obviously were oxidized to free iodine, as evidenced by the yellow color of the solutions. The iodine, or more likely I_3^- ions, combine with HEMA, producing varying degrees of yellow color in the gel depending on the solution concentration.

Alkali Sulfates

The results of the swelling experiments with PHEMA gel in alkali sulfate aqueous solutions are given in Figure 5. The three sulfates tested showed about the same deswelling or salting-out power for PHEMA.

Miscellaneous Salts

Sodium acetate in water was found to increase the swelling capacity of PHEMA hydrogel, which reached a maximum swelling in relatively low salt dilutions decreasing its swelling power as the concentration of the salt was raised in Figure 5.

In the concentrations tested both sodium trichloroacetate and sodium thiocyanate were found to be strong swelling agents for PHEMA hydrogel (Fig. 5).

DISCUSSION

The primary structure of homogeneous PHEMA hydrogel is a covalently linked three-dimensional network. In conjunction with this covalently bonded structure, PHEMA chains are held together by some noncovalent forces in a secondary structure giving the hydrogel, independent of its history, its characteristic swelling stability in water. A significant amount of hydrogen bonding between polymer segments is unlikely in water; hence, the feasibility that these bonds contribute in any considerable way to the stabilization of the secondary structure of PHEMA hydrogel is very slight. Interaction of the hydrophobic portions of the polymers with each other, the so-called hydrophobic bonding, is probably a very important factor in holding together PHEMA segments in an aqueous environment. The hydrophobic interaction may be localized between the α -methyl groups of the repeating units, or perhaps, but less likely, distributed throughout the whole hydrophobic backbone of the network.

By analogy to globular proteins,⁶ and more closely paralleled with un-ionized poly(methacrylic acid) in aqueous solutions,^{7,8} as was indicated in the introduction to this report, it is safe to assume that hydrophobic bonds play a very important, perhaps the most important role in the stabilization of PHEMA hydrogel. The addition of microsolute to the hydrogel seems to confirm this hypothesis. The hydrogel swells beyond its swelling equilibrium in water when some juncture points in the network are broken by the effect of some addends. These broken juncture points are obviously the noncovalent crosslinks, since the covalent bonds are stable under these circumstances. Solutes that decrease the solvent power of water for PHEMA will induce the creation of additional bonding between hydrophobic residues in the polymer segments, creating a tighter network and less swollen gel than in pure water.

The ability of urea to stabilize the unfolded form of protein molecules is believed to originate mainly from its capacity to diminish hydrophobic

interactions between nonpolar groups. Nevertheless, the mode of action of urea is a complex one influencing the state of aggregation of polymers in water by a more complex mechanism than the dissociation of hydrophobic bonds alone. In any case, the result is an increased affinity of the water for the polymer segments.⁹ Urea is a very effective swelling agent for PHEMA hydrogel, but this effect cannot be attributed also to a hydrophobic mechanism alone, especially at the low concentrations of Figure 1. There is no precedent, apparently, of urea affecting the structure of globular proteins at these low concentrations. Nevertheless, the power of urea and its derivatives to swell PHEMA hydrogel at higher concentrations (Fig. 2) fits reasonably well as a hydrophobic mechanism. It is apparent that, within the concentration range studied, substitutions of methyl groups for hydrogen atoms on urea decrease the effectiveness of these compounds to swell PHEMA. One might expect that they would show a more marked affinity for the hydrophobic portions of PHEMA than unsubstituted urea. The higher swelling power found for the dimethyl, in comparison with the monomethyl derivative, could be due to impurities in the commercial products used. In general, urea and its methyl derivatives were found to swell PHEMA hydrogel above its swelling equilibrium in water, and it would be safe to assume that this effect, though not exclusively so, is probably due mainly to the breaking of hydrophobic bonds in the hydrogel.

Organic solvents like alcohol and acetone, which are much less polar than water, act as strong denaturing agents toward proteins.¹⁰ These addends increase the solubility of the nonpolar groups of the polymers in the aqueous medium and are considered to be breakers of hydrophobic bonds. Acetone and ethanol, by their selective action over the hydrophobic groups in PHEMA, induce a marked swelling of the hydrogel above its swelling equilibrium in water.

Detergents, which are also denaturing agents for proteins, produce their effect by interaction with hydrophobic groups.¹⁰ Nevertheless, cetylpyridinium chloride (CPC) does not affect PHEMA in the expected manner. CPC induces slight deswelling on PHEMA hydrogel from the normal swelling state in water, and it seems that the salting-out effect of the ionic end of these compounds predominates over the interaction of the hydrophobic portion with that of the PHEMA network.

In general, it is believed that the effect neutral salts have on the conformation of a polymer in aqueous medium is a direct consequence of the action of the ions on the structure of water surrounding the polymer segments. Any modification of the water structure will induce a change in the water-polymer interaction, resulting in a different polymer conformation.

Observation of the swelling curves of PHEMA hydrogel in ionic solutions seems to indicate that the anions, rather than cations, are the dominant species affecting the conformation of the polymer in water.

Some electrolytes, like chlorides and sulfates, decrease the solubility of

PHEMA segments in water (salting-out effect). These salts strengthen hydrophobic bonds in the polymer, being manifested by the formation of a tighter, less swollen hydrogel. Bromides behave indifferently toward the structure of PHEMA in water, with hydration of the gel remaining almost unchanged in solutions containing this anion. Conversely, the iodide, acetate, trichloroacetate, and the thiocyanate ions exercise a dissociating, or salting-in effect on PHEMA. These findings are in good general agreement with the position of these ions in the lyotropic series.

The swelling behavior of PHEMA in electrolyte solutions can be interpreted from the standpoint of ion-polymer interactions rather than ion-water interactions. In analogy with the work of Lunberg et al.¹¹ on the interactions of inorganic salts with poly(ethylene oxide), it appears that the anion is the species directly associating with the polymer. Thus the iodide, acetate, trichloroacetate, and thiocyanate ions are probably adsorbed at some points in the polymer network, inducing a polyelectrolyte effect. At low salt concentrations the ionic repulsions between bound ions will induce network swelling, while at higher ionic concentrations the charges may be shielded from each other, in which case the swelling effect should decrease. This latter effect perhaps is shown in the shape of the curve of the swelling of PHEMA in sodium acetate solutions.

There is a direct indication of the association of iodide (or more likely the triiodide anion) with PHEMA evidenced by a yellow color that the hydrogel takes on in solutions containing these ions. This association of small molecules with PHEMA is probably of the same nature as that observed in other neutral polymers.¹² The mechanism by which ion-polymer interactions occur is not known, but in the case of the iodide ion it is very likely to be ion-dipole interactions. Perhaps in other cases, as with the acetate ion, it may be hydrophobic association of the polymer segments with the hydrophobic end of the ion.

Homogeneous PHEMA hydrogel, when prepared by solution polymerization in a mixture of an organic solvent (usually ethylene glycol) and water, will turn opaque upon introduction in water³ and then will become transparent, the alacrity of the process being dependent on the gel size. At the same time it acquires the characteristically constant degree of equilibrium swelling mentioned before. This phenomenon can be interpreted in the following way: within the limitations of the polymer's covalently linked network the polymer segments may be considered to be in solution in the solvent mixture. The polymer precipitates from this solutionlike state when the organic solvent is exchanged for water, a poor solvent, within the network. Because of the slow mobility of the polymer segments, phase separation occurs in water before the segments have a chance to rearrange into a structure in which PHEMA segments are solvated by water. This rearrangement evidently proceeds more slowly than the diffusion of the organic solvent from the gel, hence there is the precipitation of the water-insoluble segments. The water solvate structure, or, in other words, the transparent hydrogel, seems to be one in which

hydrophobic interactions bring together the hydrophobic portions of the polymer segments exposing the hydrophilic ends of the chains to the solvent water.

This investigation was supported by a Public Health Service Research Grant (NB-6456) from the National Institute of Neurological Diseases and Blindness, U.S. Public Health Service.

The author is indebted to Dr. Bela Nagy for helpful discussions, and to Mr. Kenneth Kublin for technical assistance.

References

1. O. Wichterle and D. Lím, *Nature*, **165**, 117 (1960).
2. O. Wichterle and D. Lím, U.S. Pat. 2,976,576 (Mar. 28, 1961).
3. M. F. Refojo and H. Yasuda, *J. Appl. Polymer Sci.*, **9**, 2425 (1965).
4. J. Janaček and J. Hasa, *Collection Czechoslovak. Chem. Commun.*, **31**, 2186 (1966).
5. H. Yasuda, G. Michael, and W. Stone, Jr., *J. Polymer Sci. A-1*, **4**, 2913 (1966).
6. H. A. Scheraga, in *The Proteins*, Vol. I, H. Neurath, Ed., Academic Press, New York, 1963, p. 477.
7. T. M. Birshstein, Ye. V. Anufriyeva, T. N. Nekrasova, O. B. Ptitsyn, and T. V. Sheveleva, *Vysokomolekul. Soedin.*, **7**, 372 (1965); *Polymer Sci. USSR*, **7**, 412 (1965).
8. A. M. Liquori, G. Barone, V. Crescenzi, F. Quadrioglio, and V. Vitagliano, *J. Macromol. Chem.*, **1**, 291 (1966).
9. D. R. Robinson and W. P. Jancks, *J. Am. Chem. Soc.*, **87**, 2462 (1965).
10. W. Kauzmann, *Advan. Protein Chem.*, **14**, 1 (1959).
11. R. D. Lundberg, F. E. Bailey, and R. W. Callard, *J. Polymer Sci. A-1*, **4**, 1563 (1966).
12. H. Morawetz, *Macromolecules in Solution*, Wiley, New York, 1965, p. 377.

Résumé

Un hydrogel homogène de poly-2-méthacrylate-2-hydroxyéthyl (PHEMA) manifeste un domaine étroit d'équilibre dans l'eau (pourcentage en eau 41.09 ± 0.15 d'écart standard pour la moyenne de 24 échantillons) indépendamment de la solution polymérique et du niveau relativement faible de pontage. On admet que l'hydrogel PHEMA possède, outre une structure réticulaire covalentielle, une structure secondaire stabilisée par des liaisons hydrophobes. L'addition de microsolutés à l'hydrogel semble confirmer cette hypothèse. L'hydrogel gonfle au delà de son équilibre de gonflement dans l'eau en présence d'urée et de ses dérivés méthylés. Le gonflement a également été induit par des solvants organiques tels que l'alcool et l'acétone, et par des anions tels que l'iode, l'acétate, le trichloroacétate, et le thiocyanate. Des chlorures et des sulfates produisent un hydrogel plus faiblement gonflé que l'eau pure, alors que les bromure et chlorure de cétypyridinium dans les concentrations utilisées, produisent uniquement un faible dégonflement du gel. Lorsque le gel PHEMA préparé dans des solutions solvants organiques-eau, est placé dans l'eau, le gel passe par un état opaque avant de redevenir transparent. Ce phénomène est interprété comme étant dû à l'incapacité de l'eau à dissoudre les terminaisons hydrophiles de segments polymériques non-organisés. L'homogénéité réapparaît pour un gel après le réarrangement des chaînes directement par l'interaction des portions hydrophobes des segments polymériques, exposant ainsi à l'action de l'eau et du solvant la plupart des sites hydrophiles du réseau.

Zusammenfassung

Ein homogenes, aus Poly-2-hydroxyäthylmethacrylat (PHEMA) bestehendes Hydrogel zeigt in Gleichgewicht mit Wasser einen sehr engen Quellbereich ($\% \text{H}_2\text{O}$, $41,09 \pm 0,15$ Standardabweichung des Mittelwerts von 24 Proben), unabhängig von der

Verdünnung der Monomerlösung und dem relativ niedrigen Vernetzungsgrad. Es wird angenommen, dass das PHEMA-Hydrogel zusätzlich zu seiner durch Kovalenzen verknüpften Netzwerksstruktur eine durch hydrophobe Bindungskräfte stabilisierte Sekundärstruktur besitzt. Der Zusatz niedermolekularer Stoffe zu dem Hydrogel scheint diese Hypothese zu bestätigen. Das Hydrogel quillt in Gegenwart von Harnstoff und dessen Methylderivaten über den Gleichgewichtswert in Wasser hinaus. Quellung wird auch durch organische Lösungsmittel wie Alkohol und Aceton, sowie durch Anionen wie Jodid, Acetat, Trichloracetat und Thiocyanat herbeigeführt. Chloride und Sulfate führten zu einem weniger stark gequollenen Gel als reines Wasser, während Bromide und Cetylpyridiniumchlorid in den untersuchten Konzentrationen nur eine geringe Entquellung des Gels bewirkten. Wenn ein PHEMA-Gel, das in wässrigen Lösungen organischer Lösungsmittel hergestellt worden war, in Wasser gebracht wird, durchläuft das Gel einen opaken Zustand, bevor es wieder transparent wird. Als Ursache dieses Phänomens wird die Tatsache angesehen, dass Wasser nicht in der Lage ist, die hydrophilen Enden der ungeordneten Polymersegmente zu solvatisieren. Die Homogenität des Gels wird wieder nach einer Umordnung der Ketten erreicht, die durch die Wechselwirkung der hydrophoben Teile der Polymersegmente gesteuert wird und die die Mehrzahl der hydrophilen Stellen im Netzwerk dem Lösungsmittel-Wassergemisch aussetzt.

Received April 3, 1967

Revised May 5, 1967

Prod. No. 5445A

Mechanisms of Propagation, Transfer, and Short-Chain Branching Reactions in the Free-Radical Polymerization of Ethylene

SUEO MACHI, SEIICHI KISE,
 MIYUKI HAGIWARA, and TSUTOMU KAGIYA,
*Japan Atomic Energy Research Institute,
 Takasaki Radiation Chemistry Research Establishment,
 Takasaki, Gumma, Japan*

Synopsis

The propagation, transfer, and short-chain branching reactions in the free-radical polymerization of ethylene were studied at temperatures of 20–80°C. under pressures of 160–400 kg./cm.² by means of two-stage polymerization with the use of a specially designed reaction vessel. In the first stage, the polymerization was carried out in the presence of AIBN as the initiator, and in the second stage, the propagation occurred with living radicals in the absence of the initiator. In the second stage the polymer yield is shown to increase with reaction temperature and pressure, and the molecular weight of the polymer reached constant values which were dependent upon the temperature when the contribution of the polymer formed in the first stage was very small. It is shown that in the second stage the rate of propagation, transfer, and short-chain branching are all proportional to the second power of ethylene fugacity, and that the activation energies of these reactions are 5.7, 23.4, and 10.9 kcal./mole, respectively. The polymer has no terminal vinyl group. The mechanism of these reactions is discussed on the basis of kinetic and energetic results.

INTRODUCTION

Free-radical polymerization of ethylene has been studied under such severe conditions as high pressures and temperatures.^{1–5} Recently, a few studies under milder conditions, of pressure and temperature have been reported.^{6,7} Lyubetzky et al.⁷ studied ethylene polymerization at 70°C. with azobisisobutyronitrile (AIBN) in benzene, and pointed out that the propagation reaction occurs with the living polymer radical in the crystalline phase. We have also suggested the existence of long-lived growing polymer radicals in both the γ -radiation-induced and AIBN-initiated polymerization of ethylene at relatively low temperatures.^{8–11}

In the previous work,¹¹ we reported briefly on the post-polymerization of ethylene by the long-lived radical in reactions in a specially designed reaction vessel. This paper, a continuation of the above, is concerned with the kinetics of the post-polymerization of ethylene. The mechanism of propagation, transfer, and short-chain branching is discussed.

EXPERIMENTAL

A stainless steel reaction vessel was specially designed as shown in Figure 1. It consisted of a main reactor chamber with a capacity of 75 ml. (B), a container of 2 ml. capacity (A) for the initiator, which was attached to the top cover of the reaction vessel. The container was a small, cylindrical, high-pressure vessel and could be sealed off from the main reactor chamber when lifted to the cover by rotating a handle (C). The sealing of the container was tested by an outside pressure of 450 kg./cm.². The radical initiator, crystalline AIBN, was put into the container. After being swept out several times with ethylene, the reactor was charged with ethylene to the desired pressure. The reaction was carried out in two

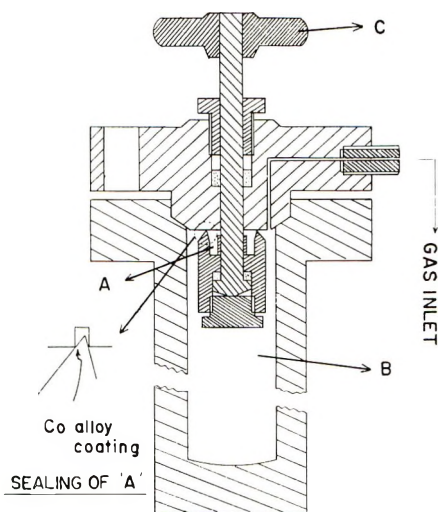


Fig. 1. Reactor assembly: (A) container of the initiator, (B) main reactor chamber, (C) handle for opening and closing the container.

stages. In the first stage, the initiator container was open to the reactor chamber under constant conditions. The container was then sealed off. After the reaction vessel was rapidly heated to the desired temperature and a part of the ethylene was vented to keep the pressure constant, the reaction in the second stage was followed under various conditions. The reactions in the first stage were always carried out under the same conditions, i.e., 40°C., 400 kg./cm.², 1.22 mmole of AIBN, and 2 hr., except for the experiments shown in Table I. The pressure was almost constant during the reaction since the polymerization was carried out to low conversion. The temperature was kept constant to within $\pm 1^\circ\text{C}$.

The ethylene used was commercially available 99.9% pure material, free of CO and H₂S and containing less than 3 ppm oxygen. Commercial grade AIBN was twice recrystallized from acetone before use. The number-average molecular weight of the polymer was determined from the in-

TABLE I
Influence of the Pressure of First Stage on the Second-Stage Polymerization

First stage ^a	Second stage ^b		Total polymerized monomer (C ₂ H ₄), mole/l.	Monomer polymerized in second stage (C ₂ H ₄), mole/l.
Pressure, kg./cm. ²	Pressure, kg./cm. ²	Time, hr.		
400	—	—	0.058 ^c	—
	250	2.0	0.155	0.097
		4.0	0.240	0.182
		6.0	0.396	0.338
		8.0	0.489	0.431
250	—	—	0.025 ^c	—
	250	2.0	0.101	0.076
		4.0	0.179	0.154
		6.0	0.316	0.291
		8.0	0.399	0.374

^a Reaction temperature, 40°C.; time, 2.0 hr.; AIBN, 1.22 mmole.

^b Reaction temperature, 40°C.

^c Polymerizations were carried out only in first stage.

trinsic viscosity by Tung's formula.¹² The concentration of methyl groups in the polyethylene was determined from the infrared absorption spectrum at 1375 cm.⁻¹ (7.25 μ) following the directions of Bryant and Voter.¹³

RESULTS AND DISCUSSION

Propagation Reaction

Figure 2 shows a plot of the amount of polymer formed against the reaction time. The amount of polymer in the second stage is considerable and proportional to the time. It is believed that radicals from AIBN pass from the container to the reactor chamber and the propagation reaction occurs, in the first stage, giving long-chain radicals. In the second stage, where the container with initiator is entirely sealed off, though no additional radical is introduced into the reactor, the amount of polymer is found to increase at a considerable rate.* This demonstrates that the growing polymer radicals introduced in the first stage survive, and the propagation reaction occurs in the second stage. The steady increase of the amount of polymer in the second stage indicates that the termination reaction is almost eliminated and the propagation reaction proceeds at a constant rate. The slope of the line of the ratio of the amount of polymer $M_{p,II}$ versus the time in the second stage t_{II} corresponds to the overall propa-

* In the second stage no initiating radical is introduced into the reactor chamber because the container of the initiator is completely sealed off. The reactor chamber is therefore entirely free of the initiator. This was proved by the experimental fact that no polymer formed when the entire polymerization was carried out with the initiator container sealed off.

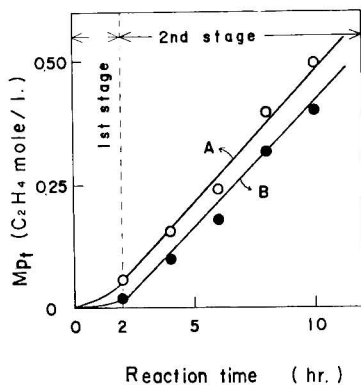


Fig. 2. Amount of monomer polymerized vs. reaction time: (A) reaction condition in the first stage, AIBN 1.22 mmole, 40°C., 400 kg./cm.²; conditions in the second stage, 40°C., 250 kg./cm.²; (B) conditions in the first stage, AIBN 1.22 mmole, 40°C., 250 kg./cm.²; conditions in the second stage same as for (A).

gation rate R_p . Two series of experiments in Figure 2 differ from each other as to the pressure in the first stage but show approximately equal rates in the second stage. This fact demonstrates that the rate of formation of the polymer radical is independent of the ethylene pressure and that the amount of the polymer radical decreases very little when a small amount of the gas is vented, with a drop in pressure from 400 to 250 kg./cm.².

The correlation between the pressure in the second stage and the amount of polymer is shown in Table II, where the conditions in the first stage are kept constant. Figures 3 and 4 show that M_{pII} increases proportionally with t_{II} at each pressure at 40 and 80°C. and the overall propagation rate increases with pressure. In Figure 5 the fugacity exponent of R_p is found to be 2. Thus, the overall propagation rate is expressed as

$$R_p = k_p [R \cdot] f_M^2 \quad (1)$$

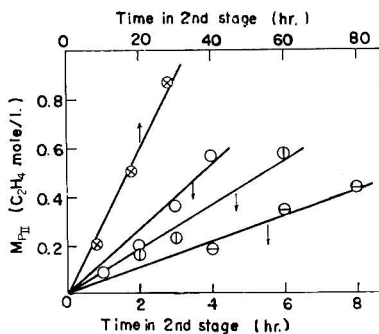


Fig. 3. Amount of monomer polymerized vs. reaction time in second stage at 40°C. under various pressures: (⊗) 160 kg./cm.²; (⊖) 250 kg./cm.²; (⊕) 360 kg./cm.²; (○) 400 kg./cm.². Condition in first stage, AIBN 1.22 mmole, 400 kg./cm.², 40°C., 2.0 hr.

where $[R\cdot]$ is the total concentration of polymer radicals irrespective of chain length in the second stage or at the end of the first stage, f_M is the fugacity of ethylene, which is a reasonable measure of ethylene activity at high pressure.

TABLE II
Results of Two-Stage Polymerization Under Various Pressures
and Temperatures^a

Conditions of second stage			Total polymerized monomer (C ₂ H ₄), mole/l.	\bar{P}_n of final polymer $\times 10^{-3}$	$N_{pt} = (M_{pt}/\bar{P}_n)$, mole/l. $\times 10^5$	Monomer polymerized in second stage (C ₂ H ₄), mole/l.	$N_{pII} = N_p$ formed in second stage, mole/l. $\times 10^5$	
Temp., °C.	Pressure, kg./cm. ²	Time, hr.						
25	300	29	0.543	25.2	2.16	0.485	1.21	
		40	0.611	25.0	2.44	0.533	1.49	
		52	0.910	28.6	3.07	0.852	2.02	
		67	1.120	27.1	4.13	1.062	3.18	
40	400	1	0.150	9.6	1.56	0.092	0.61	
		2	0.263	10.7	2.46	0.205	1.51	
		3	0.420	10.7	3.92	0.362	2.97	
		4	0.604	10.7	5.65	0.546	4.70	
	330	2	0.216	8.9	2.42	0.158	1.47	
		3	0.288	8.9	3.24	0.230	2.29	
		6	0.630	10.7	5.90	0.572	4.95	
		4	0.240	9.3	2.58	0.181	1.64	
	250	6	0.394	10.4	3.80	0.338	2.85	
		8	0.489	10.7	4.56	0.430	3.56	
		160	8	0.262	8.6	3.05	0.204	2.10
			18	0.559	10.0	5.59	0.501	4.64
60	400	28	0.925	9.6	9.64	0.867	8.69	
		2	0.509	3.6	14.1	0.460	13.2	
80	400	4	1.260	3.6	35.0	1.200	34.0	
		1	0.742	0.32	231	0.680	230	
80	400	2	1.202	0.32	376	1.140	375	
		1	0.408	0.43	96.0	0.360	95.0	
	2	0.791	0.32	251	0.730	250		
	300	3	0.378	0.35	108	0.320	107	
		4	0.484	0.32	151	0.430	150	
	160	6	0.795	0.32	246	0.741	245	

^a Reaction conditions in first stage: AIBN, 1.22 mmole; pressure, 400 kg./cm.²; temperature, 40°C.; polymerized monomer in first stage, 0.058 C₂H₄ mole/l.; \bar{P}_n , 6.1×10^3 ; number of polymer chains, 0.95×10^{-5} mole/l.

The plots of M_{pII} against t_{II} at various temperatures are shown in Figure 6. The amount of polymer increases proportionally with the time, i.e., no termination occurs even at a temperature of 80°C. It is also shown that R_p increases with temperature. The Arrhenius plot is shown in Figure 7, from which an activation energy of 5.7 kcal./mole for the overall propagation was obtained.

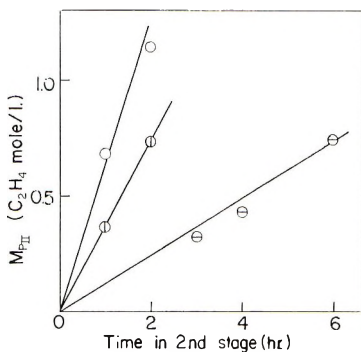


Fig. 4. Amount of monomer polymerized vs. reaction time in second stage at 80°C. under various pressures: (⊖) 160 kg./cm.²; (⊕) 300 kg./cm.²; (○) 400 kg./cm.². Condition in first stage same as in Fig. 3.

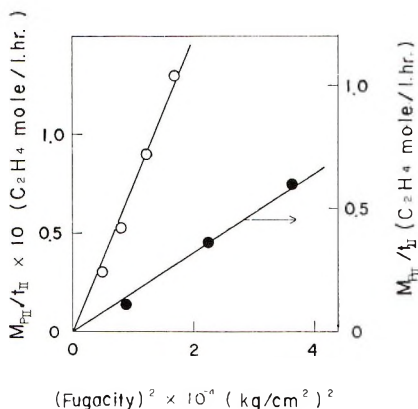


Fig. 5. Overall rate of propagation vs. square of ethylene fugacity at various temperatures: (○) 40°C.; (●) 80°C.

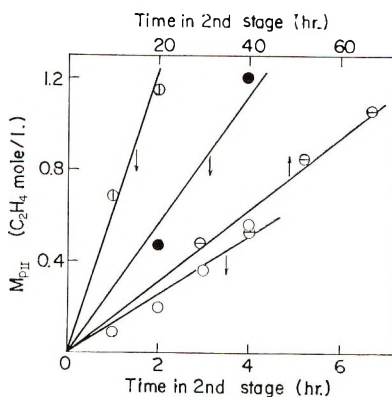


Fig. 6. Amount of monomer polymerized vs. reaction time in second stage at various temperatures: (⊖) 25°C., 300 kg./cm.²; (○) 40°C., 400 kg./cm.²; (●) 60°C., 400 kg./cm.²; (⊕) 80°C., 400 kg./cm.².

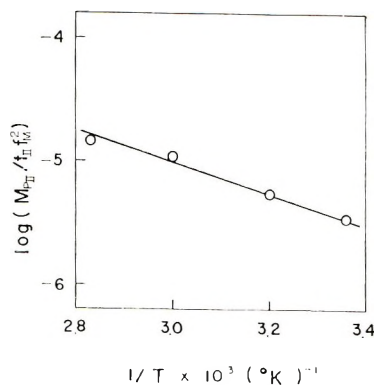


Fig. 7. Effect of temperature on the specific propagation rate at 300–400 kg./cm.², 25–80°C.

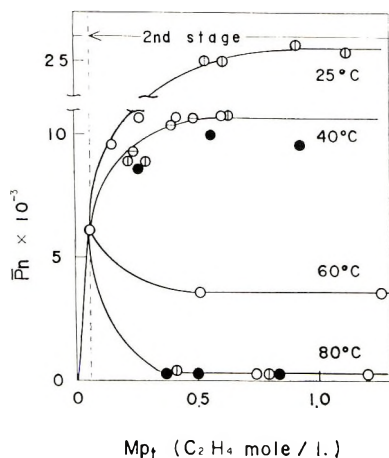


Fig. 8. Degree of polymerization vs. amount of polymerized monomer: (○) 400 kg./cm.²; (⊕) 300–330 kg./cm.²; (⊖) 250 kg./cm.²; (●) 160 kg./cm.²

Transfer Reaction

As shown in Figure 8, the degree of polymerization (\bar{P}_n) in the second stage increases with the polymer formation at the initial stage at 25 and 40°C., while it decreases at 60 and 80°C. However, at the later stage where the total amount of polymer is quite a bit larger than the amount of polymer formed in the first stage, \bar{P}_n attains constant values, which depend mainly on the temperature and do not depend on the pressure over the range of 160–400 kg./cm.². We designate the constant value of the degree of polymerization as the ultimate degree of polymerization, $[\bar{P}_n]$. It is shown that the higher the temperature, the lower $[\bar{P}_n]$ becomes. Inasmuch as initiation and termination do not occur, the value of $[\bar{P}_n]$ is determined by the ratio of the rates of chain propagation to chain transfer.

The ratio of polymer yield to molecular weight is the number of moles of the polymer chain. Therefore, the number of moles of the polymer chain formed in the second stage (N_{pII}) is given as $(M_{pt}/\bar{P}_n) - (M_p/\bar{P}_{n1})$, M_{pt} being the total amount of polymer formed. The number of polymer chains is plotted in Figures 9 and 10 against reaction time under various pressures

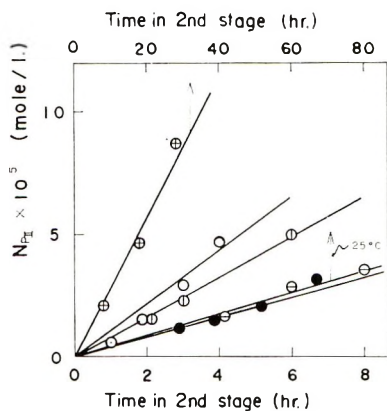


Fig. 9. Number of moles of polymer chain vs. reaction time in second stage: (●) 25°C., 300 kg./cm.²; (○) 40°C., 400 kg./cm.²; (⊕) 40°C., 330 kg./cm.²; (⊖) 40°C., 250 kg./cm.²; (⊕) 40°C., 160 kg./cm.².

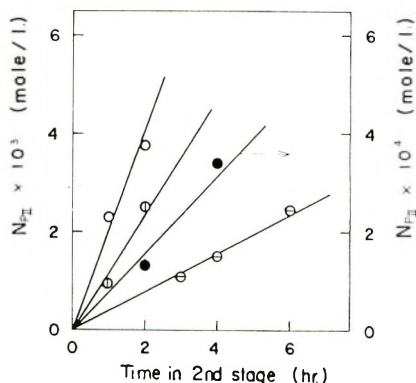


Fig. 10. Number of moles of polymer chain vs. reaction time in second stage at higher temperatures: (●) 60°C., 400 kg./cm.²; (○) 80°C., 400 kg./cm.²; (⊕) 80°C., 300 kg./cm.²; (⊖) 80°C., 160 kg./cm.².

and temperatures. These results demonstrate that N_{pII} increases proportionally with the time. In addition, the increasing rate of the number of the polymer chains was found to be linear to the second power of ethylene fugacity (cf. Fig. 11).

The number-average degree of polymerization is expressed by eq. (2):

$$\bar{P}_n = M_p / \left\{ \int R_p dt + \int R_t dt - (1/2) \int R_d dt \right\} \quad (2)$$

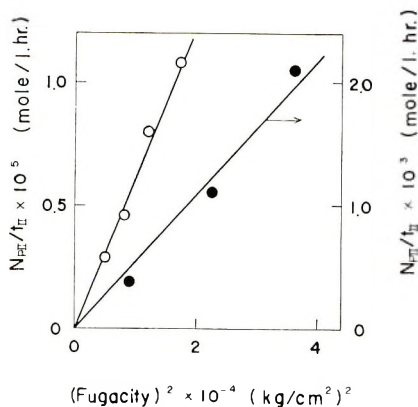


Fig. 11. Rate of increase in the number of polymer chains vs. ethylene fugacity: (O) 40°C.; (●) 80°C.

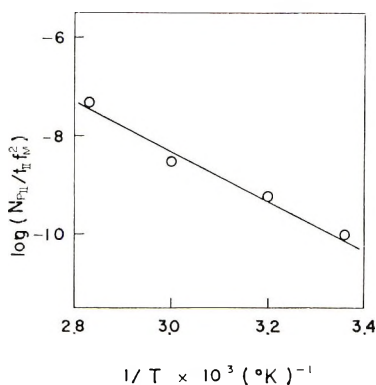


Fig. 12. Effect of the temperature on the rate of increase in the number of polymer chains at 25–80°C.

where R_i , R_{tr} , and R_t represent the rates of initiation, transfer, and termination by the recombination of radicals, respectively.

For the two-stage polymerization, M_{pII} and \bar{P}_n can be expressed by eq. (3)

$$\bar{P}_n = M_{pI} / \left\{ \int R_i dt + \int R_{tr} dt - (1/2) \int R_t dt \right\}_I + \left\{ \int R_{tr} dt \right\}_{II} \quad (3)$$

where subscripts I and II denote the first and second stage, respectively. From eqs. (2) and (3), eq. (4) is derived,

$$\left\{ \int R_{tr} dt \right\}_{II} = (M_{pI} / \bar{P}_n) - (M_{pI} / \bar{P}_{nI}) = N_{pII} \quad (4)$$

Thus,

$$R_{tr} = dN_{pII} / dt \quad (5)$$

Equation (5) indicates that in the second stage the rate of the transfer reaction is given by the rate of increase in the moles of polymer chains.

From the fact that N_{pI} is proportional to the reaction time (Figs. 9 and 10) and the rate of increase in N_{pII} is proportional to the second power of ethylene fugacity (Fig. 11), the rate equation of the transfer reaction is given as

$$R_{tr} = k_{tr}[R\cdot]f_M^2 \quad (6)$$

From eqs. (1)–(3) and (6), the degree of polymerization is given as

$$\bar{P}_n = 1 / \left\{ (M_{pI}/M_{pt})(1/\bar{P}_{nI}) + (k_{tr}/k_p)(1 - M_{pI}/M_{pt}) \right\} \quad (7)$$

When the value of M_{pI}/M_{pt} becomes very small, i.e., $M_{pt} \gg M_{pI}$ in eq. (7), the ultimate degree of polymerization is given as

$$\lim_{(M_{pI}/M_{pt}) \rightarrow 0} \bar{P}_n = [\bar{P}_n] = k_p/k_{tr} \quad (8)$$

This equation means that the ultimate degree of polymerization is equal to the ratio of the rate constant for the propagation reaction to that for the transfer reaction.

The temperature dependency of the number of polymer chains is shown in Figure 12 as an Arrhenius plot, from which an activation energy of 23.4 kcal./mole for the transfer reaction is obtained.

Short-Chain Branching Reaction

The methyl group content in the polymer was determined from the infrared absorption spectrum at 1375 cm.^{-1} (7.25μ). The terminal methyl group is eliminated in calculating the content of the methyl group in polymer side chains ($\text{CH}_3/1000\text{C}$). This value is thought to correspond to the degree of short-chain branching, which is believed to be determined by the ratio of the rate of short-chain branching to that of the propagation reaction.

Figure 13 shows that the methyl group content in side chains is independent of the ethylene fugacity. This indicates that the fugacity ex-

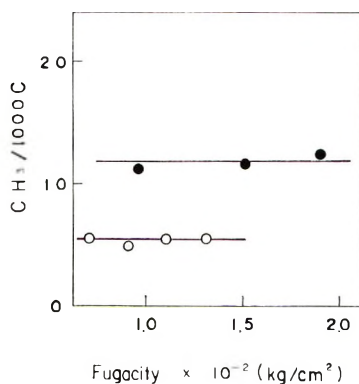


Fig. 13. Methyl group content of polymer in the side chain vs. ethylene fugacity: (O) 40°C .; (●) 80°C .

ponent of the rate of short-chain branching is the same as that of propagation. Thus, the rate equation of the short-chain branching is,

$$R_b = k_b [R \cdot] f_M^2 \quad (9)$$

where R_b and k_b represent the rate and rate constant of short-chain branching, respectively. The degree of short-chain branching, then, equals the ratio of the rate constants of the short-chain branching to the propagation reaction. Figure 14 demonstrates that the methyl group content increases with increasing reaction temperature, and the difference of activation energy between the short-chain branching and the propagation is 5.2 kcal./mole. Since the activation energy for the propagation is above shown to be 5.7 kcal./mole, that for short-chain branching is 10.9 kcal./mole.

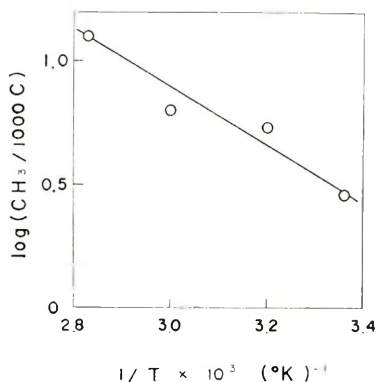


Fig. 14. Effect of the temperature on the methyl group content of polymer in side chain at 25–80°C.

Model of Coordination of Two Ethylene Molecules and Energetic Consideration of the Mechanism

As shown above, the ultimate degree of polymerization is equal to k_p/k_{tr} , and the degree of short-chain branching is k_b/k_p . These rate ratios are expressed in terms of the activation energy and activation entropy by eqs. (10) and 11.

$$[\bar{P}_n] = k_p/k_{tr} = \exp \left\{ (\Delta S_p^\ddagger - \Delta S_{tr}^\ddagger)/R \right\} \exp \left\{ -(\Delta E_p - \Delta E_{tr})/RT \right\} \quad (10)$$

$$(\text{CH}_3/1000\text{C}) = k_b/k_p = \exp \left\{ (\Delta S_b^\ddagger - \Delta S_p^\ddagger)/R \right\} \exp \left\{ -(\Delta E_b - \Delta E_p)/RT \right\} \quad (11)$$

Then,

$$\Delta S_p^\ddagger - \Delta S_{tr}^\ddagger = R \ln [\bar{P}_n] + (\Delta E_p - \Delta E_{tr})/T \quad (12)$$

$$\Delta S_b^\ddagger - \Delta S_p^\ddagger = R \ln (\text{CH}_3/1000\text{C}) + (\Delta E_b - \Delta E_p)/T \quad (13)$$

where ΔS^\ddagger and ΔE are the activation entropy and the activation energy for each reaction. The values of $(\Delta S_p^\ddagger - \Delta S_{tr}^\ddagger)$ and $(\Delta S_b^\ddagger - \Delta S_p^\ddagger)$ are

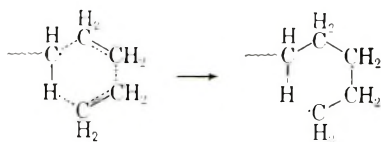
evaluated as listed in Table III. The magnitude of the activation energies and entropies decreases in the order: $\Delta E_{tr} > \Delta E_b > \Delta E_p$ and $\Delta S_{tr}^\ddagger > \Delta S_b^\ddagger > \Delta S_p^\ddagger$.

TABLE III
Activation Energy and Entropy of Elementary Steps

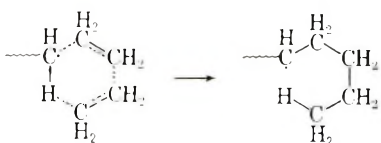
	Activation energy, kcal./mole	Activation entropy difference, e.u.
Propagation	5.7	$\Delta S_{tr} - \Delta S_p = 38.2$
Transfer	23.4	
Short-chain branching	10.9	$\Delta S_b - \Delta S_p = 19.7$

On the basis of kinetic and energetic considerations, the reaction mechanisms shown in eqs. (14)–(16) are proposed.

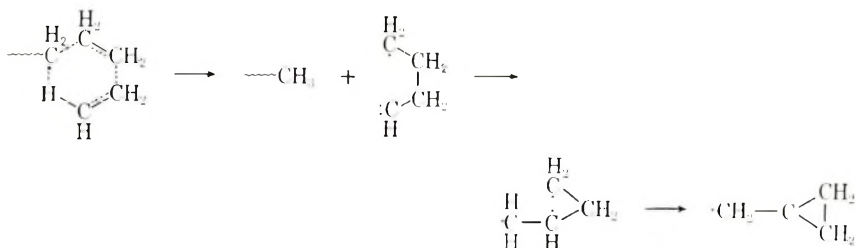
Propagation:



Chain branching:



Transfer:



Since all three elementary steps follow a second-order rate equation with respect to ethylene fugacity, the coordination of two associated monomers to the growing chain end is considered. The propagation reaction is an addition of ethylene to the radicals. Short-chain branching involves the addition of ethylene to the radicals and intramolecular hydrogen abstraction. In the transfer reaction, the growing radical abstracts the hydrogen from ethylene to form a dead polymer with a methyl group at its chain

end and a radical as an intermediate, cyclization of which takes place immediately. The cyclization is considered because of the fact that there is no vinyl group at the polymer end.

Considering that both the short-chain branching and the transfer reactions involve hydrogen abstraction and that propagation is a simple addition of ethylene to the radical, it is reasonable that the activation energy of the propagation is less than that of branching and transfer. The fact that the activation energy for the transfer reaction is greater than that for short-chain branching may be due to the fact that transfer is a complex reaction of hydrogen abstraction and cyclization of the intermediate radical.

The entropy of the transition state of short-chain branching is considered to be greater than that of the propagation because the former involves the abstraction of hydrogen from the polymer as well as the addition of ethylene to the radical, while the propagation proceeds only by the addition of ethylene. The greatest entropy is considered to be in the transition state of the transfer reaction because it is a hydrogen abstraction reaction. The order of magnitude in the activation entropy is the same as that of the entropy of transition states, since the initial states of these reactions are the same.

Thus the results of the activation energy and entropy are shown to be consistent with the proposed reaction mechanism.

References

1. S. Kodama, I. Taniguchi, S. Yuasa, T. Ota, and Y. Terada, *Kogyo Kagaku Zasshi*, **57**, 439 (1954).
2. R. K. Laird, A. G. Morrell, and L. Seed, *Discussions Faraday Soc.*, **22**, 126 (1956).
3. S. Kodama, Y. Matsushima, A. Ueyoshi, T. Shimidzu, T. Kagiya, and K. Fukui, *J. Polymer Sci.*, **43**, 389 (1960).
4. R. O. Symcox and P. Ehrlich, *J. Am. Chem. Soc.*, **84**, 531 (1962).
5. R. H. Bretton and B. F. Dodge, *Chem. Eng. Progr.*, **58**, No. 8, 50 (1962).
6. H. N. Friedlander, *J. Polymer Sci.*, **58**, 455 (1962).
7. B. L. Erussalimsky, S. G. Lyubetzky, W. W. Mazurek, S. Ya. Frenkel, and L. G. Shaltyko, *Polymer*, **3**, 639 (1962).
8. S. Machi, M. Hagiwara, M. Gotoda, and T. Kagiya, *J. Polymer Sci. A*, **3**, 2931 (1965).
9. S. Machi, M. Hagiwara, M. Gotoda, and T. Kagiya, *J. Polymer Sci. A-1*, **4**, 1517 (1966).
10. S. Machi, T. Sakai, M. Gotoda, and T. Kagiya, *J. Polymer Sci. B*, **3**, 709 (1965).
11. S. Machi, S. Kise, M. Hagiwara, and T. Kagiya, *J. Polymer Sci. B*, **4**, 585 (1966).
12. L. H. Tung, *J. Polymer Sci.*, **24**, 333 (1957).
13. W. M. Bryant and R. C. Voter, *J. Am. Chem. Soc.*, **75**, 6112 (1953).

Résumé

Les réactions de propagation, de transfert et de ramification courte en cours de polymérisation par radicaux libres de l'éthylène ont été étudiées à des températures de 20 à 80°C sous des pressions de 160 à 400 Kg/cm² au moyen de la polymérisation en deux étapes et en utilisant un réacteur spécialement conçu. Dans la première étape, la polymérisation était effectuée en présence d'AIBN comme initiateur et dans la seconde étape, la propagation résultait des radicaux vivants en absence d'initiateur. Dans la

seconde étape, le rendement en polymère croissait avec une augmentation de température et de pression, et le poids moléculaire du polymère atteignait des valeurs constantes qui dépendaient de la température lorsque la contribution du polymère formé dans la première étape était très faible. On a montré que dans la seconde étape, les vitesses de propagation, de transfert et de ramification courte étaient toutes proportionnelles à la seconde puissance de la fugacité en éthylène et que l'énergie d'activation de ces réaction était de 5,7, 23,4 et 10,9 Kcal/mole, respectivement. Le polymère n'a pas de groupe vinylique terminal. Sur la base des résultats cinétiques et énergétiques, un mécanisme de ces réactions est soumis à discussion.

Zusammenfassung

Die Wachstums-, Übertragungs- und Kurzkettenverzweigungsreaktion bei der radikalischen Polymerisation von Äthylen wurde bei Temperaturen von 20 bis 80°C, bei einem Druck von 160 bis 400 kg/cm² mittels einer Zweistufenpolymerisation unter Verwendung eines eigens konstruierten Reaktionsgefäßes untersucht. In der ersten Stufe wurde die Polymerisation unter Verwendung von AIBN als Starter ausgeführt, in der zweiten Stufe erfolgte das Kettenwachstum mit Hilfe lebender Radikale in Abwesenheit eines Starters. Wie gezeigt wurde, stieg die Polymerausbeute in der zweiten Stufe mit der Reaktionstemperatur und dem Druck an, während das Molekulargewicht konstante Werte annahm, die temperaturabhängig waren, wenn der Anteil des in der ersten Stufe gebildeten Polymeren sehr gering war. Es wurde gezeigt, dass in der zweiten Stufe die Geschwindigkeiten von Kettenwachstum, Übertragung und Kurzkettenverzweigung durchwegs dem Quadrat der Äthylenfugazität proportional sind und dass die Aktivierungsenergien dieser Reaktionen 5,7, 23,4 bzw. 10,9 Kdal/Mol betragen. Das Polymere besitzt keine endständige Vinylgruppe. Der Mechanismus dieser Reaktionen wurde auf der Grundlage der kinetischen und energetischen Ergebnisse einer Diskussion unterzogen.

Received January 4, 1967

Revised May 10, 1967

Prod. No. 5447A

Retardation of Spontaneous Polymerization of Formaldehyde by Acidic Substances

HISAO YOKOTA and MASATSUNE KONDO,
*Takarazuka Radiation Laboratory,
Sumitomo Atomic Energy Industries, Ltd., Takarazuka, Japan,*
and TSUTOMU KAGIYA and KENICHI FUKUI,
Faculty of Engineering, Kyoto University, Kyoto, Japan

Synopsis

The stability of liquid formaldehyde produced by pyrolysis of α -polyoxymethylene was studied in connection with the presence of impurities in the monomer. Liquid monomer was divided into several fractions by means of the distillation. The stability of each fraction for polymerization is dependent on the order of fraction, that is, the monomer obtained in the early fractions of distillation was much more stable with regard to polymerization than later distillate. Analyses of the monomer fractions indicated that various impurities such as carbon dioxide, water, methanol, and methyl formate were present in the early monomer distillates. From the influence of these impurities on the stability of liquid formaldehyde, it was found that small amounts of carbon dioxide and hydrogen cyanide noticeably depressed the polymerization, and that with acetic acid and maleic anhydride the rate of polymerization decreased with small amounts of these compounds but increased with an excess of additive. On the other hand, the addition of these acidic substances did not affect the molecular weight of the polymer produced. From the fact that the acidic substance retards only the initiation of polymerization, it has been concluded that the spontaneous polymerization of formaldehyde in bulk or in toluene solution is initiated by an anionic species.

INTRODUCTION

It is well known that a highly pure sample of liquid formaldehyde polymerizes even at temperature of -80°C . after several hours.¹ Satisfactory agents for inhibiting polymerization have not yet been discovered, although hydroquinone was reported to increase the stability of formaldehyde to a slight extent.² Formaldehyde is soluble in nonpolar solvents such as diethyl ether, chloroform, or toluene, but its stability is little improved by solvation.¹

Staudinger³ observed that oxygen inhibited the rate of spontaneous polymerization of formaldehyde and concluded that an alkali in the reaction system, for example on the glass wall of the reaction vessel, may initiate the polymerization. On the other hand, Enikolopyan et al.^{4,5} and Macháček et al.⁶ reported that acids such as formic acid and carbon dioxide terminate the growth of the polymer chain in polymerization of formaldehyde by anionic catalysts, causing a decrease in both the rate

of polymerization and the degree of polymerization. The role of formic acid as a chain transfer agent has been described in the literature.⁷

The present investigation centered on the stability of liquid formaldehyde in connection with impurities in the monomer. It was found that a suitable quantity of acid and acid anhydride effectively retards the rate of spontaneous polymerization, yet has no effect on the degree of polymerization of the resulting polymer. On the basis of these results, an anionic mechanism for the spontaneous polymerization of formaldehyde is proposed.

EXPERIMENTAL

α -Polyoxymethylene was dried *in vacuo* at 50°C. and stored in a desiccator over silica gel before use. A 100 g. portion of α -polyoxymethylene was put into a 500 ml. flask and pyrolyzed by heating in a closed system under reduced pressure. The gaseous product was passed through a tube packed with silica gel which was maintained at -15°C. and was condensed into a reservoir at -78°C.

The content of impurities in the monomer was determined by gas chromatography (Yanagimoto, Type GCG-3D) with poly(ethylene glycol) or diglycerol.

Glass ampules of 30 ml. capacity were used as reaction vessels; they were baked under vacuum before use. The monomer was fractionally distilled *in vacuo* and each fraction was separately condensed into an ampule at -78°C. In another experiment, the first fraction (ca. 10 vol.-%) was discarded, and only the middle fraction being simultaneously condensed into several ampules at -78°C.

Toluene used as solvent was dried over metallic sodium and was distilled before use. Additives such as telluric acid, boric acid, stearic acid, pivalic acid, acetic acid, maleic anhydride, and carbon dioxide were commercial products. Hydrogen cyanide was prepared by decomposition of potassium cyanide by sulfuric acid according to the usual method.

Solid additives were put in the ampule before addition of monomer. In the case of liquid and gaseous additives purified toluene and liquid additive dissolved in toluene or the gaseous additive were introduced by syringe into the ampule through a rubber stopper which fitted into a side arm of the ampule. The ampule was then sealed off and maintained at $0 \pm 1^\circ\text{C}$. After a given time, the ampule was cooled again to -78°C. Cooled diethyl ether was added to prevent the polymerization of unreacted monomer during separation. The polymer formed was filtered off under cooling and dried *in vacuo* at room temperature and weighed.

The inherent viscosity of polymer was measured with an Ostwald viscometer, starting with a solution containing 0.5 g. of polymer in 100 ml. of *p*-chlorophenol containing 2% of α -pinene at 60°C. When not enough polymer for viscosity study was obtained in the 30-min. polymerization time separate experiments with a longer polymerization time were carried out to produce polymer for this purpose.

RESULTS AND DISCUSSION

Impurities Contained in the Monomer and the Polymerization Rate

The purified monomer was analyzed by gas chromatography and the content of impurities detected was 0.12–0.16 vol.-% water, 0.07–0.13 vol.-% methanol, 0.006–0.007 vol.-% methyl formate, and 0.17–0.21 vol.-% carbon dioxide. In order to observe the influence of these impurities on the rate of polymerization of the monomer, the purified monomer

TABLE I
Polymerization Yield of the Distillate
and the Content of Carbon Dioxide^a

No. of distillate	Distillate, vol.-%	Content of CO ₂ , mole-%	Polymerization yield, wt.-%
1	0–11	3.26	0
2	11–25	0.55	9.8
3	25–40	0.04	ca. 100

^a Monomer concentration, 50 vol.-% in toluene solution; temperature, 0°C.; reaction time, 30 min.

was fractionated by distillation into four parts of distillate, and the polymerization yield of the monomer from each part of distillate was measured at 0°C. in toluene solution at a concentration of 50 vol.-%. Of these impurities, only the presence of carbon dioxide was related to the polymerization yield of the monomer, as shown in Table I. It was found that the increase of carbon dioxide markedly decreased the polymerization yield.

Influence of Added Carbon Dioxide on the Stability of Liquid Formaldehyde

To determine the quantitative effect of carbon dioxide on the stability of liquid formaldehyde, carbon dioxide was added to the monomer in bulk, and the polymer yield was examined 30 min. later after holding at 0°C. In this experiment the monomer used was simultaneously distilled into the ampules in order to equalize the initial concentration of carbon dioxide. From the results shown in Figure 1, it was found that carbon dioxide at a concentration of above 2 mole-% inhibited the polymerization of formaldehyde. Furthermore, liquid formaldehyde in a homogeneous solution containing 50 mole-% carbon did not polymerize at –78°C. even after a month.

Influence of the Addition of Various Acids and Acid Anhydrides on the Stability for Polymerization of Formaldehyde Solution

A detailed study of the influence of some weakly acidic substances on the stability of the monomer was carried out.

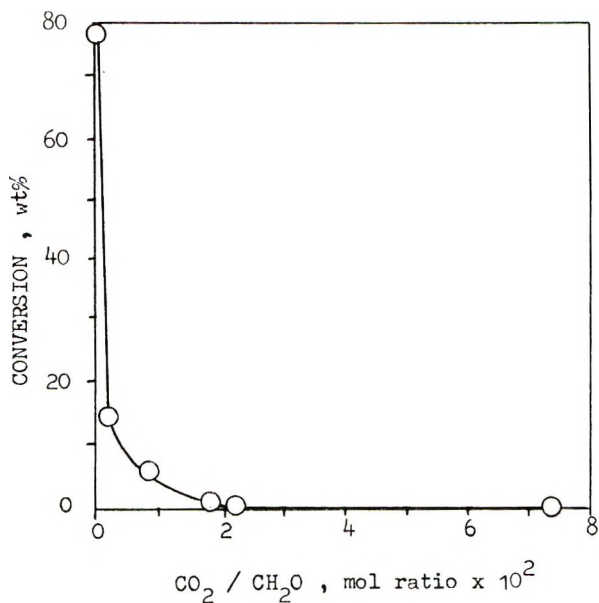


Fig. 1. Influence of the addition of carbon dioxide on the stability of liquid formaldehyde; 5 g. monomer in 30-ml. ampule; 0°C.; 30 min.

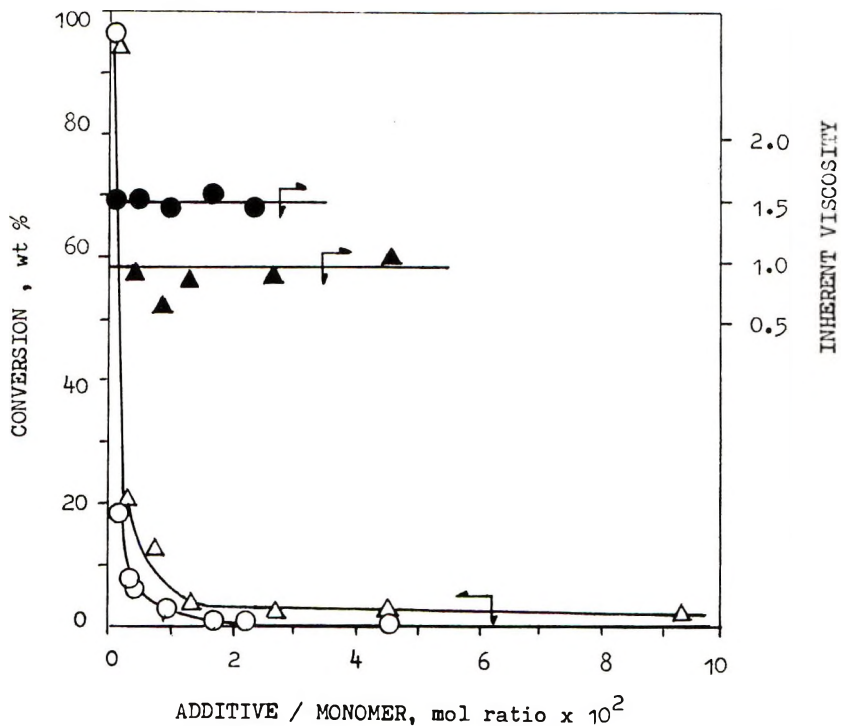


Fig. 2. Influence of (O, ●) carbon dioxide and (Δ , \blacktriangle) hydrogen cyanide on the polymerization rate and the inherent viscosity of polymer in toluene solution; monomer concentration, 50 vol.-%; 0°C., 30 min.

TABLE II
Influence of the Addition of Acidic Substances on the Stability of Formaldehyde^a

Additive	Mole ratio of additive to monomer	Conversion, %	Inherent viscosity	K_a^b
None	—	97	0.78-1.80	—
Inorganic acids				
Telluric	0.6×10^{-4}	0	0.91 ^c	2.1×10^{-8}
Boric	1.1×10^{-4}	0	—	6.5×10^{-11}
Hydrogen cyanide	2.2×10^{-2}	1.0	0.82 ^d	4.8×10^{-11}
Organic acids				
Stearic	0.3×10^{-4}	21.3	1.18	3×10^{-5}
Acetic	1.7×10^{-4}	11.3	1.12	1.6×10^{-6}
Pivalic	1.1×10^{-4}	32.2	1.00	1.1×10^{-4}
Acid anhydrides				
Carbon dioxide	1.0×10^{-1}	0	0.95 ^e	(5×10^{-11})
Maleic anhydride	5.5×10^{-2}	3.7	—	(1.4×10^{-2})

^a Monomer concentration, 50 vol.-% in toluene; temperature, 0°C.; time, 30 min.

^b Dissociation constant of the acid in water at 25°C.

^c Polymer obtained after polymerization for 25 hr. at 0°C.

^d Polymer obtained after polymerization for 17.3 hr. at 0°C.

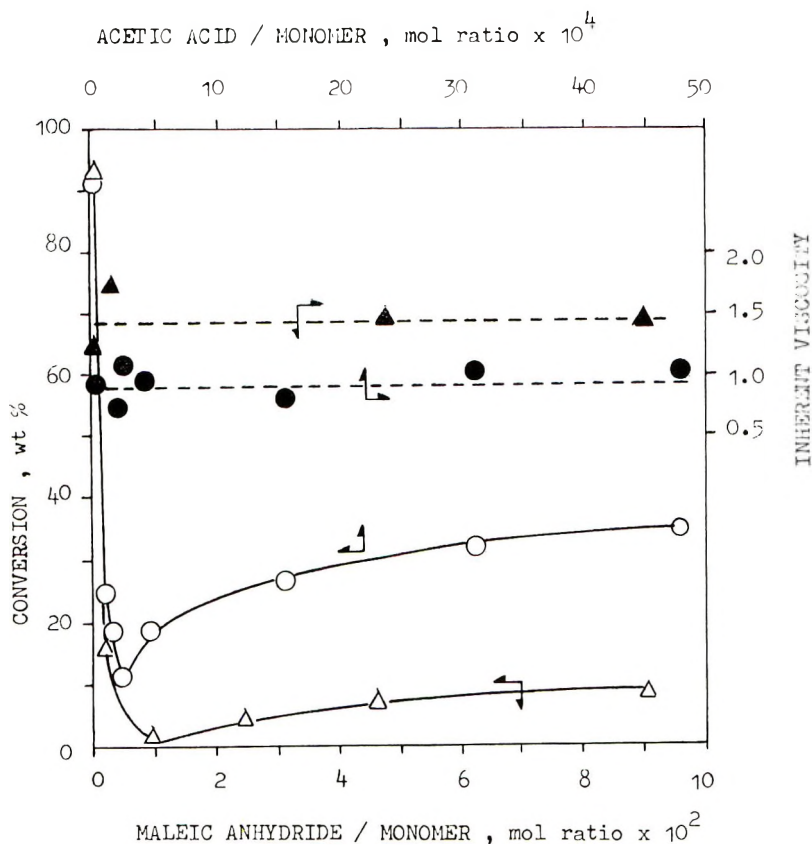


Fig. 3. Influence of (O, ●) acetic acid and (Δ, ▲) maleic anhydride on the polymerization rate and the inherent viscosity of polymer in toluene solution; monomer concentration, 50 vol.-%; 0°C.; 30 min.

The monomer used in the experiment was found by analysis to contain 0.09 vol.-% carbon dioxide, 0.13 vol.-% water, and 0.10 vol.-%, methanol as impurities. The impurities contents of the monomer used in subsequent experiments were almost the same as described above.

The polymerization was carried out in toluene solution at a monomer concentration of 50 vol.-% at 0°C. for 30 min.; results are shown in Table II. The rate of polymerization was depressed by the addition of acidic substances, especially inorganic compounds such as telluric acid, boric acid, hydrogen cyanide, and carbon dioxide, while the molecular weight of the polymer obtained was not affected by the addition of these acidic substances.

Figures 2 and 3 show the influence of hydrogen cyanide, carbon dioxide, maleic anhydride, and acetic acid on the stability of the monomer in toluene solution. The polymer yield decreased rapidly with addition of these compounds. A marked depressing effect was observed with carbon dioxide, while a slight increase in the rate of polymerization was

seen with addition of excess acetic acid or maleic anhydride. It was also found that the degree of polymerization was not affected by the addition of acidic substances.

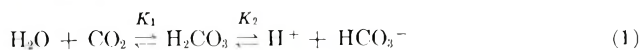
Role of Acidic Substances in the Polymerization

It has been reported that cationic and anionic catalysts easily give polymerization of formaldehyde.⁸⁻¹¹ However, the mechanism of spontaneous polymerization of anhydrous formaldehyde in a condensed phase has not been elucidated clearly. Only the ionic initiation of this polymerization has been proposed in early studies.

As described above, addition of small amounts of acidic substances generally reduces the rate of spontaneous polymerization of formaldehyde, but these acidic substances do not affect the molecular weight of the polymer produced over the entire range of concentration studied. This means that an acidic substance retards only the initiation of polymerization, which should be caused by an anionic species in the reaction system. If acidic substances examined terminate the growth of polymer chain, as Enikolopyan et al.⁵ reported, the molecular weight of the resultant polymer should be affected. The role of hydroquinone, reported by Spence,² can be also understood as that of proton donor.

Addition of excess acetic acid or maleic anhydride slightly increased the polymerization yield. The optimum amount of acid depressing polymerization varied with the dissociation constant of acid used. It is considered that the concentration of proton produced by dissociation of acid in the reaction system increases with the acidity of acidic substance used, and when the proton concentration is comparable to the concentration of an anionic initiating species the polymerization is the most effectively depressed. An excess of proton causes a cationic polymerization of the monomer.

Acid anhydride acts as acid in cooperation with water present in the monomer used. Thus, proton is produced from carbon dioxide by dissociation equilibrium with water, according to eq. (1):



where K_1 and K_2 are the equilibrium constants. Thus, the proton concentration is inversely proportional to the square root of the concentration of carbon dioxide.

$$\begin{aligned} [\text{H}^+] &= K_2^{1/2}[\text{H}_2\text{CO}_3]^{1/2} \\ &= K_1^{1/2}K_2^{1/2}[\text{CO}_2]^{1/2}[\text{H}_2\text{O}]^{1/2} \end{aligned} \quad (2)$$

The rate of polymerization should be, therefore, inversely proportional to the square root of the concentration of carbon dioxide. This relationship between the rate of spontaneous polymerization and the concentration of carbon dioxide is satisfied in Figure 4, which was calculated by using the experimental values shown in Figure 2.

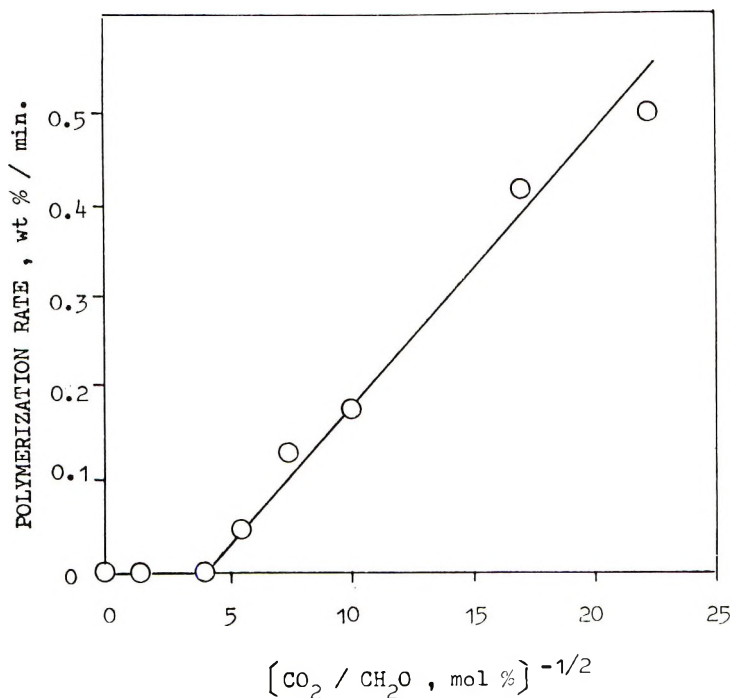


Fig. 4. Relation between the concentration of carbon dioxide and the polymerization rate.

From the fact that the acidic substance retards only the initiation of polymerization, it may be concluded that the spontaneous polymerization of formaldehyde in bulk or in a toluene solution is initiated by an anionic species.

The authors wish to express their thanks to Dr. K. Fujimura, Director of Takarazuka Radiation Laboratory, who gave us useful advice on the research work and the permission for the publication of this paper, and also to Mr. Y. Otsuka and Mr. T. Nishida for much helpful assistance.

References

1. J. F. Walker, *Formaldehyde*, 3rd Ed., Reinhold, New York, 1964, pp. 46, 52.
2. R. Spence, *J. Chem. Soc.*, **1933**, 1193.
3. H. Staudinger, *Die Hochmolekularen Organischen Verbindungen*, Springer, Berlin, 1932, pp. 257-63.
4. N. S. Enikolopyan, *J. Polymer Sci.*, **58**, 1301 (1962).
5. N. F. Poroshlyakova, I. F. Sanaya, and N. S. Enikolopyan, *Vysokomolekul. Soedin.*, **5**, 1776 (1963).
6. Z. Macháček, J. Mejzlík, and J. Pác, *J. Polymer Sci.*, **52**, 309 (1961).
7. Brit. Pat. 796,862 (1958), to E. I. du Pont de Nemours & Co., Inc.
8. H. Staudinger, R. Signer, H. Johner, H. Luthy, M. Kern, D. Russidis, and O. Schweitzer, *Ann.*, **474**, 145 (1929).
9. J. F. Walker, *J. Am. Chem. Soc.*, **55**, 2823 (1933).

10. C. E. Schweitzer, R. N. MacDonald, and J. O. Punderson, *J. Appl. Polymer Sci.*, **1**, 158 (1959).

11. K. Fukuda and H. Kakiuchi, *Kogyo Kagaku Zasshi*, **65**, 2054 (1962).

Résumé

La stabilité du formaldéhyde liquide produit par pyrolyse d' α -polyoxyméthylène a été étudiée en rapport avec des impuretés contenues dans le monomère. Le monomère liquide était divisé en différentes fractions au moyen de la distillation. La stabilité de chaque fraction du point de vue de la polymérisation dépendait de l'ordre de la fraction, c'est-à-dire, le monomère obtenu dans les fractions premières de distillation était très stable pour la polymérisation comparées aux dernières fractions. Des résultats analytiques du monomère formé indiquaient que diverses impuretés tel que du CO_2 , de l'eau, du méthanol et du formiate de méthyle étaient présents dans le monomère. Au départ de ces résultats sur l'influence des impuretés sur la stabilité du formaldéhyde liquide on a trouvé que de faibles quantités de CO_2 et d'acide cyanhydrique diminuaient remarquablement la polymérisation et qu'en présence d'acide acétique et d'anhydride maléique la vitesse de polymérisation décroissait avec la quantité de ces composés, mais qu'elle reaugmentait avec une quantité en excès. Par ailleurs l'addition de substances acides n'effectuait pas le poids moléculaire du polymère produit. Du fait que la substance acide ne retarde que l'initiation de la polymérisation, on en conclut que la polymérisation spontanée du formaldéhyde en bloc ou en solution toluénique est initiée par une espèce anionique.

Zusammenfassung

Die Stabilität von flüssigem, durch Pyrolyse von α -Polyoxymethylen hergestelltem Formaldehyd wurde in Verbindung mit einer im Monomeren enthaltenen Verunreinigung untersucht. Das flüssige Monomere wurde mittels Destillation in mehrere Fraktionen geteilt. Die Stabilität jeder Fraktion im Hinblick auf Polymerisation hängt davon ab, um die wievielte Fraktion es sich handelt, d.h. das in der Anfangsfraktion der Destillation erhaltene Monomere war äusserst polymerisationsbeständig, mehr als das in einer späteren Fraktion enthaltene Monomere. Eine analytische Untersuchung des gebildeten Monomeren ergab, dass verschiedene Verunreinigungen wie Kohlendioxyd, Wasser, Methanol und Methylformiat im Monomeren enthalten sind. Aus Untersuchungen über den Einfluss dieser Verunreinigungen auf die Stabilität flüssigen Formaldehyds ging hervor, dass kleine Mengen an Kohlendioxyd und Cyanwasserstoff die Polymerisation beträchtlich hemmen und dass bei Zusatz von Essigsäure und Maleinsäureanhydrid die Polymerisationsgeschwindigkeit mit der Konzentration dieser Verbindungen zunächst abnahm, während sie bei Zugabe eines Überschusses anstieg. Andererseits hatte der Zusatz dieser aciden Substanzen keinen Einfluss auf das Molekulargewicht der entstandenen Polymeren. Aus der Tatsache, dass die Substanzen mit Säurecharakter nur den Polymerisationsstart verlangsamten, wurde geschlossen, dass die spontane Polymerisation von Formaldehyd in Substanz oder in Toluollösung durch eine anionische Spezies ausgelöst wird.

Received February 20, 1967

Revised April 1, 1967

Prod. No. 5456A

Polymerization of Alkylene Oxides by Dialkylzinc-Lewis Base Systems

JUNJI FURUKAWA, NARIYOSHI KAWABATA, and AKIRA KATO,
*Department of Synthetic Chemistry, Kyoto University,
Kyoto, Japan*

Synopsis

Dialkylzinc-Lewis base systems are found to be active catalysts for the polymerization of alkylene oxides. The diethylzinc-dimethyl sulfoxide system is especially effective in the preparation of high polymers of ethylene oxide and propylene oxide. Diethylzinc does not react with dimethyl sulfoxide, but there is strong association between the compounds. The proton magnetic resonance spectrum of a poly(ethylene oxide) prepared by the catalyst system suggests that the *n*-butoxyl group is attached to the end of the polymer chain. Polymerization of ethylene oxide seems to be initiated by the ethyl-zinc bond. The active species of the system seems to be diethylzinc coordinated with dimethyl sulfoxide. The efficiency of the catalyst system for the formation of high molecular weight polymer is 10^{-1} - 10^{-2} . The other part of the catalyst is responsible for the formation of low polymers.

INTRODUCTION

Various catalyst systems containing metal-oxygen or metal-nitrogen bonds have been reported to induce the polymerization of alkylene oxides, yielding polymer of extremely high molecular weight.¹ Metal alkyls themselves are generally only slightly active in the polymerization of alkylene oxide, and hence various cocatalysts containing active hydrogen are proposed. These cocatalysts react with a metal alkyl to form the metal-oxygen or the metal-nitrogen bonds. In the present paper is described the catalytic activity of dialkylzinc-Lewis base systems, a new type of catalyst systems, in the high polymerization of alkylene oxides.

EXPERIMENTAL

Reagents

Diethylzinc was purified by distillation, b.p. 117°C. The concentration of the solutions of diethylzinc was determined by chelatometry.² Dimethyl sulfoxide was refluxed over calcium hydride and distilled under reduced pressure. Tetramethylene sulfoxide and diphenyl sulfoxide were prepared according to the procedures of Tarbel³ and Shriner,⁴ respectively. Triethylamine was distilled in the presence of acetic anhydride, dried

over alumina, and redistilled. Ethylene oxide was dried over calcium hydride and distilled three times. Propylene oxide was refluxed over potassium hydroxide pellets, dried over calcium hydride, and fractionated. Epichlorohydrin was purified by distillation. Benzene, toluene, tetrahydrofuran, *p*-dioxane, and acetonitrile were purified by the usual methods.⁵ Nitrogen was purified by passage through a tube containing copper turnings in a furnace at 200°C. followed by passage through a dioxane solution of the metal ketyl produced from sodium and benzophenone. Other reagents were commercial products and were used without further purification.

Procedure

Polymerizations were carried out under a nitrogen atmosphere in sealed Pyrex test tubes. The polymer was recovered by evaporating the solvent and unchanged monomer at room temperature *in vacuo*. The recovered poly(ethylene oxide) was dissolved in acetonitrile containing methanol, the solution was centrifuged, and the upper layer was dried *in vacuo*. Poly(ethylene oxide) of low molecular weight was washed several times with isopropanol and purified by freeze-drying from benzene. The recovered poly(propylene oxide) was dissolved in benzene containing methanol, the solution was centrifuged, and the upper layer was dried by the frozen benzene technique. The viscosity of poly(ethylene oxide) and poly(propylene oxide) solutions was measured at 30°C. in acetonitrile and at 25°C. in benzene, respectively, with an Ubbelohde-type viscometer. The molecular weight of poly(ethylene oxide) was calculated by use of eq. (1).⁶

The calculation of the \bar{M}_v value from the viscosity data in acetonitrile by eq. (1) was assumed not to lead us into serious error, although the equation had been obtained in water at 30°C.

$$[\eta] = 1.25 \times 10^{-4} \bar{M}_v^{0.78} \quad (1)$$

The number-average molecular weight of poly(ethylene oxide) of low molecular weight was measured with a Mechrolab vapor-pressure osmometer. The acetone-insoluble fraction of poly(propylene oxide) was measured at 0°C. by separating it from a 1% solution of the polymer.⁷ The volume of the evolved gas from catalyst systems was measured by a gas buret at 25°C. Vapor-phase chromatographic analysis of the evolved gas was made on a Yanagimoto 3DH gas chromatograph with the use of squalane as the liquid phase. The chemical analysis for sulfur in the polymers was performed according to the sodium azide method.⁸ The fractionation of poly(ethylene oxide) was made at 0°C. by means of the acetonitrile-isopropanol system. The infrared spectra of catalyst systems were measured with a Hitachi EPI-G double-beam spectrophotometer at room temperature under nitrogen atmosphere. The proton magnetic resonance spectra were obtained with a Japan Electron Optics Lab.

3H-60 spectrometer using tetramethylsilane as the internal standard in deuteriochloroform at room temperature.

RESULTS AND DISCUSSION

Polymerization of Alkylene Oxides by Dialkylzinc-Sulfoxide Systems

The catalytic activity of diethylzinc in the polymerization of ethylene oxide and propylene oxide is greatly enhanced when an appropriate amount of dimethyl sulfoxide (DMSO) is added as a cocatalyst. The catalytic activity of the system is not very sensitive to the ratio of DMSO to diethylzinc, although the optimum mole ratio lies between 1 and 2.

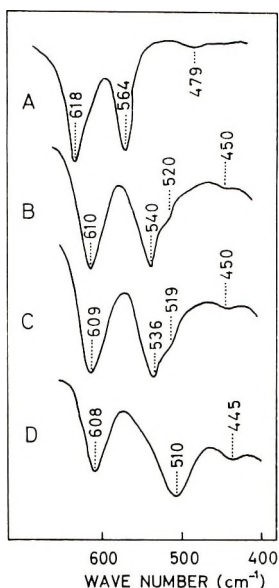


Fig. 1. Comparison of the infrared spectrum of diethylzinc with those of various diethylzinc-DMSO systems: (A) without DMSO; (B) just after mixing; (C) after aging for 1 hr. at 80°C.; (D) after aging for 10 hr. at 110°C. Toluene was used as solvent; DMSO:diethylzinc = 1.

The catalytic activity of the system is further enhanced by thermal aging of the catalyst at elevated temperatures before polymerization. Some typical results of the polymerization of ethylene oxide and propylene oxide by the diethylzinc-DMSO system are shown in Table I, where the catalyst system was used after aging at 110°C. for 10 hr. The polymerizations proceed homogeneously in toluene. In hexane, however, the polymerizations proceed heterogeneously. The catalyst system affords crystalline poly(propylene oxide) which is insoluble in cold acetone.*

* The insoluble fraction is about 20% of the polymer.

TABLE I
 Polymerization of Alkylene Oxides by the Diethylzinc-DMSO System^a

Alkylene oxide ^b	Alkylene oxide, concn., mole/l.	DMSO/Et ₂ Zn mole ratio	Et ₂ Zn, mole-%	Time, hr.	Conversion, %	$[\eta]$, dl./g. ^c
PO	7.15	1.0	0.1	40	77	9.6
PO	7.15	1.0	0.2	40	100	12.6
PO	13.83	1.0	0.01	240	44	3.7
PO	13.82	2.0	0.2	40	100	10.2
PO	13.82	2.0	0.02	287	50	8.5
EO	6.67	1.0	0.1	20	88	5.6
EO	8.33	1.0	0.1	4	19	16.0
EO	8.33	1.0	0.1	7	39	20.2
EO	8.33	1.0	0.1	9	58	19.8
EO	8.33	1.0	0.05	5	35	5.3
EO	8.33	1.0	0.05	20	100	7.5
EO	8.33	1.0	0.025	48	31	3.2
EO	8.33	1.0	0.025	80	40	3.8
EO	8.33	1.0	0.01	126	21	5.1
EO	8.33	1.0	0.01	240	30	6.2
EO	6.67	2.0	1.0	15	68	22.7
EO	6.67	0.5	1.0	15	9	37.0

^a Polymerization was carried out at 70°C. in toluene solution.

^b PO = propylene oxide; EO = ethylene oxide.

^c Viscosity of poly(ethylene oxide) and poly(propylene oxide) was measured at 30°C. in acetonitrile and at 25°C. in benzene, respectively.

The catalyst system has some slight activity in the polymerization of epichlorohydrin. The diethylzinc-tetramethylene sulfoxide system is less effective than the diethylzinc-DMSO system in the polymerization of ethylene oxide and propylene oxide. The diethylzinc-diphenyl sulfoxide system shows even less activity in the polymerization.

Reaction of Diethylzinc with DMSO

The reaction of diethylzinc with DMSO was examined in order to clarify the active species of the catalyst system. When DMSO was added to a toluene solution of diethylzinc, no evolution of gas was observed during the aging of the system both at 90°C. and at 110°C. for a long time, and the catalyst system after aging was still capable of evolving gas on hydrolysis by the addition of methanol. The volume of the evolved gas as measured by a gas buret was nearly equal to the calculated value if we assumed that the diethylzinc remained unchanged during the heat treatment. The evolved gas was ascertained by use of vapor-phase chromatography to be pure ethane. These facts indicate that diethylzinc does not react with DMSO under these reaction conditions.

TABLE II
Gases Evolved on Quenching the Diethylzinc-DMSO System
by Methanol-[A]^a

DMSO/ Et ₂ Zn mole ratio	Et ₂ Zn, mole/l.	Catalyst system, ml.	Evolved gas	
			ml.	%
0	1.000	0.500	23.77	—
1.0	0.932	0.536	23.60	99.3
2.0	0.874	0.572	23.68	99.6

^a The catalyst system was aged at 90°C. for 2 hr. Toluene was used as the solvent.

TABLE III
Gases Evolved on Quenching the Diethylzinc-DMSO System
by Methanol-[B]^a

DMSO/ Et ₂ Zn mole ratio	Et ₂ Zn, mole/l.	Catalyst system, ml.	Evolved gas	
			ml.	%
0	1.000	0.500	24.68	—
1.0	0.932	0.536	24.32	98.5
2.0	0.874	0.572	24.60	99.8

^a The catalyst system was aged at 110°C. for 10 hr. Toluene was used as the solvent.

Infrared Studies on the Diethylzinc-DMSO System

The infrared spectra of the catalyst system were obtained in order to determine whether the diethylzinc-DMSO system was only a mixture

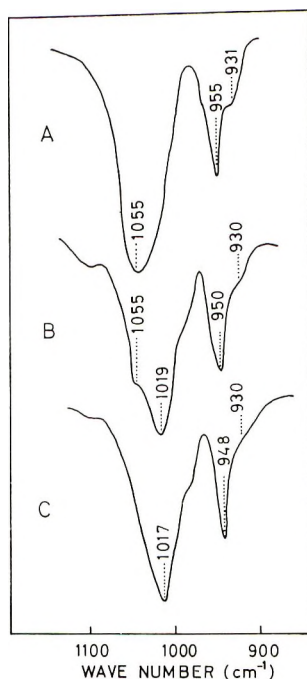


Fig. 2. Infrared spectra of DMSO with or without diethylzinc: (A) without diethylzinc; (B) just after mixing; DMSO:diethylzinc = 1; (C) after aging for 10 min. at 110°C ., DMSO:diethylzinc = 1. Toluene was used as solvent.

of diethylzinc and DMSO or whether the compounds associated with each other. When DMSO was added to a toluene solution of diethylzinc, the absorption bands of diethylzinc shifted to a lower frequency, as can be seen in Figure 1. Figure 2 shows infrared spectra of DMSO in the catalyst system which indicate some shifts of bands to lower frequency on the addition of diethylzinc. These facts suggest that the diethylzinc-DMSO system is a system of strongly associated compounds rather than a mixture of diethylzinc and DMSO.

Proton Magnetic Resonance Spectrum of Poly(ethylene Oxide) Prepared by the Diethylzinc-DMSO System

On the assumption that the active species of the diethylzinc-DMSO system for the polymerization of alkylene oxides is the diethylzinc coordinated with DMSO, the ethyl group of diethylzinc might be presumed to be attached to the endgroup of the polymer chain. The proton magnetic resonance spectrum of a polyethylene oxide was taken at an elevated sensitivity in deuteriochloroform, which is shown in Figure 3. The poly(ethylene oxide) was prepared in toluene by use of the diethylzinc-DMSO system. The number-average molecular weight of the polymer was about 1000. In Figure 4 is shown the proton magnetic resonance spectrum of diethylene glycol di-*n*-butyl ether. Comparing Figure 3 with Figure 4,

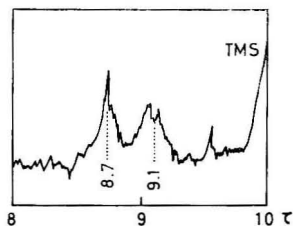


Fig. 3. Proton magnetic resonance spectrum of a poly(ethylene oxide) in CDCl_3 . The polymer was prepared by use of the diethylzinc-DMSO system in toluene.

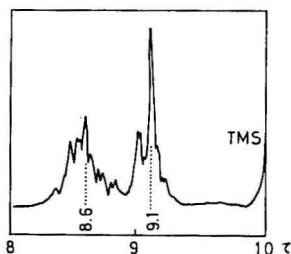
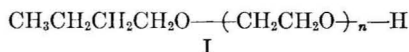
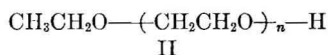


Fig. 4. Proton magnetic resonance spectrum of diethylene glycol di-*n*-butyl ether in CDCl_3 .

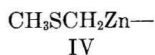
we concluded that the *n*-butoxyl group was attached to the end of the polymer chain (I). The peak at 9.1 τ was assigned to the methyl group and that at 8.7 τ was assigned to the two methylene groups adjacent to the methyl group.



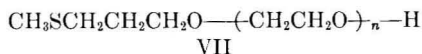
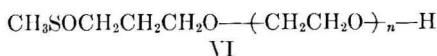
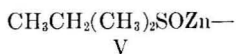
In the case where DMSO acts as an oxidizing agent for diethylzinc and the ethoxyl group initiates the polymerization of ethylene oxide, the ethoxyl group will be attached to the end of the polymer chain (II), and the peak due to the methyl group will appear at 8.8 τ and no absorption at 9.1 τ . The possibility can be ruled out from the spectrum shown in Figure 3.



Other possibilities of initiations by the species like III, IV, and V are also ruled out by the negative results of a chemical analysis for sulfur* in the polymers of structures of VI, VII, and VIII.



* Analysis would be able to detect the presence of 1 sulfur atom per 1000 polymer chains, but the results were still negative.



The active species of the diethylzinc–DMSO system for the high polymerization of alkylene oxides is concluded to be diethylzinc coordinated with DMSO.

Efficiency of the Diethylzinc–DMSO System in the Polymerization of Ethylene Oxide

The poly(ethylene oxide) prepared by use of the catalyst system was separated into two parts by dissolving the polymer in acetonitrile followed by pouring the solution into diethyl ether. The number-average molecular weight of the polymer of the soluble part was determined by vapor-pressure osmometry.* The polymer of the insoluble part was further fractionated

TABLE IV
Fractionation Data of the Ether-Insoluble Part of Poly(ethylene Oxide)
Prepared by the Diethylzinc–DMSO System^a

Fraction	$w_i \times 100$	$[\eta]_i$, dl./g.
1	4.6	1.85
2	4.7	3.45
3	7.3	5.00
4	17.5	6.45
5	21.1	6.65
6	42.3	8.05
7	2.5	9.05

^a $(\bar{M}_v)_0 = 1.16 \times 10^6$.

into several parts of different molecular weight by use of the isopropanol–acetonitrile system. Table IV indicates the molecular weight distribution, and Figure 5 shows the cumulative amount of the polymer as a function of the reduced viscosity-average molecular weight.⁹ The dashed curve in Figure 5 shows the most probable distribution.¹⁰ As is obvious in Figure 5, the ratio \bar{M}_w/\bar{M}_n for the insoluble part of the polymer lies between 1 and 2. The \bar{M}_v value of the insoluble part of the polymer is not appreciably different from the \bar{M}_n value.

* The soluble polymer was purified as follows. A small amount of methanol was added to an acetonitrile solution of polymer, the solution was centrifuged, and the upper layer was dried *in vacuo*. Subsequently, the polymer was washed several times with isopropanol and purified by freeze drying from benzene.

TABLE V
Efficiency of the Catalyst in the Polymerization of Ethylene Oxide by the Diethylzinc-DMSO System^a

Catalyst, mole-%	Time, hr.	Conversion, %	Ether-soluble polymer ^b			Ether-insoluble polymer ^b		
			Fraction, %	$\bar{M}_n \times 10^{-3}$	$f_1 \times 100$	Fraction, %	$\bar{M}_v \times 10^{-5}$	$f_2 \times 100$
0.1	10	52	9	2.9	49	91	15.9	1
0.1	30	97	20	8.7	32	80	29.7	1
0.05	9	52	9	3.4	67	91	4.3	5
0.05	15	63	6	6.0	35	94	7.5	4

^a Polymerization was carried out in toluene at 70°C. DMSO/Et₂Zn = 1. The concentration of ethylene oxide was 8.33 mole/l.

^b The poly(ethylene oxide) was separated into the soluble and the insoluble portions by pouring an acetonitrile solution of the polymer into diethyl ether.

The efficiency of the catalyst system for the formation of soluble and insoluble polymer was calculated from eqs. (2) and (3), respectively.

$$f_1 = \frac{\text{g. of polymer}}{\bar{M}_n \text{ of polymer}} \times \frac{1}{2 \text{ (moles of diethylzinc used)}} \quad (2)$$

$$f_2 = \frac{\text{g. of polymer}}{\bar{M}_v \text{ of polymer}} \times \frac{1}{2 \text{ (moles of diethylzinc used)}} \quad (3)$$

The efficiency is based upon the assumption that two ethyl groups of diethylzinc are active in starting a chain. Results are given in Table V.

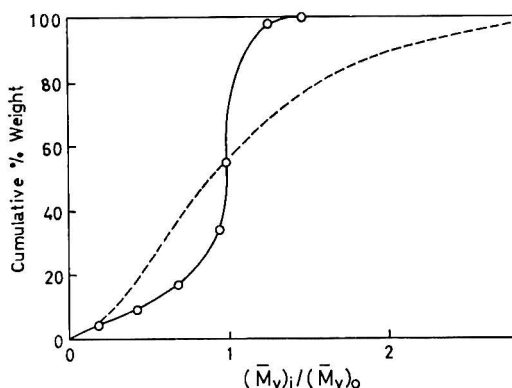


Fig. 5. Reduced molecular weight distribution: (—) experimental, for the ether-insoluble part of poly(ethylene oxide) prepared by the diethylzinc–DMSO system: (---) most probable distribution.

As can be seen in Table V, the efficiency of the diethylzinc–DMSO system in the preparation of high molecular weight polymer is 10^{-1} – 10^{-2} and is extremely high as compared with most catalysts for the coordinated anionic polymerization of alkylene oxides whose efficiencies are 10^{-3} – 10^{-4} . However, the catalyst efficiency is still not quantitative. The other part of the catalyst is responsible for the formation of low polymers.

Polymerization of Propylene Oxide by Other Diethylzinc–Lewis Base Systems

Triethylamine, tetramethylenediamine, and triethylenediamine show low but significant cocatalytic activity towards diethylzinc in the polymerization of propylene oxide. The results of the polymerization of propylene oxide by the diethylzinc–triethylamine system are shown in Table VI.

On the other hand, tetrahydrofuran does not show any cocatalytic activity with diethylzinc in the polymerization of propylene oxide, although it is well known that dimethylzinc forms a coordination complex with tetrahydrofuran.¹¹

TABLE VI
Polymerization of Propylene Oxide by
the Diethylzinc-Triethylamine System^a

Diethylzinc, mole-%	Conversion, %	$[\eta]$, dl./g. ^b
5.0 ^c	49	1.5
1.0 ^c	9	0.65
5.0 ^d	100	5.7
1.0 ^d	14	2.3

^a Polymerization was carried out in toluene solution at 70°C. for 250 hr. The concentration of propylene oxide is 7.15 mole/l.; $\text{Et}_2\text{Zn}/\text{Et}_3\text{N} = 2$.

^b Viscosity at 25°C. in benzene.

^c The catalyst system was used without aging.

^d The catalyst system was aged at 90°C. for 10 hr. prior to the polymerization.

References

1. J. Furukawa and T. Saegusa, *Polymerization of Aldehydes and Oxides*, Interscience, New York, 1963, Chap. III.
2. K. Ueno, *Chelatometric Titration*, Nankodo, Tokyo, 1960.
3. D. S. Tarbell and C. Weaver, *J. Am. Chem. Soc.*, **63**, 2939 (1941).
4. R. L. Shriner, H. C. Struck, and W. J. Jorison, *J. Am. Chem. Soc.*, **52**, 2060 (1930).
5. A. Weissberger, E. S. Proskauer, J. A. Riddick, and E. E. Toops, Jr., Eds., *Organic Solvents*, Interscience, New York, 1955.
6. F. E. Bailey, Jr., J. L. Kucera, and L. G. Imhof, *J. Polymer Sci.*, **32**, 517 (1958).
7. S. Inoue, T. Tsuruta, and N. Yoshida, *Makromol. Chem.*, **79**, 34 (1964).
8. T. Uno, *Organic Quantitative Analysis*, Kyoritsu, Tokyo, 1966, p. 33.
9. C. Booth, W. C. E. Higginson, and E. Powell, *Polymer*, **5**, 479 (1964).
10. P. J. Flory, *Principles of Polymer Chemistry*, Cornell Univ. Press, Ithaca, N. Y., 1953, p. 318.
11. K. H. Thiele, *Z. Anorg. Allgem. Chem.*, **319**, 183 (1962).

Résumé

Des systèmes zinc-dialcoyle-base de Lewis sont des catalyseurs actifs pour la polymérisation d'oxydes d'alkylène. Le système diéthylzinc-diméthyl sulfoxyde est particulièrement efficace dans la préparation de hauts polymères d'oxyde d'éthylène et d'oxyde de propylène. Le diéthylzinc ne réagit pas avec le diméthyl sulfoxyde, mais ces corps s'associent facilement les uns aux autres. Le spectre de résonance magnétique protonique d'oxyde de polyéthylène préparé avec ces systèmes catalytiques suggère que le groupe *n*-butoxylique est attaché à l'extrémité de la chaîne polymérique. La polymérisation de l'oxyde d'éthylène semble être initiée par le lien zinc-éthyl. Les espèces actives des systèmes semblent être le diéthylzinc coordonné avec le diméthyl sulfoxyde. L'efficacité de ce système catalytique pour la formation de polymère de poids moléculaire élevé est de 10^{-1} - 10^{-2} . L'autre partie du catalyseur est responsable de la formation de polymères bas.

Zusammenfassung

Systeme aus Dialkylzink und Lewis-Basen stellen, wie gefunden wurde, aktive Katalysatoren für die Polymerisation von Alkylenoxyden dar. Das Diäthylzink-Dimethylsulfoxyd-System ist bei der Herstellung von Hochpolymeren des Äthylenoxyds und Propylenoxyds besonders wirksam. Diäthylzink reagiert zwar nicht mit Dimethyl-

sulfoxyd; beide Verbindungen sind aber stark miteinander assoziiert. Das protonenmagnetische Resonanzspektrum eines mit diesem Katalysatorsystem hergestellten Polyäthylenoxyds deutet an, dass die *n*-Butoxylgruppe an ein Ende der Polymerkette gebunden ist. Die Äthylenoxydpolymerisation scheint durch die Äthyl-Zinkbindung gestartet zu werden. Die aktive Spezies des Systems dürfte das mit Dimethylsulfoxyd koordinierte Diäthylzink sein. Der Nutzeffekt des Katalysatorsystems für die Bildung von Polymeren hohen Molekulargewichts beträgt 10^{-1} – 10^{-2} . Der andere Teil des Katalysators ist für die Bildung niedermolekularer Polymerer verantwortlich.

Received February 28, 1967

Prod. No. 5448A

Persulfate-Initiated Polymerization of Acrylamide*

J. P. RIGGS† and F. RODRIGUEZ,

*Geer Laboratory for Rubber and Plastics, School of Chemical Engineering,
Cornell University, Ithaca, New York 14850*

Summary

A dilatometric technique was used to obtain conversion-time data for the polymerization of acrylamide initiated by potassium persulfate in water. The results are summarized by the empirical rate expression, $-d[M_1]/dt = R_p = k_{1,25}[K_2S_2O_8]^{0.5}[M_1]^{1.25}$, and $k_{1,25} = 1.70 \times 10^{11} \exp \{-16,900/RT\} 1.0^{75}/\text{mole}^{-0.75}\text{-min}$. Persulfate was varied over the range 9.5×10^{-4} to 5.2×10^{-2} mole/l., and initial monomer concentration $[M_1]$ was varied from 0.05 to 0.4 mole/l. The temperature range was 30–50°C. Results of analysis of the kinetics and energetics of the polymerization favor a cage-effect theory rather than a complex-formation theory to explain the order with respect to monomer.

The present work examines the mechanism by which acrylamide is polymerized by persulfate, a simple free-radical initiator which is also a component of many redox couples. In further work, the system will be extended to the redox couple persulfate-thiosulfate.^{1,2}

Acrylamide ($\text{CH}_2=\text{CHCONH}_2$) is a white, water-soluble, crystalline solid, melting at 84.5°C. and possessing good thermal stability in the solid form.³ The polymerized form of acrylamide, and, hence, the growing radical, is also water soluble. The monomer has been polymerized by a number of techniques: γ -ray initiation,⁴ ultrasonic waves,⁵ and photopolymerization.^{6,7} Dainton and co-workers made detailed studies of the polymerization kinetics in aqueous solution using x-rays and γ -rays for initiation⁸ and also studied the photosensitized initiation by hydrogen peroxide and ferric ion.⁹ Redox polymerizations of acrylamide include the initiation systems chlorate-sulfite,¹⁰ persulfate-metabisulfite,¹¹ Ce(III)-3-chloro-1-propanol,¹² and ferric ion-bisulfite.¹³ There is apparently no published work on the polymerization of acrylamide induced by the conventional peroxidic or azo dissociative initiators alone.

Dainton^{8,9} used dilatometry and rotating-sector experiments. In general, his results follow the classical pattern for free-radical polymerizations, with first-order dependence of rate on monomer concentration. However, with the chlorate-sulfite redox system, Suen¹⁰ found that,

* Presented to the Division of Polymer Chemistry, 149th Meeting, American Chemical Society, Detroit, April 1965.

† Present address: Celanese Corp. Research Center, Summit, N. J.

although initial rates depended on the first power of monomer concentration, the conversion-time data were best fitted by a five-halves power on the monomer concentration. Suen's hypothesis that monomer is adsorbed by polymer was not borne out in a subsequent study with persulfate-metabisulfite as the initiation system,¹¹ but the five-halves power persisted.

EXPERIMENTAL

Water used as solvent in the kinetic studies was singly distilled and further purified by percolation through an ion-exchange demineralizer. Acrylamide was supplied by the Borden Chemical Company and was recrystallized from chloroform. The recrystallized product was washed several times with benzene, aspirated briefly in a Büchner funnel, and then dried under vacuum, at room temperature, for 12–15 hr. The purified acrylamide was stored in the dark over calcium chloride. The inorganic salts used were of analytical grade and were not purified further.

The basic parts of the apparatus consisted of two deaeration units, a dilatometer, constant temperature baths, a magnetic stirrer used to

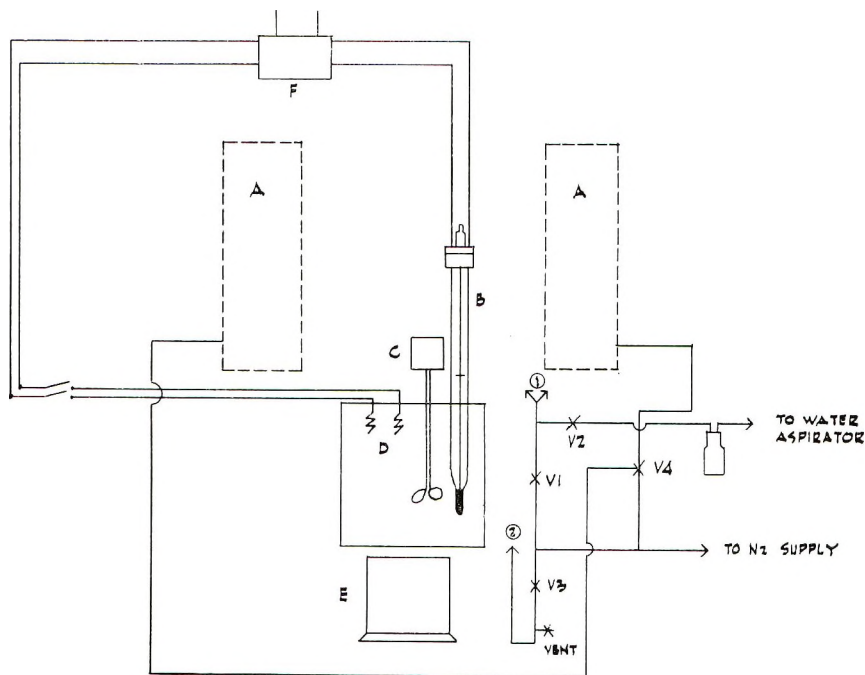


Fig. 1. Schematic of polymerization: (A) deaeration units (see Fig. 2); (B) adjustable contact thermometer; (C) variable-speed agitator; (D) 150 w. lamps; (E) variable-speed magnetic stirrer; (F) on-off valve; (V1) 7 $\frac{1}{2}$ -turn brass needle valve; (V2) polyethylene needle valve; (V3) polyethylene needle valve; (V4) three-way T-bore, Pyrex stopcock; (1) glass Y connecting to dilatometer heads via flexible tubing; (2) flexible tubing connection to dilatometer capillary.

spin a small, Teflon-coated stirring bar in the bulb of the dilatometer, and a tubing system to purge and blanket the reactant solutions with nitrogen. Figure 1 shows a schematic of the polymerization equipment.

For deaeration (Fig. 2), solutions were introduced into a central cylinder, 21 cm. long, constructed by fusing a section of 28-mm. tubing to a fritted-glass filter which functioned as a porous plate for dispersing nitrogen evenly into small bubbles over the entire cross-section. A system of glass tubing connected the cylinder to three, three-way stopcocks which permitted both deaeration and evacuation of the reactant solutions in the central cylinder and, in conjunction with the dilatometer heads, provided a closed system for transfer of deaerated solutions to the dilatometer.

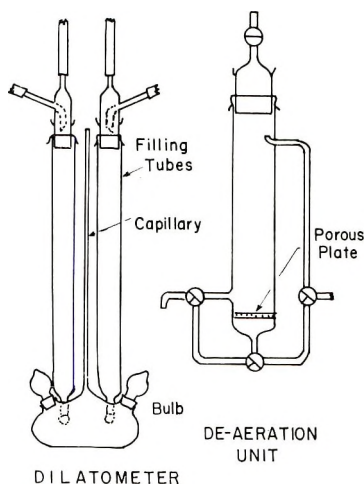


Fig. 2. Dilatometer and deaeration unit (stopcocks connecting filling tubes and reaction bulb not shown).

The dilatometer (Fig. 2) consisted of two filling tubes fitted with special heads and connected to a stirred reaction bulb on which was mounted a long, precision-bore capillary. The 1 mm. bore of the capillary permitted measurement of volumetric contraction of the reaction mixture from the height h of the liquid in the capillary.

Kinetic data were taken regularly to high conversions and, in many cases the reaction was followed to more than 80% conversion. In all runs, the polymerization was allowed to continue in the dilatometer to at least 95% completion, after which the product was transferred to a test tube, and held at temperature for an additional 3-4 hr.

By assuming the fraction of monomer converted is directly proportional to the decrease in volume accompanying the polymerization, and long chains, one obtains for the rate of polymerization

$$R_p = - d[M]/dt = \left\{ [M]_0 / (h_0 - h_\infty) \right\} (dh/dt) \quad (1)$$

The difference in capillary height at zero and infinite time ($h_0 - h_\infty$) depends on the initial monomer concentration and the particular shrinkage characteristics of the monomer-polymer system in a given medium. The shrinkage factor reported by Dainton⁸ of $5.0 \pm 0.25 \times 10^{-5}$ mole acrylamide polymerized for each millimeter contraction in a 1-mm. capillary was confirmed in this work and used throughout.

RESULTS AND DISCUSSION

Initiator Concentration

The influence of persulfate was studied over a 55-fold concentration range, and the results are compiled in Table I. The half-order dependence

TABLE I
Initial Polymerization Rate (R_{p0}) versus Persulfate Concentration^a

$[\text{K}_2\text{S}_2\text{O}_8]_0$, mole/l. $\times 10^3$	R_{p0} , mole/l.-min. $\times 10^3$	Initial pH	Final pH
0.953	0.402	4.08	4.20
2.96	1.08	4.21	4.21
4.16	1.16	3.98	3.94
7.81	1.58	3.88	3.90
10.4	1.79	3.74	3.68
14.1	2.12	3.68	3.62
18.2	2.26	3.58	3.62
40.0	3.43	3.34	3.33
52.1	4.21	3.20	3.20

^a $[\text{M}]_0 = 0.238$ mole/l.; $T = 30^\circ\text{C}$.

of initial rate on initiator concentration (Fig. 3) is the usual result for a reaction uncomplicated by transfer or termination reactions involving the initiator or related species. On the other hand, the conversion-time data are not conventional, and are best correlated, to high conversions, on the basis of a 1.25-order with respect to monomer (Fig. 4).

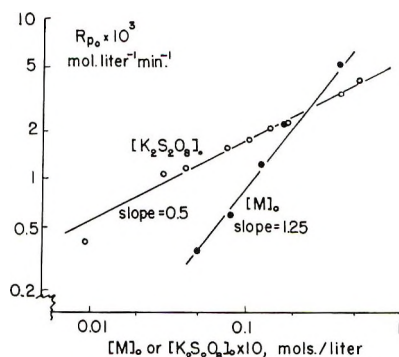


Fig. 3. Dependence of the initial rate of polymerization R_{p0} on the initial concentrations of initiator $[\text{K}_2\text{S}_2\text{O}_8]_0$ and monomer $[\text{M}]_0$.

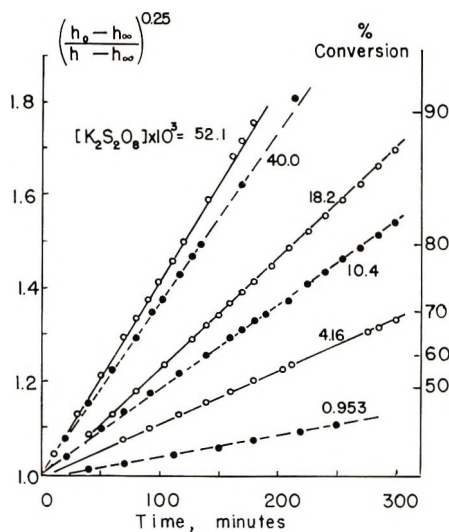


Fig. 4. Course of polymerization in terms of dilatometer reading h plotted assuming the rate proportional to monomer concentration to the 1.25 power.

Monomer Concentration

All results (Table II and Fig. 3) are satisfactorily correlated within experimental uncertainty by a line with a slope of 1.25, in agreement with

TABLE II
Initial Polymerization Rate versus Monomer Concentration^a

$[M]_0$, mole/l.	R_p , mole/l.-min. $\times 10^3$	Initial pH	Final pH
0.0498	0.362	3.40	3.41
0.0798	0.612	3.40	3.50
0.125	1.26	3.50	3.53
0.175	2.22	3.50	3.48
0.398	5.27	3.49	—

^a $[K_2S_2O_8]_0 = 2.61 \times 10^{-2}$ mole/l.; $T = 30^\circ C$.

the data of Figure 4. It should be recalled that the previously cited work^{10,11} on the redox-initiated polymerizations showed a five-halves order dependence over the course of the reaction and a first-order dependence on initial monomer concentration, in contrast to the results of this study. The data obtained here then cast further doubt on the plausibility of the purely physical monomer-adsorption hypothesis.

Molecular weights were difficult to measure and reproduce. Some solutions were unstable and crosslinked on standing a few days. Based on the rate dependence, it is expected that molecular weight should depend more on monomer concentration than on initiator. If initiator concentrations are ignored, an exponential dependence on monomer concentration

TABLE III
Concentration Dependence of Molecular Weight

Monomer concn., mole/l.	Initiator concn., mole/l. $\times 10^2$	Molecular weight $\bar{M}_v \times 10^{-5}$ ^a
0.0498	2.61	0.53
0.125	2.61	2.18
0.125	9.03	1.49
0.175	2.61	3.63
0.176	2.20	4.94
0.238	0.0953	10.6
0.238	1.04	2.84
0.353	6.70	3.90
0.404	0.452	8.04
0.940	0.807	14.3

^a $\bar{M}_v = (1470 [\eta])^{1.51}$, data of Collinson et al.⁸

to the 1.09 power is obtained, in reasonable agreement with the rate dependence on 1.25 (Table III and Fig. 5). The corresponding correlation with initiator concentration—taking into account monomer dependence—is not as satisfying (Fig. 6).

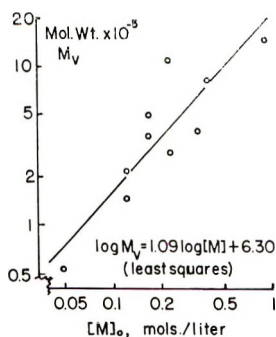


Fig. 5. Viscosity-average molecular weight \bar{M}_v as a function of initial monomer concentration.

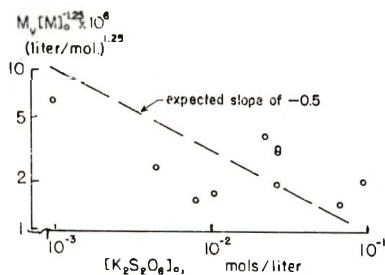


Fig. 6. Viscosity-average molecular weight as a function of initial persulfate concentration.

Temperature

A plot of the empirical rate constant, $k_{1.25}$ against the reciprocal of the absolute temperature yields values of 16.9 kcal./mole for the collective activation energy and 1.7×10^{11} l.^{0.75}/mole^{-0.75}-min. for the Arrhenius factor (Fig. 7).

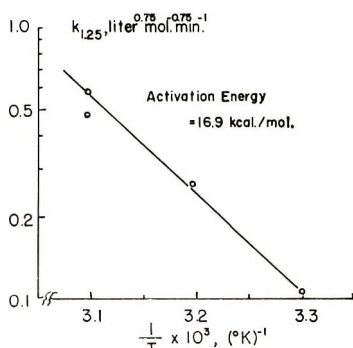


Fig. 7. Arrhenius plot to determine activation energy.

pH

Initial and final pH's for runs at variable initiator and monomer concentrations are listed in Tables I and II. Both studies show no appreciable change in pH over the course of the reaction, and for the five runs at constant initiator concentration, there is little change in initial pH. There does, however, seem to be a decrease in initial pH with increasing persulfate. At this point, it should be noted that investigations of the decomposition of persulfate in aqueous solution have shown the reaction is pH-independent in the range covered here.¹⁴ Consequently, one would not expect the rate of initiation to be influenced by the acidity, and, indeed, this is indirectly confirmed by the half-order dependence of rate on persulfate concentration.

Also, a recent study¹⁵ over the pH range 1-13 has shown that although the propagation constant k_p and the termination constant k_t decrease as pH increases, the ratio $k_p/k_t^{0.5}$ is almost constant.

Analysis

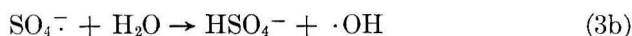
The kinetic results can be summarized in the empirical rate expression

$$R_p = k_{1.25} [\text{K}_2\text{S}_2\text{O}_8]^{0.5} [\text{M}]^{1.25} \quad (2)$$

where $k_{1.25} = 1.70 \times 10^{11} \exp \{ -16,900/RT \}$ l.^{0.75}/mole^{-0.75}-min. At 30°C., $k_{1.25} = 0.108 \pm 0.003$, an average value from seven runs. Interpretation of these results, especially the unusual order with respect to monomer, is logically pursued by first considering the kinetics of the thermal decomposition of persulfate. Then, the various postulates

regarding polymerization which will lead to deviations from first-order behavior can be evaluated.

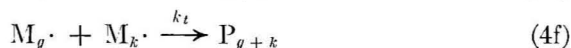
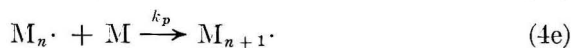
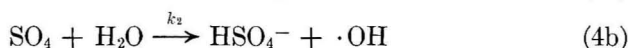
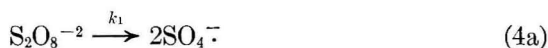
It has been known for some time¹⁶ that the persulfate decomposition in aqueous solution follows a first-order law, and evidence that the measured process is fission of the peroxide bond was provided by Eager and Winkler¹⁷ in a study of the oxidation of mercaptans by potassium persulfate. Subsequently, Bartlett and Cotman,¹⁸ who used neutral and alkaline solutions, proposed the scheme of eqs. (3) for their results:



where dots denote free radicals.

These results were confirmed in a detailed study by Kolthoff and Miller,¹⁴ who, using ¹⁸O-labeled solvent, showed that the oxygen evolved came from the water. They also showed that in addition to the primary process above, a secondary, acid-catalyzed decomposition occurs which is insignificant above a pH of 3.

With this information, it is evident that the thermal decomposition of persulfate yields two species capable of initiating polymerization, the sulfate radical-ion and the hydroxyl radical. In the presence of monomer, a straightforward scheme is as shown in eqs. (4).



where the letter subscripts denote the degree of polymerization of radical (M·) and polymer (P) species.

Reactions (4b) and (4c) compete for the sulfate radical-ion. So, if the hydroxyl radical were a poor initiator of polymerization, the rate of initiation would depend on monomer concentration, yielding (5) for the rate of polymerization if $k_{i2} = 0$:

$$R_p = \frac{k_p}{k_t^{1/2}} (2k_1 k_{i1})^{1/2} [\text{S}_2\text{O}_8^{-2}]^{1/2} \frac{[\text{M}]^{3/2}}{(k_2 + k_{i1}[\text{M}])^{1/2}} \quad (5)$$

(As shown below, a rate equation of this form does describe the experimental results.) However, there is good evidence for the high reactivity of hydroxyl radicals, and, in particular, the opinion that acrylamide is a

very efficient scavenger for hydroxyl radicals.^{8,19,20} Indeed, recent data²¹ indicate that k_{t2} has a value of 1.1×10^{11} l./mole-min. Hence, this reaction scheme is quite conventional, and the rate of polymerization is given by

$$R_p = k_p(2k_1/k_t)^{1/2}[\text{S}_2\text{O}_8^{-2}]^{1/2}[\text{M}] \quad (6)$$

which differs from the empirical results by the power on the monomer concentration. Nevertheless, one can use this scheme, with the empirical exponent on the monomer concentration, to obtain some information about the initiation process and some idea of the agreement between this and previous work on the magnitude of the rate coefficients. Adjusting Dainton's results to 30°C., one obtains $k_p/k_t^{0.5} = 38 \text{ l.}^{0.5}/\text{mole}^{0.5}\text{-min.}^{0.5}$, with $E_p - E_t/2 = 1.5 \text{ kcal./mole}$. For the persulfate decomposition, Kolthoff and Miller¹⁴ report that at 30°C., $k_1 = 3.18 \times 10^{-6} \text{ min.}^{-1}$ and $E_1 = 33.5 \text{ kcal./mole}$. Using the above with a persulfate concentration of 0.01 mole/l. and a monomer concentration of 0.238 mole/l., one obtains calculated values for the initial rate R_{p0} and activation energy E_A which can be compared with the experimental values (Table IV).

TABLE IV

	R_{p0} , mole/l.-min.	E_A , kcal./mole
Experimental	1.78×10^{-3}	16.9
Calculated	1.59×10^{-3}	18.2 ^a

^a $E_p - E_t/2 - E_1/2$.

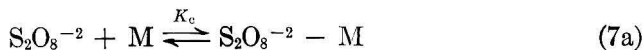
Since the collective activation energy is almost entirely determined by E_1 , the degree of agreement seen here indicates that the rate-controlling step which introduces radicals into the system is the unimolecular decomposition of persulfate. The significance of this point will become evident below.

A dependence on monomer concentration greater than first-order was observed early in the study of catalyzed polymerizations, and the theoretical treatments to explain such behavior have gone in three directions; viz., (1) the complex theory,²² (2) the cage-effect theory,²³ and (3) the solvent-transfer theory.^{24,25} These have been reviewed in the literature recently,^{26,27} and the subsequent discussion is drawn largely from these latter sources. The cage effect is also discussed by Flory²⁸ and Bevington.²⁹

First, it is clear that the solvent-transfer theory can be disregarded as far as this work is concerned. This explanation is based on retardation arising from the transfer radical being unreactive in reinitiating polymerization, and, as pointed out above, the hydroxyl radical is very reactive towards acrylamide.

Complex Theory

This theory proposes the formation of a complex between initiator and monomer, and that the rate of initiation is then determined by the rate of decomposition of the complex. For this study, the following reactions would be suitable for such a scheme in addition to reactions (4b)–(4f):



The concentration of the complex formed in reaction (7a) is given by eq. (8):

$$[\text{S}_2\text{O}_8 - \text{M}^{-2}] = K_c[\text{S}_2\text{O}_8^{-2}][\text{M}]/(1 + K_c[\text{M}]) \quad (8)$$

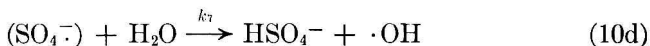
With the usual assumptions, the rate of polymerization is then given by eq. (9):

$$R_p = k_p \left(\frac{2k_3}{k_t} \right)^{1/2} \left(\frac{K_c}{1 + K_c[\text{M}]} \right)^{1/2} [\text{S}_2\text{O}_8^{-2}]^{1/2} [\text{M}]^{3/2} \quad (9)$$

This equation describes a change in the order of reaction with respect to monomer from 1.5 to 1.0 with increasing monomer concentration.

Cage-Effect Theory

This alternative explanation is based on the premise that when a catalyst decomposes into two radicals, the surrounding solvent molecules form a potential barrier to their separation by diffusion. The isolation of these "caged" radicals thus encourages their destruction by mutual recombination. The mechanism adds the (10a)–(10f) reactions to (4b)–(4f), where the parentheses indicate species contained in a solvent cage:



Reactions (10b), (10c), (10d), and (10e) are the alternative routes a primary radical within the cage might follow, i.e., recombination with its primary partner, reaction with a monomer molecule contained in the wall of the cage, reaction with one of the solvent molecules forming the cage, and diffusion out of the cage. Reactions (10f), (4b), and (4c) are analogous reactions for a random radical, but it should be remembered

that they can occur only after reaction (10e). Also, there is an important difference between reactions (10b) and (10f): While the latter is second-order with respect to the randomized radical, the former is a first-order process because the primary radicals are formed in caged pairs.

Neglecting reaction (10f) because monomer is present in reasonable concentration and making the other conventional assumptions, one derives

$$R_p = k_p \left(\frac{2k_1}{k_t} \right)^{1/2} [S_2O_8^{-2}]^{1/2} \left(\frac{k_6[M] + k_7 + k_8}{k_6[M] + k_7 + k_8 + k_5} \right)^{1/2} [M] \quad (11)$$

The steps characterized by $k_7 + k_8$ and by $k_5 [M]$ represent the different avenues by which the primary radical can escape from its cage. It is clear that the relative magnitudes of these terms will determine the dependence on monomer concentration. If $k_7 + k_8 \gg k_6 [M]$, then the rate is always first-order in monomer. On the other hand, if $k_7 + k_8 \ll k_5 [M]$, eq. (11) becomes

$$R_p = K_p \left(\frac{2k_1}{k_t} \right)^{1/2} [S_2O_8^{-2}]^{1/2} \left(\frac{k_6}{k_5 + k_6[M]} \right)^{1/2} [M]^{3/2} \quad (12)$$

Here the dependence on monomer concentration again varies from a power of 1.5 to 1.0 as the concentration increases. Thus, interpretation of kinetic orders greater than unity hinges on the dominance of a reaction between caged radicals and monomer molecules in the cage wall (However, for a different concept, see below).

Equation (12), which is of the same form as eqs. (5) and (9), can be rearranged to give:

$$\frac{[M]^3}{R_p^2} = \frac{k_t}{K k_p^2 (2k_1) [S_2O_8^{-2}]} (1 + K[M]) \quad (13)$$

where, considering the complex and cage-effect theories, $k = k_3$ or k_4 , and $K = K_c$ or k_6/k_5 . The suggested plot (Fig. 8) yields K_c or k_6/k_5 equal to 5.06 l./mole. Jenkins³⁰ has presented plots like Figure 8 for the polymerization of styrene initiated by benzoyl peroxide in toluene and of acrylonitrile initiated by azobisisobutyronitrile in dimethylformamide. Cal-

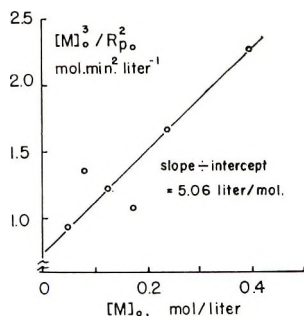


Fig. 8. Plot of eq. (13) demonstrating the predicted dependence of the cage and complex theories.

culations from his plots give values for K_c or k_6/k_5 of the order of 10^3 for each system, which is many times the result of this study.

The above treatment of the cage effect, although conceptually somewhat useful, as evidenced by Figure 8, is limited and, perhaps, misleading. Noyes³¹⁻³⁴ has discussed the kinetics of competitive processes when reactive fragments are produced in pairs, and his discussion* differs from the above in that the significant competition is considered to be between secondary recombination [reaction (10f), where the reactants are radicals from a specific dissociation which have re-encountered each other in the course of random diffusion] and initiation of polymerization [in this case, reaction (4c)]. More specifically, Noyes makes the following observations. (1) Molecules in the wall of the cage [cf. reaction (10c)] cannot compete with primary recombination [reaction (10b)] which takes place in a period that may be the order of a vibration; i.e., 10^{-13} sec.—except when the mole fraction of monomer is near unity. Comparatively, secondary recombination would be expected to occur in a maximum time of about 10^{-9} sec. (2) If $k_{i1} [M] \gg k_5 [SO_4^{\cdot-}]$, and the monomer is relatively unreactive compared to a radical-radical reaction, a limiting initiation efficiency, independent of monomer concentration, is attained, where the monomer molecules catch all radicals that escape primary and secondary recombination. To increase this efficiency, reaction of monomer with radical must compete with secondary recombination, and to do so, k_{i1} must be at least 10^7 l./mole-sec. At very large values of k_{i1} , this competition may be effective at monomer concentrations on the order of $0.01M$. (3) The fraction of radicals reacting with monomer that would otherwise have undergone secondary recombination—that is, the increase in efficiency of initiation—is, to a first approximation (with the primary assumption being that the probability a radical will react with monomer in a given time interval is not dependent on the time since the formation of the radical) given by

$$K_1 a [M]^{1/2}$$

Hence, the total rate of initiation is given by

$$R_i = K_0 + K_1 a [M]^{1/2} \quad (14)$$

where K_0 , K_1 , and a are constants, the value of K_1 being determined mainly by the magnitude of k_{i1} in reaction (4c). The parameter a , which defines the rate of increase of the enhanced initiation, depends on the frequency of diffusive displacements in the medium and, hence, is related to the molecular parameters describing diffusive motion.³²⁻³⁴

With the rate of initiation given by eq. (14), the rate of polymerization is

$$R_p = (k_p/k_t^{1/2})(K_0 + K_1 a [M]^{1/2})^{1/2} [M] \quad (15)$$

* The authors are grateful to the referee for calling their attention to this work.

and this defines an exponential dependency on monomer concentration between 1.00 and 1.25. If $K_{1a} \gg K_0$, $R_p \propto M^{1.25}$, which is the experimental result here.

Rearranging eq. (15) and using the data of Table II and Figure 3, one finds that a plot of $R_{p0}^2/[M]_0^2$ versus $[M]_0^{0.5}$ is fairly linear, although it does show more scatter than Figure 8. The data are, however, too coarse to yield a meaningful figure for the ratio of K_{1a} to K_0 .

Comparison of Cage-Effect and Complex Theories

The fact that four conceptually different approaches lead to the same kinetic conclusion is an unsatisfactory state of affairs, although not particularly unusual. The complex theory has generally been rejected for two reasons.^{26,30} Although K_c experimentally increases with temperature, the negative entropy change usually accompanying complex formation would predict the opposite; and efforts to detect the existence of a complex through melting point-composition relationships or by spectroscopic examination have been inconclusive.

The cage-effect theory has found considerably more support, although it has its critics also.^{28,30} In the present work, consideration of the primary dissociative process indicates that the cage-effect is energetically more nearly equivalent to the conventional mechanism, for which there is experimental confirmation. Formation of a complex between monomer and persulfate should alter measurably the activation energy. Inasmuch as the calculation made above demands almost exact correspondence to the activation energy for persulfate decomposition, there is substantial support for the hypothesis of cage formation. However, application of the cage-effect hypothesis to persulfate decomposition in the absence of monomer can be interpreted to be incompatible with application to the polymerization; the point is not clear.

Resolution of some of the theoretical difficulties experienced here will, perhaps, be obtained with studies with other simple, peroxidic initiation systems.

References

1. J. P. Riggs, Ph.D. Thesis, Cornell University, 1964.
2. J. P. Riggs and F. Rodriguez, *J. Polymer Sci. A-1*, **5**, 3167 (1967).
3. *Acrylamide*, Technical Bulletin, American Cyanamid Company, 1956.
4. R. Schulz, G. Renner, A. Henglein, and W. Kern, *Makromol. Chem.*, **12**, 20 (1954).
5. A. Henglein, *Makromol. Chem.*, **14**, 15, 128 (1954).
6. I. A. Arbuzova, V. N. Efremova, and I. K. Ulezlo, *Dokl. Akad. Nauk SSSR*, **112**, 645 (1957).
7. G. K. Oster, G. Oster, and G. Prati, *J. Am. Chem. Soc.*, **79**, 595 (1957).
8. E. Collinson, F. S. Dainton, and G. S. McNaughton, *Trans. Faraday Soc.*, **53**, 476, 489 (1957).
9. D. S. Dainton and M. Tordoff, *Trans. Faraday Soc.*, **53**, 499, 666 (1959).

10. T. J. Suen, Y. Sen, and J. V. Lockwood, *J. Polymer Sci.*, **31**, 481 (1958).
11. F. Rodriguez and R. D. Givey, *J. Polymer Sci.*, **55**, 713 (1961).
12. G. Mino, S. Kaizerman, and E. Rasmussen, *J. Polymer Sci.*, **38**, 393 (1959).
13. G. Talamini, A. Turolia, and E. Vianello, *Chim. Ind. (Milan)*, **45**, 335 (1953).
14. I. M. Kolthoff and I. K. Miller, *J. Am. Chem. Soc.*, **73**, 3055 (1951).
15. D. J. Currie, F. S. Dainton, and W. S. Watt, *Polymer*, **6**, 451 (1965).
16. L. Green and O. Masson, *J. Chem. Soc.*, **97**, 2083 (1910).
17. R. L. Eager and C. A. Winkler, *Can. J. Res.*, **26**, 527 (1948).
18. P. D. Bartlett and J. D. Cotman, Jr., *J. Am. Chem. Soc.*, **71**, 1419 (1949).
19. E. Collinson, F. S. Dainton, and G. S. McNaughton, *Trans. Faraday Soc.*, **53**, 357 (1957).
20. F. S. Dainton and T. J. Hardwick, *Trans. Faraday Soc.*, **53**, 333 (1957).
21. K. Chambers, E. Collinson, F. S. Dainton, and W. Seddon, *Chem. Commun. (London)*, No. **15**, 498 (1966).
22. G. V. Schulz and E. Husemann, *J. Phys. Chem.*, **B39**, 246 (1938).
23. M. S. Matheson, *J. Chem. Phys.*, **13**, 584 (1945).
24. G. M. Burnett and L. D. Loan, *Trans. Faraday Soc.*, **51**, 214, 219 (1955).
25. P. W. Allen, F. M. Merrett, and J. Scanlan, *Trans. Faraday Soc.*, **51**, 95 (1955).
26. C. H. Bamford, W. G. Barb, A. D. Jenkins, and P. F. Onyon, *The Kinetics of Vinyl Polymerization by Radical Mechanisms*, Butterworths, London, 1958.
27. I. M. Kolthoff, A. I. Medalia, and H. P. Raen, *J. Am. Chem. Soc.*, **73**, 1733 (1951).
28. P. J. Flory, *Principles of Polymer Chemistry*, Cornell Univ. Press, Ithaca, N. Y., 1955.
29. J. C. Bevington, *Radical Polymerization*, Academic Press, New York, 1961.
30. A. D. Jenkins, *J. Polymer Sci.*, **29**, 245 (1958).
31. R. M. Noyes, *J. Am. Chem. Soc.*, **77**, 2042 (1955).
32. R. M. Noyes, in *Progress in Reaction Kinetics*, G. Porter, Ed., Pergamon Press, New York, 1961, pp. 129-160.
33. R. M. Noyes, *J. Chem. Phys.*, **22**, 1349 (1954).
34. R. M. Noyes, *J. Am. Chem. Soc.*, **78**, 5486 (1956).

Résumé

Une technique dilatométrique a été utilisée pour obtenir des résultats conversion-temps pour la polymérisation de l'acrylamide initiée au persulfate de potassium dans l'eau. Les résultats sont résumés par une expression de vitesse empirique: $-d[M_1]/dt = R_p = k_{1,25} (K_2S_2O_8)^{0,5} [M_1]^{1,25}$ et $k_{1,25} = 1,70 \times 10^{11} \exp \{-16,900/RT\}$ en litre^{0,75}/mol^{+0,75} minute. La concentration en persulfate variait de $9,5 \times 10^{-4}$ à $5,2 \times 10^{-2}$ mole/litre, et la concentration initiale en monomère, $[M_1]$, était variée de 0,05 à 0,4 mole/litre. Le domaine de température s'étendait de 30 à 50°C. L'analyse de la cinétique et des données énergétiques de la polymérisation est favorable à la théorie de l'effet de cage, plutôt que la théorie de formation d'un complexe en vue d'expliquer l'ordre par rapport au monomère.

Zusammenfassung

Um den Zusammenhang zwischen Zeit und Umsatz bei der durch Kaliumpersulfat gestarteten Polymerisation von Acrylamid in Wasser zu ermitteln, wurde eine Dilatomerteknik angewandt. Die Ergebnisse lassen sich durch die empirische Gleichung für die Geschwindigkeit $-d[M]_1/dt = R_p = k_{1,25} K_2S_2O_8^{0,5} [M]_1^{1,25}$ und $k_{1,25} = 1,70 \cdot 10^{11} \exp \{-16,900/RT\}$ in Liter^{0,75} Mol^{-0,75} min⁻¹. Die Persulfatkonzentration wurde im Bereich von $9,5 \cdot 10^{-4}$ bis $5,2 \cdot 10^{-2}$ Mol/Liter variiert, während die Ausgangskonzentration an Monomerem, $[M]_1$, zwischen 0,05 und 0,4 Mol/Liter verändert wurde. Die

Temperaturen lagen zwischen 30 und 50°C. Die kinetische und energetische Analyse der Polymerisation spricht im Hinblick auf die Erklärung der Reaktionsordnung bezüglich des Monomeren eher für eine Käfigeffekt-Theorie als für eine Komplexbildungstheorie.

Received January 18, 1967

Revised May 22, 1967

Prod. No. 5450A

Polymerization of Acrylamide Initiated by the Persulfate-Thiosulfate Redox Couple

J. P. RIGGS* and F. RODRIGUEZ,
*Geer Laboratory for Rubber and Plastics,
School of Chemical Engineering,
Cornell University, Ithaca, New York 14850*

Synopsis

Conversion-time data were obtained for the polymerization of acrylamide initiated by the redox couple persulfate-thiosulfate by using a dilatometer. A plot of initial rate as a function of thiosulfate concentration shows a well-defined maximum and three distinct regions of behavior. In each region the shape of the conversion-time curves demonstrates the differences in apparent order with respect to monomer arising from changes in initiator concentration during an individual run. A reaction mechanism is proposed to explain the results, and a limiting form of the rate expression is derived for each of the three regions. The ranges of concentration studied are: persulfate, 9.5×10^{-4} – $4.7 \times 10^{-2}M$; thiosulfate, 2×10^{-5} – $2 \times 10^{-2}M$; initial monomer, 0.05–1.0M; and temperature, 30–50°C. Within these ranges the initial rate shows a half-order dependence on persulfate and a first-order dependence on initial monomer concentration.

The persulfate-thiosulfate redox couple has been investigated alone^{1,2} and as an initiation system for free-radical polymerizations; for example, it has been used in the polymerization of acrylonitrile,³ methacrylamide,⁴ and methyl acrylate.⁵ This would seem to make it a good candidate for studying acrylamide polymerization, with the objective of reconciling past kinetic studies on this monomer.^{6–10} However, the results of the present study (1) indicate that the earlier studies with the persulfate-thiosulfate system are not directly applicable in interpreting the mechanism of the acrylamide polymerization; (2) raise additional questions regarding the mechanism of the reaction between persulfate and thiosulfate; and (3) demonstrate a number of effects resulting from the generation of several transient initiator species, and from the consumption of the persulfate and thiosulfate ions throughout the course of the polymerization.

EXPERIMENTAL

Deaerated solutions were reacted in a stirred bulb and the decrease in the volume of the system was followed by measuring the height of liquid

* Present address: Celanese Corp. Research Center, Summit, N. J.

in an attached capillary. The materials and dilatometric equipment previously described¹⁰ were used. The thiosulfate solutions were de-aerated in a separate unit and added to the dilatometer bulb before monomer and persulfate solutions were added. This was done because small weights of polymer were produced in the deaeration unit when the thiosulfate and monomer were mixed and deaerated together.

RESULTS AND DISCUSSION

Effect of Thiosulfate

The dependence of initial rate on thiosulfate concentration (Fig. 1; for tabulations of all data, see ref. 11) shows three distinct regions of behavior. Runs covering the concentration range 8.20×10^{-5} – $9.96 \times 10^{-3}M$ were made with random use of the same batch of deionized solvent and two different preparations of recrystallized monomer. The remainder of the runs were made with the use of acrylamide from a third recrystallization and a second batch of deionized water. Consequently, the influence of adventitious impurities in the reagents would appear to be negligible.

The dominant maximum in the curve, occurring at a thiosulfate concentration in the vicinity of $10^{-4}M$, is well defined, and the inverse half-order dependence in the middle region also seems well established. The behavior at the two extremes of the curve are not as well defined. At the low-concentration end, the data indicate a slope greater than one-half, but it was difficult to obtain initial rates in this region. It is probable, as discussed below, that there is sufficient experimental uncertainty in the point at the lowest concentration to suspect that the actual depen-

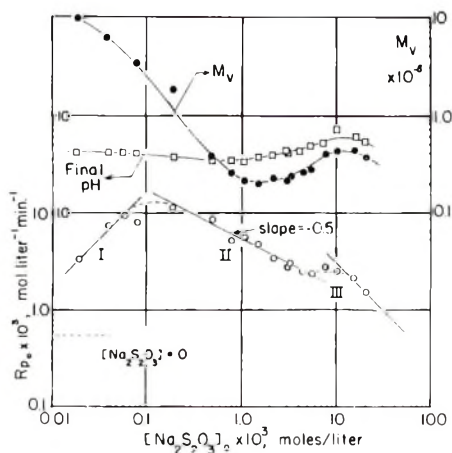


Fig. 1. Initial rate of polymerization, R_{p0} , viscosity-average molecular weight, \bar{M}_v , and final pH as a function of initial thiosulfate concentration, $[Na_2S_2O_3]_0$. Initial monomer concentration $[M_1]_0 = 0.238M$; initial persulfate concentration $[K_2S_2O_8]_0 = 9.54 \times 10^{-4}M$; $T = 30^\circ C$.

dence may be half-order, which is theoretically more tenable. A detailed analysis of the kinetic and molecular weight effects obtaining at a high ratio of persulfate to thiosulfate will be made in a subsequent publication. Emphasis here will be on the second and third regions.

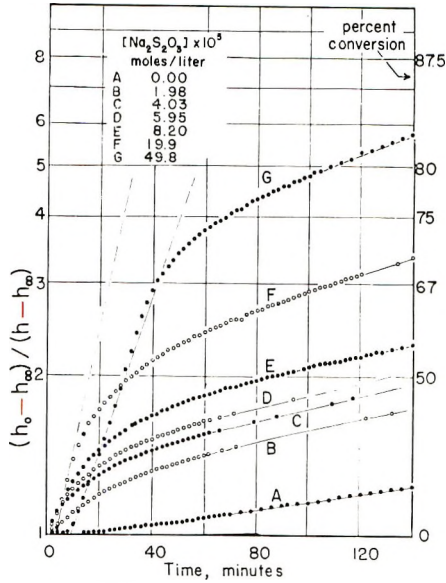


Fig. 2. Course of polymerization in terms of dilatometer reading h at various initial thiosulfate concentrations corresponding to the first and part of the second regions of Fig. 1.

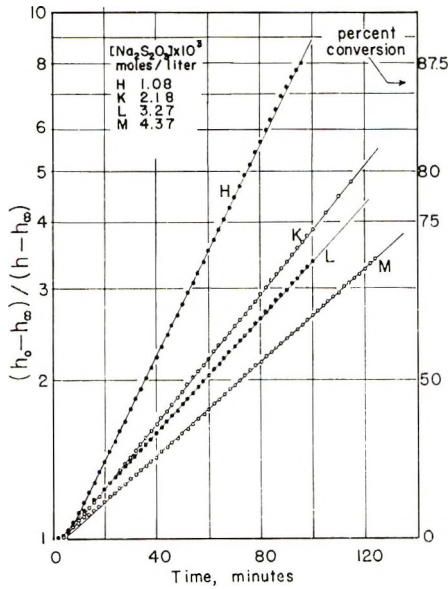


Fig. 3. Course of polymerization in terms of dilatometer reading at various initial thiosulfate concentrations corresponding to region II of Fig. 1.

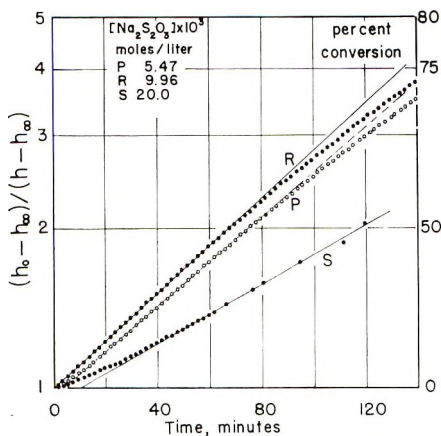


Fig. 4. Course of polymerization in terms of dilatometer reading at various initial thiosulfate concentrations corresponding to region III of Fig. 1.

At the high-concentration end, the rate appears to level off—approaching zero-order with respect to thiosulfate—and then decreases rapidly. Although not firmly established experimentally, mechanistic considerations developed below indicate the rate falls off in this area with slope less than $-1/2$.

Such behavior strongly suggests a chain process operative in the inorganic initiation sequence and, quite surprisingly, significant termination between inorganic species.

Representative “first-order” plots showing the course of the polymerization with time in these three regions are given in Figures 2–4, and a number of general observations can be made: The pronounced curvature of the data shown in Figure 2 is characteristic of the behavior when persulfate is present in large excess, and the latter portions of these plots approach in a regular manner the rate obtained in the absence of thiosulfate, given approximately by curve *A* (see the previous paper¹⁰). This curvature and the abrupt transition from a relatively high to a low, residual rate does, of course, indicate the rapid consumption of thiosulfate and, more fundamentally, a failure to maintain stationary-state conditions. The accelerating effect of thiosulfate on the rate is also very evident. Even at the lowest concentration used, with persulfate in excess by a factor of fifty, there is a sixfold increase in the initial rate, and a comparison of curves *B* and *A* shows this activation is enough to increase appreciably the fractional conversion at a given time.

Up to a point, increasing the concentration of thiosulfate increases the percentage conversion over which first-order kinetics are obeyed, and Figure 3 shows the excellent linear behavior—up to 70–80% conversion—that exists over the lower part of the middle region of Figure 1.

The data of Figure 4 correspond to initial rates at the high-concentration end of Figure 1, and there is a definite difference in the character of these

curves as compared to the previous plots. The rates described by the upper two curves, corresponding to initial rate data on each end of the zero-order region in Figure 1, fall off slowly with increasing conversion and can be approximately characterized as first-order over about 50% of the reaction. The lower curve describes the course of reaction at the highest concentration of thiosulfate used and, although linear in the range 20–50% conversion, possesses an unusually long initial retardation period.

There is a well-defined minimum in the average molecular weight (Fig. 1) and, in close correspondence to the kinetic data, a transition region showing a local maximum at the high-concentration end. The recurrence of this behavior at high thiosulfate concentrations contributes to the "realness" of this effect.

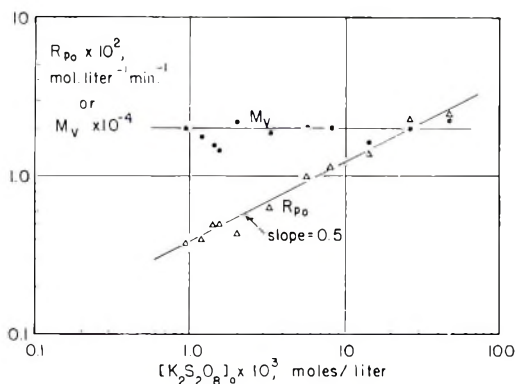


Fig. 5. Initial rate of polymerization and viscosity-average molecular weight as a function of initial persulfate concentration. $[M_1]_0 = 0.238M$; $[Na_2S_2O_3]_0 = 1.49 \times 10^{-3}M$; $T = 30^\circ C$.

Effect of Persulfate

Initial rates (Fig. 5) show a "normal" half-order dependence on persulfate. Conventionally, this is attributed to quadratic termination between polymer radicals, but this explanation is hardly consistent with the effects of thiosulfate observed here. As shown below, the effect of persulfate can be reconciled with the previous results on the basis of a quadratic termination between inorganic radicals.

The conversion-time data (Fig. 6) show features both unique to this series and similar to previous results. The curvature of the plots for the runs at the two lower concentrations (curves *A* and *B*) indicates the polymer radical concentration is steadily increasing with time. It is clear this behavior results from a decrease in thiosulfate concentration over the course of the polymerization, in confirmation of the previously noted inverse dependence on thiosulfate. Similar behavior is observed for the other two runs, and it is evident the conversion range over which this particular curvature prevails decreases with increasing persulfate

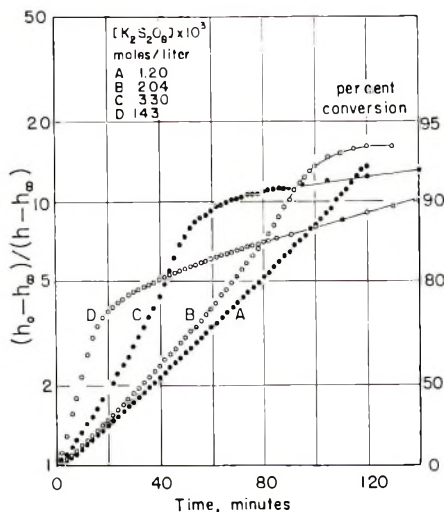


Fig. 6. Course of polymerization in terms of dilatometer reading at various initial persulfate concentrations corresponding to Fig. 5.

concentration. Analogous to the plots of Figure 2, the curves here show a transition to a much lower rate at progressively smaller conversions as the ratio of persulfate to thiosulfate—and, consequently, the rate of consumption of thiosulfate—is increased. This latter point is important, for it can be interpreted as evidence for the existence of the same rate-controlling initiation step in the first two regions of Figure 1.

The lack of any effect of persulfate on molecular weight is also shown in Figure 5. This is consistent with linear termination by thiosulfate as a dominant reaction.

Effect of Monomer

A first-order dependence of both initial rate and average molecular weight on initial monomer concentration is shown in Figure 7.

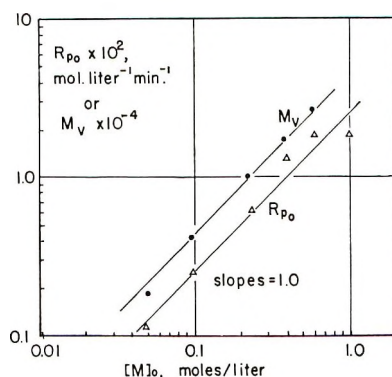


Fig. 7. Initial rate of polymerization and viscosity-average molecular weight as a function of initial monomer concentration, $[K_2S_2O_8]_0 = 2.83 \times 10^{-3}M$; $[Na_2S_2O_3]_0 = 2.98 \times 10^{-3}M$; $T = 30^\circ C$.

In reference to Figure 1, the thiosulfate concentration corresponds to the second region. However, the persulfate concentration is about twice as great, and, predictably, the course of the reaction (not shown here) has exactly the same features as curves *A* and *B* of Figure 6.

Effect of Temperature

For the second and third regions of Figure 1, lines *B* and *C* of Figure 8 demonstrate that the usual Arrhenius dependence is followed over the range 30–50°C. Slopes of these plots yield activation energies of 12.3 and 12.8 kcal./mole, respectively, and the fact that they are almost the same supports the conclusion that the primary process introducing radicals into the system is the same for the two regions, and that any competing reaction coming into dominance at high thiosulfate concentrations has

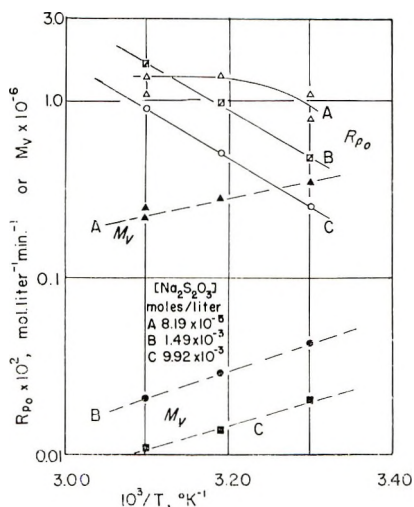


Fig. 8. Effect of temperature on the polymerization and the molecular weight at various initial thiosulfate concentrations corresponding to the three regions of Fig. 1.

a low energy requirement. Temperature dependence in the first region of Figure 1 was experimentally poorly defined, but does appear to have a lower activation energy.

The effect of temperature on molecular weight, also shown in Figure 8, is the normal behavior for an initiated polymerization. Note that, at all temperatures, the relative magnitudes of the molecular weights at the different thiosulfate concentrations follow Figure 1.

Effect of pH

Final pH data are shown as a function of thiosulfate concentration in Figure 1. The initial pH was 4.27 ± 0.08 , and comparison with the final values shows a decrease with time up to a thiosulfate concentration of about $3 \times 10^{-3}M$, after which there was an increase. The final pH

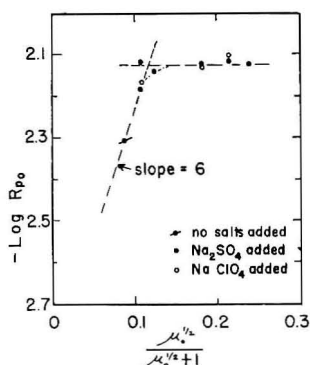


Fig. 9. Plot demonstrating the effect of initial ionic strength, μ_0 , on the rate of polymerization. $[\text{K}_2\text{S}_2\text{O}_8]_0 = 1.57 \times 10^{-3} M$; $[\text{Na}_2\text{S}_2\text{O}_3]_0 = 1.49 \times 10^{-3} M$; $[\text{M}_1]_0 = 0.238 M$; $T = 30^\circ\text{C}$.

also shows a maximum, paralleling the changes in molecular weight and kinetic behavior at this level of initiator concentration.

Sorum and Edwards² report that the rate of the persulfate-thiosulfate reaction does not depend on pH in the range 4–10.5, and Dainton et al.¹² have shown that although the propagation constant k_p and the termination constant k_t both diminish by about an order of magnitude as the pH is increased from 1 to 13; $k_p/k_t^{0.5}$ is almost constant. In this work, where linear termination by thiosulfate is important, some effect of pH on k_p would be felt, but it is not significant. This agrees with previous¹⁰ results.

Sorum and Edwards also examined the change of pH with time, and did find variation as the reaction progressed. Their results were similar to those obtained here and were attributed to side reactions which did not influence the main reaction to any extent.

Effect of Inert Salts

Sodium sulfate and sodium perchlorate were used as inert additives, and the results are shown in Figure 9, which is a plot testing the effect of ionic strength as predicted by the Brønsted-Bjerrum equation.¹³ The dashed line drawn in the low ionic strength region would be in agreement with the theoretical prediction of linear behavior. The positive effect corresponds to a reaction between ions of the same charge, but the large slope is difficult to interpret. Also, although deviation from linear behavior would be expected at the higher ionic strengths, the saturation effect found here is most anomalous.

In an early investigation,¹ a large, positive effect was observed with the addition of potassium chloride to the aqueous, persulfate-thiosulfate system. In a more recent study,² this effect has been explored in more detail: It was found that there was a large, positive, specific effect of cations, essentially no influence by anions of strong acids, and a general inhibitory effect by anions of weak acids. For example, monovalent cations affected the rate in the order $\text{K}^+ > \text{NH}_4^+ > \text{Na}^+ > \text{Li}^+$, and data

for chloride salts showed that the effect of potassium was about twice that of sodium.

Based on the limited amount of information obtained here, it is not valid to attempt a correction to the previous data. Also, the salt concentrations used in the above studies were quite a bit greater (on the order of $10^{-2}M$ for the reactions and $10^{-1}M$ for the inerts) than used for this work, and all the data to this point show a high degree of internal consistency.

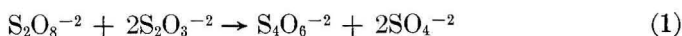
Analysis

Interpretation of these results has a twofold objective: first, it is necessary to reconcile this study with those of the persulfate,¹⁰ chlorate-sulfite,⁸ persulfate-metabisulfite,⁴ and the α - and γ -ray-initiated⁶ polymerizations; the second task is to obtain a reaction mechanism.

Apparent Order with Respect to Monomer. The five-halves order with respect to monomer reported for the chlorate-sulfite and persulfate-metabisulfite initiations was based on deviation from first-order results during the course of the polymerization. Initial rates showed a first-order dependence on initial monomer concentration. The latter behavior was also observed here, but examination of Figures 2, 3, 4, and 6 shows it is not possible to assign a fixed apparent order from the conversion-time data. There are three possibilities: results shown in Figure 2 (especially curves *B*, *C*, *D*, *E*, and *F*) could be linearized by a power on the monomer concentration greater than unity; the data of Figure 3 show first-order behavior; and the curves of Figure 6 (particularly *A*, *B*, and *C*) could be fitted to a straight line by using a kinetic order less than unity.

Since the monomer adsorption hypothesis of Suen et al.⁸ would make it impossible to obtain orders of unity or less, this work would seem to experimentally negate their postulate, and supports the conventional mechanism of initiation observed by Dainton.^{6,7} Fundamentally, the deviation from first-order kinetics must, then, result from a failure to maintain a constant concentration of growing polymer radicals, i.e., non-stationary state behavior, which, in turn, is simply a consequence of the change in the rate of initiation throughout the polymerization.

Previous Work on the Mechanism of the Persulfate-Thiosulfate Reaction. The stoichiometry is given by the reaction



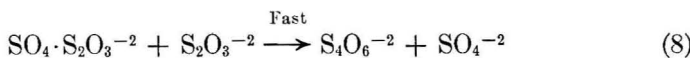
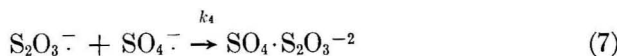
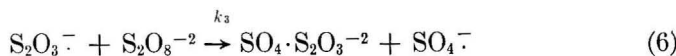
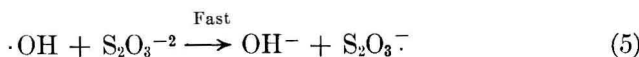
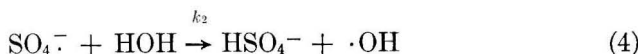
but the kinetic picture, especially in view of this work, is nebulous. Several workers^{1,2} report that the reaction is first-order with respect to persulfate and "almost, though not quite, independent of the thiosulfate concentration."

In the work of Sorum and Edwards,² it was reported that the rate of change of thiosulfate concentration with respect to its own concentration was zero-order, and that there was a first-order dependence on persulfate.

It was postulated that the disappearance of thiosulfate was governed by the relation

$$d[\text{S}_2\text{O}_3^{-2}]/dt = (k_a + k_b[\bar{X}])[\text{S}_2\text{O}_8^{-2}] \quad (2)$$

where k_b $[\bar{X}]$ is considered a dominant catalytic influence, arising from the formation of complex ions containing cations and thiosulfate. For the uncatalyzed reaction (k_a) the scheme of eqs. (3)–(8) was proposed.

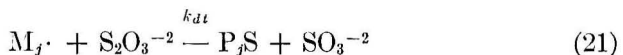
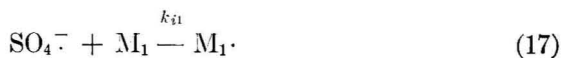
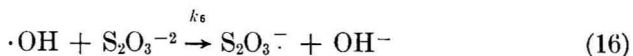
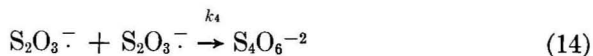
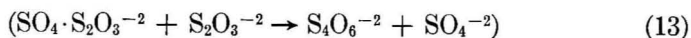
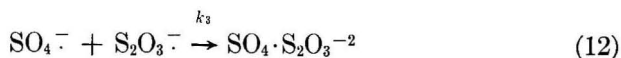
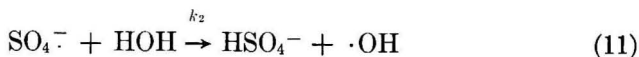


It is difficult to apply the above development to the acrylamide polymerization, since the results shown in Figures 1 and 2 are most simply interpreted by postulating a bimolecular reaction between persulfate and thiosulfate anions. It should also be noted that in the scheme presented for the uncatalyzed reaction, the induced decomposition of persulfate by reaction (6) can occur only after reaction (5). In the presence of monomer, especially acrylamide, which is highly reactive toward the hydroxyl radical,^{6,14} it is unlikely the latter would occur to any extent at low thiosulfate concentrations.

In an early study on the polymerization of acrylonitrile in aqueous solution, Morgan³ used the persulfate–thiosulfate system, both alone and catalyzed by copper. For the uncatalyzed polymerization, it was reported that the rate of polymerization was independent of thiosulfate concentration. This is hardly consistent with the data for the acrylamide polymerization, and the tentative mechanism proposed by Morgan is not applicable to this work.

Proposed Mechanism of the Persulfate–Thiosulfate-Initiated Polymerization of Acrylamide. The data of this study were obtained at generally lower concentrations than used previously, and over a much greater range of thiosulfate concentration. This latter point alone—in view of the very restrictive nature of the data in Figure 1 in terms of obtaining a satisfactory reaction scheme—justifies postulation of a mechanism.

The proposed mechanism is given in eqs. (9)–(21), along with rate equations (22)–(25) for the radical intermediates.



$$\begin{aligned} d[\text{SO}_4^{\cdot-}]/dt = & 2k_d[\text{S}_2\text{O}_8^{-2}] + k_1[\text{S}_2\text{O}_8^{-2}][\text{S}_2\text{O}_3^{-2}] \\ & - k_2[\text{SO}_4^{\cdot-}] - k_3[\text{SO}_4^{\cdot-}][\text{S}_2\text{O}_3^{\cdot-}] - k_{i1}[\text{SO}_4^{\cdot-}][\text{M}_1] \quad (22) \end{aligned}$$

$$d[\cdot\text{OH}]/dt = k_2[\text{SO}_4^{\cdot-}] - k_{i2}[\text{M}_1][\cdot\text{OH}] - k_6[\cdot\text{OH}][\text{S}_2\text{O}_3^{-2}] \quad (23)$$

$$\begin{aligned} d[\text{S}_2\text{O}_3^{\cdot-}]/dt = & k_1[\text{S}_2\text{O}_8^{-2}][\text{S}_2\text{O}_3^{-2}] - k_3[\text{SO}_4^{\cdot-}][\text{S}_2\text{O}_3^{\cdot-}] \\ & - k_4[\text{S}_2\text{O}_3^{\cdot-}]^2 + k_6[\cdot\text{OH}][\text{S}_2\text{O}_3^{-2}] \quad (24) \end{aligned}$$

$$\begin{aligned} d[\text{M} \cdot]/dt = & k_{i1}[\text{SO}_4^{\cdot-}][\text{M}_1] + k_{i2}[\cdot\text{OH}][\text{M}_1] \\ & - k_{dt}[\text{S}_2\text{O}_3^{-2}][\text{M} \cdot] - k_t[\text{M} \cdot]^2 \quad (25) \end{aligned}$$

The basic assumptions embodied in this scheme are that the thiosulfate radical-ion is unreactive in initiating polymerization and that, at sufficiently high concentrations of this radical, reaction (12) dominates in the competition with reaction (17), making the hydroxyl radical essentially the only initiating species. The first assumption is supported by some additional evidence, other than the kinetic prediction developed shortly. Bunn,⁴ in a (kinetically inconclusive) study of the initiation of methacrylamide polymerization by the persulfate-thiosulfate system, did

report that, by estimation of the amounts of tetrathionate produced, reaction between monomer and thiosulfate radical-ion did not occur to any extent. Also, in a study of endgroups produced in poly(methyl methacrylate) as a result of initiation by redox persulfate systems,⁵ it was found, in contrast to initiation by persulfate alone, that, with the exception of thiosulfate, hydroxyl endgroups were not present unless the concentration of the reducing sulfoxy compound was very low. In addition, the data showed that the ratio of hydrolyzable to nonhydrolyzable endgroups was the largest for the persulfate-thiosulfate couple.

In reference to Figure 1, it is evident that the various competing reactions proposed here do, in a qualitative manner, predict the observed behavior. At low thiosulfate concentrations, the increased rate (over that for the persulfate-initiated polymerization) stems from rapid production of sulfate radical-ions by reaction (10). As the initial thiosulfate concentration is increased, two changes occur: The concentration of thiosulfate radical-ion reaches a level where reactions (12) and (14) become important, and degradative termination by reaction (21) starts to compete effectively with the normal quadratic termination. These effects produce the maximum in the curve and explain the simultaneous decrease of the rate and molecular weight throughout part of the second region of Figure 1. Finally, the behavior at high thiosulfate concentrations can be understood by considering the competition introduced by reactions (15) and (16) [and, perhaps, (13)]. These steps would initially oppose each other in terms of their effect on the rate, since the consumption of thiosulfate in reaction (15) [and (13)] would increase the rate by competing with reaction (21), and the reaction with hydroxyl radical in (16) would decrease the concentration of the initiating species, thus decreasing the rate of reaction (18). With this reasoning, one would expect the rate to level out over a small range of thiosulfate concentration, and then decrease rather precipitously as the hydroxyl radical concentration is reduced. As shown in Figure 1, this is the observed behavior. Again, it is possible to cite some additional supporting evidence: Bacon¹⁵ and Morgan³ both report the addition of sodium bisulfite across the double bond of acrylonitrile, and in a later paper¹⁶ Bacon states a similar reaction occurs between acrylonitrile and sodium thiosulfate. Note also that reactions (15) and (16), especially the former, predict an increase in pH over the course of the reaction at high thiosulfate concentrations, which does agree with the results given in Figure 1. However, this pH effect has been attributed to a side reaction.² Finally, the reaction between thiosulfate and monomer would be expected to affect the final molecular weight, and the local maximum at the high concentration end of Figure 1 agrees with this prediction.

Rate Laws

In developing the quantitative rate laws obtaining with the above mechanism, there are three cases to consider, corresponding to the three

regions shown in Figure 1. The discussion here will be confined to the second and third regions which, as shown in Figures 3 and 4, can be treated by stationary-state techniques—especially the second. The kinetic and molecular weight effects attending the behavior shown in the first region will be considered in a subsequent publication.

For the cases discussed below, it is assumed that the thermal decomposition of persulfate [reaction (9)] is negligible, and that $k_4[\text{S}_2\text{O}_3^{\cdot-}] \gg k_3[\text{SO}_4^{\cdot-}]$. The resulting relations are obtained by setting equations (22)–(25) equal to zero.

Region II: In this region,

$$\begin{aligned} k_3[\text{S}_2\text{O}_3^{\cdot-}] &\gg k_2 + k_{t1}[\text{M}_1] \\ k_{t2}[\text{M}_1] &\gg k_6[\text{S}_2\text{O}_3^{-2}] \\ k_{dt}[\text{S}_2\text{O}_3^{-2}] &\gg k_t[\text{M}\cdot] \\ k_1[\text{S}_2\text{O}_8^{-2}] &\gg k_6[\cdot\text{OH}] \end{aligned}$$

With these assumptions,

$$R_{pII} = (k_p k_2 / k_3 k_{dt}) (k_1 k_4)^{1/2} ([\text{S}_2\text{O}_8^{-2}]^{1/2} / [\text{S}_2\text{O}_3^{-2}]^{1/2}) [\text{M}_1] \quad (26)$$

and, at 30°C.,

$$(k_p k_2 / k_3 k_{dt}) (k_1 k_4)^{1/2} = 2.2 \times 10^{-2} \pm 0.2 \text{ min.}^{-1} \quad (27)$$

If one approximates the activation energy for propagation E_p at 2.00 kcal./mole,¹⁷ the propagation rate coefficient, k_p is about 1.17×10^6 l./mole-min. at 30°C.⁷ This gives

$$(k_2 / k_3 k_{dt}) (k_1 k_4)^{1/2} = 1.9 \times 10^{-8} \text{ mole/l.} \quad (28)$$

This middle region is the most thoroughly investigated experimentally, and the rate equation exactly predicts the observed behavior (Figs. 1, 3, 5, and 7). The above mechanism also clarifies the difference in the shape of the curves in Figures 3 and 6. Increasing the thiosulfate concentration increases reactions (10) and (21) proportionately, while increasing the persulfate concentration increases the rate of consumption of thiosulfate by reaction (10) over the course of polymerization, and, hence, reduces the fraction of total thiosulfate consumed in the termination reaction.

Region III. The same assumptions apply here as for the second region, except that termination of hydroxyl radicals by thiosulfate, reaction (16), is considered significant, and with the possible exception of the relative magnitudes of $k_1[\text{S}_2\text{O}_8^{-2}]$ and $k_6[\cdot\text{OH}]$; however, it can be shown that the form of equation (16) is not altered if this restriction is relaxed. This results in

$$R_{pIII} = \frac{k_p k_2 k_{t2}}{k_3 k_{dt}} (k_1 k_4)^{1/2} \frac{[\text{S}_2\text{O}_8^{-2}]_0^{1/2} [\text{M}_1]_0^2}{(k_{t2} [\text{M}_1]_0 + k_6 [\text{S}_2\text{O}_3^{-2}]_0) [\text{S}_2\text{O}_3^{-2}]_0^{1/2}} \quad (29)$$

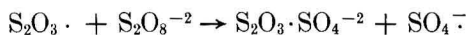
The important points to notice about this relation are (1) the strong, inverse dependence on thiosulfate concentration and (2) in view of the fact that reactions (16) and (18) are of a free-radical nature, the activation

energies obtained in the second and third regions would be expected to be nearly equal, as is shown in Figure 8.

CONCLUSIONS

This work demonstrates a wide range of effects on both kinetic effects and molecular weight dependence, resulting from the generation of different initiator species, the relative reactivity of these species, and from the change in concentration of the primary inorganic ions throughout the polymerization. It does seem that the apparent order with respect to monomer observed in two previous investigations^{8,9} is a consequence of this latter effect, and such an interpretation reconciles the results of other studies⁶⁻¹⁰ and this work.

It can also be stated that the proposed mechanism quite satisfactorily describes the experimental results, but, in view of the previous work with the persulfate-thiosulfate system, it cannot be said the mechanism of the inorganic interaction is understood. In this respect, it should be noted that consideration of a possible effect of trace impurities of copper, cited in other studies,¹⁻³ does not seem relevant here, since it has been shown¹⁸ that, assuming cuprous ions are not involved in a termination reaction, any catalysis attributable to an oxidation-reduction cycle involving cupric and cuprous oxidation states will occur only if a reaction of the type



takes place. The mechanism proposed here does not require this step.

References

1. C. V. King and O. F. Steinbach, *J. Am. Chem. Soc.*, **52**, 4779 (1930).
2. C. H. Sorum and J. O. Edwards, *J. Am. Chem. Soc.*, **74**, 1204 (1952).
3. L. B. Morgan, *Trans. Faraday Soc.*, **42**, 169 (1946).
4. D. Bunn, *Trans. Faraday Soc.*, **42**, 190 (1946).
5. P. Ghosh, S. C. Chadha, and S. R. Palit, *J. Polymer Sci. A*, **2**, 4441 (1964).
6. E. Collinson, F. S. Dainton, and G. S. McNaughton, *Trans. Faraday Soc.*, **53**, 357, 476, 489 (1957).
7. F. S. Dainton and M. Tordoff, *Trans. Faraday Soc.*, **53**, 499, 666 (1959).
8. T. J. Suen, Yun Sen, and J. V. Lockwood, *J. Polymer Sci.*, **31**, 481 (1958).
9. F. Rodriguez and R. D. Givey, *J. Polymer Sci.*, **55**, 713 (1961).
10. J. P. Riggs and F. Rodriguez, *J. Polymer Sci. A-1*, **5**, 3151 (1967).
11. J. P. Riggs, Ph.D. thesis, Cornell Univ., Ithaca, N. Y., 1964.
12. D. J. Currie, F. S. Dainton, and W. S. Watt, *Polymer*, **6**, 451 (1965).
13. A. A. Frost and R. G. Pearson, *Kinetics and Mechanism*, Wiley, New York, 1953.
14. F. S. Dainton and T. J. Hardwick, *Trans. Faraday Soc.*, **53**, 333 (1957).
15. R. G. R. Bacon, *Trans. Faraday Soc.*, **42**, 140 (1946).
16. R. G. R. Bacon, *Quart. Rev.*, **9**, 287 (1955).
17. F. S. Dainton and W. D. Sisley, *Trans. Faraday Soc.*, **59**, 1369 (1963).
18. W. K. Wilmarth and A. Haim, in *Peroxide Reaction Mechanisms*, J. O. Edwards, Ed., Interscience, New York, 1962.

Résumé

Les données conversion-temps ont été obtenues pour la polymérisation de l'acrylamide initié par un système rédox persulfate-thiosulfate; elles ont été obtenues par dilatométrie. Un diagramme de la vitesse initiale en fonction de la concentration en thiosulfate montre un maximum bien défini et trois régions de comportement distinctes. Dans chaque région, la forme des courbes conversion-temps montre les différences d'ordre apparent par rapport au monomère, résultant du changement de la concentration en initiateur au cours de chaque essai individuel. Un mécanisme de réaction est proposé en vue d'expliquer les résultats et une forme limite de l'expression de vitesse est dérivée pour chacune des trois régions. Le domaine de concentration (en mole/litre) étudié était: le persulfate, 9.5×10^{-4} à 4.7×10^{-2} ; thiosulfate, 2×10^{-5} à 2×10^{-2} ; la concentration en monomère initial de 0.05 à 1.0, tandis que la température allait de 30 à 50°C. Endéans ces domaines, la vitesse initiale montrait une dépendance en persulfate de l'ordre de un demi et une dépendance directe de premier-ordre en fonction de la concentration en monomère initial.

Zusammenfassung

Für die durch das Redox-System Persulfat-Thiosulfat gestartete Polymerisation wurden mittels eines Dilatometers die Zeit-Umsatz-Kurven aufgenommen. Eine Auftragung der Anfangsgeschwindigkeit als Funktion der Thiosulfatkonzentration zeigt ein gutausgebildetes Maximum und drei getrennte Verhaltensbereiche. In jedem Bereich veranschaulicht die Gestalt der Zeit-Umsatz-Kurve die Unterschiede in der scheinbaren Reaktionsordnung bezüglich des Monomeren, die sich aus den Änderungen der Starterkonzentration während jedes einzelnen Versuchs ergeben. Zur Erklärung der Resultate wird eine Reaktions-mechanismus vorgeschlagen und ausserdem eine Grenzform der Geschwindigkeitsausdrücke für jeden der drei Bereiche abgeleitet. Die untersuchten Konzentrationen (Mol/Liter) lagen in folgenden Bereichen: Persulfat $9.5 \cdot 10^{-4}$ bis $4.7 \cdot 10^{-2}$; Thiosulfat $2 \cdot 10^{-5}$ bis $2 \cdot 10^{-2}$; Anfangsmonomerkonzentration 0,05 bis 1,0; die Temperatur lag zwischen 30 und 50°C. Innerhalb dieser Bereiche zeigt die Anfangsgeschwindigkeit eine Wurzelabhängigkeit von der Persulfatkonzentration und eine Abhängigkeit erster Ordnung von der Anfangsmonomerkonzentration.

Received January 18, 1967

Revised May 22, 1967

Prod. No. 5451A

A Redox-Initiated Xylan-Poly(sodium Acrylate) Graft Copolymer

JOHN A. CHURCH, *Princeton Laboratory, American Can Company,
Princeton, New Jersey 08540*

Synopsis

An aspen 4-*O*-methylglucuronoxylan was grafted with poly(sodium acrylate) (PSA) in 3.4*N* NaOH at 25–30°C. with the use of a persulfate-thiosulfate redox initiator system. The formation of a true graft copolymer was indicated by fractional precipitation and light-scattering studies, physical mixtures of the two pure polymers being used as references. A grafted fraction was isolated, containing no ungrafted xylan but possibly some PSA homopolymer, which contained 96.5% PSA and 3.5% xylan, or an average of 3.2 PSA chains of \bar{M}_n approximately 90,500 per xylan chain of \bar{M}_n approximately 10,500.

INTRODUCTION

The 4-*O*-methylglucuronoxylan readily obtained from temperate-zone hardwoods¹ is almost unexplored as a substrate for graft copolymerization. Recently "living" polystyrene was coupled to a permethylated aspen xylan through the esterified 4-*O*-methylglucuronic acid group in tetrahydrofuran;² however, an unmodified (albeit deacetylated) xylan of this type has apparently not been used as the host polymer in a graft copolymer. Such a substrate may also serve, with obvious limitations, as a soluble polymeric model for cellulose grafting reactions.

In the present work, an initiator-monomer combination was sought which would be soluble in an alkaline xylan solution at 25°C. and in which would be generated radicals capable of abstracting hydrogen atoms from carbohydrates. The ammonium persulfate-sodium thiosulfate redox couple³ and acrylic acid (as acrylate ion in NaOH solution) met these requirements. At appropriate concentrations, clear deoxygenated solutions containing all of these compounds underwent essentially quantitative polymerization in 35 min. at 25–30°C. Turbidity developed during polymerization except at xylan concentrations of less than 1%.

The isolated products (amorphous, white, hygroscopic materials) were characterized by fractional precipitation and light-scattering studies. The results were compared with the results of identical studies on physical mixtures of the catalyst-treated xylan and poly(sodium acrylate) (PSA) separately prepared and also obtained by hydrolysis of the suspected graft

copolymer. The observed differences supported the hypothesis that a true graft copolymer was synthesized, although the bulk of the xylan remained ungrafted.

EXPERIMENTAL

Preparation of Xylan

The xylan was extracted with 10% KOH from a neutral sulfite semi-chemical aspen pulp. It was bleached with acidified sodium chlorite and deashed with dilute HCl. Its characteristics and those of the catalyst-treated xylan used in the reference physical mixtures, all on an oven-dry basis, are listed in Table I.

TABLE I
Xylan Characteristics

Material	$[\eta]$, dl./g. ^a	\bar{P}_w ^b	\bar{M}_w ^c	$[\alpha]_D^{25}$ ^d	Ash, %	Xylose residues, σ ^e
Original xylan (H)	0.64	120	17,400	-86.2°	0.5	15.7
Catalyst- treated xylan (Na)	0.47 ^f	92	13,600	-81.2° (-82.0°) ^g	2.6	13.1

^a Intrinsic viscosity in 0.5*M* cuene at 25.00°C. with Craig-Henderson viscometer.⁴

^b Main-chain degree of polymerization, from relationship of LeBel and Goring.⁵

^c Molecular weight as Na salt.

^d Specific rotation in 5.0% NaOH.

^e Xylose residues per 4-*O*-methylglucuronosyl xylose unit.⁶

^f Inappreciably different in acid form.

^g Estimated for acid form.

Grafting Procedure

Although many grafting runs were made, the results of only one are reported here. Other reaction conditions also yielded graft copolymers.

Eastman acrylic acid and reagent grade ammonium persulfate, sodium thiosulfate pentahydrate, and sodium hydroxide were employed in making up the grafting solutions. The formulation giving the product reported here contained 80% distilled water, 14% NaOH, 4% acrylic acid, and 2% xylan (including water added with the catalyst but neglecting the catalyst itself). Both the xylan and the acrylic acid were present as their anions in the strongly alkaline medium (3.4*N* in OH⁻ after neutralization of the acid). The mixture was deoxygenated with nitrogen in a polymerization bottle equipped with a magnetic stirrer before the freshly mixed aqueous catalyst mixture was syringed in. The amount of ammonium persulfate was 1.35% of the monomer weight; a 2:1 mole ratio of thiosulfate to persulfate was used.³ The total weight of the mixture was 125.2 g.

The mixture became turbid within 1 min., and its viscosity increased rapidly. A temperature rise of about 5°C. occurred. After 35 min., when no further temperature rise or viscosity increase was noted, the products were poured slowly into excess methanol agitated moderately in a 1-gal. Waring Blendor. The finely divided, hygroscopic white precipitate was washed thoroughly with methanol and ether and dried *in vacuo* at 50°C.

Characterization of Products

Overall Composition. The product (8.15 g.; 90.0% of theory) exhibited $[\alpha]_D^{24} = -23.4^\circ$ (*c*, 1 in 5% NaOH), corresponding to a xylan content (Na form) of 28.8% (assuming a specific rotation of -81.2° for the xylan after contact with the catalyst; see Table I). The ash content by direct ignition was 23.8%, corresponding to a xylan content (Na form) of 29.0% (assuming the theoretical Na₂O content of 1.5% for the xylan and 32.9% for PSA, which are close to the figures obtained by ashing the pure polymers). Accordingly, the xylan content of the product was taken to be 28.9%. The expected xylan content was 27.8% if 100% polymerization had occurred.

Preparation of Physical Mixtures. The xylan used in the physical mixtures was obtained by subjecting the original xylan to the grafting conditions, substituting an equivalent amount of acetic acid for the acrylic acid. The characteristics of the recovered product are given in Table I. Such a treatment, often neglected in comparisons of suspected graft copolymers with physical mixtures, should make the comparison more valid.

The PSA used in the physical mixtures was separately prepared under conditions similar to the grafting reaction, except of course omitting the xylan. A range of products with varying molecular weights was prepared by varying the catalyst concentration and thiosulfate:persulfate ratio. In addition, PSA was obtained by hydrolyzing the suspected graft in refluxing 1*N* sulfuric acid and recovering the residue. The characteristics of some of these polymers are given in Table II.

TABLE II
Poly(sodium Acrylate) Characteristics

Polymer	$[\eta]$, dl./g. ^a	\bar{M}_w ^b	\bar{M}_n ^c	Ash, %
PSA-1	1.09	390,000	—	34.6
PSA-2	0.89	260,000	136,000	32.3
PSA-GP ^d	0.71	173,000	—	29.5

^a Intrinsic viscosity in 2.0*N* NaOH at 25.00°C. with Craig-Henderson viscometer.⁴

^b From relationship of Sakamoto.⁷

^c Determined in 0.5*N* NaCl with Mechrolab high-speed membrane osmometer.

^d Obtained by hydrolysis of suspected graft.

Fractional Precipitations. Exactly 1.000 g. of either the suspected graft copolymer or the physical mixture (0.289 g. catalyst-treated xylan, 0.711 g. PSA-2) was suspended in 100 ml. 0.398*N* NaOH under nitrogen and stirred magnetically several hours. In each case, a few milligrams of residue was removed by centrifugation and the slightly hazy supernatant transferred to a 250 ml. flask with a ground stopper which was clamped in a water bath thermostatted at $25.0 \pm 0.1^\circ\text{C}$. Absolute ethanol was slowly added dropwise from a microburet to the magnetically stirred solution. After turbidity appeared, the suspension was stirred 15 min. and then centrifuged 5 min. at 1000*g*. The clear supernatant was quantitatively syringed off and returned to the precipitation flask. The residue was coagulated with methanol, filtered, washed with methanol and ether, and dried *in vacuo* at 50°C . Fifteen fractions were collected in each case. Each fraction was weighed and its specific rotation determined in 5% NaOH. Overall polymer recovery was 78% for the suspected graft and 80% for the physical mixture; in both cases the percentage PSA recovered was somewhat higher than the percentage xylan recovered.

Light-Scattering Studies. Scattering ratios ($90^\circ-0^\circ$) were determined with a Brice-Phoenix Series 2000 universal light-scattering photometer with the use of the Hg green line (5461 Å.). The solutions were made up by placing 0.0100 g. of either the dry suspected graft copolymer or the dry physical mixture (0.0029 g. catalyst-treated xylan, 0.0071 g. PSA) in a 100 ml. volumetric flask, diluting to the mark with 0.398*N* NaOH, adding a micro stirring bar, flushing with nitrogen, and stirring magnetically 5 hr. at 25°C . Complete solution apparently took place. The solutions were freed of dust by filtration through sintered glass, and a 17.0 ml. aliquot was transferred into a T-101 cell and titrated with absolute ethanol. The cell was thermostatted at $25.0 \pm 0.1^\circ\text{C}$. and the solution stirred magnetically at constant rate with a micro bar. A period of 2 min. was required to add the first 3.0 ml. of ethanol; at this point ethanol addition was halted and the scattering ratio was then determined at approximately 0.1-hr. intervals. After 1.03 hr., another 1.0 ml. ethanol was added and readings were again taken at intervals for another hour. Extensive changes, especially for the physical mixtures, were observed as the coacervate droplets coagulated.

Scattering ratios for the 0.398*N* NaOH plus various amounts of ethanol were also determined. Very little change was observed in the range of 0-6 ml. ethanol addition to 17.0 ml. NaOH solution; these solutions also remained visually clear. Neither the presence of the micro bar nor variations in total solution volume (above 19.0 ml.) caused significant changes in scattering ratios.

RESULTS AND DISCUSSION

Fractional Precipitations

The fractionations of both the suspected graft and the physical mixture are subject to minor uncertainties due to the possibility of fractionating the

xylan according to xylose:uronic acid ratio as well as according to molecular weight.¹ This is manifested by variations in specific rotation of even a pure xylan fraction, those fractions having a higher xylose: uronic acid ratio exhibiting a more negative rotation. It was assumed that the xylan in the suspected graft had the same average specific rotation as the xylan which was separately subjected to catalyst treatment (-81.2° as the Na salt in

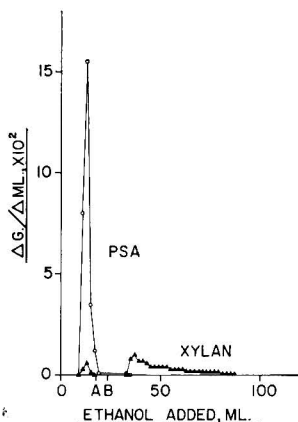


Fig. 1. Differential yield distribution curves for fractionation of suspected graft copolymer.

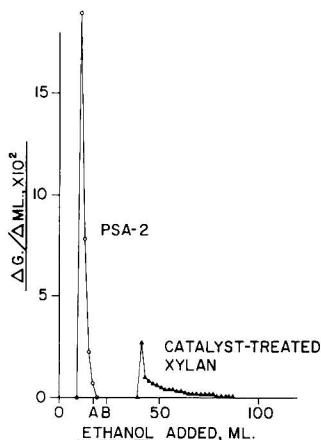


Fig. 2. Differential yield distribution curves for fractionation of physical mixture.

5% NaOH). The compositions of fractions exhibiting only slight rotations were calculated on this basis; fractions exhibiting rotations within a few degrees of the above value were assumed to consist entirely of xylan, as this only occurred far from the region of PSA precipitation.

The results of the fractionations were plotted as integral yield curves (not shown) which were graphically differentiated at 2-ml. intervals to give differential yield curves (Δ g./ Δ ml. ethanol; Figs. 1 and 2). It is

evident that excellent resolution of the two polymers in the physical mixture was achieved. However, with the suspected graft, the PSA fractions contained significant amounts of xylan, which is good evidence for the existence of a true graft copolymer.

† The total amount of xylan associated with the PSA in the case of the suspected graft (i.e., the total xylan precipitated up to the 35-ml. ethanol addition level) was 0.0214 g., or 7.4% of the total xylan present in the material. The amount of xylan recovered when only 16 ml. of ethanol had been added to the solution was 0.0190 g. (divided between seven fractions up to this point). For comparison, one large fraction was precipitated from a fresh solution of the suspected graft by the addition of 16 ml. ethanol. The amount of xylan recovered in admixture with PSA was 0.0184 g., in excellent agreement with the above result. With the physical mixture, the amount of xylan recovered at this point (and at the 35 ml. point) was nil, even when one large fraction of PSA was precipitated with 16 ml. ethanol from a fresh solution of the physical mixture in the same fashion as the suspected graft. Therefore, coprecipitation of ungrafted xylan was not a complicating factor.

No pure PSA was recovered from the suspected graft. Although it is likely that homopolymer was formed, its solubility was apparently too similar to the graft copolymer to enable its separation.

Light-Scattering Studies

It has been shown previously^{8,9} that in a graft copolymer composed of polymers with considerably differing solubilities, the coagulation of the coacervate droplets formed by addition of a nonsolvent for one of the polymers to a dilute solution of the copolymer is usually retarded as compared to the coagulation of the coacervate droplets of the less soluble homopolymer in a physical mixture of the two. In the terminology of Mysels,¹⁰ the graft may exhibit "diuturnal" behavior, while the physical mixture is "caducous." This is due to the protective action of the solvated chains of the more soluble polymer of the graft, which extend from the surfaces of the coacervate droplets into the surrounding solution. Consequently, under such conditions, the light-scattering properties of the suspension in the case of the relatively more stable graft change more slowly than the light-scattering properties of the corresponding physical mixture.

Figures 3 and 4 show the behavior of the scattering ratio ($90^\circ-0^\circ$) for dilute solutions of the suspected graft and several physical mixtures. The solvent-precipitant ratios corresponded to points in the fractional precipitations where PSA and any attached xylan precipitated but where xylan homopolymer remained in solution; the original addition (3 ml.) of ethanol corresponds to point *A* in Figures 1 and 2, and the subsequent addition of 1 ml. ethanol brought the solvent composition to point *B* in these figures. It is evident that the change in the scattering ratio was

much slower with the suspected graft than with the physical mixtures. Also, rather substantial changes in the compositions of the physical mixtures, which would surely bracket any errors in determination of the composition of the suspected graft or of its molecular weight, had negligible effects on the rate of change of the physical mixture scattering as compared to the suspected graft scattering. In addition, the fact that the scattering in the physical mixtures was due only to coagulating PSA droplets, as ex-

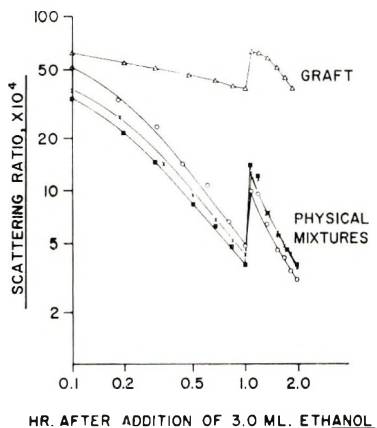


Fig. 3. Scattering ratios, $\alpha F(G_s/G_w)$, for suspected graft copolymer and physical mixtures; corrected for solvent scattering; additional 1.0 ml. ethanol added at 1.03 hr.: (Δ) suspected graft copolymer (0.0100%); (\circ) physical mixture with PSA-1 (\bar{M}_w 390,000); (\times) physical mixture with PSA-2 (\bar{M}_w 260,000); (\blacksquare) physical mixture with PSA-GP (\bar{M}_w 173,000). Physical mixtures contain 0.0071% PSA, 0.0029% catalyst-treated xylan.

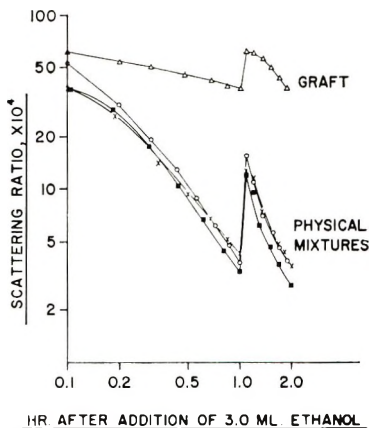


Fig. 4. Scattering ratios, $\alpha F(G_s/G_w)$, for suspected graft copolymer and physical mixtures; corrected for solvent scattering; additional 1.0 ml. ethanol added at 1.03 hr.: (Δ) suspected graft copolymer (0.0100%); (\circ) physical mixture with PSA-2, [PSA] = 0.0100%; (\blacksquare) physical mixture with PSA-2, [xylan] = 0; (\times) physical mixture with PSA-2. Physical mixtures contain 0.0071% PSA, 0.0029% catalyst-treated xylan, except as noted.

pected from the fractional precipitation results, is shown in Figure 4, where omitting the xylan from the physical mixture had no significant effect.

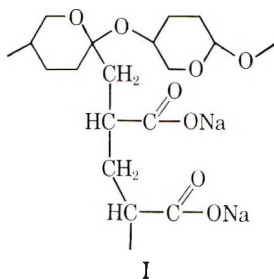
Visual observations correlated well with the instrumental results. The suspensions of the suspected graft remained nearly uniformly turbid with none or with only extremely minute particles visible to the eye; with the physical mixtures, gradual coagulation and formation of very small flocs was apparent. The flocs remained in suspension and did not settle out during the brief periods when measurements were taken and stirring consequently interrupted.

The observed behavior suggests that minute droplets of PSA were formed when limited amounts of ethanol were added to the dilute solutions of the suspected graft or the physical mixtures. In the case of the graft, highly solvated chains of xylan extended from the surfaces of the droplets into the surrounding solution and consequently inhibited coagulation of neighboring droplets. With the physical mixtures, the droplets consisted of essentially pure PSA with no such protective surfaces; hence, coagulation occurred readily.

The evidence which has been presented strongly supports the hypothesis that a true graft copolymer, consisting of a xylan backbone with attached PSA chains of relatively high molecular weight, was formed. The yield was low under the conditions employed, however, and more than 90% of the xylan charged to the reaction vessel remained ungrafted.

Proposed Structure of the Graft Copolymer

The catalyst system employed generates free hydroxyl radicals³ which are capable of abstracting hydrogen atoms from carbohydrates.¹¹ Attack may be favored at anomeric C—H bonds for reasons discussed elsewhere.¹² Assuming formation of a xylan free radical at this point, the acrylate polymer may then propagate outwards; the resultant copolymer is depicted as structure I. A LaPine-Leybold molecular model was constructed to confirm the steric possibility of such a structure.



An estimate of the average number of PSA chains per xylan chain requires a knowledge of the number-average molecular weights (\bar{M}_n) of both polymers. Since the \bar{M}_w/\bar{M}_n ratio for PSA-2 was 1.91, the \bar{M}_n for PSA-GP, isolated from the graft copolymer, was taken as 173,000/1.91, or 90,500

(not enough was available for osmometry). The value of \bar{M}_n for the grafted xylan is not known. However, for acid-degraded xyans, the \bar{M}_w/\bar{M}_n ratio was found to be about 1.3;⁵ although the degradation mechanism was different here, the value of \bar{M}_n for the grafted xylan chains was taken as 13,600/1.3, or 10,500. Up to the 35 ml. ethanol addition level in the graft fractionation, 0.5828 g. PSA and 0.0214 g. xylan had been recovered, or 6.4×10^{-6} mole PSA and 2.0×10^{-6} mole xylan. There was, therefore, an average of only 3.2 PSA chains per xylan chain, even though the graft copolymer contained 96.5% PSA. Although the amount of PSA homopolymer in this material is unknown, the fact that no xylan homopolymer could be isolated from the material precipitated up to the 35-ml. ethanol addition level indicates the presence of at least one grafted PSA chain per xylan chain, leaving a maximum of 2.2 homopolymer PSA chains per xylan chain.

References

1. T. E. Timell, *Advan. Carbohydrate Chem.*, **19**, 247 (1964).
2. J. J. O'Malley and R. H. Marchessault, *J. Polymer Sci. B*, **3**, 685 (1965).
3. C. A. Sorum and J. O. Edwards, *J. Am. Chem. Soc.*, **74**, 1204 (1952).
4. A. W. Craig and D. A. Henderson, *J. Polymer Sci.*, **19**, 215 (1956).
5. R. G. LeBel and D. A. I. Goring, in *Fourth Cellulose Conference (J. Polymer Sci. C, 2)*, R. H. Marchessault, Ed., Interscience, New York, 1963, p. 29.
6. P. J. Guttman and T. E. Timell, in *Fifth Cellulose Conference (J. Polymer Sci. C, 11)*, T. E. Timell, Ed., Interscience, New York, 1965, p. 281.
7. R. Sakamoto, *Nippon Kagaku Zasshi*, **83**, 386 (1962).
8. R. J. Ceresa, *Block and Graft Copolymers*, Butterworths, Washington, 1962, pp. 139-140.
9. F. M. Merrett, *J. Polymer Sci.*, **24**, 467 (1957).
10. K. J. Mysels, *Introduction to Colloid Chemistry*, Interscience, New York, 1959, p. 78.
11. G. O. Phillips, W. Griffiths, and J. V. Davies, *J. Chem. Soc.*, **B1966**, 194.
12. J. A. Church, *Tappi*, **48**, 185 (1965).

Résumé

Grâce à un système initiateur oxydo-réducteur à base de persulfate et de thiosulfate on a pu greffé le 4-O-méthylglucuronoxylane avec le polyacrylate de sodium (PSA) dans NaOH 3.6N à 25-30°C. La formation d'un copolymère greffé vrai était prouvée par précipitation fractionnée, par des études de diffusion lumineuse, en utilisant des mélanges physiques des deux polymères purs comme références. Une fraction greffée a été isolée, ne contenant pas du xylane non-greffé, mais peut-être quelques homopolymères PSA, qui contenaient 96.5% PSA et 3.5% de xylane, ou en moyenne 3.2 chaînes de PSA de \bar{M}_n approximativement égal à 90,500 par chaîne xylanique de \bar{M}_n approximativement égal à 10,500.

Zusammenfassung

Auf ein aus Espen stammendes 4-O-Methylglucuronoxylan wurde unter Verwendung eines Persulfat-Thiosulfat-Redox-startersystems Polynatriumacrylat (PSA) in 3,6N NaOH bei 25-30°C aufgepfropft. Fraktionierte Fällungen und Streulichtuntersuchungen, bei denen die physikalischen Gemenge der beiden reinen Polymeren als Bezugs-

substanz verwendet wurden, sprachen für die Bildung eines echten Pfropfcopolymeren. Eine der isolierten gepfropften Fraktionen, die kein ungepfropftes Xylan, aber möglicherweise etwas PSA-Homopolymeres enthielt, bestand zu 96,5% aus PSA und zu 3,5% aus Xylan. Dies entspricht einem Durchschnitt von 3,2 PSA-Ketten mit einem \bar{M}_n von ungefähr 90.500 pro Xylankette (\bar{M}_n ca. 10.500).

Received April 3, 1967

Resubmitted May 22, 1967

Prod. No. 5452A

Reactive Fiber. V. Preparation and Polymerization of *p*-Styrenesulfonyl(β -chloroethyl)amide

YOSHIO IWAKURA, KEIKICHI UNO, NOBUO NAKABAYASHI,*
and WEN-YEN CHIANG, *Department of Synthetic
Chemistry, Faculty of Engineering,
The University of Tokyo, Japan*

Synopsis

p-Styrenesulfonyl(β -chloroethyl)amide (III) was prepared and copolymerized with styrene (M_1). The monomer reactivity ratios were determined ($r_1 = 0.25 \pm 0.1$, $r_2 = 1.25 \pm 0.25$), and Q and e values were calculated (1.69 and 0.28, respectively). The polymer reacts with nucleophilic reagents such as amines and phenols in the presence of pyridine to the extent of 15–98%. Fibers from copolymers of acrylonitrile and III react with Congo Red in the presence of pyridine.

INTRODUCTION

Polymers having chemically reactive groups and their reactions have been reported in a series of studies.¹⁻⁷ Epoxy, aziridinyl, isocyanato, and β -chloroethylaminosulfonyl groups attached to polymer chains were found to be very reactive and were widely used in the preparation of reactive polymers and fibers. Monomers with sulfonyl aziridine groups were rather unstable and difficult to purify. Addition of hydrochloric acid to the sulfonyl aziridine group gives a monomer with a β -chloroethylaminosulfonyl group. The reaction of β -chloroethylaminosulfonyl groups with nucleophilic reagents in the presence of bases has been reported⁸ to be similar to that of sulfonyl aziridines.

In the present paper, the preparation and polymerization of *p*-styrenesulfonyl(β -chloroethyl)amide (III) is described. Chemical reaction of the polymer of III with nucleophilic reagents was studied. The fiber prepared from the copolymer of acrylonitrile and III reacted readily with Congo Red in the presence of pyridine. The reactivity of the dye with fiber was investigated.

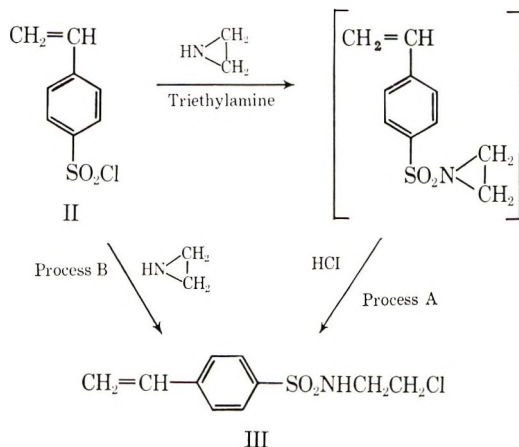
RESULTS AND DISCUSSION

Preparation of *p*-Styrenesulfonyl(β -chloroethyl)amide

p-Styrenesulfonyl chloride (II) was prepared from the reaction of potassium *p*-styrenesulfonate (I) with phosphorus pentachloride in chloro-

* Present address: Department of Chemistry, Yale University, New Haven, Conn.

form in the presence of hydroquinone. After several treatments a fraction boiling at 120–125°C./1 mm. Hg was obtained. The yield of this fraction, which might be II, was very low. It polymerized easily even when kept at Dry Ice temperature. Since isolation of II failed, crude II was used in this experiment. *p*-Styrenesulfonamide, m.p. 137–138°C. (lit.⁹ m.p. 136–137°C.), was obtained by treatment of II with ammonium hydroxide. Pure crystalline *p*-styrenesulfonyl(β -chloroethyl)amide (III) was obtained by the addition of hydrochloric acid to *p*-styrenesulfonyl aziridine. From the two processes considered for the preparation of III, process A gave III by two-step reaction involving (1) condensation of II and aziridine in the presence of triethylamine and (2) addition of concentrated hydrochloric acid to crude sulfonyl aziridine and recrystallization of III from petroleum ether. In process B, no reaction occurred, and II was recovered. Bestian¹⁰ has reported that process B is an effective method for the preparation of methansulfonyl(β -chloroethyl)amide from methansulfonyl chloride and aziridine.



III is soluble in common organic solvents. Its infrared absorption spectrum showed an N—H stretching band at 3270 cm^{-1} , sulfonate absorption bands at 1320 and 1150 cm^{-1} , double-bond bands at 3070, 1625, 983, and 910 cm^{-1} , and a *p*-phenylene band at 840 cm^{-1} .

Preparation of Polymer

III was polymerized in the presence of α, α' -azobisisobutyronitrile (AIBN). Polymers obtained by bulk polymerization at 60–90°C. were insoluble. However, polymers prepared in toluene, tetrahydrofuran (THF), or dimethylformamide (DMF) solution at monomer concentrations of 20–25% were white powders which were soluble in DMF and THF. These experiments are summarized in Table I,

TABLE I
 Polymerization of III

III, g.	AIBN, mg.	Solvent, g.	Temp., °C.	Time, hr.	Yield, %	$[\eta]$, dl./g. ^a
1.0	6	—	85-95	8	76	gel
0.5	5	—	60-80	5	70	gel
0.5	10	Toluene, 0.5	70	3	46	1.63 ^{b,c}
0.5	5	THF, 1.5	65-70	20	50	0.15
1.0	5	DMF, 4.0	60-65	19	52	0.54 ^c
0.5	5	DMF, 0.5	70	3	75	gel

^a In DMF at 30°C.

^b η_{sp}/c 0.2 g./100 ml., DMF, 30°C.

^c Calcd. for homopolymer $(C_{10}H_{12}SO_2NCl)_n$, 5.70% N; found for homopolymer, 5.66% N.

^d Found for homopolymer, 5.50% N.

Determination of Monomer Reactivity Ratios

Monomer feed versus copolymer composition is shown in Table II and Figure 1. The monomer reactivity ratios of III (M_2) with styrene (M_1) were determined and Q , e values of III were calculated as follows: $r_1 = 0.25 \pm 0.1$, $r_2 = 1.25 \pm 0.25$, $Q = 1.69$, $e = 0.28$.

 TABLE II
 Copolymerization of Styrene (M_1) and III (M_2) in Dioxane at 85°C.

Expt. no.	Monomer feed		Copolymer composition		
	$[M_1]$, mole-%	$[M_2]$, mole-%	N, %	$[M_1]$, mole-%	$[M_2]$, mole-%
1	32.92	67.08	4.97	25.74	74.26
2	39.28	60.72	4.92	27.22	72.78
3	55.95	44.05	4.38	41.56	58.44
4	60.05	39.95	4.28	43.91	56.09
5	79.81	20.19	3.45	60.61	39.39
6	90.02	9.98	2.17	79.33	20.67

Copolymerization with Acrylonitrile

Copolymerization of acrylonitrile and III was conducted by redox polymerization in aqueous dispersion and by solution polymerization. Redox polymerization gives higher conversion than solution polymerization but the polymer obtained in redox polymerization has poor solubility and tends to gel. The product of solution polymerization is more soluble in DMF and can be spun into strong fibers, while redox polymer is difficult to spin and gives weak fibers. In solution polymerization, III enters

TABLE III
Redox Polymerization

Expt. no.	AN, g. (mole-%)	III, g. (mole-%)	Solvent, ml.		Initiator, g.		Temp., °C.	Time, hr.	Yield, %	[η], dl./g. ^a
			H ₂ O	H ₂ SO ₄ (0.1N)	(NH ₄) ₂ S ₂ O ₈	Na ₂ S ₂ O ₈				
C	26.5	1.000								
	(99.19) 13.25	(0.81) 0.4177	380	3.5	0.8174	0.4088	32	2	77.7 ^b	2.2
E	(99.34) 4.4	(0.66) 0.2027	250	1.7	0.4104	0.1872	25.5	2.3	54.8	2.6
	(98.64)	(1.36)	65	0.5	0.0635 ^c	0.0291 ^d	35-38	2.5	60.0 ^e	2.65

^a In DMF at 30°C.^b III unit in the copolymer found, 1.99 mole-%.^c K₂S₂O₈ instead of (NH₄)₂S₂O₈.^d NaHSO₃ instead of Na₂S₂O₈.^e III unit in the copolymer found, 2.88 mole-%.

TABLE IV
 Solution Polymerization

Expt. no.	AN, g. (mole-%)	III, g. (mole-%)	Solvent (THF), ml.	Initiator (AIBN), g.	Temp., °C.	Time, hr.	Yield, %	$[\eta]$, dl./g. ^a	III unit in copolymer found, mole-%
11	53.0	3.6955							
	(98.5) 53.0	(1.5) 0.4879	3.5	0.035	60-65	2.3	26.5	3.1	9.03
12	(99.8) 53.0	(0.2) 1.5000	3.5	0.027	60-67	1.8	18.7	2.45	1.93
	(99.4) 53.0	(0.6) 2.0000	3.5	0.038	61-65	1.5	13.8	2.65	5.41
15	(99.2)	(0.8)	3.5	0.036	62-65	1.5	18.2	2.9	5.52

^a In DMF at 30°C.

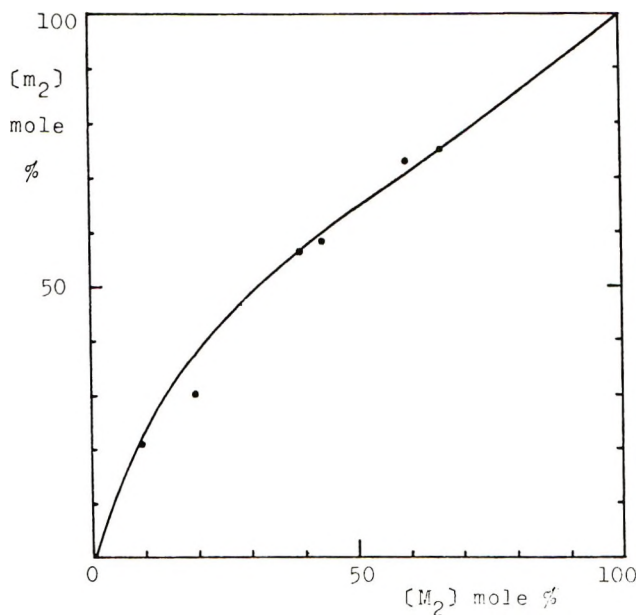


Fig. 1. Copolymerization curve for styrene (M_1)-III (M_2): (●) experimental; (—) theoretical.

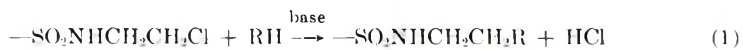
the copolymer at a faster rate than in aqueous redox polymerization. The results are shown in Tables III and IV.

Wet-Spinning of Copolymer With Acrylonitrile

Solutions (13–16 wt.-%) of the copolymer in DMF, were spun under nitrogen pressure (1 atm.) into ethylene glycol and the coagulated fiber drawn in 92–96°C. hot water. The physical properties of the fibers are shown in Table V.

Reaction of Polymer

Polymer with β -chloroethylaminosulfonyl groups was expected to react with nucleophilic reagents, such as amines and phenols in the presence of base according to eq. (1):



where RH denotes nucleophilic reagents.

Conversions in reactions with a variety of nucleophiles were calculated from elemental analyses. The results are shown in Table VI. For a comparison the reaction of *p*-toluenesulfonyl(β -chloroethyl)amide (IV) as a model compound of poly-III was studied with β -naphthylamine,

TABLE V
 Physical Properties of Fibers

Co-polymer	Solids, %	Draw ratio	Drawing temp., °C.	Denier	Dry ^a		Wet ^a	
					Tenacity, g./den.	Elongation, %	Tenacity, g./den.	Elongation, %
C	16	2.4	92	4.64	1.71	41.5	—	
E	14	3	95	3.88	1.86	12.3	11.5	
11	14	3.3	95	2.93	2.12	16.7	15.4	
12	13	4	92	3.47	1.41	8.7	9.0	
14	15	3	93	3.38	2.01	13.8	14.1	
15	13	2.6	96	2.83	2.23	10.7	10.5	

^a At room temperature.

 TABLE VI
 Reaction of Poly-III

Reagent	Wt. reagent, g.	Poly-III, g.	Solvent, ml.		Temp.	Time, hr.	N, %	Conversion, %
			DMF	Pyridine				
Aniline	1.2	0.1	3	5	Reflux	3	7.13	45.8
Aniline	1.0	0.1	3	5	"	3.5	8.97	97.5
β -Amino-propionitrile	0.03	0.04	3	5	"	4	9.55	43.4
<i>o</i> -Amino-benzoic acid	1.5	0.04	3	5	"	3	6.01	21.3
Phenol	1.1	0.06	3	5	"	6	5.15	32.4
Diethanolamine	1.0	0.1	3	5	"	3.5	7.94	58.8
<i>p</i> -Toluidine	0.8	0.6	3	5	"	3	6.75	39.6
Thiophenol	0.5	0.5	3	5	"	3	5.29	16.0

TABLE VII
 Reaction Conditions of Model Compound

Model compound	IV, g. (mole)	Reagent, g.	Base, ml.	Temp., °C.	Time, hr.	Yield, %	M.p., °C. ^a
IV-1	2.3 (0.1)	1.5	5	Reflux	5	53.0	119-120
IV-2	"	2.3	—	"	5	43.0	78-79
IV-3	"	1.1	2	"	8.5	46.0	65-65.5

^a Compounds recrystallized from CCl₄.

p-toluidine, and thiophenol in pyridine. The reaction conditions and elemental analyses are shown in Table VII and Table VIII.

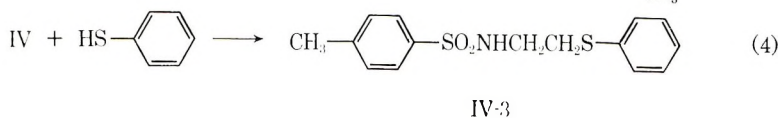
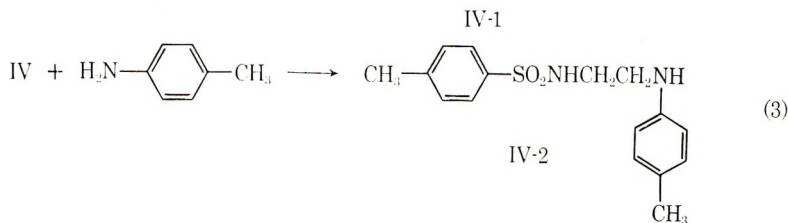
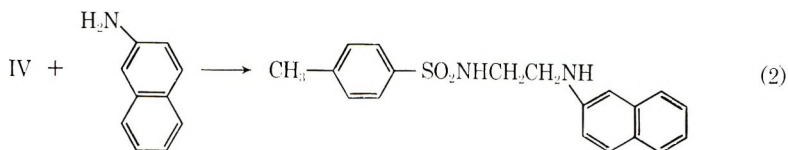


TABLE VIII
Elemental Analyses of Model Compound

Compound	C, %		H, %		N, %	
	Found	Calcd.	Found	Calcd.	Found	Calcd.
IV-1	66.91	67.04	5.56	5.92	8.01	8.23
IV-2	62.81	63.14	6.29	6.62	9.01	9.21
IV-3	58.46	58.63	5.51	5.58	4.43	4.56

Reaction of Fibers

Fibers were treated with Congo Red in aqueous solution at 95°C. for 1 hr. in the presence of pyridine. The amount of dye taken up by fiber was determined by the colorimetric method. The extraction of colored fibers with hot water and boiling acetone gave no decoloration. Therefore, the dyes taken up by the fibers seem to be combined chemically. Table IX shows the results obtained at various concentrations of pyridine in the treatment. Figure 2 shows the effect of pyridine concentration in the dye solution on the amount of dye on fiber. The low level of III in copolymer from redox polymerization gave poor dye uptake unless the pyridine concentration was over 25%, but copolymer obtained from solution polymerization was very reactive with dye even at lower pyridine concentration. Figure 3 shows the relation between the reaction time and the amount of the reaction. The amount of dye reacted is less than ca. 50% in every case, assuming equimolar reaction of Congo Red and the β -chloroethylamino group. The fiber treated with Congo Red did not dissolve in any solvent. This may indicate the reaction of Congo Red

TABLE IX
Reaction of Acrylic Fiber and Congo Red at Various Concentrations of Pyridine

Co- polymer	[C ₅ H ₅ N] = 1%		[C ₅ H ₅ N] = 5%		[C ₅ H ₅ N] = 10%		[C ₅ H ₅ N] = 15%		[C ₅ H ₅ N] = 25%		[C ₅ H ₅ N] = 50%	
	Dye, mg./g. ^a	Conv., %	Dye, mg./g. ^a	Conv., %	Dye, mg./g. ^a	Conv., %	Dye, mg./g. ^a	Conv., %	Dye, mg./g. ^a	Conv., %	Dye, mg./g. ^a	Conv., %
C	3.52	1.44	5.45	2.25	7.19	2.95	7.91	3.25	12.60	5.17	12.90	5.29
11	280.0	32.24	337.4	37.74	340.9	38.17	340.6	38.13	346.4	38.78	310.5	34.76
12	142.9	56.19	121.6	47.82	99.0	38.93	109.9	43.22	94.5	37.16	49.0	19.27
14	121.6	20.48	158.7	26.73	286.7	48.29	280.4	47.23	254.5	42.87	186.3	31.38
15	83.96	13.91	303.5	50.27	316.1	52.36	309.8	51.31	283.0	46.88	207.5	34.37

^a Dye uptake up by fiber.

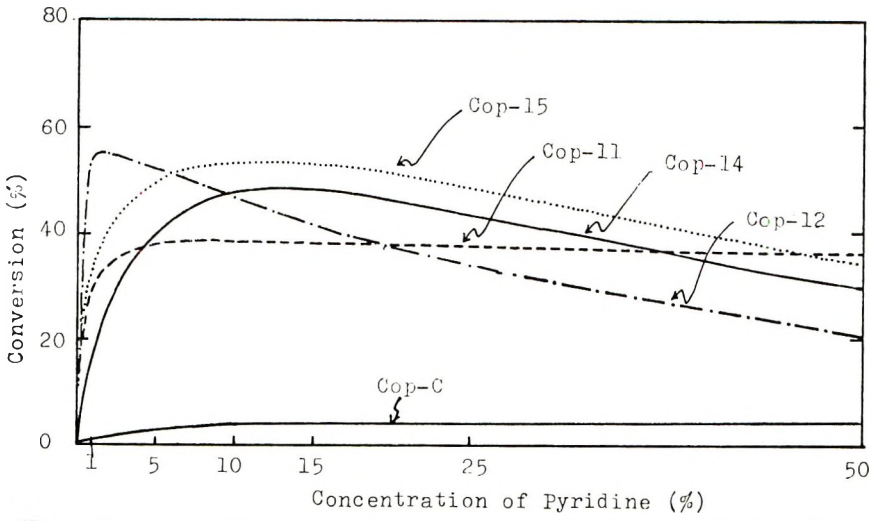


Fig. 2. Effect of pyridine concentration in the dye solution on amount of dye in fiber.

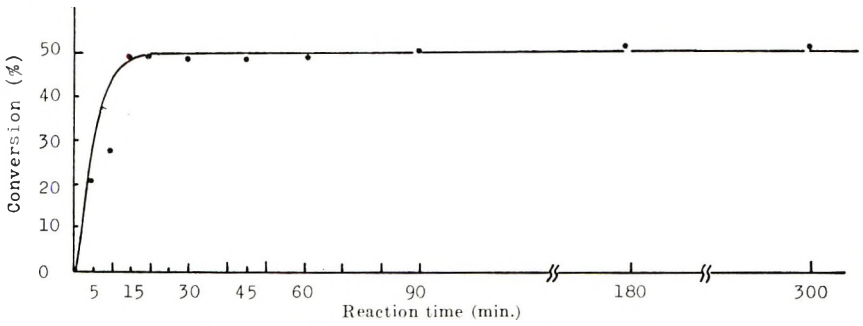
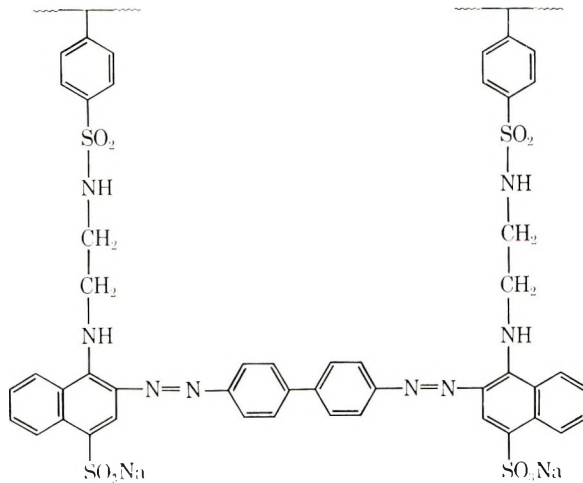


Fig. 3. Relation between reaction time and extent of reaction.

with two moles of β -chloroethylamino group and crosslinking of polymer chains (V):



V

EXPERIMENTAL

Preparation of *p*-Styrenesulfonyl(β -chloroethyl)amide

To a suspension of 100 g. (0.450 mole) of potassium *p*-styrenesulfonate (I) in 450 ml. of chloroform with 1 g. of hydroquinone, was added 120 g. (0.576 mole) of phosphorus pentachloride slowly over a period of 1 hr., with vigorous stirring with cooling by an ice-water bath. After the addition was completed the reaction was continued at 45–50°C. for 2 hr. The precipitate was removed by filtration and the chloroform was removed under reduced pressure from the filtrates. The yellow oily residue was dissolved in 500 ml. of ether and washed with ice water for several times. The organic layer was taken and dried by calcium chloride and the ether was removed under reduced pressure carefully. The crude *p*-styrenesulfonyl chloride (II) was obtained in 74.0 g. yield (81.2%).

To a solution of 74.0 g. (0.365 mole) of crude II in 200 ml. of dry toluene was added a mixture of 15.7 g. (0.365 mole) of aziridine and 37.0 g. (0.365 mole) of triethylamine dropwise with stirring at a temperature of –5 to 5°C. over 0.5–1 hr. After the addition was completed, the reaction was carried out at room temperature (20–25°C.) for 15 min. The reaction mass was filtered to remove Et₃N HCl. Excess concentrated hydrochloric acid was added dropwise into the filtrates with stirring under cooling with ice water. The organic layer was separated and washed with water several times and dried with calcium chloride. The residue after removal of the solvent was crystalline or an oil which was extracted with the large volume of petroleum ether. White, needle-shaped crystals were obtained from the petroleum ether. The recrystallization was repeated several times from petroleum ether. The yield was 20.1 g. (18.2% overall). The melting point was 77.5–78.5°C.

ANAL. Calcd. for C₁₀H₁₂SO₂NCl: C, 48.87%; H, 4.92%; N, 5.70%. Found: C, 49.17%; H, 4.90%; N, 5.76%.

Polymerization of III

A 1-g. portion of III, 0.005 g. of AIBN as an initiator, and 4 g. of DMF as a solvent were sealed in an ampule under an atmosphere of nitrogen. The ampule was kept at 60–65°C. for 20 hr. The viscous polymer solution was poured into methanol to precipitate the polymer. Reprecipitation was carried out three times with DMF–methanol.

ANAL. Calcd. for (C₁₀H₁₂SO₂NCl)_n: N, 5.70%. Found: N, 5.50%.

Determination of Monomer Reactivity Ratios

Accurately weighed portions of 3.5 g. of each of the monomers, styrene (M₁) and III (M₂), were sealed in an ampule with 5 ml. of dioxane as a solvent and 5 mg. of AIBN as an initiator under an atmosphere of nitrogen. The copolymerization was allowed to proceed below 10% conversion. The obtained polymer was reprecipitated three times with THF and

methanol. It was dried *in vacuo*. The composition of the copolymer was determined by elemental analysis.

Copolymerization of Acrylonitrile and III

Redox Polymerization. In a flask under an atmosphere of nitrogen were placed 380 ml. of distilled water, 3.5 ml. of 0.1*N* H₂SO₄, 26.5 g. (0.5 mole) of acrylonitrile, and 1.0 g. (0.004 mole) of III. The mixture was kept at 32°C. and stirred for 5 min., and then 0.8174 g. of (NH₄)₂S₂O₈ as an oxidizing agent was added. After 1 min., 0.4088 g. of Na₂S₂O₃ as a reducing agent was added. The copolymerization was carried out at 32°C. for 2 hr. The mixture was filtered and the copolymer was poured into methanol and washed several times. The yield was 21.4 g. (77.7%); $[\eta] = 2.2$ dl./g. (DMF at 30°C.).

ANAL. Found for AN-III copolymer: N, 24.62%. Calcd. for III units in the copolymer, 1.99 mole-%.

Solution Polymerization. In a flask under an atmosphere of nitrogen were placed 53 g. (1 mole) of acrylonitrile, 3.6955 g. (0.015 mole) of III, and 3.5 ml. of THF. The mixture was kept at 60–65°C., were stirred for 5 min., and then 0.035 g. of AIBN as initiator was added. The solution copolymerization was carried out at 60–65°C. for 2 $\frac{1}{4}$ hr. The copolymer was poured into methanol and washed several times. The yield was 14.5 g. (26.5%); $[\eta] = 3.1$ dl./g. (DMF at 30°C.).

ANAL. Found for AN-III copolymer N, 19.88%. Calcd. for III units in copolymer, 9.03 mole-%.

Wet-Spinning of the Copolymer

A 7-g. portion of copolymer, containing 9.03 mole-% of III units and having $[\eta] = 3.1$ dl./g. was dissolved in 43 ml. of DMF at 70–75°C. The dissolved copolymer was kept overnight at room temperature. The dope was extruded into an ethylene glycol coagulation bath at room temperature under a pressure of 1 atm. of nitrogen, through a spinneret having six holes of 0.12 mm. diameter. The fiber was drawn 3.3 times in a hot water bath kept at 95°C. The physical properties of the fiber are shown in Table V.

Reaction of Poly-III

In 3 ml. of DMF was dissolved 0.04 g. of poly-III. To the solution were added 5 ml. of pyridine and 1.1 g. of aniline. The reaction was carried out under a reflux temperature for 3.5 hr. and the solution was poured into methanol to precipitate the polymer. The polymer was washed several times. Other reactions were carried out by the same method. The results are shown in Table VI.

Reaction of Acrylic Fiber (Copolymer of AN-III) and Congo Red

The reaction of acrylic fiber and Congo Red were carried out at a 1:125 liquor ratio, that is 0.04 g. of fiber in 5 ml. of dye solution, at a temperature of 95°C. for 1 hr. The amount of dye combined chemically with the fiber was determined by a colorimetric method by using a Hitachi Photoelectric Photometer, Type EPO-B.

References

1. Y. Iwakura, T. Kurosaki, and N. Nakabayashi, *Makromol. Chem.*, **44/46**, 570 (1961).
2. Y. Iwakura and N. Nakabayashi, *Makromol. Chem.*, **66**, 142 (1963).
3. Y. Iwakura, N. Nakabayashi, and M. H. Lee, *Makromol. Chem.*, **78**, 157 (1964).
4. N. Nakabayashi and Y. Iwakura, *Makromol. Chem.*, **81**, 180 (1965).
5. Y. Iwakura, N. Nakabayashi, and H. Suzuki, *Makromol. Chem.*, **78**, 168 (1964).
6. Y. Iwakura, T. Kurosaki, K. Nagakubo, K. Takeda, and M. Miura, *Bull. Chem. Soc. Japan*, **38**, 1349 (1965).
7. Y. Iwakura, K. Uno, N. Nakabayashi, T. Tani, and W. Y. Chiang, *Kogyo Kagaku Zasshi*, **68**, 1222 (1965).
8. K. Matsui and Y. Soeda, *J. Soc. Org. Synth. Chem. Japan*, **20**, 354 (1962).
9. N. Yoda, and C. S. Marvel, *J. Polymer Sci. A*, **3**, 2229 (1965).
10. H. Bestian, *Ann.*, **566**, 210 (1950).

Résumé

Le *p*-styrènesulfonyl(β -chloroéthyl)amide (III) a été préparé et copolymérisé avec le styrène (M_1). Les rapports de réactivité monomérique ont été déterminés ($r_1 = 0.25 \pm 0.1$, $r_2 = 1.25 \pm 0.25$) et les valeurs de Q et e ont été calculées (1.69 et 0.28 respectivement). Le polymère réagit avec des réactifs nucléophiles tels que les diamines et les phénols en présence de pyridine avec des rendements variant de 15 à 98%. Des fibres au départ de copolymères d'acrylonitrile et de III réagissent avec le Rouge Congo en présence de pyridine.

Zusammenfassung

p-Styrolsulfonyl(β -chloräthyl)amid (III) wurde hergestellt und mit Styrol (M_1) copolymerisiert. Die Copolymerisationsparameter wurden bestimmt ($r_1 = 0,25 \pm 0,1$, $r_2 = 1,25 \pm 0,25$) und die Q - und e -Werte berechnet (1,69 bzw. 0,28). Das Polymere reagiert mit nukleophilen Reagenzien wie Aminen und Phenolen in Gegenwart von Pyridin in einem Ausmass zwischen 15% und 98%. Fasern aus Copolymeren von Acrylnitril und III reagieren in Gegenwart von Pyridin mit Kongorot.

Received September 22, 1966

Revised May 23, 1967

Prod. No. 5453A

NOTES

Effect of Ethyl Monochloroacetate on the Cationic Polymerization of Styrene Catalyzed by Rhenium Pentachloride

Introduction

In a previous report,¹ elementary rate constants of the polymerization of styrene catalyzed by rhenium pentachloride were obtained. In the polymerization system studied, a small quantity of ethyl monochloroacetate (ECA) was used to dissolve the catalyst. As discussed in the previous report, ECA is considered to destroy the active species and to keep the polymerization at a stationary state. In the present report, in order to clarify the effect of ECA, the induction period, the polymerization rate, and the viscosity of the polymer obtained were examined by varying the concentration of ECA at constant concentrations of catalyst and monomer.

Experimental

Although the most of data used in the present report were obtained previously,^{1,2} some additional determinations were made. By varying the concentration of ECA at a catalyst concentration of 0.550 mmole/l. and a monomer concentration of 2.61 mole/l. the polymerization was carried out at 10°C., and the change of polymer yield with time was followed. At the same time, the viscosity of the polymer obtained was measured. Details of the experiment were the same as in the previous reports.^{1,2}

Results

The change in the polymer yield with time is shown in Figure 1, and values of $[\eta]$ of the polymer obtained at various concentrations are shown in Table I, where $[\eta]$ was measured for the polymer obtained after the stationary polymerization was reached.

TABLE I^a

[ECA], mole/l.	$[\eta]$
0.095	0.244
0.189	0.236
0.473	0.210
0.567	0.211
0.946	0.201
1.892	0.181

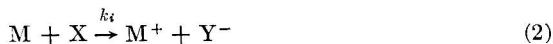
^a $[M]_0 = 2.61$ mole/l.; $[C]_0 = 0.550$ mmole/l.

Discussion

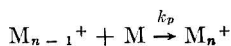
The mechanism proposed in the previous report¹ is shown in eqs. (1)–(7).
Complex formation:



Initiation:



Propagation:



Transfer:



Termination:



The relation derived according to this mechanism between the degree of polymerization P_s and the stationary-state concentration of monomer, $[M]_s$, is shown in eq. (8):

$$1/P_s = k_T/(k_p[M]_s) + k_{trm}/k_p \quad (8)$$

where

$$k_T = k_t + k_{ts}[S] + k_{ts}'[S'] \quad (9)$$

Equation (8) can be rewritten in the form:

$$1/P_s = (k_{trm} - bk_{ts})/k_p + \{ak_{ts} + k_t + (k_{ts}' - ck_{ts})[S']\}/(k_p[M]_s) \quad (10)$$

Here,

$$a = 1000d_s/W_s$$

$$b = d_s W_m / (d_m W_s)$$

$$c = d_s W_{s'} / (d_{s'} W_s)$$

and d_s , $d_{s'}$, and d_m are densities and W_s , $W_{s'}$, and W_m are molecular weights of benzene, ECA, and styrene, respectively. Therefore, when $[M]_s$ is constant, there must be a linear relationship between $[S']/[M]_s$ and $1/P_s$. This is verified in Figure 2, which was obtained from the data in Table I. Since k_{trm} and k_p were obtained previously,² k_{ts} , k_{ts}' , and k_t can be obtained from the intercept and slope of the straight line in the Figure 2 and by using eq. (9). Rate constants obtained in this way are shown in Table II.

TABLE II

Temperature, °C.	$k_{ts} \times 10^3$, l./mole-min.	$k_{ts}' \times 10^2$, l./mole-min.
0	0.12	3.90
10	2.22	4.81
20	3.04	6.02

Activation energies obtained from these values were 12.4 kcal./mole for k_{ts} and 4.55 kcal./mole for k_{ts}' , with frequency factors 7.15×10^6 and 1.62×10^2 , respectively. k_t is considered to be substantially zero, since the calculated value was very small or negative.

Table II shows that the termination effect of ECA is much higher than that of benzene. This may be due to the polar group of >C=O of ECA. Since k_p is in the range of 10–100 l./mole-min.,¹ the ratio k_{ts}'/k_p is much smaller than 1. On the other hand, the corresponding ratio for ethyl acetate was higher than 1 according to the report of Higashimura and Okamura.³ This difference may be due to the effect of the chloro function in ECA.

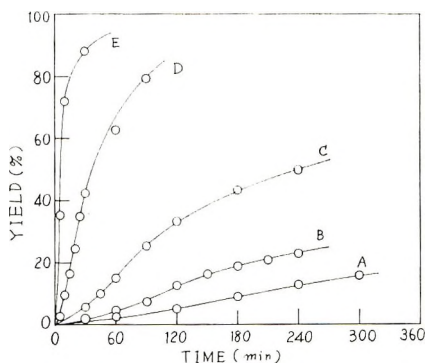


Figure 1.

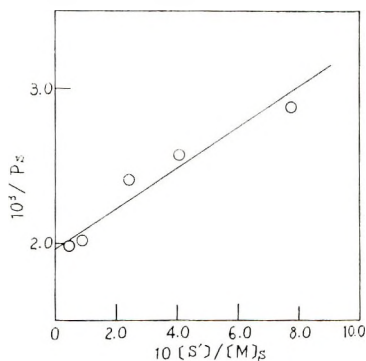


Figure 2.

In the above discussion, we used the value of k_p obtained previously.¹ However, there is a possibility that the increase of polarity with the increase of [ECA] increases k_p as described in the previous report.¹ On the contrary, the overall rate decreases increasing [ECA], as shown in Figure 1. Therefore, the termination effect of ECA is strong enough to make this polarity effect negligible. For a more detailed analysis, this effect must be taken into consideration. At present, the above described approximate estimation gives a rather satisfactory result as shown by the following discussion.

The stationary rate of polymerization R_s and the induction period τ were obtained from Figure 1 as in the previous report.² These values are plotted in Figures 3 and 4

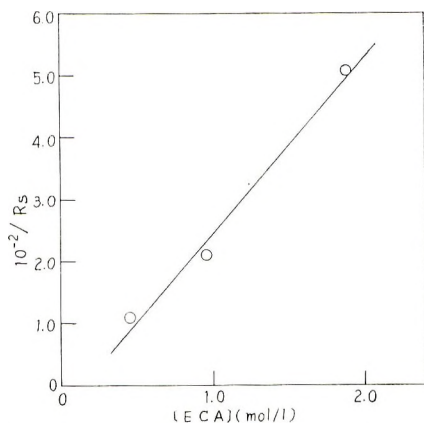


Figure 3.

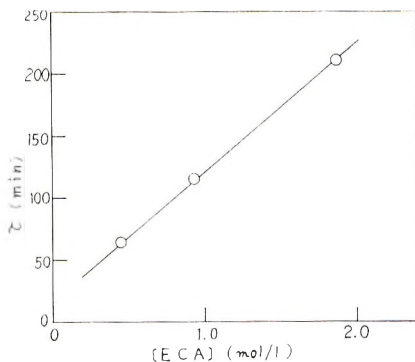


Figure 4.

against the concentration of ECA. As described in the previous report,² R_s and τ are given by

$$R_s = (Kk_i k_p / k_T) [C]_s [M]_s^{2.8} \tag{12}$$

$$\tau = \frac{k_T}{Kk_i k_p [C]_0 [M]_0^{1.8} \ln ([M]_s / [M]_0)}$$

According to Table II and the results in the previous report,¹ k_{ts}' is much larger than k_{ts} and k_T . Therefore, eq. (13) is obtained in the present experimental conditions.

$$k_T \approx k_{ts}' [S'] \tag{13}$$

TABLE III

	Measured	Calculated
$k_{ts}' / (Kk_i k_p [C]_s [M]_s^{2.8})$	298	399 ^a
$k_{ts}' / (Kk_i k_p [C]_0 [M]_0^{1.8} \ln [M]_s / [M]_0)$	110	102

^a $[C]_s = [C]_0$ was assumed for the calculation.

Slopes of Figures 3 and 4 give values of $k_{ts}'/(Kk_p k_p [C]_s [M]_s^{2.8})$ and $k_{ts}'/(Kk_p k_p [C]_0 - [M]_0^{1.8} \ln [M]_s/[M]_0)$, respectively. On the other hand, these values are calculated by using $k_i K$, k_p , and k_{ts}' obtained previously¹ and in the present experiment. As shown in Table III, there is good agreement between measured and calculated values.

From this agreement of kinetic parameters as well as the above discussion, the polymerization mechanism proposed by us is considered to be very reasonable.

The authors wish to express their thanks to Dr. Toshio Hoshino, Director of the Basic Research Laboratories, for permitting publication of the present report, to Mr. Kazutoshi Sugiyama for his help in the experiment, to Prof. Shunsuke Murahashi for his encouragement, and to Mr. Takashi Suzuki for reviewing the manuscript.

References

1. M. Kamachi and H. Miyama, *J. Polymer Sci.*, in press.
2. M. Kamachi and H. Miyama, *J. Polymer Sci. A*, **3**, 1337 (1965).
3. T. Higashimura and S. Okamura, *Kobunshi Kagaku*, **13**, 342 (1956).

MIRIHARU KAMACHI*
HAJIME MIYAMA

Basic Research Laboratories
Toyo Rayon Company, Ltd.
Kamakura, Japan

Received January 24, 1967

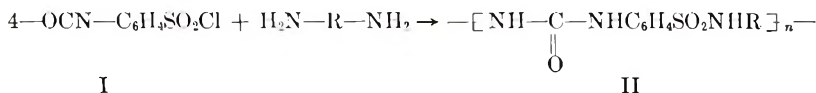
Revised June 12, 1967

* Present address: Faculty of Science, Osaka University, Toyonaka, Japan.

Polysulfonamide-Ureas

A recent publication of Iwakura and his co-workers¹ on the synthesis of polysulfonamide-ureas has prompted us to report similar findings on these types of polymers, which were produced independently in our laboratories.

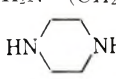
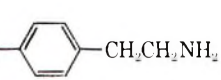
We have selected 4-isocyanatobenzenesulfonyl chloride (I) as the monomer of choice, because it can be readily obtained by direct phosgenation of sulfanilic acid. The interfacial polymerization of I with suitable diamines produces polysulfonamide-ureas (II), in which the sulfonamide group provides an acidic site for subsequent salt formation.²



The structure of the polymers was determined by comparison of their infrared and NMR spectral data with that of model compounds prepared from I and *n*-butylamine (m.p. 136°C.) and aniline (m.p. 229°C.), respectively. The polysulfonamide-ureas, being partially addition and partially condensation polymers, dissociate at their urea linkage at approximately 250–300°C. The model compounds likewise dissociate at 255 and 257°C., respectively.

The polymers are prepared by reacting I with the indicated diamines by using an interfacial polymerization method,³ and the yields are generally high (see Table I). How-

TABLE I
Polysulfonamide-Ureas from 4-Isocyanatobenzenesulfonyl Chloride
And Aliphatic Diamines

Diamine	Solvent ^a	Yield, %	η_{inh}^b	$T_{dec.}^c$ °C.
H ₂ N-(CH ₂) ₆ -NH ₂	CH ₂ Cl ₂	97	0.31	285
H ₂ N-(CH ₂) ₆ -NH ₂ ^d	Toluene	88	0.37	257
H ₂ N-(CH ₂) ₄ -CH(CH ₃)-NH ₂	Toluene	58	0.22	241
H ₂ NCH ₂ -C(CH ₃) ₂ -CH ₂ CH(CH ₃)-(CH ₂) ₂ NH ₂	Toluene	94	0.11	268
H ₂ N-(CH ₂) ₁₂ -NH ₂	CH ₂ Cl ₂	92	0.10	254
	Toluene	84	0.07	309
H ₂ NCH ₂ CH ₂ -  -CH ₂ CH ₂ NH ₂	Toluene	93	0.13	264

^a Aqueous sodium carbonate was used as the acid acceptor.

^b The inherent viscosities were measured in DMF (1% concn.) at 30.8°C.

^c The decomposition temperature was determined on a Perkin-Elmer (DSC-1) differential scanning calorimeter.

^d A 1:1 mixture of 4-isocyanatobenzenesulfonyl chloride and 1,3-benzenedisulfonyl dichloride was used.

ever, no significant changes with regard to the molecular weights were observed with a variety of organic solvents. Although the yields somewhat vary, depending on the solvent used, the inherent viscosity of the obtained polymers was of the same magnitude. The polymers are insoluble in most organic solvents, with the exception of DMF, DMSO, and hexafluoroisopropanol. All of the polymers produced were thermoplastic materials, which could be melt-pressed into films. The film quality depended upon the molecular weight and ranged from brittle to tough.

The use of a mixture of I and 1,3-benzenedisulfonyl chloride as monomers gives only slight improvement of the polymer properties.

The ease of formation as well as the high yields obtained from I and a variety of commercially available diamines provides attractive economics, which renders these polymers useful for intermediate temperature thermoplastic polymers.

Experimental

4-Isocyanatobenzenesulfonyl Chloride (I). To a suspension of 259.58 g. (1.5 moles) of sulfanilic acid in 900 ml. of *o*-dichlorobenzene at 165°C. simultaneously 13 g. (5% by weight) of *N,N*-dimethylformamide in 100 ml. of *o*-dichlorobenzene and phosgene is added (rate: 1 g./min.) until a clear solution is obtained. Approximately 3 moles of phosgene are required for complete reaction. In the absence of DMF catalyst, a huge excess of phosgene and long reaction times are necessary to achieve conversion.⁴ After purging with nitrogen for 90 min. and removal of the solvent 247.5 g. (76%) of 4-isocyanatobenzenesulfonyl chloride, b.p. 115–120°C./0.5–0.7 mm., m.p. 50–52°C., is obtained by vacuum distillation.

The monomer was redistilled and its purity was checked by vapor-phase chromatography (retention time 4.7 min. at 180°C. using a Perkin-Elmer 15 ft. \times $\frac{1}{8}$ in. S.E. 30 column with 2.5% steroid packing). Isocyanate equivalent determination⁵ indicated 99.6% purity.

Polysulfonamide-Ureas. General Method. A 10 g. portion of I (0.046 mole) was placed in 300 ml. of dry methylene chloride. The aqueous phase consisted of 5.3 g. of Na_2CO_3 and 5.9 g. of hexamethylenediamine in 300 ml. of deionized water. The reactants were cooled with an ice-salt bath. The aqueous phase was placed in a home blender, and the organic phase was rapidly added to the aqueous phase with high-speed stirring. The polymer formed immediately and precipitated as a white granular material. Stirring was continued for 10 min., after which time 200 ml. of water was added to the blender and the polymer was filtered off. The filtered polymer was again placed in the blender with 200 ml more of water and stirred, and then filtered on a sintered glass filter. It was washed several more times with water (to neutral pH) on the filter and then dried in a circulating air oven followed by drying in a vacuum oven. The yield was 14 g. (97%), $\eta_{inh} = 0.31$ (1% solution in DMF at 30.8°C.).

References

1. Y. Iwakura, K. Hayashi, and K. Inagaki, *Makromol. Chem.*, **100**, 22 (1967).
2. L. D. Taylor, M. Plukar, and L. E. Rubin, *J. Polymer Sci. B*, **5**, 73 (1967).
3. P. W. Morgan, *Condensation Polymers: By Interfacial and Solution Methods*, Interscience, New York, 1965.
4. D. Bellone and R. Magnagnoli, German Pat. 1,147,483; *Chem. Abstr.*, **60**, 701 (1964).
5. S. Siggia and J. G. Hanna, *Anal. Chem.*, **20**, 1084 (1948).

L. M. ALBERINO
HENRI ULRICH
A. A. R. SAYIGH

The Upjohn Company
D. S. Gilmore Research Laboratories
North Haven, Connecticut

Received July 3, 1967

Reaction of Nitrogen Dioxide with Polystyrene Films

No fundamental work is available on the effect of NO_2 gas on polymers, except for some scattered observations and one paper by Japanese workers on the effect of NO_2 gas on polyethylene.^{1,2} The reaction with small molecules such as olefins, however, has been investigated.³

The present work is concerned with the reaction of NO_2 gas with polystyrene films from the standpoint of main-chain rupture.

EXPERIMENTAL

Materials

All solvents were of analytical reagent grade. Polystyrene was supplied by The Dow Chemical Company; it was prepared isothermally and had a weight-average molecular weight of 3.72×10^5 (as measured in our laboratory by light scattering by Mr. C. McDonald) and a $\overline{M}_w/\overline{M}_n$ ratio of 2.3.

The polymer was purified by dissolving in methyl ethyl ketone and twice precipitating with ethanol. It was dried to constant weight *in vacuo* at 60°C. NO_2 gas was obtained from the Matheson Company, Inc.

Apparatus

An all-glass high vacuum apparatus, evacuated to about 10^{-5} – 10^{-6} mm. Hg was used. Pressures were measured with a Pyrex spoon gauge, which was used as a zero pressure indicator; the NO_2 pressure was compensated by outside air pressure, measured with a mercury manometer, as NO_2 gas reacts with mercury. Polymer films were kept in separate containers (attached to the vacuum system). The reaction temperature was kept constant by immersing these containers into a water bath. Ordinary high vacuum grease and silicone grease were attacked by NO_2 , but Fluorolube GR-544 (Hooker Chemical Corp.) was found to be satisfactory.

Preparation of Polymer Films

Glass rings of 2.6 cm. diameter and about 2 cm. in height, polished on either end, were placed on aluminum foil, which was spread on a horizontal and optically flat metal surface. A 6% (w/v) polystyrene solution in benzene was placed inside the glass rings.

The solvent was allowed to evaporate at a definite rate, which was controlled by partially covering the ring. In this way transparent films of even thickness, except for the edge of the film adhering to the glass ring, were obtained. Films of varying thicknesses, from about 10 to several hundred microns could be made in this way by varying the rate of vaporization. Films of about 20 μ were taken for the experiments. It was shown by separate experiments, that for films up to about 60 μ , diffusion effects were negligible. The films were dried *in vacuo* at 60°C. for about 2 days prior to exposure to NO_2 . Intrinsic viscosities before and after various periods of exposure were measured in a Cannon-Fenske viscometer at $25.00 \pm 0.02^\circ\text{C}$.

Results

The films were exposed to NO_2 for various periods of time and to a range of temperatures and NO_2 pressures. After exposure, their intrinsic viscosities were determined in benzene solutions.

The intrinsic viscosities were transformed into number-average chain lengths as follows. The weight-average molecular weights of the unexposed sample and one sample exposed for 22 hr. to 30 cm. Hg of NO_2 gas at 55°C. were measured by light scattering. The initial sample had a ratio of weight-average to number-average molecular weight equal to 2.3, typical for a random distribution. Thus, the weight-average chain lengths

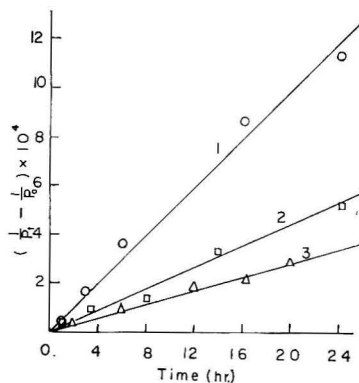


Fig. 1. Random degradation of polystyrene as a function of NO_2 pressure at 55°C .: (1) 60 cm. Hg; (2) 30 cm. Hg; (3) 15 cm. Hg.

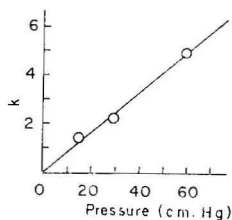


Fig. 2. Random rate constants as function of NO_2 pressure.

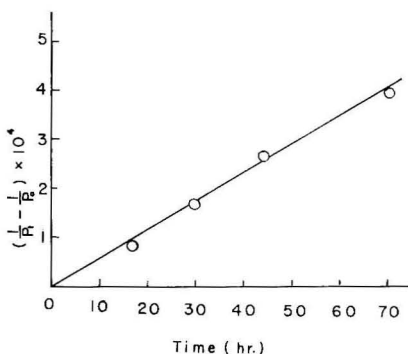


Fig. 3. Degradation at NO_2 pressure of 30 cm. Hg and 35°C .

of these samples, divided by two, gave the corresponding number-average chain lengths. A sample having the random distribution obeys the relationship (1):

$$[\eta] = K \overline{M}_n^\gamma \quad (1)$$

The parameters K and γ can be determined if the number-average molecular weights and the intrinsic viscosities for at least two samples are known. This was the case, and the number-average molecular weights for any degraded sample can be found. The unexposed sample had a weight-average molecular weight of 3.72×10^5 and the exposed sample of one of 1.57×10^5 ; their respective intrinsic viscosities were 1.067 and 0.53 dl./g. Finally the molecular weights were transformed into number-average chain lengths. The values for K and γ were 0.585×10^{-4} and 0.81, respectively.

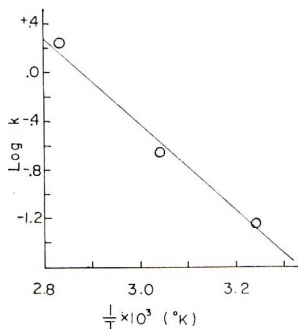


Fig. 4. Arrhenius plot for NO_2 pressure of 30 cm. Hg.

Figure 1 shows the results for exposure at 60, 30, and 15 cm. Hg NO_2 pressure at 55°C . plotted according to the random theory. Figure 2 gives the rate constants as a function of NO_2 pressure at 55°C . Figure 3 gives an example of a random plot for 30 cm. Hg of NO_2 gas at 35°C . Figure 4 shows the Arrhenius plot for 30 cm. Hg of NO_2 gas, which gives an equation as follows:

$$k = 1.66 \times 10^6 e^{-16200/RT} \text{ hr.}^{-1}$$

As the rate constants are directly proportional to the pressure, the equation can be written as:

$$k = P(5.52 \times 10^4 e^{-16200/RT}) \text{ hr.}^{-1}$$

The NO_2 pressures were measured at room temperature as centimeters of mercury while the container with the films is at the reaction temperature.

Infrared spectra of the unexposed and one exposed sample (19.5 hr., 30 cm. Hg, 80°C .) showed the presence of stretching vibrations due to the NO_2 group on an aliphatic chain in the exposed sample (aliphatic stretching vibration is located at 6.19–6.49 μ and at 7.20–7.5 8μ).⁴

DISCUSSION

The chain scission reaction is a typical random process. The most reactive point in the polystyrene molecule is the α -hydrogen atom. In a previous publication,⁶ "weak points" were postulated in polystyrene, consisting of some hydroperoxide groups which led to chain scission with a lower energy of activation than that characteristic of normal main chain links. This view has recently been substantiated by experiments with isotactic polystyrene,⁵ which do not show any weak links, but give the energy of activation for normal links from the very start of the degradation reaction.

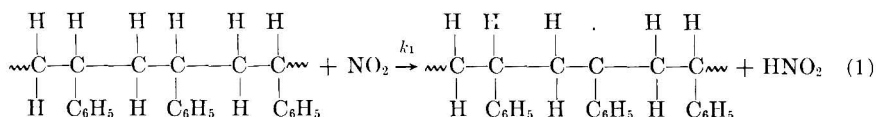
The energies of activation for bulk degradation were previously⁶ found to be as follows: 24.5 kcal./mole for weak links and 44.7 kcal./mole for normal links.

For initial rates of oxidative degradation, the energy of activation amounts to 26.2 kcal./mole.^{7,8} All these energies of activation are appreciably larger than the one obtained in the presence of NO_2 . Original weak links would, therefore, not be noticeable at relatively large and constant NO_2 pressures, but could interfere at very low pressures of NO_2 .

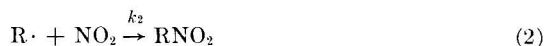
If one assumes that the same Arrhenius equation, $k = P(5.52 \times 10^4 e^{-16200/RT}) \text{ hr.}^{-1}$, can also be used for very small NO_2 pressures, one obtains, for instance, for the rate constant for a NO_2 pressure of 7.6×10^{-3} mm. Hg, with respect to health the maximum acceptable pressure in air for humans a value of $k = 5.66 \times 10^{-11} \text{ hr.}^{-1}$ at 25°C . Thus it will take 4.11×10^5 days to produce one chain scission on the average in one original

chain of the investigated sample. In the presence of daylight and oxygen, this time will probably be much shorter.

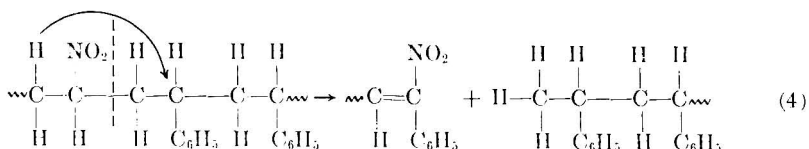
The reaction of NO_2 gas with polystyrene may be formulated on similar lines as the thermal⁶ and oxidative^{7,8} bulk degradation of polystyrene and the reaction of NO_2 gas with polyethylene, which was investigated by determining infrared spectra as functions of time and temperature.^{1,2} The initiation reaction is assumed to consist of the reaction of NO_2 with an α -hydrogen atom to form a polymer radical:



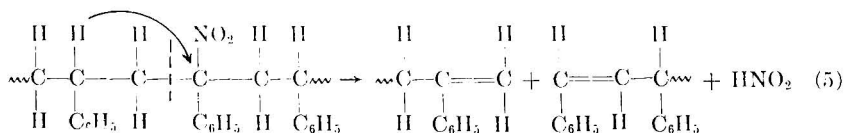
The polymer radicals may react with additional NO_2 gas, yielding nitro and nitrite groups, respectively, (where $\text{R}\cdot$ stands for the polymer radical):



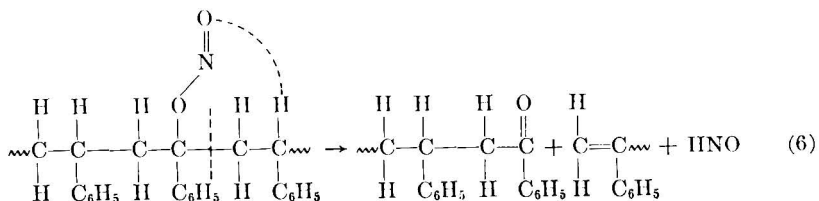
Some of these nitro and nitrite groups may lead to main chain scission, without subsequent monomer formation at low temperatures (at elevated temperatures, however, a depropagation reaction may be operative).



or



For the nitrite, one can formulate the process as shown in eqs. (6) and (7):



As already pointed out, at higher temperatures, a depropagation reaction may become operative leading to monomer and some nitrated monomer.

Termination may be first or second order.

These reactions are, of course, speculative. The infrared spectra show aliphatic nitro groups, confirming that not all of these groups lead to chain scission. The energy of activation of 16.2 kcal./mole may well be that for the abstraction of the α -hydrogen

atom, which would then be the rate-determining step.¹ Thus the rate of reaction for this case is given by

$$-d[n]/dt = k'[\alpha\text{-H}][\text{NO}_2] = k[\alpha\text{-H}]p_{\text{NO}_2} \quad (8)$$

where $[n]$ is the concentration of main-chain links at time t and $[\alpha\text{-H}]$ the concentration of α -hydrogen atoms. Equation (8) leads for moderate chain scission to:

$$(1/\overline{\text{DP}}_{n,t}) - (1/\overline{\text{DP}}_{n,0}) = kp_{\text{NO}_2} \quad (9)$$

Here

$$[n] = [\alpha\text{-H}] \cong [n_0] \quad (10)$$

where $[n_0]$ is the initial concentration of main chain links of α -hydrogen atoms, which remains practically constant for small numbers of main-chain ruptures. Equation (9) is obeyed by the experimental results. Depropagation is not considered for the temperatures employed in this work.

This work was made possible by a Grant from the Bureau of State Services, Public Health Service, Division of Air Pollution, No. 1-RO-1-AP-00486, for which the authors are grateful.

References

1. T. Ogihara, S. Tsuchiya, and K. Kuratani, *Bull. Chem. Soc. Japan*, **38**, 978 (1965).
2. T. Ogihara, *Bull. Chem. Soc. Japan*, **36**, 58 (1963).
3. R. J. Cvetanović, *J. Air Poll. Control Assoc.*, **14**, No. 6, 208 (1946).
4. R. T. Conley, *Infrared Spectroscopy*, Allyn and Bacon, Boston, 1966.
5. A. Nakajima, F. Hamada, and T. Shimuzu, *Makromol. Chem.*, **90**, 229 (1966).
6. H. H. G. Jellinek, *J. Polymer Sci.*, **3**, 850 (1948).
7. H. H. G. Jellinek, *J. Polymer Sci.*, **4**, 1 (1949).
8. H. H. G. Jellinek, *Discussions Faraday Soc.*, (The Labile Molecule), No. **2**, 402 (1947).

H. H. G. JELLINEK
Y. TOYOSHIMA

Department of Chemistry
Clarkson College of Technology
Potsdam, New York 13676

Received April 26, 1967

Revised July 12, 1967

Polymerization of β -(2-Furyl)acrolein in Solution by Ionizing Radiation

The polymerization of β -(2-furyl)acrolein derivatives by some catalysts has been reported by Usmanov et al.^{1,2} In general, polymerization of α,β -substituted ethylenic compounds is difficult except for a few monomers. Actually, polymerization of β -(2-furyl)acrolein does not occur with γ -ray irradiation in the solid state nor in the liquid state above the melting point (54°C.). We have, however, found that the monomer can be polymerized in some organic solvents by γ -ray irradiation.

Experimental

β -(2-Furyl)acrolein was synthesized from furfural and acetaldehyde^{3,4} and then purified by distillation and sublimation at reduced pressure. The mixture of the purified monomer and an organic solvent was sealed in glass ampules under vacuum (1×10^{-4} – 1×10^{-5} mm. Hg) and irradiated by γ -ray from a ⁶⁰Co source. Dose rates of 6.5–18.4 $\times 10^4$ r./hr. were employed. The solvent was evaporated quickly after the irradiation, and ethyl ether was added to the residue. The precipitated polymer was separated by centrifugation.

Results and Discussion

β -(2-Furyl)acrolein was irradiated in several organic solvents at 25 or 28°C. The results are summarized in Table I. The polymers obtained in alkyl chloride solution

TABLE I
Effect of the Type of Solvent on the Polymerization of
 β -(2-Furyl)acrolein at a Monomer Concentration of 1 g./2 cc. Solvent

Solvent	Irradiation		Dose, Mr.	Conversion, %
	temp., °C.	Dose rate \times 10^{-5} , r./hr.		
Dioxane	25	1.84	8.2	1.35
Methylene chloride	28	0.65	3.5	8.04
Chloroform	28	0.65	3.5	8.42
Carbon tetrachloride	28	0.65	3.5	2.56
<i>n</i> -Butyl chloride	28	0.65	3.5	0.94
Diethyl ketone	28	0.65	3.5	0.57
Isobutyl alcohol	28	0.65	3.5	0.61

are black or dark-brown, and the others are yellow or red. The polymers prepared in methylene chloride or chloroform are insoluble in benzene, dimethylformamide, dimethyl sulfoxide, and sulfuric acid, though the polymer prepared in dioxane is partly soluble in dioxane.

The polymerization in methylene chloride was studied by a dilatometric method at 0, 28, and 42°C. with a dose rate of 6.5×10^4 r./hr. The rate of polymerization increased with the increasing temperature. The Arrhenius plot was almost linear, and the apparent activation energy for the polymerization was 5.8 kcal./mole.

Post-irradiation polymerization was observed at 42 and 0°C. in methylene chloride solution. The monomer solution in methylene chloride was irradiated for 88 hr. at 0°C. with a dose rate of 6.5×10^4 r./hr, and then the sample was kept at the same temperature. As is seen in Figure 1, the rate of in-source polymerization increased with time, and the post-irradiation polymerization was fairly remarkable.

In the infrared spectrum of polymer prepared in alkyl chloride (polymers I and II), there are several weak bands (3120, 1560, 1510, 885 cm.^{-1}) which are due to the furan

TABLE II
Elementary Analysis Data of Polymers

	C, %	H, %	Cl, %	O, %
Polymer prepared in chloroform	69.26	4.68	2.10	23.96
Polymer prepared in methylene chloride	69.79	4.68	1.65	23.88
Monomer (calcd.)	68.86	4.92	0.00	26.22

The chlorine content indicates that fragments of the solvent molecules participate in the polymerization.

From the above results, radiation-induced polymerization of this monomer in alkyl chloride solution can be explained by assuming that the polymerization is initiated by a certain irradiation product from the solvent, probably by HCl.⁸ The assumption is supported by the following facts: (1) hardly any polymerization was observed without the solvents; (2) the polymer yield depended markedly on the type of the solvents; (3) post-irradiation polymerization was observed even in solution; (4) there was a marked acceleration in the consumption of monomer during the irradiation.

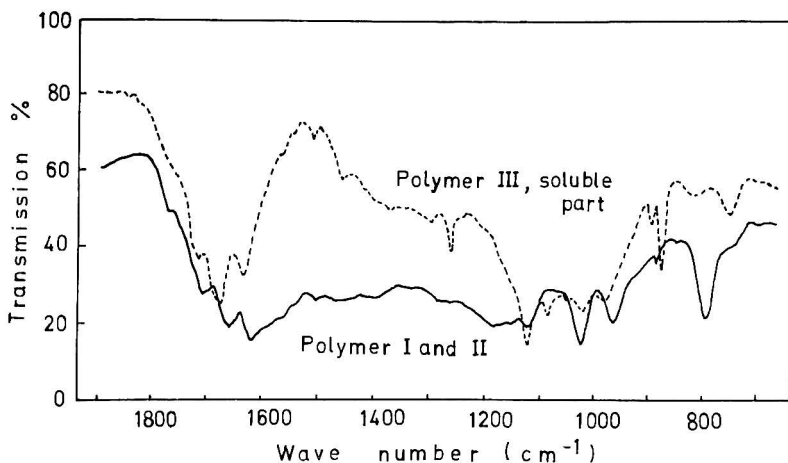


Fig. 2. Infrared spectra of β -(2-furyl)acrolein polymers. Polymer I: prepared in methylene chloride; Polymer II: prepared in chloroform; Polymer III: prepared in dioxane.

The polymer prepared in dioxane solution is partly soluble, and the infrared spectrum of this soluble polymer (polymer III, Fig. 2) is different from that of the other. The absorption bands at 870–890 and 1510 cm^{-1} may be attributed to the furan ring,⁵ which seems to suggest a linear structure of soluble polymer, while these bands disappear almost completely in the insoluble fraction, which shows the decomposition of furan ring. The mechanism of the polymerization in dioxane, diethyl ketone, and isobutyl alcohol is not clear yet, but the marked difference in color of the polymers obtained suggests that the polymerization mechanism in these solvents is different from that in alkyl chloride solutions.

References

1. Z. Usmanov, I. V. Kamenskiĭ, and M. Tadzhieva, *Uzbek. Khim. Zh.*, **7**, 76 (1963).
2. M. Tadzhieva, Z. Usmanov, and I. V. Kamenskiĭ, *Uzbek. Khim. Zh.*, **8**, 58 (1964); *Chem. Abstr.*, **61**, 12146 (1964).
3. I. F. Bel'skii, N. I. Shuikin, and R. A. Karakhanov, *Izv. Akad. Nauk SSSR Ser. Khim.*, **1964**, No. 2, 326.
4. A. Hinz, G. Meyer, and G. Schücking, *Ber.*, **76**, 681 (1943).
5. Y. Nakamura and M. Saito, *Kogyo Kagaku Zasshi*, **62**, 114 (1959).
6. R. C. Schulz, *Makromol. Chem.*, **17**, 62 (1955-1956).
7. R. C. Schulz and W. Kern, *Makromol. Chem.*, **18**, 4 (1956).
8. M. Haissinsky, *Nuclear Chemistry and its Applications*, Addison-Wesley, Reading, Mass., 1964, p. 411.

HIROMI YAMAKITA
KIYOSHI HAYAKAWA

Government Industrial Research Institute, Nagoya
Hirate-machi, Kita-ku, Nagoya, Japan

Received August 2, 1967

AUTHOR INDEX, VOLUME 5

- Aasen, J. O.: see Ugelstad, J.
- Adams, F. P., Carmichael, J. B., and Zeman, R. J.: Kinetics of non-equilibrium methylsiloxane polymerization and rearrangement, 741
- Akita, K., and Kase, M.: Determination of kinetic parameters for pyrolysis of cellulose treated with ammonium phosphate by differential thermal analysis and thermal gravimetric analysis, 833
- Alberino, L. M., Ulrich, H., and Sayigh, A. A. R.: Polysulfonamide-ureas, 3212
- Allcock, H. R.: Structural effects in heteroatom systems. II. The calculated influence of steric effects on polymerization-depolymerization equilibria in the siloxane and oxy-methylene series. Comparisons with the phosphazene system, 355
- Allen, E. E., Jr.: see BeMiller, J. N.
- Alliet, D.: Analysis of the negative peaks in gel permeation chromatography, 1783
- Amdur, S., and Shavit, N.: Kinetics and mechanism of acrylonitrile polymerization by *p*-toluenesulfonic acid. II. Polymerization mechanism, 1297
- and —: Kinetics and mechanism of acrylonitrile polymerization by *p*-toluenesulfonic acid. III. Initiation through disproportionation, 1307
- Anand, L. C., Deshpande, A. B., and Kapur, S. L.: Polymerization of styrene with the $\text{VOCl}_3\text{-AlEt}_2\text{Br}$ catalyst system, 665
- , —, and —: Polymerization of styrene with VOCl_3 -aluminum alkyls, 2079
- Anderson, C. A.: see Dyer, E.
- Anderson, W. S.: α,ω -Diols from polymerization of ethylene, 2693
- : Polymerization of 1,3-butadiene on cobalt and nickel halides, 429
- Angelo, R. J.: see Kreuz, J. A.
- Arita, K.: see Matsuzaki, K.
- Armour, M., Davies, A. G., Upadhyay, J., and Wasserman, A.: Colored electrically conducting polymers from furan, pyrrole, and thiophene, 1527
- Arnold, F. E., Cantor, S., and Marvel, C. S.: Aromatic polysulfonamides, 553
- Asahina, M.: see Kakutani, H.
- Aubrey, D. W., and Barnatt, A.: Low molecular weight by-products in the Ziegler polymerization of higher terminal olefins, 1191
- Bacskaï, R.: Cationic and free-radical polymerization of optically active 1-olefins, 619
- Bajjal, M. D.: see Blanchard, L. P.
- Baldwin, M. G., and Johnson, K. E.: Free-radical polymerization of vinyl ferrocene, 2091
- Banas, E. M., and Juveland, O. O.: NMR study of α -methylstyrene-*p*-methyl- α -methylstyrene copolymers, 397
- Barlow, A.: see Kamath, P. M.
- Barnatt, A.: see Aubrey, D. W.
- Barth, W. E.: see Kreuz, J. A.
- Bar-Zakay, S., Levy, M., and Vofsi, D.: Studies on anionic polymerization of lactams. Part III. Copolymerization of pyrrolidone and caprolactam, 965
- Bauer, R. S.: Linear polymers from diepoxides, 2192
- Beachell, H. C., and Smiley, L. H.: Oxidative degradation of polystyrene, 1635
- Bell, V. L., and Jewell, R. A.: Synthesis and properties of polyimidazopyrrolones, 3043
- BeMiller, J. N., and Allen, E. E., Jr.: Acid-catalyzed methanolysis of tri-*O*-methylamylose and tri-*O*-methylcellulose, 2133
- Berlin, A. J.: see Ketley, A. D.
- Bilbo, A. J., and Sharts, C. M.: Copolymerization of *trans*-2,6-diazidohexaphenylcyclophosphonitrile tetramer with 1,4-bis(diphenylphosphine)butane or 4,4'-bis(diphenylphosphino)biphenyl, 2891
- Bilow, N., Lawrence, R. E., and Patterson, W. J.: Synthesis and polymerization of 1,3-bis(2,3-epoxy-propylphenyl)tetramethyldisiloxanes and related compounds, 2595

- Biswas, A. M.: see Mukherjee, A. R.
- Blair, E. A.: see Price, C. C.
- Blanchard, L. P., and Baijal, M. D.:
A study of the molecular weights of tetrahydrofuran-propylene oxide copolymers by gel permeation chromatography and other methods, 2045
- Borchert, A. E.: see Field, N. D.
- Boss, C. R.: see Chien, J. C. W.
- Boyd, R. H.: Theoretical depolymerization kinetics. IV. Effect of a volatile fraction on the degradation of an initial "most probable" polymer, 1573
- Boyles, J. G., and Toby, S.: Kinetics of polymerization of gaseous formaldehyde, 1705
- Breed, L. W., Elliott, R. L., and Whitehead, M. E.: Arylene-modified siloxanes, 2745
- Brockway, C. E., and Seaberg, P. A.:
Grafting of polyacrylonitrile to granular corn starch, 1313
—, and —: Grafting of polyacrylonitrile to granular corn starch by initiation with cerium, 2967
- Brown, J. R., Gillman, G. P., and George, M. H.: Poly-1,6-diselenahexamethylene, 1,2-diselanane, and their effects on vinyl polymerizations, 903
- Bruck, S. D.: Volatile degradation products of organotin polyesters, 2458
- Buchenauer, R. L.: see Ehlers, G. F.
- Burkett, J. L.: see Ehlers, G. F.
- Burks, R. E., Jr.: see Greene, J. L., Jr.
- Burlant, W.: see Liu, K.-J.
- Burnett, G. M., Ross, F. L., and Hay, J. N.: Environmental effects in free-radical polymerizations. Part III. Vinyl chloride and *n*-butyraldehyde, 1467
- Burton, C. K.: see Parrish, C. F.
- Butler, G. B., Vanhaeren, G., and Ramadier, M.-F.: Studies in cyclocopolymerization. III. Copolymerization of divinyl ether with certain nitrogen-containing alkenes, 1265
- Byrd, J. D.: see Dunnivant, W. R.
- Caiola, R. J.: see D'Alelio, G. F.
- Calderon, N., Ofstead, E. A., and Judy, W. A.: Ring-opening polymerization of unsaturated alicyclic compounds, 2209
—, and Scott, K. W.: Polymerization of propylene oxide with a dialkylzinc-hydrazine catalyst, 917
- Campbell, D.: see Marcotte, F. B.
- , and Turner, D. T.: ESR study of radicals trapped in amorphous and crystalline samples of poly(ethylene terephthalate) after γ -irradiation, 2199
- Canter, N. H.: see Kennedy, J. P.
- Cantor, S.: see Arnold, F. E.
- Cantow, M. J. R., and Johnson, J. F.:
Gel permeation chromatography:
Effect of pore-size distribution, 2835
—, Porter, R. S., and Johnson, J. F.:
Effect of temperature and polymer type on gel permeation chromatography, 987
—, —, and —: Method of calibrating gel permeation chromatography with whole polymers, 1391
- Carmichael, J. B.: see Adams, F. P.
- Cassidy, H. G.: see Hashimoto, M.
- Chang, S.-P., Miwa, T. K., and Wolff, I. A.: Alkyl vinyl esters of brassylic (tridecanedioic) acid, 2547
- Chapman, F. W.: see Michel, R. E.
- Chiang, W.-Y.: see Iwakura, Y.
- Chien, J. C. W., and Boss, C. R.:
Polymer reactions. V. Kinetics of autoxidation of polypropylene, 2091
—, and —: Polymer reactions. VI. Inhibited autoxidation of polypropylene, 1683
- Choudhury, P. K.: see Das, B.
- Chow, R. C. L., and Marvel, C. S.:
Copolymers of methyl 12-acryloxy-stearate and vinyl chloride, 2949
- Chujo, R.: see Ohsumi, Y.
- Church, J. A.: A redox-initiated xylan-poly(sodium acrylate) graft copolymer, 3183
- Ciaperoni, A., Gechele, G. B., and Mariani, L.: Polymerization of β -isovalerolactone, 891
- Clarke, D. H.: see Suh, K. W.
- Claver, G. C.: see Cotman, J. D., Jr.
- Cleaveland, J. A.: see Marcotte, F. B.
- Clendinning, R. A.: see Hale, W. F.
—: see Johnson, R. N.
- Cohen, M. S.: see Mayes, N.
- Combs, R. L., Slonaker, D. F., Joyner, F. B., and Coover, H. W., Jr.: Influence of preparative conditions on molecular weight and stereoregularity distributions of polypropylene, 215
- Connolly, K. M.: see O'Driscoll, K. F.
- Coover, H. W., Jr.: see Combs, R. L.
- Cotman, J. D., Jr.: see Symcox, R. O.
—, Gonzalez, M. F., and Claver, G. C.:

- Studies on poly(vinyl chloride). III. The role of the precipitated polymer in the kinetics of polymerization of vinyl chloride, 1137
- Culbertson, B. M.: see Schuller, W. H.
- Cunningham, R. E.: Course of the terpolymerization of ethylene, propylene, and dicyclopentadiene. I. Single initial addition of dicyclopentadiene, 243
- : Course of the terpolymerization of ethylene, propylene, and dicyclopentadiene. II. Two-step addition of dicyclopentadiene, 251
- Curry, J. E.: see Dunnivant, W. R.
- Da Chow, C.: see Fitch, R. M.
- D'Alelio, G. F., and Caiola, R. J.: Preparation and polymerization of some vinyl monomers containing the 1,3-dioxolane group, 287
- , and Evers, R. C.: Linear polymers of acrylic monomers containing an acetylenic moiety, 813
- , and —: Linear polymers of some vinyl monomers containing a terminal acetylenic group, 999
- , and Hoffend, T. R.: Linear polymers of allyl acrylate and allyl methacrylate, 323
- , and —: Linear polymers of vinyl aryl monomers containing another unsaturated group, 1245
- , and Huemmer, T. F.: Copolymerization parameters of acrolein and acidic vinyl monomers, 77
- , and —: Preparation and polymerization of some vinyl monomers containing the 2-oxo-1,3-dioxolane group, 307
- Das, B., and Choudhury, P. K.: Molecular parameters of sodium cellulose xanthate in dilute solution, 769
- Davies, A. G.: see Armour, M.
- Delman, A. D., Kelly, J. J., Stein, A. A., and Simms, B. B.: On the thermal behavior of 4-(*o*-carboranyl)-1-butylmethyl siloxane-dimethyl siloxane copolymers, 2119
- De Schryver, F., and Marvel, C. S.: Polymers with quinoxaline units. II. 545
- Deshpande, A. B.: see Anand, L. C.
- , Subramanian, R. V., and Kapur, S. L.: Role of heterogeneous Cr-(AcAc)₃-AlEt₃ catalyst system in isoprene polymerization, 761
- De Venuto, A.: see Wiley, R. H.
- De Venuto, G.: see Wiley, R. H.
- Dietrich, H. J., Karabinos, J. V., and Raes, M. C.: Poly(chloral-1,3-dioxolane diol), 1395
- Dungan, C. H.: see Grant, D.
- Dunnivant, W. R., Markle, R. A., Stickney, P. B., Curry, J. E., and Byrd, J. D.: Synthesis of polyaryloxysilanes by melt-polymerizing dianilino- and diphenoxysilanes with aromatic diols, 707
- Dyer, E., and Anderson, C. C.: Preparation of polymeric amines from polymeric amines from poly- (Schiff bases), 1659
- Ehlers, G. F. L.: see Evers, R. C.
- , Buchenauer, R. L., and Burkett, J. L.: Poly(arylene sulfones) prepared by Friedel-Crafts reactions, 1802
- Eldred, R. J.: see Mao, T. J.
- Elliott, R. L.: see Breed, L. W.
- Empen, J. A.: see Stille, J. K.
- Empey, R.: see Wrasidlo, W.
- Evers, R. C.: see D'Alelio, G. F.
- , and Ehlers, G. F. L.: Poly-*m*-phenoxyethylene sulfonamides, 935
- , and —: Preparation and Thermal properties of some piperazine polysulfonamides, 1797
- Farnham, A. G.: see Hale, W. F.
- : see Johnson, R. N.
- Field, N. D., Kieras, J. A., and Borchert, A. E.: Polyethers. I. Polymerization of 2-methyl-2-butene oxide, 2179
- Fisher, L. P.: see Ketley, A. D.
- Fitch, R. M., and Da Chow, C.: Synthesis of an arylene/alkylene polyether from diphenolic acid and Rosenmund reduction to the polyether aldehyde, 381
- Floutz, W. V.: see Frisch, K. C.
- Friedman, M.: see Krull, L. H.
- Frisch, K. C., Reegen, S. L., Floutz, W. V., and Oliver, J. P.: Complex formation between catalysts, alcohols, and isocyanates in the preparation of urethanes, 35
- Fueno, T.: see Hayakawa, Y.
- : see Kobuke, Y.
- Fujii, S.: see Matsuda, T.
- Fukui, K.: see Kagiya, T.
- : see Yokota, H.
- Furukawa, J.: see Hayakawa, Y.
- : see Kobuke, Y.

- , Kawabata, N., and Kato, A.: Polymerization of alkylene oxides by dialkylzinc-Lewis base systems, 3139
- Gabara, W.: see Porejko, S.
- , and Porejko, S.: Grafting of maleic anhydride on polyethylene. I. Mechanism of grafting in a heterogeneous medium in the presence of radical initiators, 1547
- , and —: Grafting in reaction of polyethylene and poly(maleic anhydride), 1539
- Gaylord, N. G.: see Štěpán, V.
- Gechele, G. B.: see Ciaperoni, A.
- George, M. H.: see Brown, J. R.
- Gillman, G. P.: see Brown, J. R.
- Go, S.: see Soga, K.
- Golubeva, I. A.: see Paushkin, Ya. M.
- Gonzalez, M. G.: see Cotman, J. D., Jr.
- Gosnell, R. B.: see Hollander, J.
- Graham, R. K.: see Powell, J. A.
- Grant, D., Van Wazer, J. R., and Dungan, C. H.: α,ω -Disubstituted polymethylphosphates and polyphenylphosphates from condensation polymerization, 57
- Green, J.: see Mayes, N.
- Greene, J. L., Jr., Huffman, E. L., Burks, R. E., Jr., Sheehan, W. C., and Wolff, I. A.: Nylon 1313: Synthesis and polymerization of monomers, 391
- Haas, H. C., Schuler, N. W., and Kolesinski, H. S.: Aroyl peroxides containing reactive functional groups, 2964
- Hagiwara, M.: see Machi, S.
- : see Mitsui, H.
- Haldon, R. A., and Hay, J. N.: Dehydrochlorination reactions in polymers. Part II. Chlorinated polystyrene, 2297
- Hale, W. F.: see Johnson, R. N.
- , Farnham, A. G., Johnson, R. N., and Clendinning, R. A.: Poly(aryl ethers) by nucleophilic aromatic substitution. II. Thermal stability, 2399
- Hamada, M.: see Matsuzaki, K.
- Hamann, S. D.: Polymerization of maleic anhydride by an intense shock wave, 2939
- Hanada, T.: see Ueno, Y.
- Harada, S.: see Negi, Y.
- Harmer, D. E.: see Parrish, C. F.
- Harris, F. W.: see Mukamal, H.
- Hashimoto, M., Uno, K., and Cassidy, H. G.: Electron-transfer polymers. XXVIII. Synthesis of vinyl hydroquinone derivatives by means of the Wittig reaction, 993
- Hatta, M.: see Kagiya, T.
- Hay, J. N.: see Burnett, G. M.
- : see Haldon, R. A.
- Hayakawa, K.: see Yamakita, H.
- Hayakawa, Y., Fueno, T., and Furukawa, J.: Catalysts for asymmetric-induction polymerization of benzofuran. II. Properties and catalyses of some binary systems containing the menthoxy group, 2099
- Hayano, F.: see Iwakura, Y.
- Hayashi, K.: see Kaetsu, I.
- : see Tsuji, K.
- Heath, J. E., and Jeffries, R.: The formylation of cellulose, 2465
- Hecht, J. K., and Marvel, C. S.: Preparation of hydroxyl-terminated polysiloxanes by diborane reduction of corresponding acids, 685
- , —, and Campbell, T. W.: α,ω -Glycols from copolymers of isobutylene and 2,5-dimethyl-2,4-hexadiene, 1486
- Heller, J., and Miller, D. B.: Stereoregular polymerization of 1-vinylnaphthalene, 2-vinyl-naphthalene, and 4-vinylbiphenyl, 2323
- Hergenrother, P. M., and Levine, H. H.: Phenyl-substituted polyquinoxalines, 1453
- Hermann, H.: See Rösinger, S.
- Herp, A.: see Rickards, T.
- Higashimura, T.: see Kusudo, S.
- : see Miki, T.
- : see Ohsumi, Y.
- , Tanaka, A., Miki, T., and Okamura, S.: Copolymerization of tetraoxane with styrene catalyzed by $\text{BF}_3\cdot\text{O}(\text{C}_2\text{H}_5)_2$, 1937
- , —, —, and —: Copolymerization of trioxane with styrene catalyzed by $\text{BF}_3\cdot\text{O}(\text{C}_2\text{H}_5)_2$, 1927
- Hillman, J. J.: see Stille, J. K.
- Hirayama, T.: see Matsuda, M.
- Hladký, E.: see Kučera, M.
- Hoffend, T. R.: see D'Alelio, G. F.
- Hoffman, D. J.: see Whistler, R. L.
- Hollander, J.: Trischler, F. D.
- , Trischler, F. D., and Gosnell, R. B.: Synthesis of polyurethanes from fluorinated diisocyanates, 2757
- Hornyak, J.: see Prince, M.
- Hosoi, F.: see Mitsui, H.
- Hsu, L.-C.: see Kovacic, P.

- Hudgin, D. E.: see McCain, G. H.
Huemmer, T.: see D'Alelio, G. F.
Huffman, E. L.: see Greene, J. L., Jr.
Husar, A.: see O'Driscoll, K. F.
Ichida, T.: see Kagiya, T.
Ichikura, Y.: see Iwakura, Y.
Ide, F.: see Joh, Y.
Ikeda, K.: see Tohyama, S.
—: see Yoda, N.
Imai, Y.: Aromatic polyhydantoin from bisiminoacetate and diisocyanates, 2289
—: see Joh, Y.
Inami, A.: see Morimoto, K.
Indictor, N., and Linder, C.: Applications of limiting conversion free-radical polymerizations. I. *tert*-butyl hydroperoxide-initiated polymerization of styrene, in benzene, 1101
—, Mogolesko, P., and Jaffe, H.: Applications of limiting conversion free-radical polymerizations. II. Azobisisobutyronitrile-initiated polymerization of methyl methacrylate in benzene, 1107
Ishida, A.: see Matsuzaki, K.
Ishida, E.: see Morimoto, K.
Ishida, S., and Saito, S.: Polymerization of itaconic acid derivatives, 689
Ishizuka, O.: see Negi, Y.
Ishihara, A.: Comments on the theories of the intrinsic viscosity of chain polymers, 2883
Iwahori, K.: see Shibukawa, T.
Iwakura, Y.: see Uno, K.
—, Nabeya, A., Hayano, F., and Kurita, K.: Polyoxazolidones, 1865
—, Nakabayashi, N., Sagara, K., and Ichikura, Y.: Hydrogen-transfer polymerization of cinnamide, 675
—, Toda, F., and Suzuki, H.: Synthesis and polymerization of *N*-[1-(1-substituted-2-oxopropyl)]acrylamides and -methacrylamides. Copolymerization of these monomers with styrene and substituent effects, 1599
—, —, Torii, Y., and Sekii, R.: Base-catalyzed polymerization of acryloyl- and methacryloyl- α -amino acid amides, 1585
—, Uno, K., Nakabayashi, N., and Chiang, W.-Y.: Reactive fiber. V. Preparation and polymerization of *p*-styrenesulfonyl(β -chloroethyl)-amide, 3193
—, —, and Oya, M.: Polymerization of DL-alanine NCA and L-alanine NCA, 2867
Iwamoto, T.: see Tsuji, K.
Iwatsuki, S., and Yamashita, Y.: Studies on the charge-transfer complex and polymerization. Part XIII. Dilution and solvent effects in radical terpolymerization, 1753
Izu, M.: see Kagiya, T.
Izumi, Z.: Emulsion polymerization of acrylonitrile. Part II. Mechanism of emulsion polymerization of acrylonitrile, 469
—, and Kitagawa, H.: Effect of reaction medium on copolymerization of acrylonitrile and methyl acrylate, 1967
—, Kiuchi, H., and Watanabe, M.: Emulsion polymerization of acrylonitrile. Part I. Role and effect of emulsifiers in the emulsion polymerization of acrylonitrile, 455
Jaffe, H.: see Indictor, N.
Jain, R. K.: see Nanda, V. S.
Jarovitzky, P. A.: see Overberger, C. G.
Jedlínski, Z., and Paprotny, J.: Synthesis and polymerization studies of some *N*-alkylolacrylamides. III. Polymerization of 2-methacrylamide-2-methyl-propanediol-1,3 and 2-methacrylamide-2-methylpropanol-1, 2957
Jeffries, R.: see Heath, J. E.
Jellinek, H. H. G., and Toyoshima, Y.: Reaction of nitrogen dioxide with polystyrene films, 3214
Jerina, D. M.: see Letsinger, R. L.
Jewell, R. A.: see Bell, V. L.
Joh, Y., Kotake, Y., Yoshihara, T., Ide, F., and Nakatsuka, K.: Stereospecific polymerization of methacrylonitrile. I. Characterization of crystalline polymethacrylonitrile, 593
—, —, —, and —: Stereospecific polymerization of methacrylonitrile. II. Influence of polymerization conditions on polymerization and on properties of polymers, 605
—, Yoshihara, T., Kotake, Y., Imai, Y., and Kurihara, S.: Stereospecific polymerization of methacrylonitrile. III. Some new catalysts for isotactic polymethacrylonitrile, 2503
Johnson, J. F.: see Cantow, M. J. R.
Johnson, K. E.: See Baldwin, M. G.
Johnson, R. N.: see Hale, W. F.

- , and Farnham, A. G.: Poly(aryl ethers) by nucleophilic aromatic substitution. III. Hydrolytic side reactions, 2415
- , —, Clendinning, R. A., Hale, W. F., and Merriam, C. N.: Poly(aryl ethers) by nucleophilic aromatic substitution. I. Synthesis and properties, 2375
- Joyner, F. B.: see Combs, R. L.
- Judy, W. A.: see Calderon, N.
- Juveland, O. O.: see Banas, E. M.
- Kaetsu, I., Tsuji, K., Hayashi, K., and Okamura, S.: Radiation-induced solid-state polymerization in binary systems. IV. Solid-state polymerization in the glassy phase, 1899
- Kagiya, T.: see Machi, S.
- : see Mitsui, H.
- : see Yokota, H.
- , Ichida, T., Narisawa, S., and Fukui, K.: Radical-initiated copolymerization of carbon monoxide and ethylenimine in the presence of ethylene, 2031
- , Izu, M., Hatta, M., Matsuda, T., and Fukui, K.: Synthesis of polyamides by the polyaddition of bisimidazoline with dicarboxylic acids, 1129
- , —, Kawai, S., and Fukui, K.: Radiation-induced bulk polymerization of maleimide, 1415
- , —, Matsuda, T., and Fukui, K.: Synthesis of polyamides by the polyaddition of bisuccinimides with diamines, 15
- , Maruta, I., Ichida, T., Narisawa, S., and Fukui, K.: Influence of addition of olefins on the alternating copolymerization of carbon monoxide and ethylenimine by azobisisobutyronitrile or by γ -ray irradiation, 1645
- , Nakayama, T., Nakai, Y., and Fukui, K.: Isomerization polymerization of 2-vinyl-1,3-dioxolane by α,α -azobisisobutyronitrile or by γ -ray irradiation, 2351
- Kakutani, H., and Asahina, M.: Dielectric properties of vinylidene chloride-vinyl chloride copolymers, 1717
- Kamachi, M., and Miyama, H.: Effect of ethyl monochloroacetate on the cationic polymerization of styrene catalyzed by rhenium pentachloride, 3207
- Kamath, P. M., and Barlow, A.: Quantitative determination of short branches in high-pressure polyethylene by gamma radiolysis, 2023
- Kamogawa, H.: Redox behavior in photosensitized crosslinking of vinyl polymers containing *N*-hydroxymethylacrylamide as a component, 2705
- Kapur, S. L.: see Anand, L. C.
- : see Deshpande, A. B.
- Kar, I.: see Palit, S. R.
- Karabinos, J. V.: see Dietrich, H. J.
- Kasabo, T.: see Ueno, Y.
- Kase, M.: see Akita, K.
- Kasuya, T.: see Minoura, Y.
- Kataoka, T., and Ueda, S.: Viscosity of polydimethylsiloxane blends, 3071
- Kato, A.: see Furukawa, J.
- Kawabata, N.: see Furukawa, J.
- Kawamura, S.: see Minoura, Y.
- Keii, T.: see Soga, K.
- Kelly, J. J.: see Delman, A. D.
- Kennedy, J. P., and Canter, N. H.: Aspects of cationic polymerization of isobutene with butadiene and isoprene, 2455
- , and —: Effect of temperature on diene incorporation into isobutylene-diene copolymers, 2712
- Kern, W.: see Schnecko, H.
- Ketley, A. D., Berlin, A. J., and Fisher, L. P.: Rearrangements of the propagating chain end in the cationic polymerization of vinylcyclopropane and related compounds, 227
- Kieras, J. A.: see Field, N. D.
- Kise, S.: see Machi, S.
- Kishimoto, A., and Kitahara, T.: Differential permeation and absorption of water vapor in polyacrylamide film, 2147
- Kitagawa, H.: see Izumi, Z.
- Kitahara, T.: see Kishimoto, A.
- Kiuchi, H.: see Izumi, Z.
- Kobayashi, K.: see Sumitomo, H.
- Kobuke, Y., Furukawa, J., and Fueno, T.: Relative reactivities of the *cis* and *trans* crotonic compounds in anionic polymerization, 2701
- Kohn, D. H.: see Narkis, M.
- Kolesinski, H. S.: see Haas, H. C.
- Kolinský, M.: see Štokr, J.
- Komoto, H.: see Saotome, K.
- Kondo, M.: see Yokota, H.
- Konen, T. P.: see O'Driscoll, K. F.
- Kössler, I.: see Štěpán, V.
- Kösters, B.: see Overberger, C. G.
- Kotake, Y.: see Joh, Y.

- Kovacic, P., Uchic, J. T., and Hsu, L.-C.: Polymerization of aromatic nuclei.
XII. Oligomerization of halobenzenes by aluminum chloride-cupric chloride, 945
- Kovács, J., and Marvel, C. S.: New synthetic route to α -alkylacrylonitriles and a study of their homopolymerization and copolymerization reactions, 563
—, and —: Synthesis of 1,4,5,6,7,7-hexachloro- and hexabromo-bicyclo-[2,2,1]-5-heptene-2-carboxylic acid vinyl esters and copolymerization with acrylonitrile, 1279
- Koyano, T.: see Tsutsui, M.
- Kreuz, J. A., Angelo, R. J., and Barth, W. E.: Hydrolysis of some aromatic cyclic anhydrides, 2961
- Krull, L. H., and Friedman, M.: Anionic graft polymerization of methyl acrylate to protein functional groups, 2535
- Kubota, H.: see Ogiwara, Y.
—, and Morawetz, H.: Polymerization of gaseous diazomethane on silicone grease, 585
- Kubota, K.: Xylene-stream method for obtaining thin polyethylene specimens for electron microscopy, 1179
- Kučera, M., Hladký, E., and Majerová, K.: Kinetics of the bulk polymerization of dioxolane in the presence of water, 1881
—, —, and —: Kinetics of the solution polymerization of dioxolane in the presence of water, 1889
- Kulesza; see Porejko, S.
- Kuntz, I.: The initiation process in the polymerization of tetrahydrofuran with carbonium ion salts, 193
- Kurihara, M.: see Tohyama, S.
—: see Yoda, N.
—, and Yoda, N.: Cyclopolycondensations. V. New high-temperature aromatic polyquinazolinediones by solution polymerization in poly(phosphoric acid), 1765
- Kurihara, S.: see Joh, Y.
- Kurita, K.: see Iwakura, Y.
- Kuroda, T.: see Ohsumi, Y.
- Kusudo, S.: see Mizote, A.
- L'Abbe, G., and Smets, G.: Polymerization of methyl methacrylate with butyllithium-diethylzinc complex, 1359
- Lal, J., and McGrath, J. E.: Identification of volatile products produced during the peroxide vulcanization of poly(vinyl alkyl ethers), 785
—, —, and —: Effect of temperature and solvents on stereospecific polymerization of vinyl alkyl ethers catalyzed by aluminum sulfate-sulfuric acid complex, 795
- Landis, W. R.: see Perrine, T. D.
- Laurence, R. L., and Slattery, J. C.: Diffusion in ethylene-propylene rubber, 1327
- Lawrence, R. E.: see Bilow, N.
- Lawrence, R. V.: see Schuller, W. H.
- Letsinger, R. L., and Jerina, D. M.: Reactivity of ester groups on insoluble polymer supports, 1977
- Levine, H. H.: see Hergenrother, P. M.
- Levy, M.: see Bar-Zakay, S.
—: see Saunders, T. F.
- Li, G. T. C.: see Winston, A.
- Liepins, R., and Marvel, C. S.: Homopolymers and copolymers of acrylates and methacrylates of homoterpenylmethyl carbinol and α -campholenol, 1489
—, and —: Reaction of triethyl phosphite with vinyl esters, 2453
—, —, and Lyon, C. K.: Polymers of the vinyl esters of perchlorocyclopentadiene adducts of petroselinic and oleic acids, 1809
—, —, and Magne, F. C.: Homopolymers and vinyl chloride copolymers of vinyl esters of chlorinated fatty acids from *Umbelliferae* and *Limnanthes douglasii*, 2899
—, —, and —: Vinyl chloride acrylate of methoxy poly(ethylene glycol) copolymers, 2946
- Lím, D.: see Štokr, J.
- Linder, C.: see Indictor, N.
- Lini, D. C.: see Ramey, K. C.
- Lintz, W.: see Schnecko, H.
- Lipscomb, N. T., and Weber, E. C.: Kinetics of the γ -radiation-induced polymerization of methyl methacrylate in the solid state, 779
- Liu, K.-J., and Burlant, W.: High-resolution NMR of crosslinked polymers: Effects of crosslinked density and solvent interaction, 1407
- Lumin, A. F.: see Paushkin, Ya. M.
- Lyon, C. K.: see Liepins, R.
- MacCallum, J. R., and Werninck, A.: Kinetics of bulk polymerization of trimeric phosphonitrilic chloride, 3061

- Machi, S.: see Mitsui, H.
- , Kise, S., Hagiwara, M., and Kagiya, T.: Mechanisms of propagation, transfer, and short-chain branching reactions in the free-radical polymerization of ethylene, 3115
- Machus, F. F.: see Paushkin, Ya. M.
- Magne, F. C.: see Liepins, R.
- Maiti, S.: see Mukherjee, A. R.
- , and Saha, M. K.: Detection and incorporation of amino endgroups in free-radical polymerization of methyl methacrylate, 151
- Majerová, K.: see Kučera, M.
- Makishima, K.: see Miyasaka, K.
- Makita, M.: see Uno, K.
- Mao, T. J.: see Michel, R. E.
- , and Eldred, R. J.: Photopolymerization initiated by triphenylphosphine, 1741
- Marcotte, F. B., Campbell, D., Cleveland, J. A., and Turner, D. T.: Photolysis of poly(ethylene terephthalate), 481
- Mariani, L.: see Ciaperoni, A.
- Markle, R. A.: see Dunnivant, W. R.
- Markov, Yu. Ya.: see Paushkin, Ya. M.
- Martin, L. F., and Rowland, S. P.
- Gel permeation properties of cellulose, I. Preliminary comparison of unmodified and crosslinked, decrystallized cotton cellulose, 2563
- Maruta, I.: see Kagiya, T.
- Marvel, C. S.: see Arnold, F. E.
- : see Chow, R. C. L.
- : see De Schryver, F.
- : see Hecht, J. K.
- : see Kovács, J.
- : see Liepins, R.
- : see Narayan, T. V. L.
- : see Neufeld, C. H. H.
- : see Sowa, J. R.
- Matsuda, M., and Hirayama, T.: Polymerization initiated by an electron donor-acceptor complex. Part I. Polymerization of methyl methacrylate initiated by liquid sulfur dioxide-pyridine complex in the presence of carbon tetrachloride, 2769
- Matsuda, T.: see Kagiya, T.
- , and Fujii, S.: Radiation-induced polymerization of 1,1,2-trichlorobutadiene, 2617
- Matsuzaki, K., Hamada, M., and Arita, K.: Stereoregularity of poly(vinyl ether), 1233
- , Uryu, T., Ishida, A., Ohki, T., and Takeuchi, M.: Stereoregularity of poly(methyl acrylate), 2167
- , and Yasukawa, T.: Mechanism of stereoregular polymerization of butadiene by homogeneous Ziegler-Natta catalysts. I. Effects of the species of transition metals, 511
- , and —: Mechanism of stereoregular polymerization of butadiene by homogeneous Ziegler-Natta catalysts. II. Effects of the nature of bases and halogens, 521
- Mayes, N., Green, J., and Cohen, M. S.: Carborane polymers, IV. Polysiloxanes, 365
- McCain, G. H., Hudgin, D. E., and Rosen, I.: Poly(chloroaldehydes). IV. Copolymerization of chloral and dichloroacetaldehyde catalyzed by organometallic compounds, 975
- McGrath, J. E.: see Lal, J.
- McGuchan, R., and McNeill, I. C.: Radiochemical determination of low unsaturations in polyisobutene. Stoichiometry of the reaction between chlorine and branched double bonds, 1425
- McNeill, I. C.: see McGuchan, R.
- Meller, A.: Some considerations of the kinetics of the acid hydrolysis of poly- and oligosaccharides. Part III. The disaccharides 2-O-(α -D-glucopyranosyluronic acid)-D-xylose, and 2-O-(4-O-methyl- α -D-glucopyranosyluronic acid)-D-xylose, and 2-O-(4-O-methyl- α -D-glucopyranosyl)-D-xylitol, 1443
- Merriam, C. N.: see Johnson, R. N.
- Metz, D. J., Potter, R. C., and Thomas, J. K.: Pulse radiolysis studies of styrene, 877
- Meyer, V. E.: Reactivity ratios of styrene and methyl methacrylate at 90°C., 1289
- Meyersen, K., and Wang, J. Y. C.: Chemical modifications of polycyclopentadiene, 725
- , and —: Cyclocopolymerization of bicyclopentene and other dicyclic dienes with sulfur dioxide to fused ring systems, 1827
- , and —: Cyclocopolymerization of dicyclic dienes and maleic anhydride to fused ring systems, 1845

- Michel, R. E., Chapman, F. W., and Mao, T. J.: Decay of the ESR signal in ultraviolet-irradiated poly(methyl methacrylate), 677
- Michel, R. H.: Polymerization of 9-ethynylanthracene, 920
- Miki, T.: see Higashimura, T.
- , Higashimura, T., and Okamura, S.: Changes in concentration of tetraoxane produced during the solution polymerization of trioxane catalyzed by $\text{BF}_3 \cdot (\text{C}_2\text{H}_5)_2$, 2977
- , —, and —: Effect of solvent on the amount of tetraoxane produced in the solution polymerization of trioxane catalyzed by $\text{BF}_3 \cdot \text{O}(\text{C}_2\text{H}_5)_2$, 2989
- , —, and —: Polymerization of tetraoxane at low concentration catalyzed by $\text{BF}_3 \cdot \text{O}(\text{C}_2\text{H}_5)_2$, 2997
- , —, and —: Rates of polymer formation and monomer consumption in the solution polymerization of trioxane catalyzed by $\text{BF}_3 \cdot \text{O}(\text{C}_2\text{H}_5)_2$, 95
- Miller, D. B.: see Heller, J.
- Minoura, Y.: see Ueno, Y.
- , Kasuya, T., Kawamura, S., and Nakano, A.: Block copolymerization of methyl methacrylate with poly(ethylene oxide) radicals formed by high-speed stirring, 43
- , Shiina, K., and Yoshikawa, K.: Synthesis of poly-3,3-bis(chloromethyl)oxacyclobutane (penton) derivatives, 2843
- , Tadokoro, T., and Suzuki, Y.: Radical copolymerization of crotonyl compounds with styrene, 2641
- , Urayama, S., and Noda, Y.: Syntheses of optically active polymers by condensation polymerization of *d*-tartaric acid with some diamines, 2441
- Mitsui, H., Machi, S., Hagiwara, M., Hosoi, F., and Kagiya, T.: Effect of oxygen on the γ -radiation-induced polymerization of ethylene, 2731
- , —, —, and —: Mechanism of initiation in the γ -radiation-induced polymerization of ethylene, 1073
- Miwa, T. K.: see Chang, S.-P.
- Miyama, H.: see Kamachi, M.
- Miyasaka, K., and Makishima, K.: Transition of nylon 6 γ -phase crystals by stretching in the chain direction, 3017
- Mizote, A., Kusudo, S., Higashimura, T., and Okamura, S.: Cationic polymerization of α,β -disubstituted olefins. Part II. Cationic polymerization of propenyl *n*-butyl ether, 1727
- Mogolesko, P.: see Indictor, N.
- Molau, G. E.: Computer program for calculations and automatic data plotting in binary copolymerization, 401
- Monahan, A. R.: Photochemistry of poly(*tert*-butyl acrylate). Effect of ester spatial conformation on the cyclo-elimination process, 2333
- Moore, D. E.: Emulsion polymerization of vinyl stearate, 2665
- Morawetz, H.: see Kubota, H.
- Mori, S., and Okazaki, K.: Direct determination of ϵ -caprolactam in the presence of nylon 6 and its oligomers by infrared spectroscopy, 231
- Morimoto, K., Ishida, E., and Inami, A.: Organic photoconductors. VIII. Photoconductors obtained from the reaction products of poly(9-vinyl anthracene), 1699
- Morimoto, M.: see Teramoto, A.
- Mörk, P. C.: see Ugelstad, J.
- Mukamal, H.: see Overberger, C. G.
- , Harris, F. W., and Stille, J. K.: Diels-Alder polymers. III. Polymers containing phenylated phenylene units, 2721
- Mukherjee, A. R., Pal, R. (Mitra), Biswas, A. M., and Maiti, S.: Redox-initiated vinyl polymerization with thiourea as the reductant, 135
- Murano, M.: see Yamadera, R.
- , and Yamadera, R.: Studies on tacticity of polyacrylonitrile. II. High-resolution nuclear magnetic resonance spectra of 2,4-dicyanopentanes, 1855
- Murata, K.: Polymerization of *N*-vinylphthalimide by γ -ray radiation, 2942
- : see Terada, A.
- Nabeya, A.: see Iwakura, Y.
- Nakabayashi, N.: see Iwakura, Y.
- Nakai, Y.: see Kagiya, T.
- Nakanishi, R.: see Yoda, N.
- Nakano, A.: see Minoura, Y.
- Nakatsuka, K.: see Joh, Y.
- Nakayama, T.: see Kagiya, T.
- Nakayama, Y., and Smets, G.: Radical and Anionic homopolymerization of maleimide and *N*-*n*-butylmaleimide, 1619

- Nanda, V. S., and Jain, R. K.: Effect of impurities and the initiation and transfer rate constants on the statistical character of anionic polymers, 2269
- Nandi, U. S.: see Raghuram, P. V. T.
- Narayan, T. V. L., and Marvel, C. S.: Polybenzimidazoles. VI. Polybenzimidazoles containing aryl sulfone linkages, 1113
- Narisawa, S.: see Kagiya, T.
- Narkis, M., and Kohn, D. H.: Copolymerization of styrene. II. Emulsion copolymerization with styrene derivatives containing nitrile groups in the side chain, 1033
- , and —: Copolymerization of styrene. III. Physical and mechanical properties of copolymers with styrene derivatives containing nitrile groups in the side chain, 1049
- Needles, H. L.: Crosslinking of gelatin by aqueous peroxydisulfate, 1
- Negi, Y., Harada, S., and Ishizuka, O.: Cyclocopolymerization of diallylamine derivatives in dimethyl sulfoxide, 1951
- Negishi, S., and Tamura, Y.: Polymerization of vinylbenzamides, 2911
- Neufeld, C. H. H., and Marvel, C. S.: Synthesis and evaluation of a series of regular polyampholytes, 537
- Ninomiya, T.: see Uno, K.
- Nishijima, Y.: see Teramoto, A.
- Nisova, S. A.: see Paushkin, Ya. M.
- Noda, Y.: see Minoura, Y.
- O'Driscoll, K. F., Konnen, T. P., and Connolly, K. M.: Kinetics of Polymerization of styrene initiated by substituted benzoyl peroxides. IV. Decomposition induced by substituted diethylanilines, 1789
- , Wertz, W., and Husar, A.: Influence of intrachain interactions on the kinetics of styrene polymerization and copolymerization, 2159
- Ofstead, E. A.: see Calderon, N.
- Ogiwara, Y., Ogiwara, Y., and Kubota, H.: Effects of carbonyl and aldehyde groups in the graft copolymerization of methyl methacrylate on cellulose with a ceric salt, 2791
- Ohki, T.: see Matsuzaki, K.
- Ohsumi, Y., Higashimura, T., and Okamura, S.: NMR studies on the stereospecific polymerization of methyl vinyl ether. Part I. Polymerization by metal halides: Penultimate effect, 849
- , —, —, Chujo, R., and Kuroda, T.: Diisotacticity of poly(methyl propenyl ether) and double-bond opening of methyl propenyl ether in cationic polymerization, 3009
- Okamura, S.: see Higashimura, T.
- : see Kaetsu, I.
- : see Kusudo, S.
- : see Miki, T.
- : see Ohsumi, Y.
- : see Tazuke, S.
- Okazaki, K.: see Mori, S.
- Oliver, J. P.: see Frisch, K. C.
- Omarov, O. Yu.: see Paushkin, Ya. M.
- Onozuka, M.: Mechanism of thermal stabilizers for poly(vinyl chloride). II. Synergistic effect of combination of metal soaps, 2229
- Otsuka, Y.: see Yokota, H.
- Overberger, C. G., Jarovitzky, P. A., and Mukamal, H.: Mechanism of Ziegler-Natta polymerization of propylene and α -*d*-propylene, 2487
- , Kösters, B., and St. Pierre, T.: Synthesis of 5(6)-vinylbenzimidazole and of 2-vinylbenzimidazole, 1987
- Owens, F. H.: see Powell, J. A.
- Oya, M.: see Iwakura, Y.
- Pal, R. (Mitra): see Mukherjee, A. R.
- Palit, S. R., and Kar, I.: Polynomial expansion of log relative viscosity and its application to polymer solutions, 2629
- Paprotny, J.: see Jedlínski, Z.
- Parrish, C. F., and Harmer, D. E.: Solid-state polymerization of 1,2,3,4-diepoxybutane initiated by cobalt-60 γ -radiation, 1015
- , Trinler, W. A., and Burton, C. K.: Solid-state polymerization studies. I. 2-vinylnaphthalene post-polymerization initiated by ^{60}Co γ -irradiation, 2557
- Patalakh, I. I.: see Paushkin, Ya. M.
- Patterson, W. J.: see Bilow, N.
- Paushkin, Ya. M., Vishnyakova, T. P., Nisova, S. A., Lunin, A. F., Omarov, O. Yu., Markov, Yu. Ya., Machus, F. F., Golubeva, I. A., Polak, L. S., Patalakh, I. I., Stychenko, V. A., and Sokolinskaya, T. A.: Some new polymeric semiconductors, 1203
- Peebles, L. H.: On the chromophore of polyacrylonitrile, 2637

- Perrine, T. D., and Landis, W. R.: Analysis of polyethylenimine by spectrophotometry of its copper chelate, 1993
- Peyser, P., Tutas, D. J., and Stromberg, R. R.: Conformation of polyesters adsorbed on solid surfaces, 651
- Pigman, W.: see Rickards, T.
- Pittman, C. U., Jr.: Organometallic polymers. I. Synthesis of ferrocene-containing poly(phosphine oxides) and poly(phosphine sulfides), 2927
- Polak, L. S.: see Paushkin, Ya. M.
- Porejko, S.: see Gabara, W.
- , Gabara, W., and Kulesza, J.: Grafting of maleic anhydride on polyethylene. II. Mechanism of grafting in a homogeneous medium in the presence of radical initiators, 1563
- Porter, R. S.: see Cantow, M. J. R.
- Potter, R. C.: see Metz, D. J.
- Powell, J. A., Whang, J. J., Owens, F. H., and Graham, R. K.: Post-lactonization of vinyl polymers containing pendent ester and hydroxymethyl groups, 2655
- Preston, J., and Black, W. B.: New high temperature polymers. VI. Ordered heterocycle copolymers, 2429
- Price, C. C., and Blair, E. A.: Polymerization of thietane, 171
- , Spector, R., and Tumolo, A. L.: Head-to-head units in poly(propylene oxide) by ozonation, 407
- , and Tumolo, A. L.: Isotactic sequence lengths by ozonation of poly(propylene oxide), 175
- Prince, M., and Hornyak, J.: High-Pressure reactions. II. γ -Ray polymerization of acrylamide, 531
- , and —: High-pressure reactions. III. Hydrolysis of polyacrylonitrile, 161
- Raes, M. C.: see Dietrich, H. J.
- Raghuram, P. V. T., and Nandi, U. S.: Studies on the polymerization of ethyl acrylate. I. Kinetic studies, 2005
- Ramadier, M.-F.: see Butler, G. B.
- Ramey, K. C., Lini, D. C., and Statton, G. L.: NMR study of poly(vinyl formate), 257
- Rao, S. P., and Santappa, M.: Graft polymers: Chain transfer and branching, 2681
- Reader, A. M., and Rulison, R. N.: Elastomers based on cyclohexylidene bisphenol polycarbonates, 927
- Reegen, S. L.: see Frisch, K. C.
- Refojo, M. F.: Hydrophobic interaction in poly(2-hydroxyethyl methacrylate) homogeneous hydrogel, 3103
- Rickards, T., Herp, A., and Pigman, W.: The kinetics of depolymerization of hyaluronic acid by L-ascorbic acid, and the inhibition of this reaction by anions of the lyotropic series, 931
- Riggs, J. P., and Rodriguez, F.: Persulfate-initiated polymerization of acrylamide, 3151
- , and —: Polymerization of acrylamide initiated by the persulfate-thiosulfate redox couple, 3167
- Rijke, A. M., and Taylor, G. L.: Stress-strain behavior of swollen polymeric networks, 1433
- Rodia, J. S.: Role of *para*-substituted phenols in curing resole-type phenolic resins, 2807
- Rodriguez, F.: see Riggs, J. P.
- Rosen, I.: see McCain, G. H.
- Rösinger, S., Hermann, H., and Wiessermel, K.: Copolymerization of trioxane by γ -radiation, 183
- Ross, F. L.: see Burnett, G. M.
- Rowland, S. P.: see Martin, L. F.
- Rubin, I. D.: Homopolymerization of ethylene and copolymerization with 1-butene in the presence of bis(cyclopentadienyl)titanium dichloride and diisobutylaluminum chloride, 1119
- Rulison, R. N.: see Reader, A. M.
- Ryska, M.: see Štokr, J.
- Saha, M. K.: see Maiti, S.
- Saito, S.: see Ishida, S.
- Sandler, S. R.: Preparation of mono and poly-2-oxazolidones from 1,2-epoxides and isocyanates, 1481
- Santappa, M.: see Rao, S. P.
- : see Venkatarao, K.
- Saotome, K., and Komoto, H.: *N*-Alkyl-substituted polyamides and copolyamides having long methylene chain units, 107
- , and —: Polyurethanes and polyureas having long methylene chain units, 119
- Saunders, F. L.: Crystalline poly-*p*-*tert*-butylstyrene, 2187
- Saunders, T. F., Levy, M. F., and Serino, J. F.: Mechanism of the tertiary amine-catalyzed dicyandiamide cure of epoxy resins, 1609

- Sawanda, H.: Thermodynamics of polymerization. Part IV. Free energy changes of binary copolymerization systems, 1383
- Sayigh, A. A. R.: see Alberino, L. M.
- Schnecko, H., Lintz, W., and Kern, W.: Polymerization with heterogeneous metalorganic catalysts. VI. Differences in polymerization activity of α -olefins and some kinetic results on butene-1 polymerization, 205
- Schneider, B.: see Štokr, J.
- Schuler, N. W.: see Haas, H. C.
- Schuller, W. H., Lawrence, R. V., and Culbertson, B. M.: Some polyimide-amides from maleopimaric acid, 2204
- Scott, K. W.: see Calderon, N.
- Seaberg, P. A.: see Brockway, C. E.
- Seely, T.: Hydrodynamics of a porous sphere molecule, 3029
- Segara, K.: see Iwakura, Y.
- Sekii, R.: see Iwakura, Y.
- Serino, J. F.: see Saunders, T. F.
- Sharts, C. M.: see Bilbo, A. J.
- Shavit, N.: see Amdur, S.
- Sheehan, W. C.: see Greene, J. L., Jr.
- Shibasaki, Y.: Boundary effect on the thermal degradation of copolymers, 21
- Shibukawa, T., Sone, M., Uchida, A., and Iwahori, K.: Endgroup study of chlorate-sulfite-initiated acrylonitrile copolymer, 2857
- Shiina, K.: see Minoura, Y.
- Simms, B. B.: see Delman, A. D.
- Slattery, J. C.: see Laurence, R. L.
- Slonaker, D. F.: see Combs, R. L.
- Smets, G.: see L'Abbe, G.
—: see Nakayama, Y.
- Smiley, L. H.: see Beachell, H. C.
- Soga, K., Takano, Y., Go, S., and Keii, T.: Influence of SeOCl_2 on the polymerization of propylene by $\text{TiCl}_3\text{-Al}(\text{C}_2\text{H}_5)_3$, 2815
- Sokolinskaya, T. A.: see Paushkin, Ya. M.
- Sone, M.: see Shibukawa, T.
- Sowa, J. R., and Marvel, C. S.: Polymerization of methyl 12-acryloxystearate, *N,N*-dimethyl 12-acryloxystearamide, and methyl 14-acryloxyeicosanoate, 1501
- Spector, R.: see Price, C. C.
- Stannett, V.: see Wellons, J. D.
- Statton, G. L.: see Ramey, K. C.
- Stein, A. A.: see Delman, A. D.
- Štěpán, V., Vodehnal, J., Kössler, I., and Gaylord, N. G.: Cyclo- and cyclized diene polymers. XIII. γ -Ray-initiated polymerization of 1,3-dienes, 503
- Stickney, P. B.: see Dunnivant, W. R.
- Stille, J. K.: see Mukamal, H.
—, and Empen, J. A.: Polymerization of cyclic sulfides, 273
—, and Hillman, J. J.: Cyclopolymerization of diastereomeric diepoxides, 2067
—, and Hillman, J. J.: The polymerization of styrene oxide by the triisobutyl-aluminum-water system, 2055
- Štokr, J., Schneider, B., Kolínský, M., Ryska, M., and Lím, D.: Determination of tacticity in poly(vinyl chloride) by infrared spectroscopy, 2013
- St. Pierre, T.: see Overberger, C. G.
- Stromberg, R. R.: see Peyser, P.
- Stychenko, V. A.: see Paushkin, Ya. M.
- Subramanian, R. V.: see Deshpande, A. B.
- Suh, K. W., and Clarke, D. H.: Cohesive energy densities of polymers from turbidimetric titrations, 1671
- Sumitomo, H., and Kobayashi, K.: Polymerization of β -cyanopropionaldehyde. II. Crystalline poly-(cyanoethyl)oxymethylene, 2247
- Suzuki, H.: see Iwakura, Y.
- Suzuki, Y.: see Minoura, Y.
- Svegliado, G., Talamini, G., and Vidotto, G.: Stereoregularity of polyacrylonitrile determined by NMR, 2875
- Symcox, R. O., and Cotman, J. D., Jr.: Ionic polymerization of *p*-vinylbenzyl methyl ether, 417
—, and —: Kinetics of free-radical polymerization of *p*-vinylbenzyl methyl ether: Crosslinking by initiator free radicals, 1165
- Tadokoro, T.: see Minoura, Y.
- Takano, Y.: see Soga, K.
- Takeuchi, M.: see Matsuzaki, K.
- Talamini, G.: see Svegliado, G.
- Tamura, Y.: see Negishi, S.
- Tanaka, A.: see Higashimura, T.
- Taylor, G. L.: see Rijke, A. M.
- Tazuke, S., and Okamura, S.: Effects of metal salts on polymerization. Part III. Radical polymerizabilities and infrared spectra of vinylpyridines complexed with zinc and cadmium salts, 1083

- , Tjoa, T. B., and Okamura, S.: Effects of metal salts on polymerization. Part IV. Polymerization of *N*-vinylcarbazole initiated by oxidizing metal nitrates, 1911
- Terada, A., and Murata, K.: Aminobutadienes. V. Polymers of 1-phthalimido-1,3-butadiene and 1-succinimido-1,3-butadiene, 2219
- Teramoto, A., Morimoto, M., and Nishijima, Y.: Studies of the micro-Brownian motion of a polymer chain by the fluorescence polarization method. III. Fluorescent conjugates of polyethyleneimine, 1021
- Thomas, J. K.: see Metz, D. J.
- Tjoa, T. B.: see Tazuke, S.
- Toby, S.: see Boyles, J. G.
- Toda, F.: see Iwakura, Y.
- Tohyama, S.: see Yoda, N.
- , Kurihara, M., Ikeda, K., and Yoda, N.: Cyclopolycondensations. VII. Preparation of aromatic poly(ureido acids) by the low-temperature solution polymerization and cyclodehydration to fully aromatic polyquinazolinediones, 2523
- Torii, Y.: see Iwakura, Y.
- Toy, M. S.: Stereoregular condensation polymers. I. Synthesis and comparison of optically active and inactive polycamphorates and polycamphoramides, 2481
- Toyoshima, Y.: see Jellinek, H. H. G.
- Trick, G. S.: see Lal, J.
- Trinler, W. A.: see Parrish, C. F.
- Trischler, F. D.: see Hollander, J.
- , and Hollander, J.: Preparation of fluorine-containing polyethers, 2343
- Tsuji, K.: see Kaetsu, I.
- , Iwamoto, T., Hayashi, K., and Yoshida, H.: Electron spin resonance study of irradiated monomer and polymer of 3,3-bis(chloromethyl)oxetane, 265
- Tsutsui, M., and Koyano, T.: Elemental organic compounds. Part XX. Ethylene dimerization to butene-1, 681
- , and —: Elemental organic compounds. Part XXI. Polymerization of ethylene by dibenzenechromium, 683
- Tomolo, A. L.: see Price, C. C.
- Turner, D. T.: see Campbell, D.
- : see Marcotte, F. B.
- Tutas, D. J.: see Peyser, P.
- Uchic, J. T.: see Kovacic, P.
- Uchida, A.: see Shibukawa, T.
- Ueda, S.: see Kataoka, T.
- Ueno, Y., Kasabo, T., Hanada, T., and Minoura, Y.: Cationic graft copolymerization of styrene onto natural rubber, 339
- Ugelstad, J., Mörk, P. C., and Aasen, J. O.: Kinetics of emulsion polymerization, 2281
- Ulrich, H.: see Alberino, L. M.
- Uno, K.: see Hashimoto, M.
- : see Iwakura, Y.
- Iwakura, Y., Makita, M., and Ninomiya, T.: Syntheses of polymerizable dyes and their graft copolymerization to cellulose and polypropylene fibers, 2311
- Upadhyay, J.: see Armour, M.
- , and Wassermann, A.: Conjugated double bonds in deeply colored polymers, 395
- Urayama, S.: see Minoura, Y.
- Uryu, T.: see Matsuzaki, K.
- Vanhaeren, G.: see Butler, G. B.
- Van Wazer, J. R.: see Grant, D.
- Venkatarao, K., and Santappa, M.: Uranyl ion-sensitized polymerization of acrylamide and methacrylamide in aqueous solution, 637
- Vidotto, G.: see Svegliado, G.
- Vijayaraghavan, N. V.: see Vittimberga, B. M.
- Vishnyakova, T. P.: see Paushkin, Ya. M.
- Vittimberga, B. M., Vijayaraghavan, N. V., and Winslow, E. C.: Thermal stability of imide-crosslinked poly(vinylphthalic anhydride), 2202
- Vodehnal, J.: see Štěpán, V.
- Vofsi, D.: see Bar-Zakay, S.
- Wang, J. Y. C.: see Meyersen, K.
- Warwicker, J. O.: Effect of chemical reagents on the fine structure of cellulose. Part IV. Action of caustic soda on the fine structure of cotton and ramie, 2579
- Wasserman, A.: see Armour, M.
- : see Upadhyay, J.
- Watanabe, M.: see Izumi, Z.
- Weber, E. C.: see Lipscomb, N. T.
- Wellons, J. D., Williams, J. L., and Stannett, V.: Preparation and characterization of some cellulose graft copolymers. Part IV. Some properties of

- isolated cellulose acetate-styrene graft copolymers, 1341
- Weissmerel, K.: see Rösinger, S.
- Werninck, A.: see MacCallum, J. R.
- Wertz, W.: see O'Driscoll, K. F.
- Wang, J. J.: see Powell, J. A.
- Whistler, R. L., and Hoffman, D. J.:
Preparation and polymerization of a sugar dithiol, 2111
- Whitehead, M. E.: see Breed, L. W.
- Wiley, R. H., De Venuto, G., and De Venuto, A.: 1,2,4- and 1,3,5-trivinylbenzenes. Vapor-phase chromatographic and nuclear magnetic resonance characterization, 1805
- Williams, J. L.: see Wellons, J. D.
- Winslow, E. C.: see Vittimberga, B. M.
- Winston, A., and Li, G. T. C.: Copolymerization of the cyclic monomer, 5,5-dichloro-4-hydroxy-2,4-pentadienoic acid lactone, 127
- , and —: Copolymerization of 4-cyclopentene-1,3-dione with *p*-chloro-styrene and vinylidene chloride, 1223
- Wolff, I. A.: see Chang, S.-P.
- : see Greene, J. L., Jr.
- Worsfold, D. J.: Anionic copolymerization of styrene and isoprene in cyclohexane, 2783
- Wrasidlo, W., and Empey, R.: Pyrolysis of polyaromatic heterocyclics, 1513
- Yamadera, R.: see Murano, M.
- , and Murano, M.: The determination of randomness in copolyesters by high resolution nuclear magnetic resonance, 2259
- , and —: Studies on tacticity of polyacrylonitrile. I. High-resolution nuclear magnetic resonance spectra of polyacrylonitrile, 1059
- Yamakita, H., and Hayakawa, K.: Polymerization of β -(2-Furyl)acrolein in solution by ionizing radiation, 3219
- Yamashita, Y.: see Iwatsuki, S.
- Yasuda, H.: Basic consideration of permeability of polymer membrane to dissolved oxygen, 2952
- Yasukawa, T.: see Matsuzaki, K.
- Yoda, N.: see Kurihara, M.
- : see Tohyama, S.
- , Ikeda, K., Kurihara, M., Tohyama, S., and Nakanishi, R.: Cyclopolycondensations. VI. Fully aromatic polybenzoxazinones from aromatic poly(amic acids), 2359
- Yokota, H., Kondo, M., Kagiya, T., and Fukui, K.: Retardation of spontaneous polymerization of formaldehyde by acidic substances, 3129
- , Otsuka, Y., Kagiya, T., and Fukui, K.: Kinetics of γ -ray polymerization of formaldehyde in the presence of carbon dioxide, 2825
- Yoshida, H.: see Tsuji, K.
- Yoshihara, T.: see Joh, Y.
- Yoshikawa, K.: see Minoura, Y.
- Zeman, R. J.: see Adams, F. P.
- Zola, H.: Dissociation constants of onuphic acid, 2707

SUBJECT INDEX, VOLUME 5

- Absorption and differential permeation of water vapor in polyacrylamide film, 2147
- Acetylenic group, terminal, linear polymers of vinyl monomers containing, 999
- Acetylenic moiety, linear polymers of acrylic monomers containing, 813
- Acid-catalyzed methanolysis of tri-*O*-methylamylose and tri-*O*-methylcellulose, 2133
- Acidic substances, retardation of spontaneous polymerization of formaldehyde by, 3129
- Acidic vinyl monomers, copolymerization parameters of, 77
- Acids, dicarboxylic, synthesis of polyamides by polyaddition of bisimidazolines with, 1129
- petroselinic and oleic, perchlorocyclopentadiene adducts of, vinyl esters of, polymers of, 1809
- Acid vinyl esters, 1,4,5,6,7,7-hexachloro- and hexabromobicyclo-[2,2,1]-5-heptene-2-carboxylic acid, and copolymerization with acrylonitrile, synthesis of, 1279
- Acrolein vinyl monomers, copolymerization parameters of, 77
- Acrylamide, and methacrylamide in aqueous solution, uranyl ion-sensitized polymerization of, 637
- persulfate-initiated polymerization of, 3151
- polymerization of, initiated by persulfate-thiosulfate redox couple, 3167
- γ -ray polymerization of, 531
- Acrylate, vinyl chloride, of methoxy poly(ethylene glycol) copolymers, 2946
- Acrylates and methacrylates, homopolymers and copolymers of, of homoterpenylmethyl carbinol and α -campholenol, 1489
- Acrylic monomers containing an acetylenic moiety, linear polymers of, 813
- Acrylonitrile, copolymer of, endgroup of chlorate-sulfite-initiated, 2857
- copolymerization with, synthesis of 1,4,5,6,7,7-hexachloro- and hexabromobicyclo-[2,2,1]-5-heptene-2-carboxylic acid vinyl esters and, 1279
- mechanism of emulsion polymerization of, 469
- and methyl acrylate, copolymerization of, effect of reaction medium on, 1967
- polymerization by *p*-toluenesulfonic acid, kinetics and mechanism of, 1297, 1307
- role and effect of emulsifiers in emulsion polymerization of, 455
- 12-Acryloxystearate and vinyl chloride, copolymers of, 2949
- Acryloyl- and methacryloyl- α -amino acid amides, base-catalyzed polymerization of, 1585
- DL-Alanine NCA and L-alanine NCA, 2867
- Alcohols, complex formation with catalysts and isocyanates in preparation of urethanes, 35
- Aldehyde and carbonyl groups, effects of, in graft copolymerization of methyl methacrylate on cellulose with ceric salt, 2791
- Alicyclic compounds, unsaturated, ring-opening polymerization of, 2209
- Alkenes, nitrogen-containing, copolymerization of divinyl ether with certain, 1265
- α -Alkylacrylonitriles, new synthetic route to, and homopolymerization and copolymerization reactions, 563
- Alkylene/arylene polyether, synthesis of, from diphenolic acid and Rosenmund reduction to polyether aldehyde, 381
- Alkylene oxides, polymerization of, by dialkylzinc-Lewis base systems, 3139
- N*-Alkylolacrylamides, 2957
- N*-Alkyl-substituted copolyamides with long methylene chain units, 107
- N*-Alkyl-substituted polyamides with long methylene chain units, 107
- Alkyl vinyl esters of brassylic (tridecanedioic) acid, 2547

- Allyl acrylate and allyl methacrylate, linear polymers of, 323
- Allyl methacrylate and allyl acrylate, linear polymers of, 323
- Alternating copolymerization of carbon monoxide and ethylenimine by azobisisobutyronitrile or by γ -ray irradiation, influence of addition of olefins on the, 1645
- Aluminum chloride-cupric chloride, oligomerization of halobenzenes by, 945
- Aluminum sulfate-sulfuric acid complex, effect of temperature and solvents on stereospecific polymerization of vinyl alkyl ethers catalyzed by, 795
- Amine-catalyzed dicyandiamide cure, tertiary, of epoxy resins, mechanism of, 1609
- Amines, polymeric, from poly(Schiff bases), preparation of, 1659
- Aminobutadienes, 2219
- Amino endgroups, detection and incorporation of, in free-radical polymerization of methyl methacrylate, 151
- Amorphous and crystalline samples of poly(ethylene terephthalate), ESR study of radicals trapped in, after γ -irradiation, 2199
- Ammonium phosphate, determination of kinetic parameters for pyrolysis of cellulose and cellulose treated with, by differential thermal analysis and thermal gravimetric analysis, 833
- Anhydrides, aromatic cyclic, hydrolysis of, 2961
- Anionic copolymerization of styrene and isoprene in cyclohexane, 2783
- Anionic graft polymerization of methyl acrylate to protein functional groups, 2535
- Anionic polymerization, of lactams, 965 relative reactivities of *cis* and *trans* crotonic compounds in, 2701
- Anionic polymers, statistical character of, effect of impurities and the initiation and transfer rate constants on, 2269
- Anionic and radical homopolymerization of maleimide and *N-n*-butylmaleimide, 1619
- Aromatic cyclic anhydrides, hydrolysis of, 2961
- Aromatic nuclei, polymerization of, 945
- Aromatic poly(amic acids), fully aromatic polybenzoxazinones from, 2359
- Aromatic polybenzoxazinones from aromatic poly(amic acids), 2359
- Aromatic polyhydantoins from bisiminoacetate and diisocyanates, 2289
- Aromatic polyquinazolinodiones, fully, cyclodehydration to, 2523
- Aromatic polysulfonamides, 553
- Aromatic poly(ureido acids) by low-temperature solution polymerization and cyclodehydration to fully aromatic polyquinazolinodiones, 2523
- Aromatic substitution, nucleophilic, poly(aryl ethers) by, 2399 nucleophilic, poly(aryl ethers) by, 2415
- Aroyl peroxides containing reactive functional groups, 2964
- Arylene/alkylene polyether, synthesis of, from diphenolic acid and Rosenmund reduction to polyether aldehyde, 381
- Arylene-modified siloxanes, 2745
- Aryl sulfone linkages, polybenzimidazoles containing, 1113
- L-Ascorbic acid, kinetics of depolymerization of hyaluronic acid by, and inhibition of reaction by anions of lyotropic series, 931
- Asymmetric-induction polymerization of benzofuran, catalysts for, 2099
- Autoxidation, inhibited, of polypropylene, 1683 of polypropylene, kinetics of, 2091
- Azobisisobutyronitrile-initiated polymerization of methyl methacrylate in benzene, 1107
- α,α -Azobisisobutyronitrile or γ -ray irradiation, isomerization polymerization of 2-vinyl-1,3-dioxolane by, 2351
- Base-catalyzed polymerization of acryloyl- and methacryloyl- α -amino acid amides, 1585
- Benzene, azobisisobutyronitrile-initiated polymerization of methyl methacrylate in, 1107 *tert*-butyl hydroperoxide-initiated polymerization of styrene in, 1101
- Benzofuran, catalysts for asymmetric-induction polymerization of, 2099
- $\text{BF}_3 \cdot \text{O}(\text{C}_2\text{H}_5)_2$, changes in concentration of tetraoxane produced during

- solution polymerization of trioxane, 2977
- copolymerization of tetraoxane with styrene catalyzed by, 1937
- copolymerization of trioxane with styrene catalyzed by, 1927
- effect of solvent on amount of tetraoxane produced in solution polymerization of trioxane catalyzed by, 2989
- polymerization of tetraoxane at low concentration catalyzed by, 2997
- Bicyclopentene and other dicyclic dienes, cyclocopolymerization of, with sulfur dioxide to fused ring systems, 1827
- Binary copolymerization, computer program for calculations and automatic data plotting in, 401
- free energy changes of, 1383
- Binary systems, radiation-induced solid-state polymerization in, 1899
- 3,3-Bis(chloromethyl)oxetane, irradiated monomer and polymer of, electron spin resonance study of, 265
- Bis(cyclopentadienyl)titanium dichloride and diisobutylaluminum chloride, homopolymerization of ethylene and copolymerization with 1-butene in presence of, 1119
- 4,4'-Bis(diphenylphosphino)biphenyl or 1,4-bis(diphenylphosphino)butene, copolymerization of, with *trans*-2,6-diazaidohexaphenylcyclophosphonitrile, 2891
- 1,4-Bis(diphenylphosphino)butene or 4,4'-bis(diphenylphosphino)biphenyl, copolymerization of, with *trans*-2,6-diazaidohexaphenylcyclophosphonitrile, 2891
- 1,3-Bis(2,3-epoxypropylphenyl)tetramethyldisiloxanes, 2595
- Bisimidazolines with dicarboxylic acids, synthesis of polyamides by polyaddition of, 1129
- Bisiminoacetate and diisocyanates, aromatic polyhydantoins from, 2289
- Bissuccinimides, polyaddition of, with diamines in synthesis of polyamides, 15
- Block copolymerization of methyl methacrylate with poly(ethylene oxide) radicals, 43
- Boundary effect on thermal degradation of copolymers, 21
- Brassylic (tridecanedioic) acid, alkyl vinyl esters of, 2547
- Bulk polymerization, of dioxolane, kinetics of, in presence of water, 1881
- kinetics of, of trimeric phosphonitrile chloride, 3061
- Butadiene, and isoprene, cationic polymerization of isobutene with, 2455
- mechanism of stereoregular polymerization of, by homogeneous Ziegler-Natta catalysts, effects of the nature of bases and halogens, 521
- mechanism of stereoregular polymerization of, by homogeneous Ziegler-Natta catalysts, effects of the species of transition metals, 511
- 1,3-Butadiene on cobalt and nickel halides, polymerization of, 429
- 1-Butene, copolymerization with, homopolymerization of ethylene and, in presence of bis(cyclopentadienyl)titanium dichloride and diisobutylaluminum chloride, 1119
- ethylene dimerization to, 681
- kinetic results on polymerization with heterogeneous metalorganic catalysts, 205
- tert*-Butyl hydroperoxide-initiated polymerization of styrene in benzene, 1101
- Butyllithium-diethylzinc complex, polymerization of methyl methacrylate with, 1359
- N-n*-Butylmaleimide, radical and anionic homopolymerization of maleimide and, 1619
- α -Campholenol, homopolymers and copolymers of acrylates and methacrylates of homoterpenylmethyl carbinol and, 1489
- ϵ -Caprolactam, direct determination of, in presence of nylon 6 and its oligomers by infrared spectroscopy, 231
- Caprolactam and pyrrolidone, copolymerization of, 965
- Carbon dioxide, kinetics of γ -ray polymerization of formaldehyde in presence of, 2825
- Carbonium ion salts, initiation process in polymerization of tetrahydrofuran with, 193
- Carbon monoxide and ethylenimine, alternating copolymerization of, by

- azobisisobutyronitrile or by γ -ray irradiation, influence of addition of olefins on, 1645
- radical-initiated copolymerization of, in the presence of ethylene, 2031
- Carbon tetrachloride, polymerization of methyl methacrylate initiated by liquid sulfur dioxide-pyridine complex in presence of, 2769
- Carbonyl and aldehyde groups, effects of, in graft copolymerization of methyl methacrylate on cellulose with ceric salt, 2791
- Carborane polymers, polysiloxanes, 365
- 4-(*o*-Carboranyl)-1-butylmethyl siloxane-dimethyl siloxane copolymers, thermal behavior of, 2119
- Catalyses and properties of some binary systems containing the menthoxy group, 2099
- Catalysts, for asymmetric-induction polymerization of benzofuran, 2099
- complex formation with alcohols and isocyanates in preparation of urethanes, 35
- new, for isotactic polymethacrylonitrile, 2503
- Cationic and free-radical polymerization of optically active 1-olefins, 619
- Cationic graft copolymerization of styrene onto natural rubber, 339
- Cationic polymerization, of α,β -disubstituted olefins, 1727
- double-bond opening of, in methyl propenyl ether, 3009
- of isobutene with butadiene and isoprene, 2455
- of propenyl *n*-butyl ether, 1727
- of styrene catalyzed by rhenium pentachloride, effect of ethyl monochloroacetate on, 3207
- of vinylcyclopropane and related compounds, rearrangements of the propagating chain end, 227
- Caustic soda, action of, on fine structure of cotton and ramie, 2579
- Cellulose, and cellulose treated with ammonium phosphate by differential thermal analysis and thermal gravimetric analysis, determination of kinetic parameters of pyrolysis, 833
- cotton, crosslinked decrystallized, 2563
- fine structure of, effect of reagents on, 2579
- formylation of, 2465
- gel permeation properties of, 2563
- graft copolymerization of methyl methacrylate on, with ceric salt, effects of carbonyl and aldehyde groups in, 2791
- Cellulose acetate-styrene graft copolymers, isolated, 1341
- Cellulose graft copolymers, preparation and characterization of, 1341
- Ceric salt, effects of carbonyl and aldehyde groups in graft copolymerization of methyl methacrylate on cellulose with, 2791
- Cerium, grafting of polyacrylonitrile to granular corn starch by initiating with, 2967
- Chain transfer and branching, 2681
- Chloral and dichloroacetaldehyde, copolymerization of, catalyzed by organometallic compounds, 975
- Chlorate-sulfite-initiated acrylonitrile copolymer, endgroup of, 2857
- Chlorinated fatty acids, homopolymers and vinyl chloride copolymers of vinyl esters of, from *Umbelliferone* and *Limnanthes douglasii*, 2899
- Chlorinated polystyrene, 2297
- p*-Chlorostyrene and vinylidene chloride, copolymerization of 4-cyclopentene-1,3-dione with, 1123
- Chromophore of polyacrylonitrile, 2637
- Cinnamide, hydrogen-transfer polymerization of, 675
- Cobalt halide and nickel halide, polymerization of 1,3-butadiene on, 429
- Cobalt-60 γ -radiation, solid-state polymerization of 1,2,3,4-diepoxybutane initiated by, 1015
- Cohesive energy densities of polymers from turbidimetric titrations, 1671
- Complex formation between catalysts, alcohols, and isocyanates in the preparation of urethanes, 35
- Computer program for calculations and automatic data plotting in binary copolymerization, 401
- Condensation polymerization, α,ω -disubstituted polymethylpolyphosphonates and polyphenylpolyphosphonates, 57
- of *d*-tartaric acid with diamines, syntheses of optically active polymers by, 2441
- Condensation polymers, stereoregular, 2481

- Conjugated double bonds in deeply colored polymers, 395
- Conjugates, fluorescent, of polyethyleneimine, 1021
- Copolyesters, randomness in, determination of, by high resolution nuclear magnetic resonance, 2259
- Corn starch, granular, grafting of polyacrylonitrile to, 1313
- granular, grafting of polyacrylonitrile to, by initiation with cerium, 2967
- Cotton cellulose, crosslinked decrystallized, 2563
- Cotton and ramie, action of caustic soda on fine structure of, 2579
- Cr(AcAc)₃-AlEt₃ catalyst system, heterogeneous, in isoprene polymerization, 761
- Crosslinked, decrystallized cotton cellulose, 2563
- Crosslinking of gelatin by aqueous peroxydisulfate, 1
- Crosslinking by initiator free-radicals, 1165
- Crotonic compounds, *cis* and *trans*, relative reactivities of, in anionic polymerization, 2701
- Crotonyl compounds, radical copolymerization of, with styrene, 2641
- Crystalline and amorphous samples of poly(ethylene terephthalate), ESR study of radicals trapped in, after γ -irradiation, 2199
- Crystalline poly-*p*-*tert*-butylstyrene, 2187
- Crystalline poly(cyanoethyl)oxymethylene, 2247
- β -Cyanopropionaldehyde, polymerization of, 2247
- Cyclocopolymerization, of bicyclopentene and other dicyclic dienes with sulfur dioxide to fused ring systems, 1827
- of diallylamine derivatives in dimethyl sulfoxide, 1951
- of dicyclic dienes and maleic anhydride to fused ring systems, 1845
- Cyclo- and cyclized diene polymers, γ -ray-initiated polymerization of 1,3-dienes, 503
- Cyclodehydration to fully aromatic polyquinazolinediones, 2523
- Cycloelimination process, effect of ester spatial conformation on, 2333
- Cyclohexane, anionic copolymerization of styrene and isoprene in, 2783
- Cyclohexylidenebisphenol polycarbonates, elastomers based on, 927
- 4-Cyclopentene-1,3-dione, copolymerization of, with *p*-chlorostyrene and vinylidene chloride, 1123
- Cyclopolycondensations, 2359, 2523
- Cyclopolymerization of diastereomeric diepoxides, 2067
- Decay of the ESR signal in ultraviolet-irradiated poly(methyl methacrylate), 677
- Decrystallized, crosslinked cotton cellulose, 2563
- Degradation, of an initial "most probable" polymer, effect of volatile fraction on, 1573
- oxidative, of polystyrene, 1635
- thermal, of copolymers, boundary effect on, 21
- Degradation products, volatile, of organotin polyesters, 2458
- Dehydrochlorination reactions in polymers, 2297
- Densities, cohesive energy of, of polymers from turbidimetric titrations, 1671
- Depolymerization kinetics, theoretical, 1573
- Dialkylzinc-hydrazine catalyst, polymerization of propylene oxide with, 917
- Dialkylzinc-Lewis base systems, polymerization of alkylene oxides by, 3139
- Diallylamine derivatives, cyclocopolymerization of, in dimethyl sulfoxide, 1951
- Diamines, condensation polymerization of *l*-tartaric acid with, syntheses of optically active polymers by, 2441
- polyaddition of bisuccinimides with, in synthesis of polyamides, 15
- Dianilinoxysilanes and diphenoxysilanes, synthesis of polyaryloxysilanes by melt-polymerizing, with aromatic diols, 707
- Diastereomeric diepoxides, cyclopolymerization of, 2067
- trans*-2,6-Diazidohexaphenylcyclophosphonitrile tetramer, copolymerization of, with 1,4-bis(diphenylphosphino)butane or 4,4'-bis(diphenylphosphino)biphenyl, 2891
- Diazomethane, gaseous, polymerization of, on silicone grease, 585
- Dibenzenechromium, polymerization of ethylene by, 683

- Diborane reduction of corresponding acids, preparation of hydroxyl-terminated polysiloxanes by, 685
- Dicarboxylic acids, synthesis of polyamides by polyaddition of bisimidazolines with, 1129
- Dichloroacetaldehyde and chloral, copolymerization of, catalyzed by organometallic compounds, 975
- 5,5-Dichloro-4-hydroxy-2,4-pentadienoic acid lactone, copolymerization of, 127
- Dicyandiamide cure, tertiary amine-catalyzed, of epoxy resins, mechanism of, 1609
- 2,4-Dicyanopentanes, high-resolution nuclear magnetic resonance spectra of, 1855
- Dicyclic dienes, bicyclopentene and other, cyclocopolymerization of, with sulfur dioxide to fused ring systems, 1827
and maleic anhydride, cyclocopolymerization of, to fused ring systems, 1845
- Dicyclopentadiene, single initial addition of, in terpolymerization of ethylene, propylene, and dicyclopentadiene, 243
two-step addition of, in terpolymerization of ethylene, propylene, and dicyclopentadiene, 251
- Dielectric properties of vinylidene chloride-vinyl chloride copolymers, 1717
- Diels-Alder polymers, 2721
- Diene incorporation into isobutylene-diene copolymers effect of temperature on, 2712
- Dienes, cyclo- and cyclized, γ -ray-initiated polymerization of, 503
dicyclic, bicyclopentene and other, cyclocopolymerization of, with sulfur dioxide to fused ring systems, 1827
dicyclic, and maleic anhydride, cyclocopolymerization of, to fused ring systems, 1845
- Diepoxides, linear polymers from, 2192
- 1,2,3,4-Diepoxybutane initiated by cobalt-60 γ -radiation, solid-state polymerization of, 1015
- Differential permeation and absorption of water vapor in polyacrylamide film, 2147
- Diffusion in ethylene-propylene rubber, 1327
- Diisobutylaluminum chloride, homopolymerization of ethylene and copolymerization with 1-butene in presence of bis(cyclopentadienyl)titanium dichloride and, 1119
- Diisocyanates, and bisiminoacetate, aromatic polyhydantoins from, 2289
fluorinated, polyurethanes from, 2757
- Diisotacticity of poly(methyl propenyl ether) and double-bond opening of methyl propenyl ether in cationic polymerization, 3009
- N,N*-dimethyl 12-acryloxystearamide, polymerization of, methyl 12-acryloxystearate, and methyl 14-acryloxyeicosanoate, 1501
- Dimethyl sulfoxide, cyclocopolymerization of diallylamine derivatives in, 1951
- Diols, aromatic, synthesis of polyaryloxysilanes by melt-polymerizing dianilino- and diphenoxysilanes with, 707
 α,ω -Diols from polymerization of ethylene, 2693
- Dioxolane, bulk polymerization of, kinetics of, in presence of water, 1881
solution polymerization of, kinetics of, in presence of water, 1889
- 1,3-Dioxolane group, preparation and polymerization of vinyl monomers containing, 287
- Diphenolic acid, synthesis of an arylene/alkylene polyether from, 381
- Diphenoxysilanes and dianiloxysilanes, synthesis of polyaryloxysilanes by melt-polymerizing, with aromatic diols, 707
- Disproportionation, initiation through, 1307
- Dissociation constants of onuphic acid, 2707
- α,β -Disubstituted olefins, cationic polymerization of, 1727
- α,ω -Disubstituted polymethylphosphonates, from condensation polymerization, 57
- Divinyl ether, copolymerization of, with certain nitrogen-containing alkenes, 1265
- Double-bond opening of methyl propenyl ether in cationic polymerization, 3009

- Dyes, polymerizable, and their graft copolymerization, syntheses of, to cellulose and polypropylene fibers, 2311
- Elastomers based on cyclohexylidene biphenol polycarbonates, 927
- Electrically conducting polymers, colored, from furan, pyrrole, and thiophene, 1527
- Electron donor-acceptor complex, 2769
- Electron microscopy, xylene-stream method for obtaining thin polyethylene specimens for, 1179
- Electron spin resonance study of irradiated monomer and polymer of 3,3-bis(chloromethyl)oxetane, 265
- Electron-transfer polymers, 993
- Elemental organic compounds, ethylene dimerization to butene-1, 681
- Emulsion copolymerization with styrene derivatives containing nitrile groups in the side chain, 1033
- Emulsion polymerization, of acrylonitrile, role and effect of emulsifiers, 455
kinetics of, 2281
of vinyl stearate, 2665
- Endgroup of chlorate-sulfite-initiated acrylonitrile copolymer, 2857
- Energy densities, cohesive, of polymers from turbidimetric titrations, 1671
- Epoxy resins, mechanism of tertiary amine-catalyzed dicyandiamide cure of, 1609
- ESR signal in ultraviolet-irradiated poly(methyl methacrylate), decay of, 677
- ESR study of radicals trapped in amorphous and crystalline samples of poly(ethylene terephthalate) after γ -irradiation, 2199
- Ester groups, reactivity of, on insoluble polymer supports, 1977
- Esters, acid vinyl, 1,4,5,6,7-hexachloro- and hexabromobicyclo-[2,2,1]-5-heptene-2-carboxylic acid, and copolymerization with acrylonitrile, synthesis of, 1279
alkyl vinyl, of brassylic (tridecanedioic) acid, 2547
vinyl, polymers of, of perchlorocyclopentadiene adducts of petroselinic and oleic acids, 1809
vinyl, reaction of triethyl phosphite with, 2453
- Ester spatial conformation, effect of, on the cycloelimination process, 2333
- Ethyl acrylate, polymerization of, 2005
- Ethylene, dimerization to butene-1, 681
 α,ω -diols from polymerization of, 2693
effect of oxygen on γ -radiation-induced polymerization of, 2731
homopolymerization of, and copolymerization with 1-butene in presence of bis(cyclopentadienyl)titanium dichloride and diisobutylaluminum chloride, 1119
mechanism of initiation in the γ -radiation-induced polymerization of, 1073
polymerization of, by dibenzenechromium, 683
propagation, transfer, and short-chain branching in free-radical polymerization of, 3115
radical-initiated copolymerization of ethylenimine and carbon dioxide in presence of, 2031
terpolymerization of, with propylene and dicyclopentadiene, two-step addition of dicyclopentadiene, 251
terpolymerization of, with propylene and dicyclopentadiene, single initial addition of dicyclopentadiene, 243
- Ethylene-propylene rubber, diffusion in, 1327
- Ethylenimine and carbon monoxide, alternating copolymerization of, by azobisisobutyronitrile or by γ -ray irradiation, influence of addition of olefins on, 1645
radical-initiated copolymerization of, in presence of ethylene, 2031
- Ethyl monochloroacetate, effect of, on cationic polymerization of styrene catalyzed by rhenium pentachloride, 3207
- 9-Ethynylantracene, polymerization of, 920
- Fatty acids, chlorinated, homopolymers and vinyl chloride copolymers of vinyl esters of, from *Umbelliferae* and *Limnanthes douglassii*, 2899
- Ferrocene-containing poly(phosphine oxides) and poly(phosphine sulfides), 2927
- Fibers, cellulose and polypropylene, syntheses of polymerizable dyes and their graft copolymerization to, 2311
- Films, polystyrene, reaction of nitrogen dioxide with, 3214

- Fine structure of cellulose, effect of reagents on, 2579
- Fluorescence polarization method, studies of micro-Brownian motion of a polymer chain by, 1021
- Fluorescent conjugates of polyethyleneimine, 1021
- Fluorinated diisocyanates, polyurethanes from, 2757
- Fluorine-containing polyethers, preparation of, 2343
- Formaldehyde, gaseous, polymerization of, kinetics of, 1705
- γ -ray polymerization of, in presence of carbon dioxide, kinetics of, 2825
- spontaneous polymerization of, by acidic substances, retardation of, 3129
- Formylation of cellulose, 2465
- Free energy changes of binary copolymerization systems, 1383
- Free-radical polymerization, of ethylene, propagation, transfer, and short-chain branching in, 3115
- of methyl methacrylate, detection and incorporation of amine endgroups in, 151
- of *p*-vinylbenzyl methyl ether, kinetics of, 1165
- of vinyl ferrocene, 2091
- Free radicals, initiator, crosslinking by, 1165
- Furan, pyrrole, and thiophene, colored electrically conducting polymers from, 1527
- β -(2-Furyl)acrolein, polymerization of, in solution by ionizing radiation, 3219
- Fused ring systems, cyclocopolymerization of bicyclopentene and other dicyclic dienes with sulfur dioxide to, 1827
- cyclocopolymerization of dicyclic dienes and maleic anhydride to, 1845
- Gamma radiolysis, quantitative determination of short branches in high-pressure polyethylene by, 2023
- Gaseous formaldehyde, polymerization of, kinetics of, 1705
- Gelatin, crosslinking of, by aqueous peroxydisulfate, 1
- Gel permeation chromatography, 2835
- effect of temperature and polymer type on, 987
- and other methods, molecular weights of tetrahydrofuran-propylene oxide copolymers by, 2045
- Gel permeation properties of cellulose, 2563
- Glassy phase, solid-state polymerization in, 1899
- Graft copolymerizations, of gaseous vinyl chloride and vinylidene chloride on preirradiated polypropylene, 439
- of methyl methacrylate on cellulose with ceric salt, effects of carbonyl and aldehyde groups in, 2791
- Graft copolymers, isolated cellulose acetate-styrene, 1341
- Grafting, in a heterogeneous medium in the presence of radical initiators, mechanism of, 1563
- of maleic anhydride on polyethylene, 1547
- of polyacrylonitrile to granular corn starch, 1313
- of polyacrylonitrile to granular corn starch by initiation with cerium, 2967
- in reaction of polyethylene and poly(maleic anhydride), 1539
- Graft polymerization, anionic, of methyl acrylate to protein functional groups, 2535
- Graft polymers, cellulose, preparation and characterization of, 1341
- chain transfer and branching, 2681
- Granular corn starch, grafting of polyacrylonitrile to, 1313
- grafting of polyacrylonitrile to, by initiation with cerium, 2967
- Halides, cobalt and nickel, polymerization of 1,3-butadiene on, 429
- metal, NMR studies on the stereospecific polymerization of methyl vinyl ether, polymerization by, 849
- Halobenzenes, oligomerization of, by aluminum chloride-cupric chloride, 945
- Halogens and bases, effects of nature of, on mechanism of stereoregular polymerization of butadiene by homogeneous Ziegler-Natta catalysts, 521
- Heteroatom systems, structural effects in, 355
- Heterocycle copolymers, ordered, 2429
- Heterocyclics, polyaromatic, pyrolysis of, 1513
- Heterogeneous medium in the presence of radical initiators, mechanism of grafting in, 1563

- 1,4,5,6,7,7-Hexachloro- and hexabromobicyclo-[2,2,1]-5-heptene-2-carboxylic acid vinyl esters and copolymerization with acrylonitrile, synthesis of, 1279
- High resolution nuclear magnetic resonance, determination of randomness in copolyesters by, 2259
- Homopolymers, and copolymers of acrylates of homoterpenylmethyl carbinol and α -campholenol, 1489
and vinyl chloride copolymers of vinyl esters of chlorinated fatty acids from *Umbelliferae* and *Limnanthes douglasii*, 2899
- Homoterpenylmethyl carbinol and α -campholenol, homopolymers and copolymers of acrylates and methacrylates of, 1489
- Hyaluronic acid, kinetics of depolymerization of, by L-ascorbic acid, and inhibition of reaction by anions of lyotropic series, 931
- Hydrodynamics of a porous sphere molecule, 3029
- Hydrogel, homogeneous poly(2-hydroxyethyl methacrylate), hydrophobic interaction in, 3103
- Hydrogen-transfer polymerization of cinnamide, 675
- Hydrolysis, of aromatic cyclic anhydrides, 2961
of polyacrylonitrile, 161
- Hydrolytic side reactions, 2415
- Hydrophobic interaction in poly(2-hydroxyethyl methacrylate) homogeneous hydrogel, 3103
- Hydroquinone derivatives, vinyl, synthesis of, by the Wittig reaction, 993
- Hydroxyl-terminated polysiloxanes, preparation of, by diborane reduction of corresponding acids, 685
- N-Hydroxymethylacrylamide, redox behavior in photosensitized crosslinking of vinyl polymers containing, 2705
- Hydroxymethyl and pendent ester groups, post-lactonization of vinyl polymers containing, 2655
- Imide-crosslinked poly(vinylphthalic anhydride), thermal stability of, 2202
- Impurities and the initiation and transfer rate constants, effect of, on the statistical character of anionic polymers, 2269
- Infrared spectra of vinylpyridines complexed with zinc and cadmium salts, radical polymerizabilities and, 1083
- Infrared spectroscopy, determination of tacticity in poly(vinyl chloride) by, 2013
direct determination of ϵ -caprolactam in presence of nylon 6 and its oligomers by, 231
- Inhibited autoxidation of polypropylene, 1683
- Initial "most probable" polymer, effect of volatile fraction on degradation of, 1573
- Initiation, through disproportionation, 1307
in the γ -radiation-induced polymerization of ethylene, mechanism of, 1073
and transfer rate constants and impurities, effect of, on the statistical character of anionic polymers, 2269
- Initiator free radicals, crosslinking by, 1165
- Initiators, radical, mechanism of grafting in a heterogeneous medium in the presence of, 1563
- Insoluble polymer supports, reactivity of ester groups on, 1977
- Intrachain interactions, influence of, on the kinetics of styrene polymerization and copolymerization, 2159
- Intrinsic viscosity of chain polymers, theories of, 2883
- Ionic polymerization of *p*-vinylbenzyl methyl ether, 417
- Ionizing radiation, polymerization of β -(2-furyl)acrolein in solution by, 3219
- Irradiated monomer and polymer of 3,3-bis(chloromethyl)oxetane, electron spin resonance study of, 265
- γ -Irradiation, or α,α -azobisisobutyronitrile, isomerization of polymerization of 2-vinyl-1,3-dioxolane by, 2351
- ^{60}Co , 2-vinylnaphthalene post-polymerization initiated by, 2557
- ESR study of radicals trapped in amorphous and crystalline samples of poly(ethylene terephthalate) after, 2199
- Isobutylene-diene copolymers, effect of temperature on diene incorporation into, 2712
- Isolated cellulose acetate-styrene graft copolymers, 1341

- Isoprene and butadiene, cationic polymerization of, 2455
- Isobutene, cationic polymerization of, with butadiene and isoprene, 2455
- Isoocyanates, complex formation with catalysts and alcohols in preparation of urethanes, 35
- Isomerization polymerization of 2-vinyl-1,3-dioxolane by α,α' -azobisisobutyronitrile or by γ -ray irradiation, 2351
- Isoprene, polymerization of, heterogeneous $\text{Cr}(\text{AcAc})_3\text{-AlEt}_3$ catalyst system in, 761
and styrene, anionic copolymerization of, in cyclohexane, 2783
- Isotactic polymethacrylonitrile, new catalysts for, 2503
- Isotactic sequence lengths by ozonation of poly(propylene oxide), 175
- β -Isovalerolactone, polymerization of, 891
- Itaconic acid derivatives, polymerization of, 689
- Kinetic parameters for pyrolysis of cellulose and cellulose treated with ammonium phosphate by differential thermal analysis and thermal gravimetric analysis, 833
- Kinetics, of autoxidation of polypropylene, 2091
of bulk polymerization of dioxolane in presence of water, 1881
of bulk polymerization of trimeric phosphonitrile chloride, 3061
of emulsion polymerization, 2281
of free-radical polymerization of *p*-vinylbenzyl methyl ether, 1165
and mechanism of acrylonitrile polymerization by *p*-toluenesulfonic acid, 1297, 1307
of non-equilibrium methylsiloxane polymerization and rearrangement, 741
of polymerization of gaseous formaldehyde, 1705
of polymerization of vinyl chloride, precipitated polymer in, 1137
of the γ -radiation-induced polymerization of methyl methacrylate in the solid state, 779
of γ -ray polymerization of formaldehyde in presence of carbon dioxide, 2825
of solution polymerization of dioxolane in presence of water, 1889
of styrene polymerization and copolymerization, influence of intrachain interactions on, 2159
theoretical depolymerization, 1573
- Kinetic studies, 2005
- Lactams, anionic polymerization of, 965
- Lewis base-dialkylzinc systems, polymerization of alkylene oxides by, 3139
- Limnanthes douglasii* and *Umbelliferae*, homopolymers and vinyl chloride copolymers of vinyl esters of chlorinated fatty acids from, 2899
- Linear polymers, of acrylic monomers containing an acetylenic moiety, 813
of allyl acrylate and allyl methacrylate, 323
from diepoxides, 2192
of vinyl aryl monomers containing another unsaturated group, 1245
of vinyl monomers containing a terminal acetylenic group, 999
- Lyotropic series, kinetics of depolymerization of hyaluronic acid by L-ascorbic acid, and inhibition of reaction by anions of, 931
- Maleic anhydride, and dicyclic dienes, cyclocopolymerization of, to fused ring systems, 1845
grafting of, on polyethylene, 1547
polymerization of, by an intense shock wave, 2939
- Maleimide and *N-n*-butylmaleimide, radical and anionic homopolymerization of, 1619
- Maleopimaric acid, polyimide-amides from, 2204
- Mechanism, of acrylonitrile polymerization by *p*-toluenesulfonic acid, kinetics and, 1307
of emulsion polymerization of acrylonitrile, 469
of stereoregular polymerization of butadiene by homogeneous Ziegler-Natta catalysts, effects of the nature of bases and halogens on, 521
of stereoregular polymerization of butadiene by homogeneous Ziegler-Natta catalysts, effects of the species of transition metals, 511
- Membrane, permeability of, to dissolved oxygen, 2952
- Metal nitrates, oxidizing, polymerization of *N*-vinyl-carbazole initiated by, 1911

- Metals, transition, effects of species of, on mechanism of stereoregular polymerization of butadiene by homogeneous Ziegler-Natta catalysts, 511
- Metal salts, effects of, on polymerization, 1083, 1911
- Metal soaps, combination of, synergistic effect of, 2229
- Methacrylamide and acrylamide in aqueous solution, uranyl ion-sensitized polymerization of, 637
- 2-Methacrylamide-2-methylpropanediol-1,3 and 2-methacrylamide-2-methylpropanol-1, 2957
- 2-Methacrylamide-2-methylpropanol-1 and 2-methacrylamide-2-methylpropanediol-1,3, 2957
- Methacrylates and acrylates, homopolymers and copolymers of, of homoterpenylmethyl carbinol and α -campholenol, 1489
- Methacrylonitrile, influence of polymerization conditions on polymerization and properties of polymers, 605
- stereospecific polymerization of, 2503
- stereospecific polymerization of, characterization of crystalline polymethacrylonitrile, 593
- Methacryloyl- and acryloyl- α -amino acid amides, base-catalyzed polymerization of, 1585
- Methanolysis, acid-catalyzed, of tri-*O*-methylamylose and tri-*O*-methylcellulose, 2133
- Methoxy poly(ethylene glycol) copolymers, vinyl chloride acrylate of, 2946
- Methyl acrylate, and acrylonitrile, copolymerization of, effect of reaction medium on, 1967
- anionic graft polymerization of, to protein functional groups, 2535
- Methyl 14-acryloxyeicosanoate, polymerization of, methyl 12-acryloxy-stearate and *N,N*-dimethyl 12-acryloxy-stearamide, 1501
- Methyl 12-acryloxy-stearate, polymerization of, *N,N*-dimethyl 12-acryloxy-stearamide, and methyl 14-acryloxyeicosanoate, 1501
- 2-Methyl-2-butene oxide, polymerization of, 2179
- Methylene chain units, *N*-alkyl-substituted polyamides and copolyamides with, 107
- polyurethanes and polyureas with, 119
- Methyl methacrylate, in benzene, azobisisobutyronitrile-initiated polymerization of, 1107
- block copolymerization of, with poly(ethylene oxide) radicals, 43
- detection and incorporation of amino endgroups in free-radical polymerization of, 151
- graft copolymerization of, on cellulose with ceric salt, effects of carbonyl and aldehyde groups in, 2791
- polymerization of, with butyllithium-diethylzinc complex, 1359
- polymerization of, initiated by liquid sulfur dioxide-pyridine complex in presence of carbon tetrachloride, 2769
- at 90°C., reactivity ratios of styrene and, 1289
- in the solid state, kinetics of the γ -radiation-induced polymerization of, 779
- Methyl propenyl ether, double-bond opening of, in cationic polymerization, 3009
- Methylsiloxane, kinetics of non-equilibrium polymerization and rearrangement, 741
- α -Methylstyrene-*p*-methyl- α -methylstyrene copolymers, NMR study of, 397
- Methyl vinyl ether, NMR studies on the stereospecific polymerization by metal halides, penultimate effect, 849
- NMR studies on the stereospecific polymerization of, by sulfuric acid-aluminum sulfate complex, enantiomorphic catalyst sites model, 863
- Micro-Brownian motion of a polymer chain by the fluorescence polarization method, 1021
- Microscopy, electron, xylene-stream method for obtaining thin polyethylene specimens for, 1179
- Molecular weight, influence of preparative conditions on, 215
- Molecular weights of tetrahydrofuran-propylene oxide copolymers by gel permeation chromatography and other methods, 2045
- "Most probable" polymer initial, effect of volatile fraction on degradation of, 1573
- Nickel halide and cobalt halide, polymerization of 1,3-butadiene on, 429

- Nitrates, oxidizing metal, polymerization of *N*-vinylcarbazole initiated by, 1911
- Nitrile groups in the side chain, emulsion copolymerization with styrene derivatives containing, 1033
physical and mechanical properties of copolymers with styrene derivatives containing, 1049
- Nitrogen-containing alkenes, copolymerization of divinyl ether with certain, 1265
- Nitrogen dioxide, reaction of, with polystyrene films, 3214
- Nuclear magnetic resonance studies, high resolution, determination of randomness in copolyesters by, 2259
high-resolution, of 2,4-dicyanopentanes, 1855
of polyacrylonitrile, 1059
of α -methylstyrene-*p*-methyl- α -methylstyrene copolymers, 397
of poly(vinyl formate), 257
on the stereospecific polymerization of methyl vinyl ether, polymerization by metal halides, penultimate effect, 849
on the stereospecific polymerization of methyl vinyl ether, polymerization by sulfuric acid-aluminum sulfate complex, enantiomorphic catalyst sites model, 863
- Nuclei, aromatic, polymerization of, 945
- Nucleophilic aromatic substitution, poly(aryl ethers) by, 2399, 2415
- Nylon 6 and its oligomers, direct determination of ϵ -caprolactam in the presence of, by infrared spectroscopy, 231
- Nylon 6 γ -phase crystals, transition of, by stretching in the chain direction, 3017
- Nylon 1313, synthesis and polymerization of monomers, 391
- Olefins, α,β -disubstituted, cationic polymerization of, 1727
higher terminal, low molecular weight by-products in Ziegler polymerization of, 1191
- α -Olefins, differences in polymerization activity of, with heterogeneous metalorganic catalysts, 205
- 1-Olefins, optically active, cationic and free-radical polymerization of, 619
- Oleic and petroselinic acids, perchlorocyclopentadiene adducts of, vinyl esters of, polymers of, 1809
- Oligomerization of halobenzenes by aluminum chloride-cupric chloride, 945
- Onuphic acid, dissociation constants of, 2707
- Optically active and inactive polycamphorates and polycamphoramides, 2481
- Optically active polymers, syntheses of, by condensation polymerization of *d*-tartaric acid with diamines, 2441
- Ordered heterocycle copolymers, 2429
- Organic photoconductors, 1699
- Organometallic polymers, 2927
copolymerization of chloral and dichloroacetaldehyde catalyzed by, 975
- Organotin polyesters, volatile degradation products of, 2458
- Oxidative degradation of polystyrene, 1635
- 2-Oxo-1,3-dioxolane group, preparation and polymerization of vinyl monomers containing, 307
- Oxygen, dissolved, permeability of membrane to, 2952
effect of, on γ -radiation-induced polymerization of ethylene, 2731
- Oxymethylene and siloxane series, calculated influence of steric effects on polymerization-depolymerization equilibria in, 355
- Ozonation, head-to-head units in poly(propylene oxide) by, 407
of poly(propylene oxide), isotactic sequence lengths, 175
- Pendent ester and hydroxymethyl groups, post-lactonization of vinyl polymers containing, 2655
- Perchlorocyclopentadiene adducts of petroselinic and oleic acids, vinyl esters of, polymers of, 1809
- Permeability of membrane to dissolved oxygen, 2952
- Peroxides, aryl, containing reactive functional groups, 2964
- Peroxide vulcanization of poly(vinyl alkyl ethers), identification of volatile products produced during, 785
- Peroxydisulfate, aqueous, crosslinking of gelatin by, 1
- Persulfate-initiated polymerization of acrylamide, 3151

- Persulfate-thiosulfate redox couple, polymerization of acrylamide initiated by, 3167
- Petroselinic and oleic acids, perchlorocyclopentadiene adducts of, vinyl esters of, polymers of, 1809
- γ -Phase crystals, nylon 6, transition of, by stretching in the chain direction, 3017
- Phenolic resins, role of *para*-substituted phenols in curing of, 2807
- Phenols, *para*-substituted, in curing resole-type phenolic resins, 2807
- Phenylated phenylene units, 2721
- Phosphazene system, comparisons with the calculated influence of steric effects on polymerization-depolymerization equilibria in siloxane and oxymethylene series, 355
- Phosphonitrilic chloride, trimeric, kinetics of bulk polymerization of, 3061
- Photochemistry of poly(*tert*-butyl acrylate), 2333
- Photoconductors, obtained from reaction products of poly(9-vinyl anthracene), 1699
organic, 1699
- Photolysis of poly(ethylene terephthalate), 481
- Photosensitized crosslinking of vinyl polymers containing *N*-hydroxymethylacrylamide, redox behavior in, 2705
- 1-Phthalimido-1,3-butadiene and 1-succinimido-1,3-butadiene, polymers of, 2219
- Polarization method, fluorescence, studies of micro-Brownian motion of a polymer chain by, 1021
- Polyacrylamide film, absorption and differential permeation of water vapor in, 2147
- Polyacrylonitrile, chromophore of, 2637
grafting of, to granular corn starch, 1313
grafting of, to granular corn starch by initiation with cerium, 2967
high-resolution nuclear magnetic resonance spectra of, 1059
hydrolysis of, 161
tacticity of, 1059, 1855
- Polyaddition, of bisimidazoline with dicarboxylic acids, synthesis of polyamides by, 1129
of bisuccinimides with diamines in synthesis of polyamides, 15
- Poly(amic acids), aromatic, fully aromatic polybenzoxazinones from, 2359
- Polyamides, synthesis of, by the polyaddition of bisimidazoline with dicarboxylic acids, 1129
synthesis of, by polyaddition of bisuccinimides with diamines, 15
- Polyampholytes, synthesis and evaluation of a series of regular, 537
- Polyaromatic heterocyclics, pyrolysis of, 1513
- Poly(aryl ethers) by nucleophilic aromatic substitution, 2399, 2415
- Polyaryloxysilanes, synthesis of, by melt-polymerizing dianilino- and diphenoxysilanes with aromatic diols, 707
- Polybenzimidazoles containing aryl sulfone linkages, 1113
- Polybenzoxazinones, fully aromatic, from aromatic poly(amic acids), 2359
- Poly-3,3-bis(chloromethyl)oxacyclobutane (Penton) derivatives, 2843
- Poly(*tert*-butyl acrylate), photochemistry of, 2333
- Poly-*p*-*tert*-butylstyrene, crystalline, 2187
- Polycamphoramides and polycamphorates, optically active and inactive, 2481
- Poly(chloroaldehydes), 975
- Poly(cyanoethyl)oxymethylene, crystalline, 2247
- Polycyclopentadiene, chemical modifications of, 725
- Polydimethylsiloxane blends, viscosity of, 3071
- Poly-1,6-diselenahexamethylene, 1,2-diselenane, and their effects on vinyl polymerizations, 903
- Polyesters, adsorbed on solid surfaces, conformation of, 651
organotin, volatile degradation products of, 2458
- Polyethers, 2179
fluorine-containing, preparation of, 2343
- Polyethylene, grafting of maleic anhydride on, 1547
high-pressure, quantitative determination of short branches in, by gamma radiolysis, 2023
and poly(maleic anhydride), grafting in reaction of, 1539

- Poly(ethylene glycol) copolymers, methoxy, vinyl chloride acrylate of, 2946
- Polyethylenimine, analysis of, by spectrophotometry of its copper chelate, 1993
fluorescent conjugates of, 1021
- Poly(ethylene oxide) radicals, block copolymerization of, with methyl methacrylate, 43
- Polyethylene specimens, thin, for electron microscopy, xylene-stream method for obtaining, 1179
- Poly(ethylene terephthalate), amorphous and crystalline samples of, ESR study of radicals trapped in, after γ -irradiation, 2199
photolysis of, 481
- Polyhydantoins, aromatic, from bisiminoacetate and diisocyanates, 2289
- Poly(2-hydroxyethyl methacrylate) homogeneous hydrogel, hydrophobic interaction in, 3103
- Polyimidazopyrrolones, 3043
- Polyimide-amides from maleopimaric acid, 2204
- Poly(maleic anhydride) and polyethylene, grafting in reaction of, 1539
- Polymethacrylonitrile, isotactic, new catalysts for, 2503
- Poly(methyl acrylate), stereoregularity of, 2167
- Poly(methyl methacrylate), ultraviolet-irradiated, decay of ESR signal in, 677
- Poly(methyl propenyl ether), diisotacticity of, and double-bond opening of methyl propenyl ether in cationic polymerization, 3009
- Polynomial expansion of log relative viscosity and application to polymer solutions, 2629
- Polyoxazolidones, 1865
- Poly-*m*-phenoxyene sulfonamides, 935
- Polyphenylpolyposphonates from condensation polymerization, 57
- Poly(phosphine oxides) and poly(phosphine sulfides), ferrocene-containing, 2927
- Poly(phosphine sulfides) and poly(phosphine oxides), ferrocene-containing, 2927
- Polypropylene, influence of preparative conditions on molecular weight and stereoregularity distributions of polypropylene, 215
inhibited autoxidation of, 1683
kinetics of autoxidation of, 2091
preirradiated, graft copolymerizations of gaseous vinyl chloride and vinylidene chloride on, 439
- Poly(propylene oxide), isotactic sequence lengths by ozonation of, 175
by ozonation, head-to-head units in, 407
- Polyquinazolinediones, fully aromatic, cyclodehydration to, 2523
- Poly(Schiff bases), preparation of polymeric amines from, 1659
- Polysiloxanes, carborane polymers, 365
hydroxyl-terminated, preparation of diborane reduction of corresponding acids, 685
- Poly(sodium acrylate)-xylan graft copolymer, redox-initiated, 3183
- Polystyrene, chlorinated, 2297
oxidative degradation of, 1635
- Polystyrene films, reaction of nitrogen dioxide with, 3214
- Polysulfonamides, aromatic, 553
- Polysulfonamide-ureas, 3212
- Polyureas with long methylene chain units, 119
- Poly(ureido acids), aromatic, by low-temperature solution polymerization and cyclodehydration to fully aromatic polyquinazolinediones, 2523
- Polyurethanes, from fluorinated diisocyanates, 2757
with long methylene chain units, 119
- Poly(vinyl alkyl ethers), identification of volatile products produced during peroxide vulcanization of, 785
- Poly(9-vinyl anthracene), photoconductors obtained from reaction products of, 1699
- Poly(vinyl chloride), 1137
determination of tacticity in, by infrared spectroscopy, 2013
thermal stabilizers of, mechanism of, 2229
- Poly(vinyl ether), stereoregularity of, 1233
- Poly(vinyl formate), NMR study of, 257
- Poly(vinylphthalic anhydride), imide-crosslinked, thermal stability of, 2202
- Pore-size distribution, 2835
- Post-lactonization of vinyl polymers containing pendent ester and hydroxymethyl groups, 2655
- Post-polymerization, 2-vinylnaphthalene, initiated by ^{60}Co γ -irradiation, 2557

- Propenyl *n*-butyl ether, cationic polymerization of, 1727
- Propylene, influence of SeOCl_2 on polymerization of, by $\text{TiCl}_3\text{-Al}(\text{C}_2\text{H}_5)_3$, 2815 and α -*d*-propylene, Ziegler-Natta polymerization of, 2487
- terpolymerization of, with ethylene and dicyclopentadiene, single initial addition of dicyclopentadiene, 243
- terpolymerization of, with ethylene and dicyclopentadiene, two-step addition of dicyclopentadiene, 251
- Propylene oxide with a dialkylzinc-hydrazine catalyst, polymerization of, 917
- α -*d*-Propylene and propylene, Ziegler-Natta polymerization of, 2487
- Protein functional groups, anionic graft polymerization of methyl acrylate to, 2535
- Pulse radiolysis studies of styrene, 877
- Pyridine-sulfur dioxide complex, polymerization of methyl methacrylate initiated by, in presence of carbon tetrachloride, 2769
- Pyrolysis, of cellulose and cellulose treated with ammonium phosphate by differential thermal analysis and thermal gravimetric analysis, determination of kinetic parameters of, 833
- of polyaromatic heterocyclics, 1513
- Pyrrrole, furan, and thiophene, colored electrically conducting polymers from, 1527
- Pyrrolidone and caprolactam, copolymerization of, 965
- Quinoxaline units, polymers with, 545
- Radiation, ionizing, polymerization of β -(2-furyl)acrolein in solution by, 3219
- γ -Radiation, cobalt-60, solid-state polymerization of 1,2,3,4-diepoxybutane initiated by, 1015
- copolymerization of trioxane by, 183
- γ -Radiation-induced polymerization of ethylene, effect of oxygen on, 2731
- mechanism of initiation in, 1073
- Radiation-induced polymerization of 1,1,2-trichlorobutadiene, 2617
- Radiation-induced solid-state polymerization in binary systems, 1899
- Radical and anionic homopolymerization of maleimide and *N*-*n*-butylmaleimide, 1619
- Radical copolymerization of crotonyl compounds with styrene, 2641
- Radical-initiated copolymerization of carbon monoxide and ethylenimine in the presence of ethylene, 2031
- Radical initiators, mechanism of grafting in a heterogeneous medium in the presence of, 1563
- Radical polymerizabilities and infrared spectra of vinylpyridines complexes with zinc and cadmium salts, 1083
- Radicals, ESR study of, trapped in amorphous and crystalline samples of poly(ethylene terephthalate) after γ -irradiation, 2199
- Radiolysis, gamma, quantitative determination of short branches in high-pressure polyethylene by, 2023
- Ramie and cotton, action of caustic soda on fine structure of, 2579
- Randomness in copolyesters, determination of, by high resolution nuclear magnetic resonance, 2259
- γ -Ray-initiated polymerization of 1,3-dienes, 503
- γ -Ray irradiation or α, α' -azobisisobutyronitrile, isomerization of polymerization of 2-vinyl-1,3-dioxolane by, 2351
- γ -Ray polymerization, of acrylamide, 531
- of formaldehyde in presence of carbon dioxide, kinetics of, 2825
- γ -Ray radiation, polymerization of *N*-vinylphthalimide by, 2942
- Reaction medium, effect of, on copolymerization of acrylonitrile and methyl acrylate, 1967
- Reactivity ratios of styrene and methyl methacrylate at 90°C., 1289
- Redox behavior in photosensitized cross-linking of vinyl polymers containing *N*-hydroxymethylacrylamide, 2705
- Redox couple, persulfate-thiosulfate, polymerization of acrylamide initiated by, 3167
- Redox-initiated vinyl polymerization with thiourea as reductant, 135
- Redox-initiated xylan-poly(sodium acrylate) graft copolymer, 3183
- Resins, epoxy, mechanism of tertiary amine-catalyzed dicyandiamide cure of, 1609
- resole-type phenolic, role of *para*-substituted phenols in curing of, 2807

- Resole-type phenolic resins, role of *para*-substituted phenols in curing of, 2807
- Rhenium pentachloride, effect of ethyl monochloroacetate on cationic polymerization of styrene catalyzed by, 3207
- Ring-opening polymerization of unsaturated alicyclic compounds, 2209
- Ring systems, fused, cyclocopolymerization of bicyclopentene and other dicyclic dienes with sulfur dioxide to, 1827
- Rosenmund reduction to polyether aldehyde, synthesis of an aryene/alkylene polyether from diphenolic acid and, 381
- Rubber, ethylene-propylene, diffusion in, 1327
natural, cationic graft copolymerization of styrene onto, 339
- Salts, metal, effects of, on polymerization, 1083
zinc and cadmium, radical polymerizabilities and infrared spectra of vinylpyridines complexed with, 1083
- SeOCl₂, influence of, on polymerization of propylene by TiCl₃-Al(C₂H₅)₃, 2815
- Short-chain branching, propagation, and transfer in free-radical polymerization of ethylene, 3115
- Side reactions, hydrolytic, 2415
- Silicone grease, polymerization of gaseous diazomethane on, 585
- Siloxane and oxymethylene series, calculated influence of steric effects on polymerization-depolymerization equilibria in, 355
- Siloxanes, aryene-modified, 2745
- Soaps, metal, combination of, synergistic effect of, 2229
- Sodium cellulose xanthate in dilute solution, molecular parameters of, 769
- Solid-state polymerization, 2557
of 1,2,3,4-diepoxybutane initiated by cobalt-60 γ -radiation, 1015
in the glassy phase, 1899
radiation-induced, in binary systems, 1899
- Solution polymerization, of dioxolane, kinetics of, in presence of water, 1889
low-temperature, poly(ureido acids) by, 2523
of trioxane catalyzed by BF₃·O(C₂H₅)₂, changes in concentration of tetraoxane produced during, 2977
of trioxane catalyzed by BF₃·O(C₂H₅)₂, effect of solvent on amount of tetraoxane produced in, 2989
- Solvent, effect of, on amount of tetraoxane produced in solution polymerization of trioxane catalyzed by BF₃·O(C₂H₅)₂, 2989
- Spatial conformation, ester, effect of, on the cycloelimination process, 2333
- Spectra, infrared, of vinylpyridines complexed with zinc and cadmium salts, radical polymerizabilities and, 1083
- Spontaneous polymerization of formaldehyde by acidic substances, retardation of, 3129
- Stability, thermal, of imide-crosslinked poly(vinylphthalic anhydride), 2202
- Stabilizers, thermal, mechanism of, for poly(vinyl chloride), 2229
- Statistical character of anionic polymers, effect of impurities and the initiation and transfer rate constants on, 2269
- Stereoregular condensation polymers, 2481
- Stereoregularity, of polyacrylonitrile by NMR, 2875
of poly(methyl acrylate), 2167
of poly(vinyl ether), 1233
- Stereoregularity distributions of polypropylene, influence of preparative conditions on, 215
- Stereoregular polymerization of 1-vinylnaphthalene, 2-vinylnaphthalene, and 4-vinylbiphenyl, 2323
- Stereospecific polymerization of methacrylonitrile, 2503
characterization of crystalline polymethacrylonitrile, 593
- Steric effects, calculated influence of, on polymerization-depolymerization equilibria in siloxane and oxymethylene series, 355
- Structural effects in heteroatom systems, 355
- Styrene, in benzene, *tert*-butyl hydroperoxide-initiated polymerization of, 1101
cationic graft copolymerization of, onto natural rubber, 339
copolymerization of, 1033, 1049
copolymerization of monomers with, 1599
copolymerization of tetraoxane with, catalyzed by BF₃·O(C₂H₅)₂, 1937
copolymerization of trioxane with, catalyzed by BF₃·O(C₂H₅)₂, 1927

- effect of ethyl monochloroacetate on cationic polymerization of, catalyzed by rhenium pentachloride, 3207
and isoprene, anionic copolymerization of, in cyclohexane, 2783
and methyl methacrylate at 90°C., reactivity ratios of, 1289
polymerization of, with VOCl_3 -aluminum alkyls, 2079
polymerization and copolymerization, influence of intrachain interactions on kinetics of, 2159
pulse radiolysis studies of, 877
radical copolymerization of crotonyl compounds with, 2641
with the VOCl_3 - AlEt_2Br catalyst System, polymerization of, 665
- Styrene derivatives containing nitrile groups in the side chain, emulsion copolymerization with, 1033
physical and mechanical properties of copolymers with, 1049
- Styrene oxide, polymerization of, by the triisobutylaluminum-water, system, 2055
- p*-Styrenesulfonyl(β -chloroethyl)amide, 3193
- Substituent effects, copolymerization of monomers with styrene and, 1599
- N*-[1-(1-Substituted-2-oxopropyl)] acrylamides and -methacrylamides, polymerization of, synthesis and, 1599
- para*-Substituted phenols in curing resole-type phenolic resins, 2807
- 1-Succinimido-1,3-butadiene and 1-phthalimido-1,3-butadiene, polymers of, 2219
- Sugar dithiol, preparation and polymerization of, 2111
- Sulfides, cyclic, polymerization of, 273
- Sulfite-chlorate-initiated acrylonitrile copolymer, endgroup of, 2857
- Sulfur dioxide-pyridine complex, polymerization of methyl methacrylate initiated by, in presence of carbon tetrachloride, 2769
- Sulfuric acid-aluminum sulfate complex, enantiomorphic catalyst sites model, NMR studies on the stereospecific polymerization of methyl vinyl ether, polymerization by, 863
- Synergistic effect of combination of metal soaps, 2229
- Tacticity, determination of, in poly(vinyl chloride) by infrared spectroscopy, 2013
of polyacrylonitrile, 1059, 1855
- d*-Tartaric acid, condensation polymerization of, with diamines, syntheses of optically active polymers by, 2441
- Terminal acetylenic group, linear polymers of vinyl monomers containing, 999
- Terpolymerization of ethylene, propylene, and dicyclopenta-diene with single initial addition of dicyclopentadiene, 243
- Tertiary amine-catalyzed dicyandiamide cure of epoxy resins, mechanism of, 1609
- Tetrahydrofuran, initiation process in polymerization of, with carbonium ion salts, 193
- Tetrahydrofuran-propylene oxide copolymers, molecular weights of, by gel permeation chromatography and other methods, 2045
- Tetraoxane, copolymerization of, with styrene catalyzed by $\text{BF}_3 \cdot \text{O}(\text{C}_2\text{H}_5)_2$, 1937
effect of solvent on amount of, produced in solution polymerization of trioxane catalyzed by $\text{BF}_3 \cdot \text{O}(\text{C}_2\text{H}_5)_2$, 2989
polymerization of, at low concentration catalyzed by $\text{BF}_3 \cdot \text{O}(\text{C}_2\text{H}_5)_2$, 2997
produced during solution polymerization of trioxane catalyzed by $\text{BF}_3 \cdot \text{O}(\text{C}_2\text{H}_5)_2$, changes in concentration of, 2977
- Thermal behavior of 4-(*o*-carboranyl)-1-butylmethyl siloxane-dimethyl siloxane copolymers, 2119
- Thermal degradation of copolymers, boundary effects on, 21
- Thermal gravimetric analysis, determination of kinetic parameters for pyrolysis of cellulose treated with ammonium phosphate by, 833
- Thermal stability, 2399
of imide-crosslinked poly(vinylphthalic anhydride), 2202
- Thermal stabilizers, mechanisms of, for poly(vinyl chloride), 2229
- Thermodynamics of polymerization, 1383
- Thietane, polymerization of, 171
- Thiophene, furan, and pyrrole, colored electrically conducting polymers from, 1527

- Thiosulfate-persulfate redox couple, polymerization of acrylamide initiated by, 3167
- Thiourea, as reductant in redox-initiated vinyl polymerization, 135
- $\text{TiCl}_3\text{-Al}(\text{C}_2\text{H}_5)_3$, influence of SeOCl_2 on polymerization of propylene by, 2815
- Titration, turbidimetric, cohesive energy densities of polymers from, 1671
- p*-Toluenesulfonic acid, acrylonitrile polymerization of, kinetics and mechanism of, 1297, 1307
- Transfer rate and initiation constants and impurities, effect of, on the statistical character of anionic polymers, 2269
- 1,1,2-Trichlorobutadiene, radiation-induced polymerization of, 2617
- Triethyl phosphite, reaction of, with vinyl esters, 2453
- Triisobutylaluminum-water system, polymerization of styrene oxide by, 2055
- Trimeric phosphonitrilic chloride, kinetics of bulk polymerization of, 3061
- Tri-*O*-methylamylose and tri-*O*-methylcellulose, acid-catalyzed methanolysis of, 2133
- Tri-*O*-methylcellulose and tri-*O*-methylamylose, acid-catalyzed methanolysis of, 2133
- Trioxane, copolymerization of, by γ -radiation, 183
- copolymerization of, with styrene catalyzed by $\text{BF}_3\cdot\text{O}(\text{C}_2\text{H}_5)_2$, 1927
- rates of polymer formation and monomer consumption in the solution polymerization of, catalyzed by $\text{BF}_3\cdot\text{O}(\text{C}_2\text{H}_5)_2$, 95
- solution polymerization of, catalyzed by $\text{BF}_3\cdot\text{O}(\text{C}_2\text{H}_5)_2$, changes in concentration of tetraoxane produced during, 2977
- solution polymerization of, catalyzed by $\text{BF}_3\cdot\text{O}(\text{C}_2\text{H}_5)_2$, effect of solvent on amount of tetraoxane produced in, 2989
- Turbidimetric titration, cohesive energy densities of polymers from, 1671
- Ultraviolet-irradiated poly(methyl methacrylate) decay of ESR signal in, 677
- Umbelliferae* and *Limnanthes douglasii*, homopolymers and vinyl chloride copolymers of vinyl esters of chlorinated fatty acids from, 2899
- Unsaturated alicyclic compounds, ring-opening polymerization of, 2209
- Unsaturated group, linear polymers of vinyl aryl monomers containing another, 1245
- Uranyl ion-sensitized polymerization of acrylamide and methacrylamide in aqueous solution, 637
- Urethanes, complex formation with catalysts, alcohols and isocyanates in preparation of, 35
- Vinyl alkyl ethers catalyzed by aluminum sulfate-sulfuric acid complex, effect of temperature and solvents on stereospecific polymerization of, 795
- Vinyl aryl monomers, linear polymers of, containing another unsaturated group, 1245
- Vinylbenzamides, 2911
- 2-Vinylbenzimidazole and 5(6)-vinylbenzimidazole, synthesis of, 1987
- 5(6)-Vinylbenzimidazole and 2-vinylbenzimidazole, synthesis of, 1987
- P*-Vinylbenzyl methyl ether, ionic polymerization of, 417
- kinetics of free-radical polymerization of, 1165
- 4-Vinylbiphenyl, 1-vinylnaphthalene, and 2-vinylnaphthalene, stereoregular polymerization of, 2323
- N*-Vinylcarbazole, polymerization of, initiated by oxidizing metal nitrates, 1911
- Vinyl chloride, and 12-acryloxystearate, copolymers of, 2949
- gaseous, graft copolymerization of, on preirradiated polypropylene, 439
- polymerization of, precipitated polymer in kinetics of, 1137
- Vinyl chloride acrylate of methoxy poly(ethylene glycol) copolymers, 2946
- Vinyl chloride copolymers and homopolymers of vinyl esters of chlorinated fatty acids from *Umbelliferae* and *Limnanthes douglasii*, 2899
- Vinylcyclopropane and related compounds, rearrangements of the propagating chain end in the cationic polymerization of, 227
- 2-Vinyl-1,3-dioxolane, isomerization polymerization of, by α,α' -azobisisobutyronitrile or by γ -ray irradiation, 2351
- Vinyl esters, acid, 1,4,5,6,7-hexachloro- and hexambromobicyclo-[2,2,1]-5-heptene-2-carboxylic acid, and copolymerization with acrylonitrile, synthesis of, 1279

- of chlorinated fatty acids, homopolymers and vinyl chloride copolymers of, from *Umbelliferae* and *Limnanthes douglasii*, 2899
- polymers of, of perchlorocyclopentadiene adducts of petroselenic and oleic acids, 1809
- reaction of triethyl phosphite with, 2453
- Vinyl ferrocene, free-radical polymerization of, 2091
- Vinyl hydroquinone derivatives synthesis of, by the Wittig reaction, 993
- Vinylidene chloride, copolymerization of 4-cyclopentene-1,3-dione with *p*-chlorostyrene and, 1123
- gaseous, graft copolymerizations of, on preirradiated polypropylene, 439
- Vinylidene chloride-vinyl chloride copolymers, dielectric properties of, 1717
- Vinyl monomers, containing 1,3-dioxolane group, preparation and polymerization of, 287
- containing 2-oxo-1,3-dioxolane group, preparation and polymerization of, 307
- containing a terminal acetylenic group, linear polymers of, 999
- 1-Vinylnaphthalene, 2-vinylnaphthalene, and 4-vinylbiphenyl, stereoregular polymerization of, 2323
- 2-Vinylnaphthalene, post-polymerization initiated by ^{60}Co γ -irradiation, 2557
- 1-vinylnaphthalene, and 4-vinylbiphenyl, stereoregular polymerization of, 2323
- N*-Vinylphthalimide, polymerization of, by γ -ray radiation, 2042
- Vinyl polymerizations, poly-1,6-diselenahexamethylene, 1,2-diselenane, and their effects on, 903
- Vinyl polymers, containing *N*-hydroxymethylacrylamide, redox behavior in photosensitized crosslinking of, 2705
- post-lactonization of, containing pendent ester and hydroxymethyl groups, 2655
- Vinylpyridines complexed with zinc and cadmium salts, radical polymerizabilities and infrared spectra of, 1083
- Vinyl stearate, emulsion polymerization of, 2665
- Viscosity, log relative, polynomial expansion of, application to polymer solutions, 2620
- of polydimethylsiloxane blends, 3071
- $\text{VOCl}_3\text{-AlEt}_2\text{Br}$ catalyst system, polymerization of styrene with, 665
- VOCl_3 -aluminum alkyls, polymerization of styrene with, 2079
- Volatile degradation products of organotin polyesters, 2458
- Volatile fraction, effect of, on the degradation of an initial "most probable" polymer, 1573
- Water, bulk polymerization of dioxolane in presence of, kinetics of, 1881
- solution polymerization of dioxolane in presence of, kinetics of, 1889
- Water vapor, absorption and differential permeation of, in polyacrylamide film, 2147
- Wittig reaction, synthesis of vinyl hydroquinone derivatives by, 993
- Xylan-poly(sodium acrylate) graft copolymer, redox-initiated, 3183
- Xylene-stream method for obtaining thin polyethylene specimens for electron microscopy, 1179
- Ziegler-Natta catalysts, homogeneous, mechanism of stereoregular polymerization of butadiene by, effect of the nature of bases and halogens on, 521
- homogeneous, mechanism of stereoregular polymerization of butadiene by, effects of the species of transition metals, 511
- Ziegler-Natta polymerization of propylene and α -*d*-propylene, 2487
- Ziegler polymerization of higher terminal olefins, low molecular weight by-products in, 1191